INVESTIGATION OF TAR CONVERSION OVER BIOMASS CHAR

Agnieszka Korus

A thesis submitted in partial fulfilment of the requirements of the University of Lincoln and the Silesian University of Technology for the degree of Doctor of Philosophy

Faculty of Energy and Environmental Engineering
Silesian University of Technology

School of Engineering
College of Science
University of Lincoln

Gliwice/Lincoln

June 2019

ACKNOWLEDGEMENTS

The main part of this work's funding was provided by the National Science Centre, Poland in the scope of the project PRELUDIUM 10 number 2015/19/N/ST8/02454 "Decomposition of aromatic hydrocarbons in a coupled coking-steam reforming process in respect of adsorptive and catalytic properties of the char" where the author was the primary investigator. The main experimental rig was financed by Silesian University of Technology Statutory Funding. Char oxidation kinetics and SEM analysis were financed by the School of Engineering, University of Lincoln.

The author would like to thank her supervisors, Prof Andrzej Szlęk and Dr Abby Samson for their guidance and advice, for sharing their knowledge and experience as well as for providing moral support.

The author would also like to express her gratitude to Mr Krzysztof Rajczykowski, Dr Krzysztof Loska and Dr Irena Korus for the help with AAEM content analysis and to Mr Philip Staton for a training in SEM analysis. Moreover, the author would like to thank Dr Anna Katelbach-Woźniak and Dr Sławomir Sładek for sharing their knowledge and experience on academic research as well as express her gratitude to Mr Zygmunt Zieliński for all the technical help with laboratory maintenance.

PREFACE

This PhD project was carried out in a dual mode at the Institute of Thermal Technology, Faculty of Energy and Environmental Engineering, Silesian University of Technology, Gliwice, Poland and the School of Engineering, University of Lincoln, Lincoln, UK in a scope of the Joint Doctoral Degree Agreement between both Universities, signed on the 16th of May 2018.

The work presented in this thesis was carried out by the author at first as a Silesian University of Technology internal grant: BKM-512/RIE6/2015 „Badania procesu zgazowania paliw stałych w warstwie nieruchomej" and continued further as a National Science Centre project PRELUDIUM 10 number 2015/19/N/ST8/02454 "Decomposition of aromatic hydrocarbons in a coupled coking-steam reforming process in respect of adsorptive and catalytic properties of the char". In both projects, the author acted as a primary investigator. Moreover, some of the analyses were performed by the author at the School of Engineering, University of Lincoln.

Supervisors:

Prof. dr hab. inż. Andrzej Szlęk

Dr Abby Samson

ABSTRACT

Tar release is one of the main challenges for a further development of gasification technology. While heavy aromatic compounds condensation causes installation clogging, lighter molecules remain in a gaseous phase, contaminating producer gas. Therefore, catalytic reforming of tar has been extensively studied. To simplify a conversion mechanism, a single tar compound is often used in a fundamental research.

In this dissertation, toluene was selected as a model tar molecule. Biochar was used as a catalyst, as its availability, as a gasification by-product, makes it an economically beneficial material. Toluene conversion over biochars prepared under uniform conditions, from three differentiated tree species, was examined. The comparison of various woods revealed, that toluene conversion over a char prepared from coniferous pine was lower, compared to deciduous-trees chars. It was attributed to less abundant active sites and lower surface area of a pine char. Moreover, a higher microporosity resulted in a quicker deactivation of this char, as suggested by a conversion decrease with time. Since one of the main distinctions between deciduous and coniferous trees is a high resin content in the letter, an acetone extraction of pinewood prior to char preparation was performed. This pre-treatment influenced pyrolysis process, yielding char with slightly improved parameters and an increased short-term performance.

Another objective of this work focused on plausible toluene conversion pathways. To this end, along with toluene conversion, a yield of its by-products was also measured. The experiment was carried out under pyrolytic conditions to enable separation of a heterogeneous, catalytic toluene conversion from the effects of an oxidising agent. Then, an H_2O/N_2 atmosphere was studied to assess the role of steam and a possibility of its interactions with toluene during reforming. It was concluded that a majority of toluene decomposed heterogeneously over char bed, yielding coke and releasing H_2. Demethylation was a competitive, less favoured pathway leading to benzene and CH_4 formation, with a selectivity up to ~15 %. Some secondary substitution and dehydrogenation reactions were also observed, leading to xylenes, ethylbenzene and styrene. The steam introduced in a reforming mode did not influence toluene conversion pathways. Its role was limited to char and coke gasification, and thus a prolongation of catalytic activity of the bed. Although the

two processes were not directly interacting, a plausible competition for char surface between steam and toluene was suspected.

An additional set of tests was designed to further clarify some of toluene conversion aspects, *i.e.* the roles of an oxidising agent, char surface chemistry and tar molecule's substituents. An intermittent toluene feeding experiment suggested that no homogeneous toluene conversion was initiated by any char-released radicals. Comparison of benzene, toluene and *p*-xylene conversion suggested an importance of methyl group presence to the compound's reactivity and its conversion pathways. An addition of an extra CH_3– group did not however improve the conversion any further, although it enhanced secondary, rearrangement reactions. Comparison of O_2 and steam as an oxidising agent suggested that while steam favoured char/coke oxidation and did not react directly with toluene, O_2 was primarily consumed by toluene in ring-opening, homogeneous reactions thus it did not regenerate catalyst bed. Char pre-treatment, applied to differentiate alkali and alkaline earth metals content, resulted in drastic changes in char's reactivity towards oxidation, yet it did not affect its performance as a catalyst in pyrolytic toluene conversion.

STRESZCZENIE

(*Abstract in Polish*)

Powstawianie smół podczas procesu zgazowania jest jednym z poważniejszych problemów eksploatacyjnych tej technologii. Podczas gdy cięższe wielopierścieniowe węglowodory aromatyczne mogą ulegać kondensacji, powodując blokowanie przewodów instalacji, lżejsze związki smół pozostają w fazie gazowej, zanieczyszczając gaz procesowy. Dlatego też, katalityczny reforming smół stał się istotnym obiektem badań. W celu uproszczenia mechanizmów konwersji, na potrzeby badań podstawowych, jako reprezentant prawdziwej smoły, będącej mieszaniną rozmaitych węglowodorów, stosowany jest często pojedynczy związek.

W niniejszej pracy rolę takiego związku pełnił toluen. Katalizatorem podczas przeprowadzonych eksperymentów był karbonizat pochodzący z biomasy drzewnej, ponieważ, jako półprodukt procesu zgazowania, jest materiałem łatwo dostępnym i ekonomicznym. Na potrzeby niniejszych badań, w kontrolowanych warunkach laboratoryjnych przygotowane zostały trzy rozdaje karbonizatu z różnych gatunków drewna: sosny, buka i olchy. Badania wykazały, że karbonizat z drewna sosnowego posiadał gorsze właściwości katalityczne, w porównaniu do pozostałych dwóch materiałów, przygotowanych z drzew liściastych. Zaobserwowana różnica korelowała z mniejszą powierzchnią właściwą i liczbą miejsc aktywnych karbonizatu z drzewa iglastego. Szybsza dezaktywacja karbonizatu z sosny została z kolei przypisana do zwiększonego udziału mikroporów w tym materiale. Oprócz różnic w ilości i budowie ligniny w drzewach iglastych i liściastych, charakterystyczną cechą drewna sosnowego jest wysoka zawartość związków ekstrakcyjnych, w tym żywic. W kolejnym etapie badań, jako katalizator wykorzystany został karbonizat przygotowany z drewna sosnowego poddanego ekstrakcji acetonem. Rezultatem usunięcia związków ekstrakcyjnych było polepszenie właściwości katalitycznych otrzymanego karbonizatu oraz krótkotrwała poprawa jego skuteczności w usuwaniu toluenu.

Przeprowadzone eksperymenty pozwoliły na zbadanie mechanizmów rozkładu toluenu. Oprócz stopnia konwersji toluenu, przeprowadzony został pomiar ilości ciekłych i gazowych produktów reakcji. Dodatkowo, pomiary prowadzone były w dwóch odmiennych atmosferach. Pirolityczna konwersja dostarczyła informacji na temat

niezakłóconych, heterogenicznych reakcji toluenu na powierzchni katalizatora. Reforming parowy pozwolił z kolei na zbadanie wpływu utleniacza na przebieg procesu. Badania wykazały, że główną ścieżką rozkładu toluenu była heterogeniczna reakcja prowadząca do adsorpcji toluenu na powierzchni karbonizatu z równoczesnym wydzielaniem się wodoru. Selektywność konwersji względem konkurencyjnego procesu, w którym produktami były benzen i metan, osiągała poziom ~15 %. Ponadto zaobserwowane zostały reakcje rekombinacji, prowadzące do powstawania śladowych ilości etylobenzenu, ksylenów oraz styrenu. Wprowadzenie pary wodnej do środowiska reakcji nie wpłynęło na mechanizm konwersji toluenu. Jej obecność skutkowała natomiast zgazowaniem karbonizatu w rezultacie przedłużając aktywność katalizatora. Pomimo iż podczas reformingu nie zaobserwowano bezpośrednich, homogenicznych reakcji pary wodnej z toulenem, oba związki najprawdopodobniej rywalizowały o dostęp do powierzchni katalizatora.

W celu poszerzenia informacji na temat roli utleniacza, właściwości karbonizatu oraz obecności metylowego podstawnika pierścienia aromatycznego w procesie jego konwersji, przeprowadzona została dodatkowa seria badań. Eksperyment z przerywanym dozowaniem toluenu wykazał brak łańcuchowych reakcji rozpadu zainicjowanych wolnymi rodnikami, potencjalnie uwalniającymi się z powierzchni karbonizatu. Z kolei porównanie konwersji benzenu i toluenu podkreśliło istotny wpływ obecności grupy metylowej na skuteczność usuwania danego związku. Dodatkowa grupa CH_3– w *p*-ksylenie nie wpłynęła z kolei na poprawę sprawności procesu, zwiększyła jedynie ilość i różnorodność produktów rekombinacji. Reforming w obecności tlenu wskazywał na występowanie bezpośredniej reakcji utleniania toluenu, w rezultacie skutkując brakiem regeneracji karbonizatu, z uwagi na preferencyjne zużycie tlenu w homogenicznych reakcjach. Eksperyment ten zasugerował zatem zróżnicowane role poszczególnych utleniaczy – w przeciwieństwie do tlenu, para wodna okazała się niezdolna do bezpośredniej reakcji z toluenem i działała jedynie jako czynnik zgazowujący karbonizat. Z kolei badanie karbonizatów o zróżnicowanej zawartości metali alkalicznych i metali ziem alkalicznych wykazało brak wpływu tych pierwiastków na skuteczność pirolitycznej konwersji toluenu, jednocześnie istotnie zmieniając reaktywność samego materiału.

TABLE OF CONTENT

LIST OF FIGURES

LIST OF TABLES

NOMENCLATURE

Acronyms

AAEM – Alkali and Alkaline Earth Metals

AAS – Atomic Absorption Spectroscopy

ATR – Attenuated Total Reflectance

BET – Brunauer−Emmett−Teller

BJH – Barrett-Joyner-Halenda

DFT – Density Functional Theory

DRIFT – Diffuse Reflectance

DTG – First Derivative of a mass loss function

EDX – Energy Dispersive X-Ray

FTIR – Fourier-Transform Infrared Spectroscopy

ICP – Inductively Coupled Plasma

MS – Mass Spectrometry

PAH – Polycyclic Aromatic Hydrocarbons

SEM – Scanning Electron Microscopy

TGA – Thermal Gravimetric Analysis

TPD – Temperature Programmed Desorption

XPS – X-ray Photoelectron Spectroscopy

Abbreviations

AA – activated alder char

AA_HCl – activated alder char washed with HCl

AA_Na – activated alder char washed with HCl and spiked with Na^+

AC – activated carbon

ASH – ash content

B – benzene

BA – activated beech char

EB – ethylbenzene

ET – *p*-ethyltoluene

FC – fixed carbon content

H2O_b – blank test of steam reforming with no compound feeding

MS – *p*-methylstyrene

m-X – *m*-xylene

o-X – *o*-xylene

P – non-activated pine char

PA – activated pine char

PAE – activated extracted pine char

PE – non-activated extracted pine char

p-X – *p*-xylene

PYR – pyrolytic mode

S – styrene

SR – steam reforming mode

T – toluene

TMB – 1,2,4-trimethylbenzene

VM – volatile matter content

Symbols

a – activity coefficient

A – pre-exponential coefficient

C_{tar} – tar concentration

E_a – activation energy

η_T – toluene conversion

k – rate coefficient

k_d – empirical parameter of activity function

m_i – mass of *i*-th by-product recovered from the impingers

M_i – mass of *i*-th by-product recovered from the impingers

m_{Tf} – total mass of toluene fed during a test run

m_{Tr} – mass of unreacted toluene

n_{CSF} – amount of carbon surface functionalities

$\dot{n}_{N_2}$ – molar flow of N_2 fed into the reactor

$n_{T,t}$ – molar amount of converted toluene

p – empirical parameter of activity function

p_1 – empirical parameter of activity function

p_2 – empirical parameter of activity function

R^2 – coefficient of determination

r_{tar} – tar conversion rate

T – temperature of a catalyst bed

t_{ex} – time of the experiment

t_f – final temperature of mass loss region

t_i – initial temperature of mass loss region

t_p – temperature of a peak of a DTG curve

τ – toluene residence time in catalyst bed

τ_{int} – time of gas sampling interval

V_a – volume of the aliquot

V_B – volume of the reaction base

V_{HCl} – volume of added acid

V_{NaOH} – volume of titrant

x_i – i-th by-product molecular yield

CHAPTER 1

INTRODUCTION

1.1. Introduction

To meet the obligations under the Renewable Energy Directive, individual EU countries issued their National Renewable Energy Action Plans that include scenarios for reaching 2020 targets [1]. Plans for both, United Kingdom and Poland strongly rely on biomass utilisation. United Kingdom strategy aims at achieving 30 % of energy production from renewable energy. The UK Renewable Energy Strategy encourages an increasing use of biomass for heat, power and transport, *i.a.* by "increasing supply through bringing more woods back into management" [2]. Polish Government plans to increase power production from renewable energy sources up to 19.13 % by 2020. The National Renewable Energy Action Plan for Poland also promotes energy production from biomass and forestry is named as one of the three main sources for biomass supply [1].

Government support for biomass utilisation promotes renewable energy technologies development and optimisation. One of the most important biomass conversion techniques is its gasification to produce syngas. Wood biomass is considered a particularly suitable gasification feedstock, due to is high calorific value [3]. This technology, although rapidly developing in recent years, still struggles with some important operational challenges.

Overcoming issues related to tar release during fuel gasification is one of the main challenges in a further development and commercialisation of this technique. Besides the operational problems, resulted from installation clogging with condensing and polymerising hydrocarbons, another negative aspect of tar formation is the deteriorated efficiency of a solid-to-gas conversion, due to a loss of chemical energy contained in created tars [3]. Therefore, instead of a physical removal of tar contaminants, an interesting alternative lies in their catalytic conversion into calorific gaseous compounds. However, a catalytic process entails additional costs and operational problems and thus using biochar catalyst, as a cheap and accessible gasification by-product, became a quickly developing area of research [4]. As the heterogeneity of both, tar compounds mixture and char structure, is obstructing the basic processes that underlie tar reforming, a research interest is often focused on fundamental studies carried out under simplified conditions. To this end, a single, model tar compound is commonly used. Char preparation and tar reforming processes are also carried out in a controlled environment with selected and monitored process parameters (temperature, gas composition, residence time, tar concentration, *etc.*) [5,6].

Therefore, fundamental research into tar conversion is important for a further development of the gasification technology.

1.2. Aims

Within a general scope of tar conversion over biomass char studies, two issues were selected as the main interest of this work:

1) Comparison of different wood species as a biochar feedstock,
2) Investigation of toluene (as tar representative) catalytic conversion over biomass char.

The research comprised laboratory scale experiments on toluene decomposition over char prepared from woody feedstock. The first objective was addressed by selecting three differentiated tree species, each used separately for char preparation. Properties and catalytic performance of the three obtained chars were thereafter compared and related to the feedstock characteristic features. The observed differences were further investigated by an application of a pre-treatment to one of the feedstocks, *i.e.* pinewood extraction prior to char preparation. The results of extraction on char properties and performance were then assessed. In order to investigate the second objective, the results of the abovementioned toluene catalytic decomposition experiment with three wood biochars were assessed to determine the most plausible conversion pathways. To this end, liquid and gaseous products sampling and analysis was carried out during the tests. Moreover, to distinguish the pyrolytic decomposition and steam reforming of toluene, two different atmospheres were used within the scope of the experiment. After the evaluation of the results obtained from the main experiment, additional tests were performed with one of the chars, to further investigate toluene conversion. In those tests, one of the main experiment parameters was changed, to determine its influence on the conversion process. For this purpose, either the feeding principle, the feeding compound, atmosphere in the reactor or char parameters were differentiated.

CHAPTER 2

LITERATURE REVIEW

2.1. Introduction

As an introduction to the results and discussion on the experiment carried out in scope of this work, a brief literature review was provided it this section. It comprises basic overview on catalysts for tar reforming, their preparation, properties and examination. A woody feedstock characterisation was also provided. Basic information on recognised toluene conversion mechanisms leading to its decomposition and coke formation were summarised. A current state-of-the-art of tar model compound heterogeneous conversion was also given as it provided a background for this work.

2.2. Tar release from solid fuels gasification

Gasification is an important method of fuel-to-fuel conversion. It allows, among others, for a solid feedstock transformation into a high quality, calorific gas. It is therefore most beneficial for low-rank fuels that can be converted at relatively low temperatures, thus utilising "low-grade thermal energy" and turning it into a "high grade chemical energy" of syngas in a so called "chemical heat pumping" process [7].

Gasification of carbonaceous materials inevitably entails tar formation. The term "tar" was determined by The International Energy Agency as "hydrocarbons with molecular weight higher than benzene" [3,8]. Tar is considered a highly undesirable product of thermochemical fuel conversion, as it can cause numerous downsides to the feasibility and efficiency of the gasification technology [3,5]. Condensable tar compounds can cause clogging of the installation downward the gasification chamber. Remaining species contaminate producer gas and prevent its direct utilisation in power generating units, *e.g*. gas turbines and gas engines [8]. Hydrocarbons are also known to polymerise into a more complex structures at elevated temperatures, thus contaminating gasification infrastructure [3]. Another disadvantage of tar formation is the occurring loss of chemical energy that decreases the efficiency of fuel conversion into syngas.

Tar formation has to be therefore address during a gasification process design. Physical methods for tar removal include filters and scrubbers, yet they require cooling down the producer gas and can create substantial amounts of wastewater. Thermal cracking, on the other hand, has to be performed at temperatures over 1000 °C, thus requiring additional energy [9]. Catalytic tar removal is considered an interesting alternative, allowing for syngas enrichment in conversion products while maintaining reasonable temperatures of 400 – 900 °C [9]. Therefore, a substantial amount of research has been devoted to various aspects of tar catalytic reforming methods [5,6,9,10].

2.3. Catalysts for tar reforming

There is a wide range of materials that exhibit catalytic effect towards hydrocarbon thermochemical conversion. They have been categorised by Anis and Zainal [4] into six groups: nickel based catalysts, non-nickel metal catalysts, alkali metal catalysts, basic catalysts, acid catalysts and activated carbon catalysts. The first two groups comprise synthesised composites where an active metal species has been dispersed on a porous, ceramic base. Their preparation process makes them relatively expensive [10]. Alkali metal catalysts are often added directly to the biomass, *e.g.* as salts, making them difficult to recover [11]. Natural ores, like dolomite or olivine are catalysts of a basic nature. They are considered cheap and moderately effective [11,12]. Typical acidic catalysts are zeolites, synthetic aluminosilicates with a well-defined pore structure and very high surface area [12]. They are prone to deactivation via coking and difficult to regenerate [4]. Therefore, it can be concluded, that the main challenges for tar conversion catalysts are cost-effectiveness and resistance to coke deposition. In this regard, activated carbons, and gasification chars in particular, are considered a promising option. Biochar is created *in-situ* during the gasification process, becoming accessible and inexpensive material [6,12,13]. Upon the interactions with gasifying agents and released volatiles, it develops a well-defined porosity and high surface area with chemical functional groups [6,14]. It usually possessed dispersed alkali and alkaline earth metal (AAEM) species due to feedstock's ash content [5]. As a carbonaceous material, deactivated char can be easily disposed by combustion or recalculation back to a gasifier [4]. Since it is reactive towards oxidising agents, it is constantly consumed during tar reforming process [13], yet this phenomenon contributes to a prolonging of char activity [15].

Carbonaceous materials, activated carbons and biochars among them, are characterised by several features that are responsible for their catalytic properties towards hydrocarbons conversion. Heterogeneous reaction between a tar molecule and carbon matrix requires a presence of so called "active sites" on the carbon surface [5,13]. Various biochar structures are considered to be catalytically active, as tar interaction could involve numerous phenomenon, including van der Waals forces as well as chemical bonds of various strength [5]. The most recognisable active sites are commonly determined as alkali and alkaline earth metals (AAEM), acidic and basic functional groups on the char surface as well as "unsaturated carbons" [5,14,16].

Alkali and alkaline earth metals presence in solid carbons greatly improves their gasification and combustion rates [17,18]. The beneficial influence of AAEM species content in char

catalyst during tar reforming was also reported [19,20]. As those experiments were carried out in a presence of steam, a concurrent char gasification along with tar reforming was occurring. As inorganics catalyse the gasification process, and char gasification, on the on the hand, affects tar reforming efficiency, the AAEM involvement in tar conversion might be an indirect result of catalyst gasification/activation, enhancement. Hosokai et al. [15] suggested that a role of alkaline inorganics is correlated mainly with char steam reforming and not heterogeneous hydrocarbon conversion. A direct effect of AAEM species content on hydrocarbons conversion has been debatable [14,16,21]. It was studied extensively in terms of methane decomposition. Dufour et al. [16] reported no significant influence of alkali metals on methane decomposition over wood char in an atmosphere of a pyrolysis gas. Also, no effect of ash in a coal char during methane decomposition in an inert atmosphere was registered by Bai et al. [22]. On the other hand, Klinghoffer et al. [14] reported a decrease in methane pyrolytic conversion upon the inorganics removal from wood char catalyst. Moreover, they stressed out the importance of metal species dispersion on the catalyst surface. This might be one of the reasons for the discrepancies in the AAEM species effect on methane decomposition. Furthermore, the acid washing applied for inorganics removal could affect the concentration of no only AAEM species but also *e.g.* transition metals such as Fe, that are considered catalytically active towards methane reforming [22]. Ash removing treatment would therefore result in overlapping effects of more than one type of inorganic species, contributing to the ambiguities of the AAEM species catalytic effect. Gasification tar is comprised of a vast variety of hydrocarbons with different functional groups and thus diversified reactivities. Therefore, a role of AAEM species on the tar molecules conversion might differ depending on their structure, *e.g.* the presence or lack of O-heteroatoms, and thus it would comprise and interesting scope for a more in-depth studies.

Another active sites on activated carbon surface are acidic and basic structures, commonly assign to oxygen-containing functional groups [6,14,23], as presented in Figure 1. Carbon acidic sites have been studied extensively and they are usually attributed to phenols, carboxylic acids, anhydrites, lactones and lactols [24]. They can be created during chemical activation of carbon as well as upon oxidation in elevated temperatures [14,23]. Tar molecules are able to bond chemically with those functionalities via hydrogen bonds. Moreover, a multilayer adsorption of some molecules, *e.g.* phenol, were reported as the electron-donating ability of hydroxyl group increases nucleophilic nature of aromatic ring, enhancing the π-π ring stacking of adsorbed molecules. Interactions with functional surface groups are more effective than physical adsorption though van der Waals forces, therefore

contributing significantly to adsorption capacity of activated carbons [25]. Acidic functional groups, however, decompose at relatively low temperatures. Carboxylic acids start to desorb from carbon surface below 400 ℃. Anhydrites and lactones release was reported at various temperatures between 350 and 900 ℃. Phenolic groups decompose at 600 – 800 ℃ [14,23,26]. Their involvement in a high temperature tar conversion is therefore considered to be of importance only at the initial stages of the conversion process [6,14]. However, as the reforming process is often carried out in a presence of an oxidising agent, acidic functionalities might be continuously re-created and thus take part in the hydrocarbon heterogeneous conversion. The O-containing active sites of a basic character include C=O based groups like carbonyls and quinones, as well as some pyrone- and chromene-like structures [23,26,27]. They are more thermally stable, with carbonyls and quinones desorbing above 700 ℃ and pyrones and chromenes decomposing above 900 ℃ [23,28,29]. Thus, they are expected to play an important role during tar conversion processes, although less studies were devoted to them so far, and their exact nature and contribution remains more ambiguous [14].

As a carbonaceous materials structure is based on graphene, it is considered non-reactive on its own, although its basal planes, rich in π-electron systems, are considered to be of a slightly basic nature. Most carbons are however, microcrystallines comprised of small graphene layers, and thus the edges and defects in the layers are often possessing unpaired electrons [27,30]. These "unsaturated" carbons in the matrix are highly active. They are often considered to be precursors for acidic and basic functionalities formation sites [14,27]. Thermal destruction of oxygenates returns those carbons to their primary, unsaturated state. Catalytic properties have been also assigned to the unsaturated carbons themselves [27,31]. Therefore, carbonaceous materials with a high content of unsaturated carbons can be active despite high temperature treatment [16,31].

Due to their ambiguous nature, a presence of unsaturated carbons would be difficult to quantify [16]. However, the physical destruction of graphene layers could result in an increase of the amount of edge and defect-related carbons. Therefore, it could be expected, that a severe thermochemical treatment of carbonaceous material, *e.g.* an activation process, would enhance the amount of unsaturated carbons, therefore increasing material's activity. Those treatments are also known to develop carbon structure, increasing its surface area and porosity [32,33]. It could be thus expected, that the surface area, which is easier to quantify, could serve as an estimation of the potential of unsaturated carbons presence, thus providing and assessment of the activity of a material.

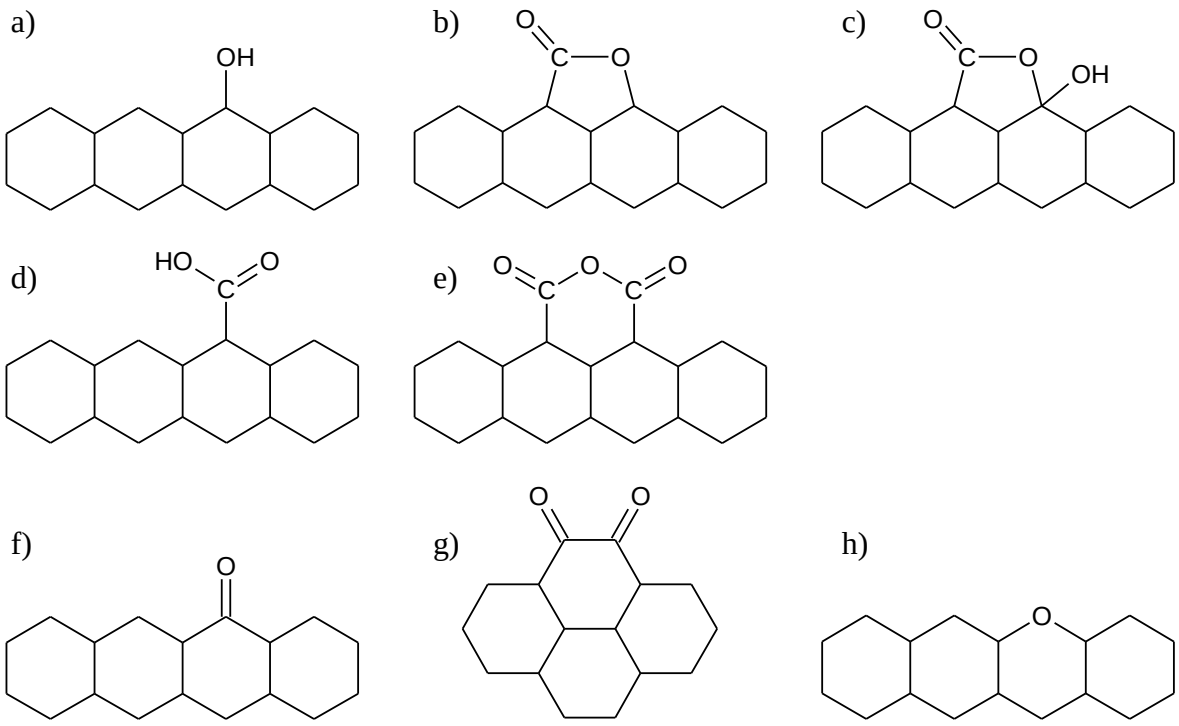

Figure 1. Carbon surface oxygen functional groups of acidic character: a) phenolic group b) lactone c) lactol d) carboxyl group e) carboxylic anhydrites as well as basic f) carbonyl group g) quinone h) O-heteroatoms in pyrone- and chromene-like structures (Adapted from [24]*)*

Indeed, extensive research has been devoted to surface area and porosity studies and their contribution to the carbon activity was well established [5,6,15,34,35]. Activated biochars surface area varies significantly, depending on the preparation process parameters. Usually, areas between 400 – 1000 m^2/g are reported for biochars, while commercial activated carbons have surface areas often exceeding 1000 m^2/g [34,36–39]. The microporosity of carbonaceous catalysts varies significantly. A share of micropores within the total pore volume is an important parameter in terms of catalytic performance of a material. Micropores were reported as particularly important during light hydrocarbons (benzene, toluene) conversion [40]. On the other hand, they are more easily deactivated due to "pore mouth blocking", therefore their importance is considered to be significant only at the initial stages of hydrocarbons conversion process [34,41]. More mesoporous structures are considered more stable with process duration due to a more "uniform poisoning" [34].

2.4. Activated char preparation

Char preparation from lignocellulosic materials involves carbonisation of the feedstock by a high temperature treatment. Pores of carbonaceous structure created during the process are often blocked by tar released at elevated temperatures. Therefore, an untreated pyrolytic char has usually poor absorbing properties. An activation process that removes pore blockages is necessary, to provide a catalyst with a well-developed surface area [32].

There are two main methods of carbon activation. Physical (or thermal) activation involves heating up the material in a presence of an oxidising agent, usually CO_2, steam or O_2. It is therefore similar in nature to the gasification process, thus char as a gasification by-product has often good catalytic properties without any additional pre-treatment [6]. Chemical activation involves impregnation of the material with a dehydrating agent, like KOH or H_3PO_4, and a consecutive heat treatment in an inert atmosphere [32].

Activated biochar structure can be therefore influenced by adjustment of both carbonisation and activation parameters. Properties of the char prepared in pyrolytic conditions strongly depend on temperature, heating rate and residence times. An increase of carbonisation temperature leads to char with significantly lower functional groups amount and decreased dispersion of inorganics [14,34,42]. Burhenne at al. [35,43] reported that spruce char surface area was proximatly 30 % higher when prepared at 800 ℃ than 500 ℃ when high heating rate was applied. On the other hand, upon the slower heating (4 instead of 30 K/min) and thus longer residence time at high temperatures the char after 500 ℃ treatment had a more developed structure. They concluded, that the prolonged exposition to high temperature resulted in an annealing of a porous structure [44]. This suggests, that various pyrolysis parameters had strong and often opposite influences on char structure. Thus, an overall outcome of the overlapping effects of the pyrolysis parameters is difficult to predict.

A following char activation can further influence its properties. Here, again, final product parameters are a common result of temperature, residence time or oxidising agent. It was established, that a type of an oxidising agent used during thermal activation influences a structure of the developing pores. CO_2 activation tends to yield more microporous materials, while steam creates mesopores [32,33]. However, it was reported by Rodríguez-Reinoso et al. [45], that dilution of steam flow during activation yielded chars with a pore distribution more similar to that after CO_2 treatment. An increase of activation temperature was reported to increase surface area of the chars [38,39]. The prolonged activation time, thus extended char burn-off, also increased an overall surface area, even for a significant char mass loss, *i.e.* burn-off > 60% [39,46]. However, changes to pore size distribution upon the activation

time and char burn-off vary, depending on the applied oxidiser. Steam was reported to widen the micropores, increasing mesoporosity of the char with activation time [39]. Keown et al. [47] reported, that steam interactions with char result in transformation of smaller aromatic ring structures of 3 – 5 rings into a larger systems with ≥6 rings.

It is therefore important, during comparison of other parameters influence, *e.g.* feedstock type, on char parameters, to maintain identical synthesis conditions, to avoid the effects of different preparation parameters.

2.5. Wood as a biochar feedstock

The main advantage of thermochemical conversion of biomass, instead of fossil fuels, is that it releases CO_2 that was relatively recently captured from the atmosphere by growing plants and thus it causes less disturbance in a CO_2 balance. It is also more evenly, worldwide distributed, therefore it can be easily used locally in a smaller scale plants fitting well within the scope of decentralized energy system idea [3].

Wood, and lignocellulosic plants in general, are considered primary biomass falling into forest biomass or energy crop (*e.g.* willow) group. However, as it can also comprise forest and industrial wastes, like sawdust, demolition wood *etc*., it can be considered a secondary biomass, that is more beneficial in terms of land-use efficiency and environmental performance [3,48]. Due to its high calorific value, wood is often utilised as a gasification fuel, thus making a wood-derived gasification char a common biochar that can be used as a catalyst directly, without any pre-treatment [3,37]. Hence, numerous studies has been devoted to a catalytic performance of wood biochars [13,14,16,34,35,37,49,50].

All woody materials are composed of three main polymers – cellulose, hemicellulose and lignin. Cellulose is a linear homopolymer of β-D-glucopyranose units connected by glycosidic bonds [51]. It thermally decomposes at around 300 °C, releasing levoglucosan, hydroxyacetaldehyde, and furfurals, leaving a small char yield <15 wt.% [52,53]. Its pyrolysis rate it the highest and decomposition temperature range the most narrow, amongst the three main wood constituents [54,55]. The other types of polysaccharides are commonly described as hemicellulose. Its chains can be linear as well as cross-linked and they comprise various pentose and hexose molecules [51]. Hemicellulose starts to decompose below 200 °C, over a slightly wider range of temperatures and with a lower intensity than cellulose, yielding approximately 30 wt.% of char [53]. The most influential, regarding wood pyrolysis process, is lignin [56]. It is a highly cross-linked polymer comprised of aromatic phenylpropane units of three types: *p*-hydroxyphenylpropane, guaiacylpropane and

syringylpropane [51]. The difference between those structures lies in the number of methoxy groups substituted to the aromatic ring, as presented in Figure 2. Decomposition of lignin, due to its highly heterogeneous nature, covers a vast range of temperatures, starting as low as 200 ℃ and continuing up to 700 ℃. It leaves the highest solid residue among the wood components > 40 wt.% [53,56].

Besides the main polymeric constituents, wood can comprise a significant amount of lighter organic compounds, referred to as "extractives", as well as some inorganic species. Lipophilic extractives are typically terpenoids and steroids, fats (fatty acid glycerol esters), waxes (fatty acid esters of fatty alcohols, terpene alcohols, and sterols) while phenolic extractives include stilbenes, lignans, tannins, and flavonoids. They decompose or vaporise at low temperatures and can be removed from wood by extraction with various solvents. Basic inorganics in wood are alkali and alkaline earth metals (AAEM), mainly calcium, potassium, and magnesium. They are present in a form of carbonates, silicates, phosphates, and oxalates or can be bound to the acid groups in wood [51]. Inorganics in biomass are usually well dispersed [7] and can be removed from wood or wood-derived carbonates by washing with strong acids, *e.g.* 2 M HCl [57].

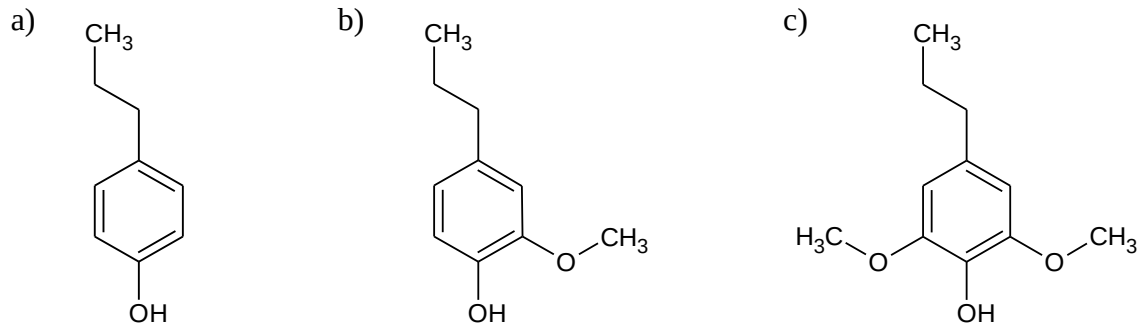

Figure 2. Main lignin units structures a) p-hydroxyphenylpropane, b) guaiacylpropane and c) syringylpropane (Adapted from [51]*)*

Although all wood is a lignocellulosic material with common structural features based on the same components, there are some characteristic differences between trees species. The main distinction can be observed between softwood and hardwoods. Coniferous trees are classified as softwoods, while deciduous trees species are typically hardwoods. Galactoglucomannans are main hemicellulose polymers in softwood, while glucuronoxylan predominates in hardwoods. The most striking difference in main polymeric constituents is however the structure of lignin. In coniferous softwoods, lignin is built almost exclusively with guaiacyl units (Figure 2 b) while hardwood comprise guaiacyl and syringyl structures

(Figure 2 b and c). A non-substituted *p*-hydroxyphenols (Figure 2 a) are typical for grassy biomass and are seldom found in wood lignin. Besides the qualitative differences, coniferous woods have also higher general lignin content (25 – 35 wt.% vs 18 – 25 wt.% in deciduous wood) [3,51]. They are also richer in extractives, present not only in parenchyma cells, but also in resin canals. Pine, as a typical conifer, contains extractives comprised mainly from resin acids (up to 97 wt. %) [58]. Additionally, there are some free fatty acids and fatty acids esters. The most abundant resins are levopimaric and palustric acid. Fatty acids are mainly present as esters, usually stearic and oleic acids esters. They are often present in a form of triglycerides. Additionally, some phytosterols, terpenes and phenolic compounds were also found in pine extractives [58–60]. The extractives content differs significantly even within the same wood species, depending on the plant age, its place of growth and the season of the year. The amount of extracted compounds is also dependant on the type of solvent and extraction process parameters. The general rule is that the increased time and number of extraction cycles increases extractives yield. Additionally, more polar solvents remove more phenolic compounds, and sometimes some inorganics, while less polar solvents are better at lipophilic extractives removal [54,59]. For beech extractions with acetone values between 0.5 and 2.5 wt.% were typically reported [54,61,62], while acetone extractives in pine varied in a wide range of 2.3 – 7.0 wt.% [61,63,64].

2.6. Analytical techniques for catalyst evaluation

As the catalytic performance of a material strongly depends on its physicochemical properties, an extensive material studies have been devoted to the subject. Chemical structures on the activated carbons catalysts involve oxygen-containing functionalities of acidic or basic character as well as inorganic species.

A variety of spectroscopic methods is often applied to study catalyst surface functional groups. Fourier-Transform Infrared Spectroscopy (FTIR) is a commonly used technique allowing for analysis of vibrational-rotational energy of bonds, providing spectra within 4000 – 400 cm^{-1} wavenumbers [65,66]. It could be used for solid, liquid and gaseous samples analysis. Solid samples analysis is often carried out by mixing an analyte with KBr and pressing it into a pellet [35]. Recently, reflectance spectroscopy methods like DRIFT or ATR are gaining popularity, due to an easy and quick nature of this analysis. Attenuated Total Reflectance (ATR) is technique suitable for solids and liquids. Solid sample could be analysed without any pre-treatment. It is pressed to the surface of a crystal with a determined refractive index (*e.g.* germanium, diamond). The IR band travels through the crystal, reflects

from the surface of the sample and is directed to the detector. Simultaneously, due to a total internal reflection phenomenon, an evanescent wave is created that penetrates the sample. Attenuation of the evanescent wave, caused by sample absorption at certain wavenumber, is thereafter detected, and transformed into a spectrum. As only the thin layer of the sample (<1 μm for Ge crystal) is penetrated, this analysis provides an information on the surface structures of the material [51]. The C–O and C=O bonds from the catalyst's surface functional groups could be therefore analysed [28,67]. However, due to an extremely heterogeneous nature of carbonaceous materials, FTIR spectra are usually comprised of a vast variety of overlapping bands, providing only general information on the wavenumber regions with an increased absorption. Another infrared technique, Raman spectroscopy, is also commonly used for char composition assessment, providing *e.g.* an information on the size of polyaromatic structures in carbon matrix [47]. A widely popular method for catalysts analysis is also X-ray photoelectron spectroscopy (XPS), providing information on a sample's elemental composition as well as some functional groups, *e.g.* C=O, C–O content [25].

Acidic sites have been of interest in catalysts applied to chemical industrial processes, thus an abundance of their evaluation methods has been developed. Typical techniques applied for conventional catalyst involve FTIR spectroscopy of adsorbed pyridine and Temperature Programmed Desorption (TPD) of a probe molecule (*e.g.* ammonia). Both methods involve a saturation of catalyst with probe molecule that chemisorbs to its acidic sites. Saturated samples can be further analysed via FTIR, where different absorption bands provide information on Brønsted and Lewis types of acidic sites on a catalyst, to which pyridine was bonded. In TPD analysis, saturated sample is heated with a fixed heating rate and the desorption of a probe molecule is registered. The evolution profile of a released probe molecule provides information on the amount of acidic sites it was bonded to [68]. Another method for acidic sites evaluation was developed by Boehm and it was aimed at carbon blacks studies [24,30]. It involves immersion of the sample in a standard solution of one of three bases of different strength, *i.e.* $NaHCO_3$, Na_2CO_3 or NaOH. As the strength of the base would determine what types of acidic structures it would react with, a measurement of an uptake of each of the solutions provides information about the amount of acidic sites of a certain strength. Titration analysis enables assessment of phenolic, lactone and carboxyl groups' distribution on a carbon's surface. Carbonaceous materials are also often studied via a Temperature Programmed Desorption without a probe molecule. The untreated sample is heated up in a controlled environment and the evolution profiles of CO and CO_2 as functions

of time/temperature are registered. As each type of oxygen functional groups, of either acidic or basic character, is decomposing into one or both of those gases at certain characteristic temperatures, the evolution profiles can provide a quantitative information on basic and acidic sites [14,23,26]. This analysis is often performed in a custom-built apparatus comprising a furnace and a detector, usually mass spectrometer [23,26]. A thermogravimetric measurement coupled with a spectroscopic analysis of the evolved gases, *e.g.* TGA-FTIR technique could be considered a Temperature Programmed Desorption experiment if a pyrolysis at slow heating rate is performed. This method was utilised, *e.g.* by Gao et al. [69] for a pine saw dust analysis.

Carbon catalyst's inorganics analysis usually comprises determination of metals content. For the biomass-derived chars, the most abundant are alkali and alkaline earth metals (AAEM). Prior to their analysis, the acid digestion of chars is performed with concentrated acid, usually HNO_3 and/or HF. Metal concentrations in digested and liquidised char can be thereafter analysed, *e.g.* via Inductively Coupled Plasma (ICP-MS, ICP-AES) or Atomic Absorption Spectroscopy (AAS) technique [20,47].

The most important analysis in catalyst's morphology assessment is a measurement of gas molecules adsorption isotherm, used to determine surface area and pore size and distribution. An analysis is commonly carried out in a dedicated apparatus, where at the amount of selected gaseous species that adsorbs on the surface of the sample is measured as a function of increasing relative pressure in the probe containing the sample. Isothermal condition of the analysis is maintained by immersion of the probe in a Dewar cooled with liquid nitrogen or a cryostat. In carbonaceous materials studies, a N_2 adsorption at 77 K or CO_2 adsorption at 273 K is usually performed. The former is the most universal method, while the latter provides better data on micropores structure [34]. Data from the adsorption analysis could be further used to calculate surface area of the sample (*e.g.* from Brunauer−Emmett−Teller BET or Langmuir model) as well as to determined external surface area (*e.g.* from t-Plot model), thus providing an estimate on micropores area, defined as the difference of those two areas. Some more complicated models could be also applied to assess pore size distribution, *e.g.* Barrett-Joyner-Halenda (BJH) analysis or a density functional theory (DFT) modelling. The adsorption/desorption experiments can reveal an occurrence of a hysteresis, that along with a general shape of an isotherm provide some information on sample's pore size and shape [37]. A visual assessment of catalyst's structure is usually performed via a scanning electron microscopy (SEM). When coupled with *e.g.* energy

dispersive X-ray (EDX) analysis, inorganics content could be also determined with this technique [5,14].

As carbonaceous catalysts used at reforming conditions can undergo oxidation themselves, an evaluation of their gasification/combustion kinetics is also often studied. The most common method is a thermogravimetric analysis (TGA). It involves heating up a sample at a set heating rate in a controlled flow of gases with a determined composition. A mass loss of a sample upon thermal treatment and/or oxidation is continuously registered, thus a kinetic of its pyrolysis or oxidation can be calculated [43].

2.7. Homogeneous conversion of hydrocarbons

Detailed mechanisms of hydrocarbon thermochemical conversion has been studied extensively by experimental methods as well as via modelling. As most of the studies were aimed at fuel combustion related polycyclic aromatic hydrocarbons (PAH) and soot growth, they comprise a homogeneous reaction at high temperatures and often high pressures [70–72]. For those severe conditions and non-catalytic conversions, many numerical calculations has been performed as well [71,73–76]. Undergoing decomposition reactions at those conditions can relate to some extent to the catalytic tar reforming process, therefore some basic information regarding current state of knowledge on this subject was presented below.

At sufficiently severe conditions, above 1000 °C, toluene can decompose into benzyl, phenyl or methylphenyl radical [70,71], presented in Figure 3, and a respective $H^{\bullet}$ or $CH_3^{\bullet}$ radical. Benzyl formation is favoured due to a lower C–H bond dissociation energy in methyl group (92 kcal/mol) than the bonds responsible for phenyl and methylphenyl (104 and 113 kcal/mol, respectively) radical creation [71]. With an increase of reaction temperature, formation of the latter two becomes more significant [77]. Hydrogen abstraction from toluene by $H^{\bullet}$ or $CH_3^{\bullet}$ radical has an order of magnitude lower activation energy than unimolecular decomposition of toluene molecule [76] and it was determined by Zimmerman and York [78], that the introduction of n-heptane enhanced toluene conversion by increasing free radical amount in the reactor. Hydrogen abstraction is usually considered as a chain propagation reaction, while the homolytic dissociation is required to initiate the decomposition [74]. Another possible initiation reaction is a reverse radical disproportionation also called molecular disproportionation where the interaction between two molecules yields two radicals. This mechanism is reported to be enhanced at lower temperatures [72,74].

Benzene formation was reported to undergo mainly via hydrogen attack on toluene molecule with a $CH_3^{\bullet}$ release, followed by benzyl and methane formation [70,76]:

$$C_6H_5CH_3 + H^{\bullet} = C_6H_6 + CH_3^{\bullet} \quad (1)$$

$$C_6H_5CH_3 + CH_3^{\bullet} = C_6H_5CH_2^{\bullet} + CH_4 \quad (2)$$

Methylated aromatics demethylation in gaseous phase has been often reported for experimental studies, *e.g.* by Lea-Langton et al. [79], Leininger et al. [72], Metcalfe et al. [80] or Zimmerman and York [78], when high pressures or reactive atmospheres were applied.

As a main toluene decomposition radical, benzyl is reported to undergo further decomposition to cyclopendadienyl radical and acetylene either directly or through a fulvenallene intermediate, eventually leading to larger aromatic structures formation and light gases release [70,71,75,80]. Three plausible mechanisms of condensed molecules, like soot and coke, are usually proposed: hydrogen abstraction – C_2H_2 addition (HACA) [81], cyclopentadienyl radical recombination (CPDR) and phenyl addition/cyclisation (PAC) [82]. It could be generally expected, that coke formation from toluene results from primary toluene conversion products (benzyl, phenyl radical) and reactive C2– and C3– species (*e.g.* propargyl radical) created during cyclopendadienyl decomposition [70].

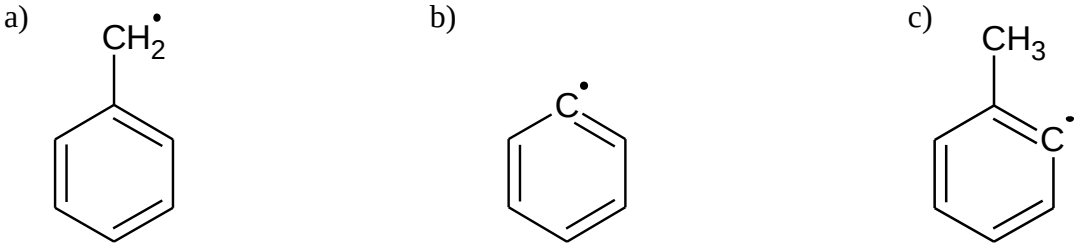

Figure 3. Radicals from toluene thermal decomposition: a) benzyl, b) phenyl and c) methylphenyl radicals

2.8. Heterogeneous conversion of hydrocarbons

Catalytic conversion of aromatic hydrocarbons, as tar representatives, has been extensively studied. A variety of compounds, including non-substituted species like benzene, naphthalene or phenanthrene, as well as alkyl-substituted species like toluene and oxygen containing aromatics, like phenol were examined at different temperatures and various atmospheres including inert N_2, as well as reactive gases like H_2O, CO_2, H_2 or producer gases. Moreover, a wide range of materials with catalytic potential were tested [13,15,20,34–

37,49,50,83]. In catalytic tar conversion experiments relatively simple molecules are used as model compounds since heavier and more substituted compounds removal undergoes more efficiently [15,36], therefore it is of a less importance in terms of process optimisation. Some more complicated structures, *e.g.* anisole, eugenol or 1-methylnaphthalene, were on the other hand commonly used in studies devoted to tar release and transformation into coke, as they better represent the structure of the majority of real tar compounds [72,79,84–86]. The most common features of model tar compound conversion over a catalyst bed were summarised in Table 1.

A possibility of biochar utilisation for tar removal was studied by El-Rub et al. [13], where a performance of biomass chars was compared with conventional materials like silica sand, olivine, dolomite or nickel catalyst. Naphthalene and phenol conversion in steam and CO_2 revealed a good biochar performance. Its prolonged longevity, resulted from the continuous regeneration of the catalyst, therefore confirming that the biochar is a promising alternative to a conventional catalysts.

Toluene catalytic conversion was studied mainly in reactive atmospheres. Bhandari et al. [87] performed toluene removal over switchgrass biochar directly form a downdraft gasifier and after chemical activation. The experiments carried out at 700 and 800 ℃ in a presence of nitrogen or a synthetic producer gas revealed an increase in toluene conversion with temperature and upon char activation. They also reported that producer gas (H_2, CH_4, CO, CO_2, N_2) decreased conversion, compared to the experiments in pure N_2, plausibly due to gas adsorption on a catalyst. Another observation was a surface area and porosity decrease with coke deposition. Mani at al. [83] calculated kinetic parameters of toluene removal over pine bark char at 600 – 900 ℃ in a presence of steam. They also reported a maintained char activity and process efficiency resulted from a continuous steam regeneration. The benzene formation was observed during the study with a selectivity of ~16 % after steady conditions were reached. Pyrolytic removal of toluene/naphthalene mixture was also examined by Ravenni et al. [6]. Performance of a residual char from spruce wood gasification was compared with commercial activated carbons within a 600 – 800 ℃. It was concluded, that char recovered directly from the gasifier, without any further treatment, was efficient and long-lasting catalyst for tar removal.

Toluene and naphthalene removal was also extensively studied by Fuentes-Cano et al. [36]. A temperature range of 750–950 ℃ and steam concentrations of 0 – 25 vol.% with a constant H_2 concentration of 8 vol.% were tested. Fixed toluene and naphthalene concentration of 8 and 12 g/Nm^3, respectively, were applied and the residence time in a catalyst bed was set

to 0.3 s. Performance of commercial coconut and coal char as well as laboratory prepared sewage sludge char were accessed. Kinetics of tar compound conversion was calculated, and an activity factor was introduced by the authors, to account for a catalyst deactivation with time. Again, a beneficial role of steam and temperature was confirmed in the experiments along with a coke deposition and char/coke gasification occurrence.

Hosokai et al. [15] studied mechanisms of non-substituted aromatics conversion over commercial activated charcoal. Their findings revealed that aromatics heterogeneous decomposition undergoes mainly via coke creation, regardless of the presence of steam or H_2. They also reported that the prolonging activity of the catalyst depends on the relation between the rate of coke formation and the rate of char/coke gasification. Micropores were attributed by the authors as a contributing factor to the coke formation. They also established that the lighter aromatics were more refractory, as the increase of the examined compound removal was in an order of: benzene < naphthalene < phenanthrene and pyrene.

Table 1. Typical settings of experiments into catalytic conversion of model tar compounds

Tar compounds:	Benzene, toluene, phenol, naphthalene, phenanthrene, pyrene, ethylbenzene	[15,34,36,37]
Atmosphere:	N_2, N_2/H_2O, $N_2/H_2O/H_2$, N_2/CO_2, producer gas	[15,34,87]
Catalyst:	Silica sand, olivine, dolomite, nickel catalyst, coal char, wood biochar, sewage sludge char, coconut/nutshell char, grass/straw char	[13,35,36]
Catalyst origin:	Natural ores, commercial catalysts, laboratory-prepared catalysts, gasification-derived chars	[13,34,37]
Catalyst particles size range:	212 – 420 μm up to 1300 – 2400 μm	[15,83]
Temperature:	600 – 1000 °C	[34,36,83]

Burhenne et al. [35] studied pyrolytic benzene decomposition that was continued by Nestler et al. [34] with a naphthalene conversion. They studied spruce-derived CO_2-activated biochars performed in laboratory conditions. A thorough char properties examination, involving FTIR analysis as well as N_2 and CO_2 adsorption isotherms measurement, revealed the importance of surface area and chemistry in the catalytic affinities of the chars.

Micropores were revealed to play an important role in an initial tar decomposition, but were also found responsible for a quicker catalyst deactivation.

An extensive research has been devoted to model tar compounds catalytic conversion. The differentiated parameters of the experiments performed so far resulted in some common conclusions regarding the process. It was established, that in a presence of a catalytically active bed at elevated temperatures, aromatic hydrocarbons undergo heterogeneous conversion, yielding coke as a main decomposition product. Tar removal via coking proved to be an efficient process, although its unavoidable repercussion is the catalyst-deactivating effect of coke. The presence of oxidising agent during tar conversion was proved to prolong catalyst activity. It was also suggested by Hosokai et al. [15], that a dominant tar conversion pathway remain a heterogeneous decomposition, regardless of if it is carried out in an inert atmosphere or in a presence of steam. It was also commonly established, that the main properties affecting catalytic performance of a material are its surface area, microporosity and acidic sites distribution [34,87]. In some studies, a presence of additional conversion by-products was detected, *e.g.* benzene creation from toluene reported by Mani et al. [83].

2.9. Research objectives

This work was aimed at extending existing knowledge on tar conversion over biochars. Since the overall data on biomass-derived chars comprises experiments carried in varying conditions, an assessment of an effect of feedstock on created char catalytic performance is impossible. Therefore, in this project, a selection of wood species was used to create activated chars prepared according to the one, common procedure, carried out in the same reactor for all examined materials, allowing for feedstock comparison. Prepared chars' performance was accessed at both inert and oxidising atmosphere to allow for a broader overview of wood char potential towards aromatic hydrocarbons removal. Moreover, repeating the same experiment for three wood chars provided an additional validation of some phenomena observed during toluene conversion.

Another focus of the work was to follow all liquid by-products formation from toluene catalytic pyrolysis and steam reforming. In-depth studies of aromatics thermochemical conversion products were usually conducted in studies devoted to tar release and polymerisation. Thus they were performed as non-catalytic processes and they involved heavier or more substituted compounds, like anisole or eugenol [84–86]. Focusing not only on the efficiency of the main compound removal but also on the formation of other species

allowed for some speculations regarding plausible, additional conversion pathways occurring along with the main one, leading to solid coke formation.

As the main differences between the examined chars occurred between coniferous and deciduous trees used as a feedstock, a further study into the char from a conifer (pine) was conducted. One of the most characteristic distinctions of conifer wood is a high content of extractives, due to an abundance of resin. Hence, the attempt to determine if the removal of extractives from pinewood, prior to biochar preparation, would diminish the impaired performance of this catalyst was made.

Besides the main experiment, designed to assess the performance of three wood chars as catalysts for toluene pyrolysis and steam reforming, a set of additional experiments with one of the chars was performed. *E.g.,* a possibility of some chain reactions initiation by the char bed was examined by changing the toluene-feeding principle. Another of the issues addressed in this second part of the work was to examine the influence of a presence of methyl groups on an aromatic ring in terms of the effectiveness of its heterogeneous conversion efficiency and pathways. To this end, benzene or *p*-xylene were used instead of toluene as a compound fed to the reactor. Otherwise same conditions as during the main toluene experiments were maintained to ensure the separation of the effect of the used compound from the interference of changing setups. A benefit of using the same test rig providing comparable data was also used to access toluene interaction with oxidiser different from steam. A test, where oxygen was supplied instead of steam was carried out to provide an insight into a nature of toluene – char – oxidiser interactions, depending on the strength of an oxidising agent. Finally, an assessment of an influence of AAEM species on toluene conversion efficiency was carried out, as their contribution to the carbonaceous material oxidation reactivity is well acknowledged, yet their role in hydrocarbons-solid carbon interactions is debatable [14,16,20].

CHAPTER 3

EXPERIMENTAL SECTION

3.1. Introduction

The general scope of this work was to investigate a process of tar conversion over biomass char. Due to a high complexity of heterogeneous catalytic reactions between tar compounds and a bed of catalyst, only selected aspects of an overall process were analysed.

Tar reforming is aimed at gasification producer gas upgrading. In commercial installations, it involves a variety of aromatic hydrocarbons reacting on a surface of an applied catalyst. Moreover, a reactive syngas introduces potential oxidising radicals that can plausibly interact with converting aromatics, deposited coke as well as carbonaceous matrix of a catalyst. Additionally, constant fluctuations of process parameters (temperature and syngas composition variations, catalyst heterogeneity, changes in tar composition, *etc.*) can obscure mechanisms of hydrocarbons catalytic conversion. Therefore, a fundamental research on tar reforming often involves laboratory scale experiments carried out under simplified conditions, *e.g.* a model tar compound is commonly used to represent real gasification tars.

In this work, toluene was selected as a main tar representative. Catalysts were prepared from selected wood species in a controlled environment in a laboratory reactor. This approach allowed for a comparison of wood species as biochar feedstocks. It also provided an insight into a light, methyl substituted aromatic hydrocarbons conversion pathways. Additionally, some modifications of the main conversion experiment were introduced in the second part of this research to further investigate biochars catalytic performance and hydrocarbons conversion principle.

Information on all materials and equipment used for this work was provided in this chapter. Moreover, all experimental procedures and analytical methods were described. Performed tests and their parameters were also listed, and methodology of calculations and experimental data evaluation was summarised.

3.2. Materials

For the purpose of this research, various biochars were examined. They were prepared in the Facilities of Institute of Thermal Technology from three different wood feedstocks. Moreover, they were further compared with a commercial, activated carbon. Information on raw biomass, its pre-treatment and char preparation procedure was summarised below.

3.2.1. Feedstock

Wood is a common gasification feedstock, thus wood-derived biochars are an abundant by-product, and can be further utilised, *e.g.* as a soil amendment. They can also be used directly

or after activation, as a filtration material, catalyst support or a catalyst itself. Therefore, wood was selected as a feedstock for biochar synthesis. To provide a better scope of the wood-derived char properties, three diversified tree species were examined. To represent coniferous softwood, pine (*Pinus sylvestris*) from the south of Poland (Silesia) was obtained. Moreover, two deciduous trees of different hardness were selected, namely beech (*Fagus sylvatica*) as a typical hardwood and alder (*Alnus glutinosa*) as a relatively soft hardwood. Feedstock selection was summarised in Table 2.

Proximate and elemental composition analysis of selected wood materials was outsourced to Zakłady Pomiarowo - Badawcze Energetyki „ENERGOPOMIAR" Sp. z o.o. and it was carried out according to PN-EN ISO 18122:2016-01 and PN-EN ISO 16948:2015-07 standards, respectively. A chemical composition was analysed at the Poznań University of Life Sciences according to PN-92/P-50092 standard.

Table 2. Wood feedstock selected for biochar production

Species	Pine (*Pinus sylvestris*)	Alder (*Alnus glutinosa*)	Beech (*Fagus sylvatica*)
Type	Coniferous, *Gymnosperms*	Deciduous, *Angiosperms*	Deciduous, *Angiosperms*
Hardness	Softwood (2 420 N)[a]	"Soft" hardwood (2 890 N)[a]	Hardwood (6 460 N)[a]

[a)] Janka Hardness Scale, based on [88]

During preliminary studies, a commercial, coal-derived activated carbon (BG 09 from CBF Vendor AB, Sweden) was used. It had particles in a range of 400 – 850 μm (as provided by the manufacturer), 14.4 wt.% (on a dry basis) ash content and a following elemental composition (wt.% on a dry basis): C=81.45±2.61, H=0.43±0.03, N=0.53±0.03, S=0.66±0.02 and O=2.53 (by diff.). Preliminary studies involved tests of toluene pyrolytic conversion over activated carbon bed. Conditions of preliminary runs were relatively similar to the ones applied during the main experiment, therefore a comparison between biochar and commercial activated carbon was included in this work.

3.2.2. Char preparation process

Each of the selected wood species was used for a separate char preparation. During a real gasification process, properties of a created char are influenced by numerous, difficult to control variables, like syngas composition, temperature gradients, volatiles-char interactions, *etc*. Therefore, in this work, chars were synthesised in a batch process in a laboratory reactor under controlled conditions to provide a more uniform, homogeneous material. Limiting fluctuations of parameters of a preparation process enabled a comparison between chars' properties in relation to their feedstock.

Each wood material, deprived of bark and knots, was dried at 60 °C for 48 h to remove most of the moisture prior to milling with a LMN-100 Testchem cutting mill and sieving. A 250 – 1000 μm fraction was separated for further use. Due to its hygroscopic nature, feedstock was further dried at 105 °C for 2 h directly before char preparation.

Char preparation procedure was comprised of two consecutive steps – pyrolysis and steam activation. A batch of approximately 20 g of wood was inserted into a vertical quartz tube reactor with i.d. of 27 mm and a heating zone of 300 mm and purged with 0.45 SLPM N_2 flow. The removal of wood volatile compounds, *i.e.* the first step of the process, was achieved by heating the feedstock up to 800 °C with an average rate of 47 K/min, followed by a 60 min isotherm. Immediately after pyrolysis, the second step of the process was initiated by steam introduction into the reactor. The char was held at 800 °C for 80 min in a flow of 15.5/84.5 vol.% H_2O/N_2 mixture and the same superficial velocity as during the pyrolysis step was maintained. The activated char was cooled down in a N_2 stream and stored in a desiccator. Char preparation conditions (*e.g.* temperature, steam concentration) were selected based on the parameters reported for similar studies [15,36].

An examination of char properties prior to its activation was also required for some of the samples. Therefore, char synthesis where a process was terminated after the first, pyrolytic step was also performed. Thus obtained, non-activated char was then cooled down to ambient in N_2 flow and stored in a desiccator for a further analysis.

3.2.3. Pine wood extraction

A main difference between coniferous and deciduous trees, beside their lignin content and structure, is that conifers are usually rich in extractives, mainly resin acids. Therefore, to further investigate the differences between biochars from pine and the ones from alder and beech, an extraction of a raw pinewood was carried out as a pre-treatment.

Extracted pine was prepared from a dried and milled wood in a FOSS Soxtec Avanti 2055 apparatus. Each extraction run involved 60 min of boiling and 90 min of rinsing of 3 grams of a sample with 70 mL of acetone. Gravimetrically determined extractives content for 42 repetitions was 8.5 ±0.3 wt.% on a dry basis. A solvent was chosen based on the similar studies, where acetone and ethanol were the most common compounds used for a thorough lipophilic species removal, with a partial extraction of phenolic compounds [59,89,90]. Acetone extraction was therefore considered more suitable to target resins extraction than *e.g.* hot water washing, which removes mainly polar compounds and metal ions [91]. An efficient removal of extractives achieved with this procedure could be confirmed by a comparison of extractives yield from the applied pre-treatment with an extractives content determined during pine chemical composition analysis by a standard method, *i.e.* 7.14 wt.%. Extracted pinewood was then used to prepare extracted-pine derived biochar, following the procedure described in section 3.2.2.

3.3. Tar conversion experiments

The main scope of this research comprised experiments on model tar conversion over wood-derived biochars prepared according to a procedure described in section 3.2.2. For the main experiment, toluene was chosen as a tar-representing compound. Real gasification tar is comprised mainly of heavier, polyaromatic hydrocarbons (PAHs). However, they are prone to condense after leaving a high temperature reaction zone and, although they tend to cause technical issues related to installation clogging, they do not contribute significantly to a syngas contamination [3]. It was generally established, that refractoriness of a tar compound increases with decreasing amount of fused rings and substituents in its molecule [36,92]. Therefore, in terms of producer gas upgrading by a catalytic reforming, efficiency of light compounds removal is of the biggest interest. Hence, a single ring compound was selected for these studies. Although benzene molecule is considered the most refractory aromatic hydrocarbon, a compound with one, simple functional group was selected to provide more conversion pathways possibilities. The substituents were however limited to one alkyl group, so that a GC-FID analysis could facilitate an identification of all the conversion by-products. For the same reason, no molecules with heteroatoms (*e.g.* O) were examined in this study. Toluene has also been commonly used as a model tar in catalytic reforming experiments [36,37,83,87], thus it was considered a good tar representative for the purpose of this work. The main experiment involved toluene conversion tests for three biochars prepared from

alder, beech or pine carried out in two different modes – pyrolysis (PYR) and steam reforming (SR).

Results of the main experiment led to a further investigation of catalysts performance as well as tar conversion principles. These additional experiments were comprised of modified test runs where one, selected parameter of the process was changed. All experiments were carried out in the main test rig, described in this section. Details of the experiment procedure, reaction products analysis methodology and information on reagents purity and origin were also provided.

3.3.1. Experimental test rig

The main part of the performed study comprised the investigation of toluene heterogeneous decomposition over wood-derived activated chars. Conversion was measured as a function of time of the char being exposed to a constant flow of toluene in a gaseous state. The tests were performed in isothermal conditions at high temperature. For each char, a series of seven tests with varying toluene feeding times were performed in order to obtain a conversion change with char time-on-stream. Two main conversion modes were examined – one with a toluene pyrolytic conversion in N_2 flow, denoted as PYR, and another with the presence of steam, *i.e.* stream-reforming mode SR. SR mode provided information on toluene behaviour in an environment closer to the one in a real gasifier (with an reactive atmosphere), while PYR mode provided an insight into the undisturbed toluene-char interactions, thus it was useful for a conversion pathways investigation.

The experiment was carried out in a laboratory scale, custom-built test rig, comprised of a toluene/carrier gas mixture preparation section (I), a vertical quartz tube reactor enclosed in an electrical furnace (II) and the conversion products sampling train (III), as presented in Figure 4. The reactants mixture was prepared by feeding a controlled flow of nitrogen to a top part of a tube reactor with 20 mm i.d. At this end of the reactor, a steel capillary and PTFE tubing were introduced as well. In steam reforming (SR) mode, water was supplied through the capillary (1), while toluene (or other compound in additional tests) was fed via the tubing (2), both dosed with a constant flow forced by a two-syringe infusion pump. Liquid compounds were then captured in a quartz wool plug inserted in the upper section of the furnace (3) – namely the evaporator. This 200 mm long heating zone with a separate control system was kept at 200 °C to enable liquids vaporisation and mixing with a carrier gas. Thus, prepared mixture passed though the main reactor (4), comprised of a 300 mm long high temperature zone. In this part of a tube, fixed bed of studied char was placed,

secured from the top and bottom with quartz wool plugs. The height at which the bed was inserted was selected to fit within a uniform temperature region, as presented in Figure 5. A thermocouple, inserted from the bottom of the reactor, was used to monitor temperature of the bed.

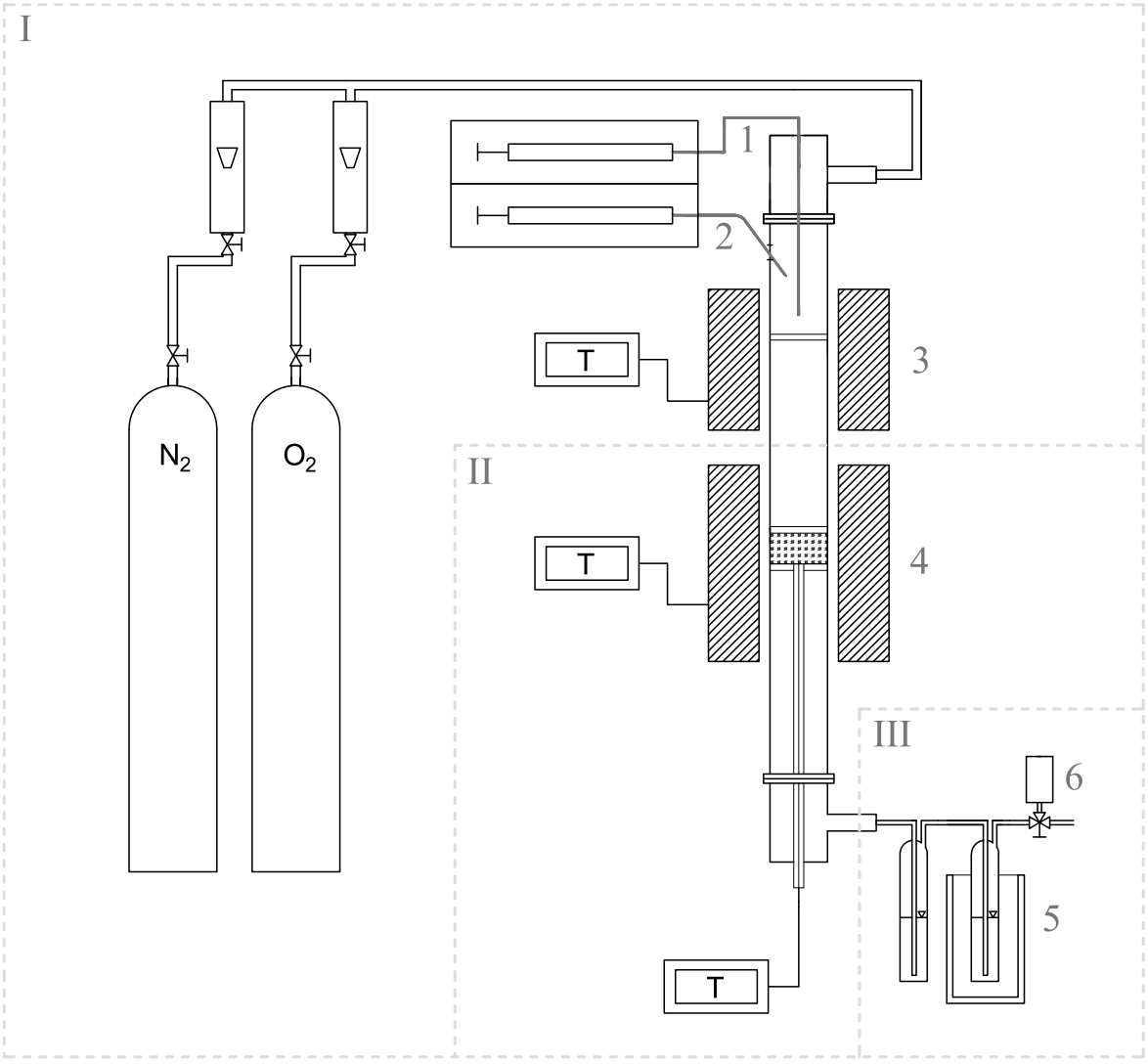

Figure 4. A diagram of the test rig comprised of: I – gas mixture preparation section, II – reaction zone, III – sampling train (1 – capillary for water feeding, 2 – tubing for tar compound feeding, 3 – evaporator, 4 – reaction zone with a catalyst, 5 – impinger bottles, 6 – gas bag)

The reactive mixture was forced to pass through the char bed, were it underwent heterogeneous conversion on catalyst's surface. Unreacted toluene as well as condensable reaction by-products were collected below the reactor via a heated transfer line, connected to a set of two impinger bottles (5) with G3 frits, each filled with 50 mL of dichloromethane.

First impinger was kept at room temperature, while the second one was immersed in the bath cooled to -25 °C. The temperature gradient was introduced, because the evaporation of the solvent from the first bottle has been claimed to improve the condensation of liquid products in the following bottles [93]. Since most of the recovered compounds were captured in the first bottle, and only traces of products were found in the second impinger, extending the sampling train was not necessary.

After removal of the condensable species, gaseous products were collected into Tedlar bags (6) via a three-way valve. Gas was sampled with 90 s intervals and it was analysed post-run. As the maximum experiment time was 60 min, the gas collection was carried out during 30 and 60 min tests, for the initial 30 min and the second 30 min of the test, respectively. This way, functions of gas yields in respect to toluene feeding time were obtained for the whole length of the experiment.

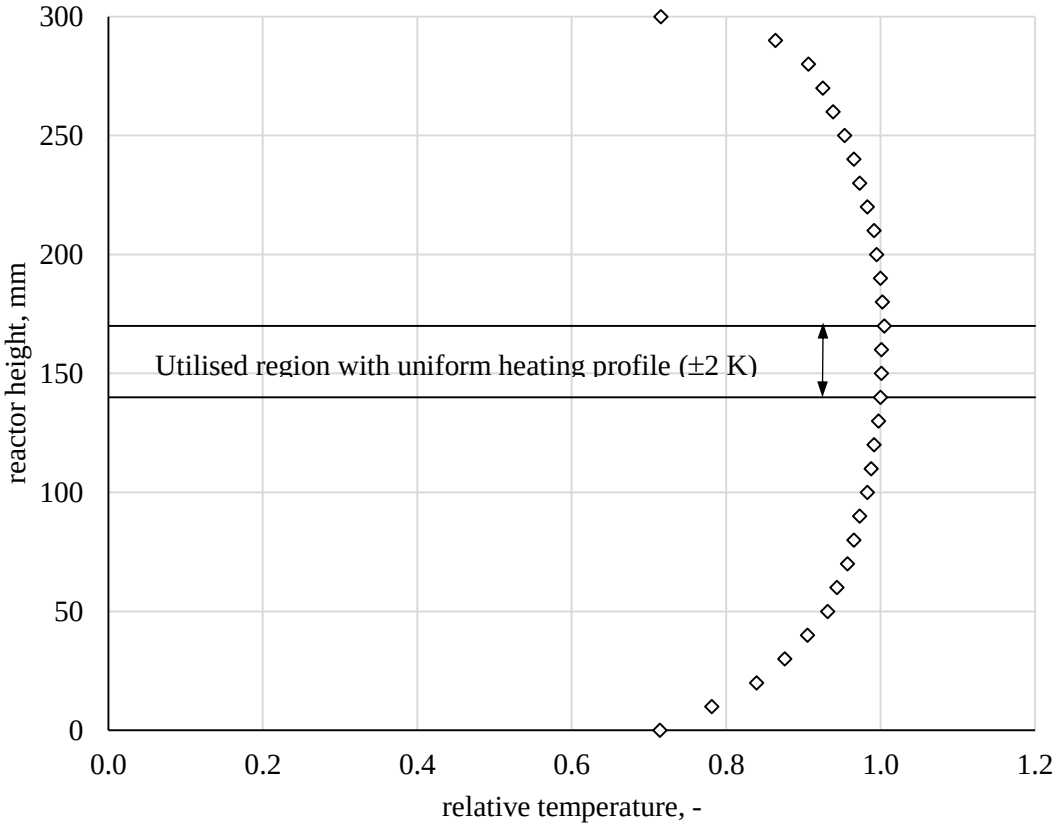

Figure 5. Lower heating zone temperature profile with the region where the fixed bed was placed (temperature measurement uncertainty was ±1 K)

The airtightness of the reactor and the feeding system as well as the efficiency of the sampling train were examined by performing tests with an empty reactor and both furnaces

set to 200 ℃. Toluene recovery under these conditions, when no conversion was expected, was maintained above 99 %.

Additionally, tests at a target experiment temperature of 800 ℃, but without a presence of a catalytic bed, were performed to determine if any homogenous, non-catalytic toluene conversion occurred. It was however observed, that when only a quartz wool plug, and no char, was inserted into the reactor, toluene recovery in both, pyrolytic (PYR) as well as steam reforming (SR) tests was above 96 %. This suggested that homogeneous toluene conversion during both, PYR and SR modes was negligible.

3.3.2. Catalytic tar conversion procedure

Each test run was performed by placing 0.5 g of an examined char inside the tube reactor at the level of the lower furnace. After sealing the reactor, it was purged with N_2 and the evaporator and transfer line were heated up. Then, the lower zone with an incorporated bed was heated up to a desired temperature (800 ℃ for the main experiment), with an average rate of *ca.* 47 K/min. After reaching the given isotherm, the impinger bottles were connected, and in a steam reforming (SR) mode, the water feeding was started. After 5 min of purging, tar compound (toluene in the main experiment) feeding was initiated. It was carried out for a selected run time between 5 and 60 min. For the 30 and 60 min runs, released gases were sampled as described in section 3.3.1. Then, tar compound (and water in the SR mode) flow was terminated and the reactor was purged for 15 min with N_2 flow. In the next step, the impinges were disconnected and secured for the analysis, while the spent char bed was cooled down to ambient in N_2 flow and then removed from the reactor and stored in a desiccator.

In the PYR mode, N_2 flow with linear velocity of 0.094 m/s (on empty reactor at 800 ℃) was maintained throughout the whole experiment. In the SR mode, during the water feeding, N_2 flow was readjusted so that the same, constant velocity was maintained, while the carrier gas mixture composition was set to 15.5 vol.% H_2O in N_2, since this steam concentration was reported by Hosokai et al. [15] as the most favourable. Following reports on similar catalytic conversion studies, toluene concentration in the gas was set to 12 g/Nm^3 [15,36].

3.3.3. Liquid and gaseous products analysis

All the collected liquid and gaseous products of a model tar conversion were analysed post-run. Content of each impinger was transferred quantitatively into a volumetric flask and diluted to 100 mL. It was thereafter analysed with an Agilent 6890N gas chromatograph

fitted with an FID detector and a 30 m x 0.32 mm x 0.25 μm HP-5 column. The inlet and the detector were kept at 250 ℃ and a 1 μL sample injection with a split ratio of 10:1 was made with an Agilent 7893 autosampler. The GC method was set as follows: initial temperature was set to 50 ℃ and it was maintained for 5 min. Then, the temperature was increased to 80 ℃ at a rate of 5 K/min. The heating rate was then changed to 10 K/min until a final temperature of 200 ℃ was reached and held for 2 min. External calibration method was used to determine liquid products concentration. Calibration curves were fitted using a least-square method. Coefficients of determination (R^2) were >0.998 for all examined compounds. During each of the 30 and 60 min tests, 20 Tedlar bags with gaseous samples were collected. They were analysed with an Agilent 6890N gas chromatograph equipped with a TCD detector. The analytes were separated on the capillary J&W GS-CarbonPLOT 30 m x 0.53 mm x 3 μm column followed by the J&W HP-PLOT 30 m x 0.53 mm x 25 μm molecular sieves. For the duration of CO_2 elution, the latter was bypassed by means of a 6-way valve, to avoid sieves clogging and CO_2 retention. Concentrations were calculated using calibration curves and coefficients of determination (R^2) were >0.997 for all examined species. Gaseous compounds yields were calculated based on detected concentrations and the N_2 flow rate that was supplied to the reactor.

3.3.4. Reagents purities and manufacturers

All gas cylinders were supplied by Air Liquide S.A. N_2 (Alphagaz 1) with a 99.999 % purity was used for the main experiment. In some of the modified tests, O_2 (Alphagaz 1) with a 99.999 % purity was additionally supplied. The GC operated on a 99.9999 % purity He (Alphagaz 2). For FID detector, 99.999 % pure synthetic air with a hydrocarbon content below 0.1 ppm (Alphagaz 1) was supplied, while 99.999 % pure H_2 was generated *in-situ* with a SPE150HC hydrogen generator. Calibration gases for TCD detector were supplied by Linde AG.

To represent tar compounds, anhydrous toluene with a purity ≥99.8 %, benzene EMPLURA with a purity ≥99.5 % and *p*-xylene with a purity ≥99.0 % were purchased from Sigma Aldrich, MERCK and Avantor Performance Materials Poland S.A, respectively. For liquid products sampling, as well as for calibration standards preparation, dichloromethane with a purity ≥99.8 % from Sigma Aldrich was used. Standard solutions (benzene, toluene, ethylbenzene, *o*-xylene, *m*-xylene, *p*-xylene, styrene, benzaldehyde, *p*-ethyltoluene, 1,2,4-trimethylbenzene and *p*-methylstyrene) for FID calibration were prepared from

reagents with a purity ≥99.0 %. Pine extractions were performed with acetone EMPARTA with a purity ≥99.5 % from MERCK.

3.4. Summary of performed experiments

The first part of the research was comprised of toluene catalytic conversion over three activated biochars prepared from alder, beech or pine wood species. Conversion was carried out either in a pyrolytic (PYR) or steam reforming (SR) mode. These tests were referred to as the main experiment.

The main experiment results allowed for a comparison of a catalytic performance of biochars. Conclusions on main principles of toluene catalytic conversion under an inert and reactive atmosphere were also drawn. Perusal of the obtained data led to a further investigation of both, catalysts' properties and aromatic hydrocarbons conversion pathways. To this end, additional test runs were performed, where some of the parameters were modified to assess their influence on the process. Test runs carried out during the main experiments and additional tests were listed in this section, along with details of the applied process parameters.

The general outline of research is presented as a flowchart in Figure 6. The initial activities, such as feedstock selection and extraction, as well as char preparation were followed by the conversion experiments (main and additional). Concurrently, analytical methods were applied to examine properties of the wood and char samples. Findings of the experiments were further interpreted and the conclusions on wood-derived catalysts and tar conversion were formulated.

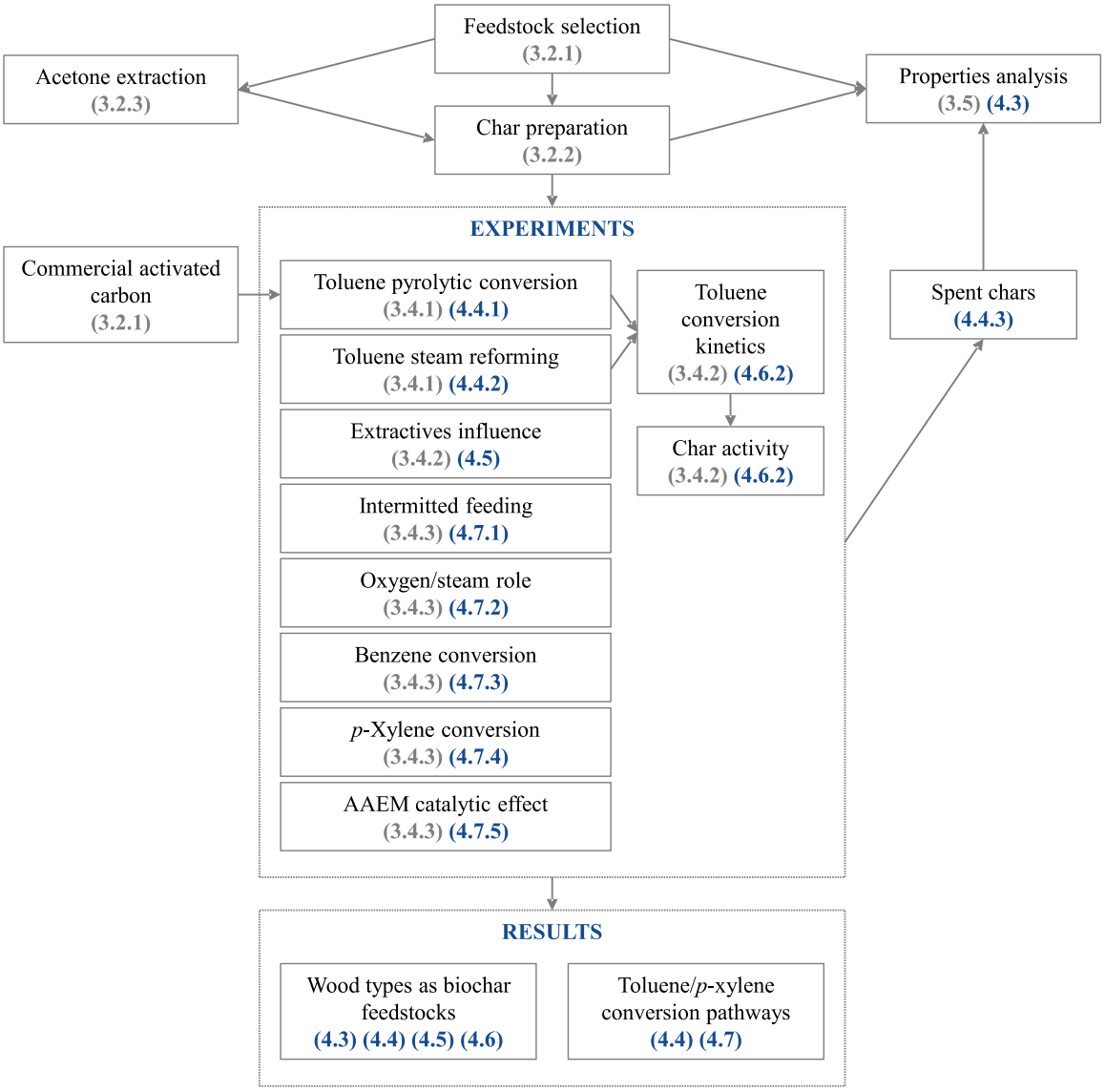

Figure 6. Flowchart of the performed research with relevant sections of the thesis (in parentheses) providing information on methods (in grey) and findings (in blue)

3.4.1. The main experiment

The main experiment was comprised of six measurement series of toluene conversion-in-time, when three chars in two reaction modes (pyrolysis and steam reforming) were tested. Conditions of these tests were summarised in Table 3. Each experimental run was performed in duplicate and the mean values were reported in this work.

Table 3. Parameters of the main experimental series and blank tests (PYR – pyrolysis mode and SR – steam reforming mode)

Series	Char feedstock	Tar compound	Feeding time	Mode	Temperature
1	Alder	Toluene	5 – 60 min	PYR	800 °C
2	Alder	Toluene	5 – 60 min	SR	800 °C
3	Beech	Toluene	5 – 60 min	PYR	800 °C
4	Beech	Toluene	5 – 60 min	SR	800 °C
5	Pine	Toluene	5 – 60 min	PYR	800 °C
6	Pine	Toluene	5 – 60 min	SR	800 °C
blank	Alder	None	60 min	SR	800 °C
blank	Beech	None	60 min	SR	800 °C
blank	Pine	None	60 min	SR	800 °C

Furthermore, to separate steam-char interactions from toluene conversion during steam reforming (SR) mode, a blank test for each char was performed as a reference. Each blank test was carried out in the same manner as an appropriate 60 min SR mode run, with the only difference that neither toluene, nor any other tar compound, was fed into the reactor. This approach allowed for an assessment of uninterrupted char-steam reactions and the results were further compared with the toluene-char-steam interactions. It is also important to stress out, that all the parameters (temperature, steam concentration, gases velocity, *etc*.) during SR mode were the same as during a second step of char preparation process. Therefore, spent chars recovered from the reactor after blank runs, where no toluene was fed, could be also considered as fresh chars with activation time prolonged from 80 to 140 min. This opportunity was used in some of the char characterisation studies for comparative purposes.

3.4.2. Further studies of catalysts

The main experiment of toluene pyrolysis and steam reforming over three activated woody biochars was followed by further tests aimed at catalyst characterisation, involving feedstock pre-treatment, comparison with commercial activated carbon as well as an assessment of toluene conversion kinetics. These extended studies required some additional, modified experimental runs, summarised in Table 4 and detailed below:

a) Feedstock modification

Although a main principle of toluene conversion was similar for all three examined chars, activated pine (PA) char had a lower performance, compared to deciduous trees chars. Since one of the most characteristic features of coniferous wood is its high content of extractive compounds, their effect on biochar performance was examined. To this end, acetone extraction of pinewood was performed, as described in section 3.2.3, and thus pre-treated feedstock was used to prepare activated char, referred to as PAE. A series of pyrolytic toluene conversion tests for seven feeding times was performed with PAE char catalyst, analogously to the runs comprised within the main experiment. Moreover, for the purpose of extractives effect examination, physicochemical properties of the PAE char were also evaluated. Due to a volatile nature of extractives, their contribution to created char properties was expected to occur during pyrolysis of a feedstock. Therefore, not only activated pine chars properties were analysed, but additionally, chars that were sampled after the first, pyrolytic step of the preparation process were also examined, and referred to as non-activated pine (P) and non-activated extracted-pine (PE) chars. Spent PA and PAE chars properties were also investigated.

Extractives influence on pyrolysis process was additionally assessed by a thermogravimetric analysis with a Netzsch STA 409 LUXX analyser for two different heating rates. 5 mg sample of either raw or extracted pinewood was pyrolysed by heating it up to 800 °C in 100 mL/min N_2 flow with a heating rate of either 10 or 50 K/min. Moreover, a decomposition of extractives derived from the pine was analysed at the same conditions as the wood samples. The first derivatives (DTG) of the mass loss curves were further used to examine the role of acetone-extractable compounds in relation to the applied heating rate. All tests were run in duplicates.

b) Catalyst bed modification

In order to assess the performance of biochars used in this study with a commercial catalytic material, results of toluene pyrolysis (PYR) runs from preliminary studies were used. They were performed with a bed of commercial activated carbon (AC) described in section 3.2.1. Process conditions during those tests were the same as during PYR mode of the main experiment, with an exception of toluene concentration and catalyst mass, which during the preliminary studies were set to 8 g/Nm^3 and 1 g, respectively. Moreover, due to a higher density of AC, a bed height in those tests was approximately half of that used in the main experiment with chars. Despite these differences in process conditions applied during

preliminary tests with AC and the main experiment with biochars, a comparison of those tests lead to some valid conclusions and thus was included in the scope of this dissertation.

c) Reaction temperature modification

To enable kinetic calculations of toluene conversion reaction, additional runs for the initial feeding times (5 min) were performed at another two temperatures, *i.e.* 700 and 750 °C. These test runs were limited to an activated alder (AA) bed and were carried out in both pyrolytic (PYR) and steam reforming (SR) mode. Except for the reaction temperature, the same parameters and test procedure as during the main experiment were maintained. Moreover, the results from preliminary studies at 700 and 750 °C for 10 min feeding times were used to calculate toluene conversion kinetics over commercial AC during a pyrolytic mode. The parameters of these runs were consistent with the experimental series of preliminary AC tests carried out at 800 °C.

Table 4. Parameters of additional test runs performed during further studies of catalysts (PYR – pyrolysis mode and SR – steam reforming mode)

	Catalyst	**Tar compound**	**Feeding time**	**Mode**	**Temperature**
a)	Extracted pine char	Toluene	5 – 60 min	PYR	800 °C
b)	Activated carbon	Toluene	5 – 50 min	PYR	800 °C
c)	Alder char	Toluene	5 min	PYR	700, 750 °C
	Alder char	Toluene	5 min	SR	700, 750 °C
	Activated carbon	Toluene	10 min	PYR	700, 750 °C

3.4.3. Further studies of tar conversion

Besides the main experimental runs with pyrolytic conversion and steam reforming of toluene over bed of fresh, activated chars from pine, alder and beech, some additional tests were performed to further investigate mechanisms of tar conversion. Test modifications involved changes of one of the following: feeding principle, oxidising agent, tar representing compound or bed material properties. As the main experiment revealed that the basic principle of toluene conversion was similar for all three chars, only one of them was selected for the additional experiments. As parameters like hardness, lignin content *etc.* of alder wood were the most moderate amongst the examined species, activated alder char was used in additional tests. The additional runs involved modifications summarised in Table 5 and detailed below:

a) Toluene feeding modification:

In order to examine a possibility of toluene gas phase chain reactions initiated by radicals released from a char surface, an additional test in pyrolysis (PYR) mode was performed. During this experiment, a feeding principle was changed, and it was further referred to as an "intermittent feeding" test. The interruption of the feeding process was introduced in order to elute gaseous reactants and cease any possible chain reactions. Two modifications were examined. In each one, toluene feeding was stopped after initial 10 or 15 min, the reactor was purged with N_2 for 15 min, after which, the feeding was resumed for a further 20 or 15 min to provide an overall char time-on-stream of 30 min. The modifications were named "10+20 min" and "15+15 min" runs, respectively. Liquid conversion by-products were collected together with unreacted toluene in a set of impinger bottles. The set was changed after the initial feeding period and N_2 purging, and a new set was connected for the second part of the run. Thus, a conversion within each feeding period could be determined, along with an overall conversion for a total 30 min test. Obtained results were compared with a conventional 30 min PYR run from the main experiment, where a continuous feeding was applied. Additionally, toluene conversion within an initial period of the 10+20 min run was compared with results obtained in a 10 min continuous run of the main experiment. Furthermore, differences between continuous 30 and 10 min run results were calculated to enable a correlation with the second part of the 10+20 min run.

b) Oxidising agent modification

As the main experiment's results suggested no direct, homogeneous toluene-steam interactions, a stronger oxidising agent was examined to further investigate a dynamic of a tar-char-oxidiser system. To this end, oxygen instead of steam was used in a reactive gas mixture. The concentration of steam (15.5. vol.%) in steam reforming (SR) mode, applied during the main experiment, provided a stoichiometric excess of oxygen for toluene oxidation. Therefore, an initial test was performed with an excess of oxygen (3.55 vol.% in N_2) and a lack of catalytic bed. Contrary to the SR mode tests with an empty reactor, a significant homogeneous toluene conversion occurred. Therefore, O_2 concentration was decreased below stoichiometric requirement and it was kept at 0.67 vol.% for the remaining tests. The second test was therefore performed with a new, lower O_2 concentration and an empty reactor. For the third test, an activated alder char (AA) bed was introduced. This test was further compared with the results of a respective run performed in a SR mode in scope of the main experiment. In order to ensure a stable state of toluene conversion during tests

with an empty reactor as well as to provide sufficient time for char-oxidiser interactions during tests with a catalyst bed, the reaction time was set to 40 min for all the tests with O_2 agent. Toluene conversion, as well as gaseous and liquid by-products were analysed to assess the effect of an oxidising agent type. Toluene reactions with O_2 yielded more compounds than the main experiment. Besides benzene, ethylbenzene, xylenes and styrene, numerous compounds with higher retention times were detected with GC-FID analysis, although only one of them was identified. This additional by-product was recognised as benzaldehyde, and its formation during toluene-oxygen reactions has been reported before [80]. Since some differences between O_2 and steam reforming modes were observed, a spent char from each experiment was examined to further investigate the role of an oxidising agent. Chemical properties of chars were assessed via ATR-FTIR and their morphology was studied by N_2 adsorption, as described further in section 3.5.

c) Compound modification – benzene

In order to determine an importance of a methyl group presence during toluene catalytic conversion, additional tests were performed, where benzene was used as a tar representing compound. A 30 min pyrolysis (PYR) and steam reforming (SR) of benzene over activated alder char was carried out. The same concentration of model tar as during the main experiment with toluene was used. A yield of gases released during benzene conversion was measured along with an analysis of trace amounts of a sole liquid by-product, *i.e.* toluene. The results were compared with corresponding toluene runs performed during the main experiment in PYR and SR modes. Due to observed differences in benzene and toluene conversions, spent char analysis with ATR-FTIR and N_2 adsorption was carried out to further investigate principles of methylated and non-methylated aromatic ring heterogeneous reactions on a catalyst surface.

d) Compound modification – *p*-xylene

Since some differences in conversion principle, and thus its efficiency, were found between a sole aromatic ring (benzene) and methyl-substituted one (toluene), in a next step, a compound with two functional groups was examined. To this end, *p*-xylene was selected. A *para* isomer was chosen in an attempt to limit any possible interactions between methyl groups as well as due to its kinetic diameter that is consistent with that of toluene and benzene (5.85 Å) [94]. In this experiment, only pyrolytic (PYR) mode was explored, yet for a wider range of feeding times, *i.e.* between 10 – 50 min. Concentration of the fed compound

was consistent with that of toluene and benzene. The results were compared with corresponding runs of the main experiment with toluene feeding. Although conversion efficiency did not improve upon an introduction of a second methyl group, a liquid by-products rage was increased. A GC-FID analysis of impinger bottles revealed eight peaks, identified as benzene, toluene, ethylbenzene, *p*-xylene/*m*-xylene, *o*-xylene/styrene, *p*-ethyltoluene, 1,2,4-trimethylbenzene and *p*-methylstyrene.

e) Char modification

Despite a well-documented catalytic influence of alkali and alkaline earth metals (AAEM) on char oxidation reactivity [17,18], their role in hydrocarbons conversion is ambiguous [14,16]. Therefore, an additional test of modified activated alder (AA) chars was performed. An activated char, as received from the synthesis process described in section 3.2.2, was subjected to a further treatment to diversify its AAEM content. In a first step of the modification, 5 g of char was shaken for 24 h in 50 mL of 2.0 M HCl solution, to remove inorganic species [57]. After washing with deionised water and oven drying at 60 °C, thus prepared char, referred to as AA_HCl, was used in an additional test. Moreover, 2 g of the AA_HCl char was subsampled and it was impregnated with Na^+ by shaking it for 24 h in 50 mL of 0.5 M solution of sodium acetate. Followed by filtration and drying at 60 °C, it was then referred to as AA_Na.

AAEM content in both modified chars was analysed according to the procedure described further in section 3.5.1. To assess any possible changes to other char parameters due to AAEM content modifications, ATR-FTIR analysis of fresh and spent AA_HCl and AA_Na chars was performed, along with a measurement of N_2 adsorption on the AA_Na char.

The additional tests of modified chars were comprised of 30 min toluene pyrolytic (PYR) conversion tests, with liquid products analysis. An assessment of AAEM species importance during toluene pyrolytic decomposition was obtained by comparison of a conversion over untreated AA char, obtained during the main experiment, with the results of washed and impregnated chars tests. Moreover, a TGA oxidation tests were performed for modified chars and their kinetic parameters were calculated, as further described in section 3.5.3. Therefore, AAEM influence on char oxidation rates was examined, by a comparison of original AA, and modified AA_HCl and AA_Na char reactivity.

Table 5. Parameters of additional test runs performed during further studies of tar conversion (PYR – pyrolysis mode and SR – steam reforming mode)

	Catalyst	Tar compound	Feeding time	Mode	Temperature
a)	Alder char	Toluene	10+20 min	PYR	800 °C
	Alder char	Toluene	15+15 min	PYR	800 °C
b)	None	Toluene	40 min	3.55 vol.% O_2 in N_2	800 °C
	None	Toluene	40 min	0.67 vol.% O_2 in N_2	800 °C
	Alder char	Toluene	40 min	0.67 vol.% O_2 in N_2	800 °C
c)	Alder char	Benzene	30 min	PYR	800 °C
	Alder char	Benzene	30 min	SR	800 °C
d)	Alder char	*p*-Xylene	10 – 50 min	PYR	800 °C
e)	Alder AA_HCl	Toluene	30 min	PYR	800 °C
	Alder AA_Na	Toluene	30 min	PYR	800 °C

3.5. Catalysts and their feedstock properties

Performance of chars as tar conversion catalysts correlates with their physicochemical properties. The main parameters often considered to have the strongest influence on the catalytic properties are the active sites available for heterogeneous reactions and the surface structure of the material, determining the accessibility of those sites. It has been generally established, that the main groups of catalytically active sites on biochars are alkali and alkaline earth metals (AAEM) species, acidic functional groups as well as so called unsaturated carbons, often understood as imperfections in the carbon matrix of the carbonaceous materials [14,16,34]. The surface area, pore shapes and size distribution are on the other hand responsible for providing access to the active sites, thus enabling tar-char interactions. Material studies that were performed within the scope of this study comprised examination of the physicochemical properties of chars and their feedstock. The details of the analysis were described in this section.

3.5.1. Chemical properties of studied materials

Presence of the main functional groups on a surface of prepared chars, activated carbon and raw wood was examined via Attenuated Total Reflectance Fourier-Transform Infrared Spectroscopy (ATR-FTIR) with a Perkin Elmer Spectrum 100 spectrometer with UATR accessory equipped with a germanium crystal. Each spectrum had the resolution of 4 cm^{-1}

and 32 scans per measurement were taken within the 4000 – 700 cm^{-1} wavenumber range. Water vapour and CO_2 corrections were applied for the scans. The baseline correction was applied as well to counteract the drift occurring in a highly carbonised aromatic materials due to a scattering effect of those structures [95]. For each sample, an average of five measurements is reported as a final spectrum. Samples were milled to a fine powder prior to the analysis to provide better contact with the crystal.

The compounds extracted from raw pinewood were studied as well. In this case, a thin layer of the extractives was pressed to the crystal's surface. The same parameters of spectra as during the powdered materials studies were maintained.

For raw and extracted pine wood analysis, a differential spectrum was also reported. It was obtained by subtracting a registered absorbance of the extracted wood from the absorbance of a raw pine, within the studied wavenumbers range.

Further investigation of the functional groups present on the surface of fresh chars was carried out by measuring the distribution of the acidic sites. To this end, the Boehm titration method was selected as it distinguishes three different strengths of the sites and it was previously used for similar materials [96–98]. Since the original method was designed for more stable carbon blacks, char samples required additional pre-treatment to remove mobile species like metal cations or labile organic carbon, *e.g.* humic acids that are characteristic to biomass derived carbonaceous materials [98]. The pre-treatment was comprised of a series of consecutive washings for unstable, soluble compounds removal and final protonation of the remaining active sites. It was performed according to the procedure proposed by Tsechansky and Graber [99]. Samples were shaken in two aliquots of 0.05 M HCl solution over 24 h, rinsed with deionised water, shaken in two aliquots of 0.05 M NaOH solution over 24 h, rinsed with deionised water and again shaken with 0.025 M HCl aliquot for 24 h to protonate all the remaining carbon surface groups. Finally, the samples were rinsed with deionised water and dried in the oven at 40 ℃ for 72 h.

Thus prepared char were further subjected to Boehm titrations, following the standardised procedure established by Goertzen et al. [96,97]. The analysis allowed for quantification of the strong, medium and weak acidic sites, *i.e.* carboxylic, lactonic and phenolic groups, respectively, by accessing the sample's uptake of the bases of different strengths. Therefore, three separate titrations are required for each experiment, using either NaOH, Na_2CO_3 or $NaHCO_3$. One gram of homogenised sample was weighted into each of three flasks and it was shaken for 24 h in 0.05 M solution of one of the bases. Samples were then filtrated on Grade 1 Whatman filter papers. A 10 mL aliquot portions were mixed with 10 mL (20 mL

for Na_2CO_3) of 0.05 M HCl, purged with N_2 flow of *ca.* 0.25 mL/min for 2 h and back-titrated with 0.05 M NaOH with N_2 purging. Potentiometric titrations were performed with a Schott Instruments GmbH TitroLine alpha plus titrator. The endpoint was determined based on a titration curve's first derivative analysis.

Following Goertzen et al. [96], the amount (mol) of carbon surface functionalities for each titration was determined from the equation:

$$n_{CSF} = \frac{n_{HCl}}{n_B}[\mathrm{B}]V_B - ([\mathrm{HCl}]V_{HCl} - [\mathrm{NaOH}]V_{NaOH})\frac{V_B}{V_a} \quad (3)$$

where $\frac{n_{HCl}}{n_B}$ is the molar ratio of acid to base, [B], [HCl] and [NaOH] are the concentrations (mol/L) of the reaction base, acid added to the aliquot and titrant, respectively. The V_B, V_{HCl}, V_{NaOH}, and V_a represents the volumes (L) of the reaction base, acid added to the aliquot, titrant and aliquot, respectively. The amount of acidic sites, expressed as μeq/g of char, that was neutralised by each reaction base was determined. According to Boehm [24], $NaHCO_3$ accepts protons only from the strongest acidic groups, *i.e.* carboxylic sites. The Na_2CO_3 reacts with carboxylic groups as well, while it also hydrolyses lactones and lactoles, which are considered as medium strength sites. NaOH neutralises all the above-mentioned functional groups as well as phenolic structures, ascribed to weak acidic sites [98]. Therefore, a subtraction of n_{CSF} obtained for Na_2CO_3 test from the n_{CSF} for NaOH one and n_{CSF} for $NaHCO_3$ test from n_{CSF} for Na_2CO_3 gave the amount of phenolic and lactonic sites, respectively. The amount of the strongest, carboxylic sites was represented directly by the n_{CSF} value from the $NaHCO_3$ test. The total acidity was understood as the sum of all three sites groups and it was therefore represented by n_{CSF} for NaOH test. All titrations were carried out in duplicates, and the relevant acidic sites amounts were calculated using averaged n_{CSF} values.

Another attempt to gain some insight into the functional groups presence on the char surface was made by performing the TPD-FTIR analysis, using a Netzsch STA 409 LUXX thermogravimeter coupled, by a heated transfer line, with a Perkin Elmer Spectrum 100 spectrometer equipped with a RedShift accessory for gaseous samples analysis. This method was applied to fresh alder char as well as an alder char after blank steam reforming (SR) run, considered as a fresh char with a prolonged activation. 100 mg char sample was heated up to 1000 °C in a 30 mL/min N_2 flow in a TGA, with a heating rate of 5 K/min. Simultaneously, released gases, namely CO and CO_2, were analysed online with a spectrometer. Spectra in a

range of 4000 – 450 cm^{-1} were taken with an interval of 8 seconds throughout the whole measurement. The evolution profiles of CO_2 and CO were assigned to absorption values at 2358 and 2162 cm^{-1}, respectively. The TGA pyrolysis provided mass loss curves of the samples and first derivatives DTG of those curves were compared with the peaks of the evolution profiles.

Appling high sample mass for the measurement was necessary to enable gaseous species detection, yet the quality of the spectra were relatively poor. Thus, this test was expected to provide only qualitative information about the compounds released at certain temperatures. Gases released at certain temperatures, can be however assigned to characteristic functionalities on the surface of carbonaceous materials [23,26], therefore this test confirmed the presence of certain active sites on the studied materials.

Alkali and alkaline earth metals (AAEM) content in the fresh chars was determined by a SpectrAA 880 Varian Atomic Absorption Spectrometer after digestion with HNO_3 in a Milestone MLS1200 MEGA microwave. The experiment was carried out in triplicate and the averaged values were reported in this work

3.5.2. Physical properties of studied materials

A structure of the chars was examined by analysing their surface area and porosity. Physical adsorption technique was used by measuring the N_2 adsorption isotherm at 77 K. The analysis of all pine chars as well as fresh alder and beech chars was outsourced to the Centre for Functional Nanometrics at Maria Skłodowska Curie University, where the samples were analysed with a Micromeritics ASAP 2420 instrument. Further assessment of spent alder chars and activated carbon was performed at the Institute of Thermal Technology facilities, with a Micromeritics TriStar II 3020 analyser.

Samples were outgassed under N_2 flow, at 200 °C, for 24 h prior to the analysis. Adsorption was carried out for relative pressures (P/P_0) within the range of 0.0002 to 0.95. Smaller intervals were applied for lower pressures to better capture adsorption in micropores. Desorption isotherm was also registered to determine occurrence of a hysteresis and thus provide an insight into pore shapes. The total surface area was estimated using BET model and a pressure range for the calculations was narrowed to the $P/P_0<0.2$ due to a microporous nature of the samples. The *t*-Plot method was used to assess the micropores area using Harkins and Jura thickness equation. Pooled standard deviations for BET surface area and micropores area determination were ±5 m^2/g and ±7 m^2/g, respectively.

Surfaces of selected chars were further examined by taking scanning electron micrographs with a JCM-5000 NeoScope microscope.

3.5.3. Char oxidation kinetics

Char reactivity was assessed by kinetic parameters of oxidation reaction obtained from the thermogravimetric analysis performed with a Netzsch TG 209 F3 Tarsus instrument. Samples were heated up to 800 ℃ at a 10 K/min rate in a continuous 85 mL/min flow of a 12/88 vol.% O_2/N_2 mixture. Prior to the analysis, char particles were milled and sieved under 36 μm to diminish mass and heat transfer limitations. 2.5 mg sample of char, providing a thin, evenly distributed layer covering the bottom of the crucible, was subsampled for each run.

A first order reaction was assumed in the kinetic parameters calculations, since it is often used to describe char combustion reactions [100]. This simplification can be especially justified since the purpose of thus obtained data is the comparison between relatively similar materials, rather than implementation into more general kinetic models. Due to its high accuracy, a temperature integral approximation method using Senum and Yang's 4^{th} degree rational approximation [101] was used for the activation energy and pre-exponential coefficient calculations.

The oxidation process during thermogravimetric analysis inevitably differed from the reactions that char was undergoing during the main experiment. However, the TGA analysis was performed for the purpose of the estimation of the char's potential towards reacting with oxidising agent. Therefore, the reactivity during the initial stages of char decomposition was of interest, rather than the kinetics of the overall oxidation process. Thus, for the kinetic parameters estimation, only the initial sample mass loss in the range of 3 – 10 wt.% was considered. This assumption allowed for a comparison between the dynamics and the temperatures of the char-O_2 reaction initiation. All tests were run in duplicates. Due to a kinetic compensation effect, raw data from both repetitions was averaged prior to calculating an activation energy and a pre-exponential coefficient. Thus, instead of standard deviations, coefficients of determination were reported for each pair of kinetic parameters that were obtained.

3.6. Toluene heterogeneous conversion kinetics

Kinetic parameters of toluene conversion were calculated based on the method reported by Fuentes-Cano et al. [36]. Initial conversions at short feeding times were considered to

prevent any interference of the catalyst deactivation with deposited coke. Conversion was assumed to follow a first order reaction with respect to toluene concentration. The modified experimental runs at lowered temperatures (700 and 750 ℃) as well as the 5 min test from the main experimental series at 800 ℃ were used to calculate kinetic parameters of toluene conversion over alder char in pyrolytic (PYR) and steam reforming (SR) modes. Since initial activity of activated carbon was maintained for a longer time, 10 min runs at 700, 750 and 850 ℃ were used to calculate toluene initial pyrolytic conversion kinetics over this material. Rate coefficient was calculated based on equation:

$$k = \frac{-\ln(1-\eta_T)}{\tau} \tag{4}$$

where η_T – toluene conversion and τ – residence time in the bed (s).

Based on the *k* values for three studied temperatures (*T*), Arrhenius plot of $\ln(k) = f(1/T)$ was created for alder in PYR, alder in SR and activated carbon in PYR modes. Linear function, fitted using a least squares method, provided activation energy E_a and pre-exponential coefficient, *A*, values.

3.7. Char activity

Following the work of Fuentes-Cano et al. [36], an activity factor (a) was introduced to incorporate char deactivation, occurring during prolonged exposition to toluene, into the kinetics of its conversion. Conversion rate at any given time of experiment was therefore expressed as:

$$-r_{tar} = kC_{tar,i}a \tag{5}$$

where k was the rate coefficient (1/s) and $C_{tar,i}$ was the tar concentration (mol/m^3) in the gas at the inlet of the reactor.

Activity was defined by Fuentes-Cano et al. [36] as:

$$a = \frac{1}{1 + k_d t_{ex}^p} \tag{6}$$

and coefficient p was defined as:

$$p = p_1 + p_2(T/1023) \quad (7)$$

where p_1, p_2, k_d were empirical parameters, T was the temperature (K) of the catalyst's bed and t_{ex} was the time (s) of the experiment (feeding time).

Conversion data from experimental series could be therefore used to fit the values of p_1, p_2 and k_d parameters. This way, an activity function $a = f(t_{ex})$ was obtained for the toluene conversion during the main experimental tests, *i.e.* at 800 °C.

For the alder and activated carbon conversions, the rate coefficient *k* determined from the kinetic calculations was used. For the remaining experimental series, a coefficient for a single studied temperature (800 °C) was calculated and used in activity function estimation.

3.8. Experimental data evaluation

Assessment of a significance of the obtained results was carried out by means of the analysis of variance (ANOVA). This method has been considered as suitable for testing the significance of differences between the sets of data and it has been commonly used in similar studies [34,43]. Analysis of variance is a parametric test allowing for comparison of the means of groups of measured data. Two-way ANOVA with replication is particularly convenient when groups are cross-examined by two different factors (char type and feeding time). Moreover, this approach incorporates both, errors derived from measuring equipment accuracy as well as uncertainties related to a heterogeneous nature of studied materials. Therefore, it was considered a good evaluation method for the purpose of this work.

A significance level α=0.05 was specified as a threshold. When the calculated probability value (*p*-value) was lower than α, the rejection of the null hypothesis is justified. Two-way ANOVA analysis of toluene conversion as well as its by-products yields was carried out for two factors – char type and experiment time. Therefore, for each analysis, three null hypotheses were tested: 1) there is no significant difference in toluene conversion (or conversion product yield) between the studied chars, 2) there is no significant difference in toluene conversion (or conversion product yield) for different experiment times, 3) the interaction effect between char types and experiment times does not exist. Within each of two examined modes (PYR and SR), data series for all tree chars were cross-examined, *i.e.* significances of the differences between alder and pine, alder and beech and pine and beech chars were studied.

All experimental runs were carried out in duplicate and pooled standard deviations were incorporated in the conversion and products yields plots.

3.9. Concluding remarks

Tar conversion over biomass chars was performed in a laboratory scale in controlled conditions. The experiment was designed to provide fundamental knowledge of the heterogeneous reactions between carbonaceous material and light aromatics. Tar was represented by toluene, and the chars were prepared from three different wood species.

A laboratory-scale test rig was designed and built for the purpose of this study. It was used for char preparation as well as the tar conversion experiments. The physicochemical properties of chars and their feedstocks were examined in a series of analytical tests. Obtained results were presented and discussed in Chapter 4.

CHAPTER 4

RESULTS AND DISCUSSION

4.1. Introduction

Results of all performed experiments described in Chapter 3 were presented below. A discussion on the data in relation to the current state of knowledge on hydrocarbons conversion was also provided. Results were divided into six sections regarding: feedstock properties, biochars properties, the main experiment on toluene conversion, further investigation on pine extractives, biochars and commercial activated carbon comparison and additional tests on conversion mechanisms.

4.2. Feedstock characterisation and comparison

Biomass derived char was the main catalytic material studied within the scope of this project. Different wood species were selected as a feedstock for char production. This approach allowed for comparison between the materials similar in nature and properties, however diversified enough to help establish the correlation between their features and their suitability for catalysing tar conversion. In order to assure a thorough assessment of woody biomass as a biochar feedstock, examined species were picked amongst the various wood types.

As presented in Table 6, all three wood materials had similar elemental composition, with carbon comprising approximately half of the organic matter. As the youngest among carbonaceous fuels, they had high oxygen content and significant amount of hydrogen. As opposed to some coal types and some other biomass feedstock, like sewage sludge or manure, they had low nitrogen and sulphur content. As most woody biomass, all examined feedstocks had low ash content and were rich in volatiles, therefore obtained char yields were relatively low. However, abundance of highly volatile species as well as high oxygen content made the material more reactive and therefore more prone to activation during char preparation process.

The diversification of the selected feedstocks becomes visible when the chemical composition of the woods is considered. As a general rule, softwoods have considerably higher lignin content than hardwoods [51]. This trend can be observed in the composition of studied materials, with pine having almost 1.5 times more lignin than beech. A structure of this polymer also differs distinctively between conifers and deciduous trees. With the similar cellulose composition, hemicellulose content was higher in wood with a higher hardness. It has been reported that the structure of this constituents varies between hard and softwoods [51]. All hemicellulose compounds are being released from the sample at relatively low temperatures, and the char yielded from the wood samples comprises mainly the remains of

lignin and cellulose, along with the inorganic matter. Another distinctive feature of conifers (softwoods) is their high content of extractives, *i.e.* low-molecular, volatile compounds that can be easily removed from the polymeric constituents due to their solubility in organic solvents. Coniferous extractives are comprised mainly of resin acids, which are not present in the deciduous trees at all [51,58]. The analysis of selected samples revealed, that pine had 2 – 3 times more extractives than alder and beech. The expected differences in wood composition were therefore confirmed by the chemical composition analysis.

Table 6. Composition of wood used as biochars feedstock

Elemental composition, wt.% daf

	C	H	N	S	O (by diff.)
Alder	50.28 ±1.42	6.26 ±0.27	0.32 ±0.30	0.02 ±0.01	43.12
Beech	49.77 ±1.34	6.14 ±0.25	0.22 ±0.01	0.01 ±0.01	43.86
Pine	52.57 ±1.48	6.29 ±0.28	0.12 ±0.01	0.01 ±0.01	41.01

Proximate analysis, wt.% dry

	VM	ASH	FC (by diff.)
Alder	84.7 ±3.9	0.44 ±0.02	14.86
Beech	84.4 ±3.9	0.51 ±0.02	15.09
Pine	87.4 ±0.5	0.20 ±0.01	12.41

Chemical composition, wt.% dry

	cellulose	hemicellulose	lignin	extractives
Alder	42.46 ±0.06	33.67 ±2.17	23.71 ±0.45	3.68 ±0.34
Beech	39.53 ±0.20	37.11 ±0.65	20.97 ±0.46	2.54 ±0.13
Pine	44.10 ±0.25	27.81 ±1.52	29.75 ±0.20	7.14 ±0.08

The FTIR analysis of wood samples (Figure 7) revealed similarity of alder and beech structure as well as some differences between those two species and a pine. All recorded spectra were comprised of few characteristic regions [65,66]. Within a 3700 – 3200 cm^{-1}, O–H vibrations could be detected, although due to the overlapping effects they often create a wide band which does not provide any detailed information, which was the case in examined wood samples, where only a general presence of hydroxyl groups could be confirmed. Within a 3000 – 2840 cm^{-1} region, C–H stretching vibrations in hydrocarbons occur. The characteristic absorption bands were 2962 and 2872 cm^{-1} for asymmetrical and symmetrical stretching in methyl groups, respectively. Methylene groups absorbed at 2926

and 2853 cm^{-1}. It could be determined from the spectra, that all samples comprised aliphatic structures. Pine had a more pronounced 2926 cm^{-1} methylene band, suggesting more aliphatic chains, plausibly due to significant amount of extractives, comprised of resin and fatty acids.

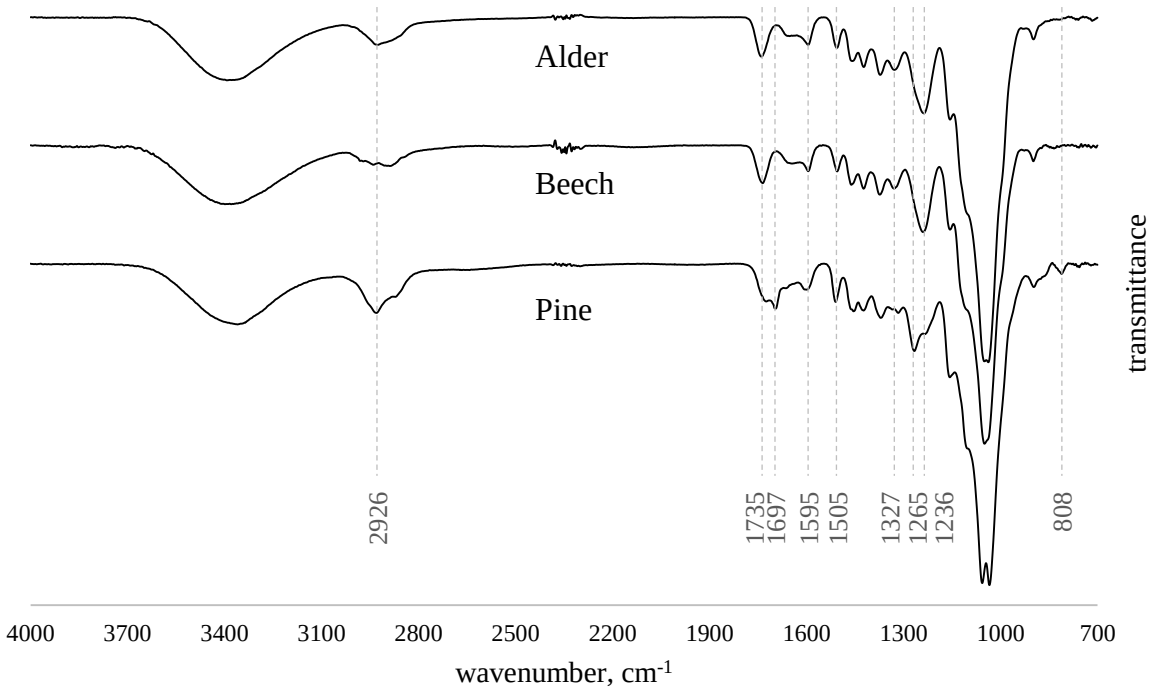

Figure 7. FTIR spectra of fine powdered woods used as feedstocks

Flat spectra in the 2260 – 2100 cm^{-1} region gave evidence to the lack of any C≡C structures in wood. C=O stretching bonds, among others in carboxylic acids, absorbs in the region of 1800 – 1600 cm^{-1}. All examined spectra confirmed a presence of carboxyls (1735 cm^{-1}), in wood present mainly in hemicellulose, *e.g.* xylans [102]. The absorption band at 1697 cm^{-1} is commonly attributed to the C=O bond in resin acids [103]. It was clearly pronounced in the pine spectrum, while it was lacking in the deciduous tree ones. Aromatic rings stretching vibrations absorb at 1600 – 1585 cm^{-1} and 1500 – 1400 cm^{-1}. While built into lignin polymeric structure, they are usually attributed to the 1595 and 1505 cm^{-1} bands [102]. The relative intensity of those two bands depends on the type of lignin [104]. Softwood lignin typically has a higher 1505/1595 absorption ratio – this could be observed in the obtained spectra, where the ratio was 1.21 for pine, while only 1.08 and 1.00 for alder and beech, respectively.

The next three bands in all spectra resulted from the C–H deformations. Following, the 1327 cm^{-1} band could be observed. It arose from the C–O stretching in syringyl units, which are unique to hardwood lignin type. As expected, it was very prominent in alder and beech spectra, while it was lacking in the pine one. Analogous stretching in guaiacyl units absorb at 1265 cm^{-1} [105]. While hardwood lignin is comprised of both types of those aromatic rings, softwood lignin contains only guaiacol derivatives. This phenomenon, combined with the overall higher lignin content in conifers, resulted in a much more pronounced 1265 cm^{-1} band in pine than the in other two spectra. Absorption at 1236 cm^{-1} has been attributed to polysaccharides [102] and it was expectedly more pronounced in hardwoods, which are more abundant in holocellulose.

Within the next region of 1200 – 800 cm^{-1}, miscellaneous C–O stretches along with C–C vibrations of hydrocarbons matrix occurred [66], resulting in a generally high-intensity area of the spectra. Deciduous trees spectra peaked at 1049 cm^{-1}, which is a typical absorption band for polysaccharides. There were two distinguishable bands in a pine spectrum, namely 1054 and 1033 cm^{-1}, originating from polysaccharides and methoxy groups, respectively [104,105]. The differences most likely arose from the diversified composition of hemicellulos among wood species.

The 808 cm^{-1} band in pine spectrum, along with increased absorption around 850 cm^{-1}, confirmed an abundance of guaiacyl units, as those wavenumbers are characteristic for C–H vibrations in their rings [106].

Summarising the spectroscopic wood analysis, three main differences between pine and deciduous trees were confirmed:

a) An abundance of aliphatic chains and carboxylic groups, particularly originating from resin acids, was visible in pine spectrum, as opposed to the other two materials. This observation correlated well with increased extractives content in a raw pine.
b) Lower absorption at some wavenumbers characteristic to hemicellulose, as well as a different shape of the main 1100 – 1000 cm^{-1} band in pine spectrum reinforced the presumption of the different composition and lower content of polysaccharides.
c) Intensities of characteristic lignin absorption bands confirmed a presence of both, syringyl and guaiacyl units in alder and beech, while they indicated abundant guaiacyl structures and a lack of syringyl ones in pine. This confirmed a presence of characteristic softwood and hardwood lignin types in examined pine and deciduous woods, respectively. Moreover, strong lignin bands in pine spectrum aligned with a higher content of this constituent revealed by chemical composition analysis.

The studies were therefore based on three diversified tree species, providing a relatively wide overview of woody biochar feedstocks. The main differences can be observed between pine and the other two samples, *i.e.* between coniferous and deciduous trees representatives.

4.3. Properties of the synthesised chars

As catalysts in the main experiment, the three chars prepared in laboratory conditions in the two-stage process described in section 3.2.2 of Chapter 3 were used. Physicochemical properties of these fresh, steam activated biochars prepared from alder, beech and pine as well as their reactivity towards oxidation were summarised in this section.

4.3.1. Chemical properties of fresh, activated chars

Alkali and alkaline earth metals (AAEM) are commonly known as potential active sites for char oxidation. They are therefore expected to play a role in the interactions between biochar and volatiles. Four main AAEM species content in biochars was therefore analysed, and the results were presented in Figure 8. The highest impact on char gasification reactivity has been commonly assigned to potassium, followed by sodium, calcium and magnesium [17]. The most important feature of the chars would be therefore their K content, as the most abundant as well as the most influential of the analysed metals. Its concentration was high in deciduous-trees chars, especially in beech char. Pine char comprised significantly less K and the main AAEM in this char can be assign to Ca. All studied chars comprised negligible amounts of Na. Mg concentrations were relatively low as well. Ca concentration was moderate and similar in all examined chars. Measured AAEM concentrations suggested that two deciduous-trees chars were likely to be more reactive during oxidation reactions.

Other possible active sites, besides metal species, are attributed *i.a.* to functional surface groups. Various O-containing groups are the structures that are most likely to occur on carbonaceous materials [24]. The elemental analysis of feedstocks revealed presence of some nitrogen and sulphur as well, yet those elements were rather expected to be released from the material at the early stages of devolatilisation. Although reducing atmosphere of the pyrolytic step of char preparation removed most of the oxygen as well, it was later re-introduced during the activation step, creating miscellaneous structures built into the carbon lattice of the char. The main functionalities of acidic character occurring on activated carbons are carboxylic acids and their anhydrides, lactones, lactols as well as phenolic structures. The carbonyl and quinone structures, as well as some O-heteroatoms built directly into carbon rings have on the other hand of a basic nature [24].

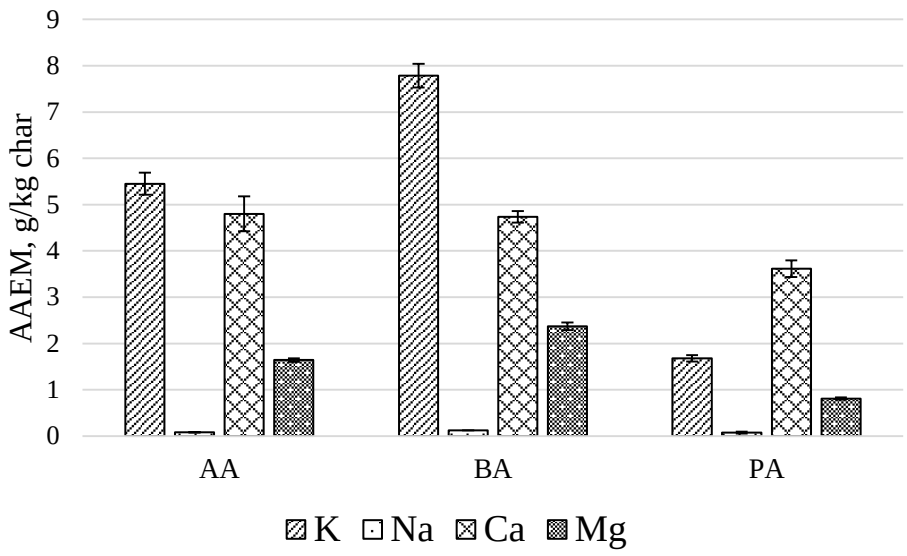

Figure 8. AAEM species content in fresh, activated chars from alder (AA), beech (BA) and pine (PA)

As presented in Figure 9, spectra of all examined chars had two main absorption regions, namely 1630 – 1420 and 1300 – 900 cm^{-1}, and three less pronounced ones at 2000 – 1660, 900 – 700 and 1420 – 1320 cm^{-1}, the last one appearing as a shoulder on one of the main peaks. At higher frequencies, the vibrations of O–H groups were expected, yet in the registered spectra, no detectable increase of absorption occurred above 2200 cm^{-1}. This might be caused by the scattered character of O–H bands and generally low intensity of ATR-FTIR spectra. Therefore, no unambiguous conclusions about the presence and nature of hydroxyl groups on char surfaces can be drawn from the analysis. It could be however assumed, that no significant amounts of –OH functionalities and aliphatic structures occurred on the samples. To enhance the readability of the most important part of the spectra, only a 2200 – 700 cm^{-1} region was depicted in Figure 9.

The first of the main absorption regions, *i.e.* 1630 – 1420 cm^{-1}, comprised the wavenumbers typical for aromatic rings absorption. Due to a high diversity of aromatic structures within char matrix, two doublet bands that can typically be distinguished in a pure compound spectrum [66] overlapped into one, wide region of increased absorption. Presence of aromatic structures can be further affirmed by numerous bands at 900 – 700 cm^{-1}, which originated from C–H bending vibrations in aromatic rings. The diversity of char structure could be confirmed, as each ring conformation has characteristic absorption wavenumbers in this area and in the registered spectra, again, they overlapped into one region of overall

increased absorption. Some overtones of aromatic rings stretching were also expected to contribute to the broad band within 2000 – 1660 cm^{-1} [66].

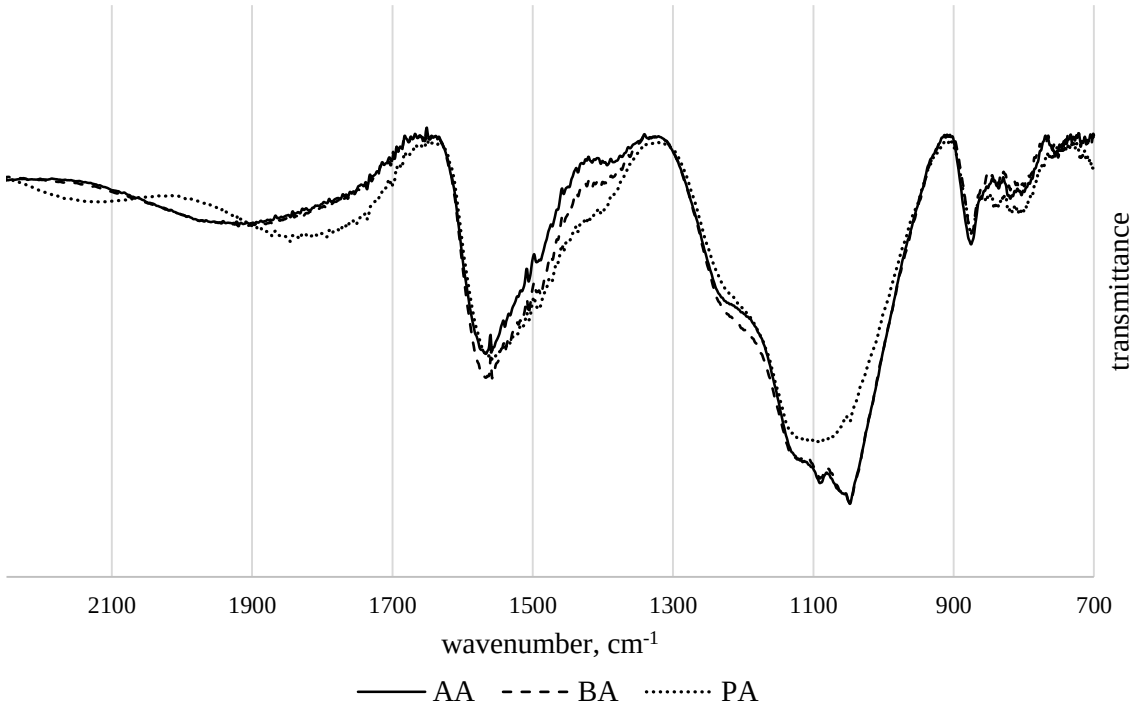

Figure 9. FTIR spectra of fresh, activated chars from alder (AA), beech (BA) and pine (PA)

Besides aromatic rings incorporated in a carbonaceous matrix, some functional groups were expected on a char surface, mostly the ones comprising oxygen atoms. One of possible structures is a carbonyl group in miscellaneous conformations. The overall absorption region for this functionality is reported to stretch as wide as from 1870 to 1540 cm^{-1} [66]. In conjugated and heavily substituted structures, especially if the intramolecular hydrogen bonding occurs, C=O absorption can shift to lower frequencies. There is therefore a possibility, that the presence of C=O attached to a dense, numerously substituted aromatic structure, *e.g.* some forms of quinones, could partially contribute to the 1630 – 1420 cm^{-1} broad absorption region. Most likely, however, C=O structures would occur at higher wavenumbers (1800 – 1660 cm^{-1}), in the form of free carboxylic acids, acid esters, lactones, ketones and quinones. Unequivocal affirmation of the presence of those structures based on the obtained spectra is unfortunately impossible, due to an overlap with the aromatic rings overtones region.

The most pronounced absorption can be observed within the fingerprint region, *i.e.* 1300 – 900 cm^{-1}. Miscellaneous single bonds absorb at these frequencies. The shape of this region is therefore often very characteristic in pure compound spectrum and enables identification of the examined species [65,66]. A heterogeneous nature of biochar diminishes diagnostic value of this part of the spectrum. The main contribution to this absorption region was most likely introduced by C–C interactions in structures of a carbonaceous matrix. Although C–H in hydrocarbons usually absorbs at around 1400 or 800 cm^{-1}, some in-plane C–H bending vibrations can occur at fingerprint region as well [65].

Moreover, it is the most typical part of an IR spectrum for vibrations of various bonds of oxygen with carbon atoms. Free carboxylic acids C–O as well as C–C(=O)–O conformation of esters and lactones absorb at higher wavenumbers, *i.e.* 1320 – 1111 cm^{-1}. Simultaneously, C–C–O vibrations in alcohol-derived part of esters occur between 1164 – 1100 cm^{-1}. Ether C–O–C group is characterised by asymmetrical stretching at higher wavenumbers, *i.e.* 1200 – 1100 cm^{-1} as well as symmetrical ones at 1070 – 1020 cm^{-1}. C–C–O in alcohols also absorbs in wide region of 1250 – 1000 cm^{-1}. Carboxylic acid anhydrides C–C(=O)–O–C(=O)–C structure vibrations occur at relatively low wavenumbers, *i.e.* 1050 – 900 cm^{-1}. Since all these functional groups fall within the registered increased absorption region of 1300 – 900 cm^{-1}, they were all plausible to occur on the examined char surfaces. However, the lack of any pronounced absorption bands around 3500 – 3000 cm^{-1} would suggests, that no significant amounts of O–H groups were present. This might suggest that free carboxylic acids and alcohols were less likely char functionalities. As free carboxylic acids thermally decompose at relatively low temperatures, below 400 °C [26], it is likely, that they were not recreated during high temperature treatment, even under oxidising conditions.

A small shoulder in the range of 1420 – 1320 cm^{-1} might result from the C–H bending in esters and lactones as well as in ketones and aldehydes. If a resonance effect occurs in the molecule, the energy of the bond between C and O atom falls between that of a single and double bond, resulting in the absorption wavenumbers correlating with this shoulder region as well. Some C–H bending vibrations in aliphatic functionalities occur in this region, however no absorption was detected at 3000 – 2800 cm^{-1}, where associated stretching of these bonds would appear. In the same manner, the C–O–H in free carboxylic acids also absorbs at these wavenumbers, although lack of absorption at the O–H stretching vibrations region suggested that it was a less plausible functional group.

Concluding, the overall shape of the obtained spectra did not unambiguously determine the structures present on a char surface, however, it could suggest a range of possible

conformations that were in alignment with the functionalities previously reported in carbonaceous material studies [14,23,24]. The carbonyl groups and C–O–C structures, as well as aromatic rings were the most probable ones to occur. No significant amounts of aliphatic and hydroxyl substituents were found on the surfaces. Phenolic and carboxylic groups were therefore expected to be present in a form of ethers and esters, rather than in a free, protonated state.

Although the major outline of the char spectrum is similar for all three samples, some differences can be distinguished, especially between pine (PA) and deciduous-trees chars, alder (AA) and beech (BA). PA absorption was slightly more pronounced within 1500 – 1350 cm^{-1} and 900 – 700 cm^{-1}, which might suggest a more aromatic nature of this char. More pronounced bands within the 1900 – 1700 region and the 1420 – 1320 cm^{-1} shoulder could also indicate higher content of carbonyl groups, *i.e.* ketones and quinones, in pine char. AA and BA absorption had on the other hand significantly higher intensity within 1200 – 1000 cm^{-1} part of the main absorption region. These lower frequencies of the C–O vibrations area are most likely resulting from oxygen bridges in ethers, esters and acid anhydrides. The higher frequencies part of the main region, *i.e.* 1300 – 1200 cm^{-1} is most likely correlated with lactones as well as some esters. At these wavenumbers, absorption was relatively similar in all samples' spectra. It is therefore plausible, that AA and BA had a higher esters and acid anhydrides content than a PA char.

A characteristic feature of AA and BA chars was also a presence of two sharp peaks at 1091 and 1049 cm^{-1}. Unfortunately, the intrinsic heterogeneity of biochar makes the unambiguous identification of the structures responsible for those peaks impossible. The presence of two sharp bands arising from the wide region of generally increased absorption suggested, however, specific types of functional groups that were abundant in alder and beech chars. Pine spectrum, on the other hand, did not suggest that it possessed any particular, favoured structures. The similarity between the 1049 cm^{-1} band in raw alder and beech wood and their char spectra did not necessarily mean that there were some hemicellulose remains left in the char. As shown further in section 4.5, wood material after pyrolytic step of char preparation lost most of its functional groups, and they were only later recreated during the steam activation step. It is however plausible, that some structures similar to the ones originally present in a raw wood were created under oxidising conditions.

Comparison of the three chars spectra suggested, that while all samples had some aromatic structures, along with oxygen functionalities mainly in form of carbonyls and oxygen bridges, the alder and beech char surface contained more groups of acidic character, like

carboxylic acid anhydrides. Pine char on the other hand might have had slightly increased amount of aromatic rings as well as carbonyls of a basic nature. The transformation from a raw wood to an activated char underwent with an intermediate step of pyrolysis under reducing atmosphere and most of the activated-char structures were re-created upon the interactions with steam. It can be however noticed that pinewood, which was more abundant in aromatic rings, because of its higher lignin content, provided a plausibly more aromatic char. Alder and beech chars, on the other hand, had more C–O structures while their raw feedstocks had higher content of hemicellulose, which absorbed at the same frequencies.

The presence of oxygen containing functional groups of acidic nature was further examined by Boehm titration method (Table 7). As the method involved sample immersion in a standard solution of a selected base and its aliquot was subsampled for further analysis, it was important for char samples to comprise only stable structures that would not dissolve into the base solution, so that the base uptake would not be affected by any labile compounds. Char pre-treatment, involving HCl and NaOH washing, was therefore necessary [99]. This however, caused an inevitable intervention into char surface groups. Although the pre-treatment proposed by Tsechansky and Graber [99] was developed in a manner that would assure the removal of the interfering species without an oxidation of reaming carbon lattice, the final step of the method involved protonation of all acidic sites. Hence, the obtained results of Boehm titrations represent the maximum number of surface functional groups. This might explain that while the FTIR spectra did not point towards any significant amounts of free carboxylic acids and phenolic groups, they were detected during titrations. It is likely, that before the protonation, they were present in a form of anhydrites and/or esters suggested by the fresh char spectra.

Table 7. Acidic sites distribution on a surface of activated alder (AA), beech (BA) and pine (PA) char, determined by the Boehm titration method

Acidic sites type, μeq/g	AA		BA		PA	
phenolic	72	±08	71	±13	69	±06
lactonic	50	±08	43	±03	57	±14
carboxylic	201	±04	208	±02	149	±14

The main acidic sites found on all char surfaces were attributed to carboxylic acids, with significantly lower amounts of weaker, lactonic and phenolic groups. The ANOVA analysis

of the obtained results suggested no significant differences between alder (AA) and beech (BA) chars. The variations between PA and AA as well as PA and BA chars should be however considered as statistically significant. This observation correlates well with the similarity between AA and BA chars FTIR spectra and their distinction from the pine (PA) char. The acidic sites distribution suggested that the main difference lied in carboxylic groups amount. This would suggest that the higher and more pronounced 1200 – 1000 cm^{-1} region in AA and BA spectra resulted from esters and anhydrides that after char pre-treatment (including protonation) resulted in increased amount of carboxylic functionalities. The Boehm titration is a common method for functional groups estimation, however, it has substantial limitations in biocarbons analysis. Besides abovementioned necessity for a char pre-treatment and therefore its structure alteration, another downside is a large amount of the sample required for the experiment. However, the main drawback of the Boehm method application is that it accounts only for some of the oxygen functionalities types. Therefore, in case of typical biochars, a substantial amount of oxygen surface structures cannot be detected with this analysis [26], *e.g.* quinones that have a basic character [24].

Another approach to functionalities assessment was undertaken by performing a Temperature Programmed Desorption TPD with online FTIR analysis of evolved gases. The obtained data was of a qualitative nature, due to the limitations of the experimental setup. A thermogravimeter was used to heat up a 100 mg of char sample with a constant heating rate of 5 K/min up to 1000 ℃ in N_2 flow. The sample mass loss was registered along with the CO_2 and CO evolution profiles derived from the FTIR spectra intensity at 2358 and 2162 cm^{-1}, respectively. A large sample mass, necessary to provide enough gas yield for FTIR detection, resulted in diffusional restrictions within the TGA crucible, potentially delaying the decomposition and elution of some functionalities, despite a low heating rate applied. However, registered DTG curve of char decomposition (Figure 10) reviled some characteristic temperatures, which correlated quite well with peaks of CO and/or CO_2 yields (Figure 11). The test was performed on a fresh activated alder char (AA) as well as AA char retrieved from the reactor after a steam reforming blank run (AA_H2O_b), when no tar compound was fed. Hence, the AA_H2O_b sample could be considered a fresh AA char that was steam activated for additional 60 min, as explained in section 3.4.1 of Chapter 3. The gases evolved from the samples were represented by the time profiles of the absorption at selected wavenumbers, corresponding to the carbon oxygen bond in CO_2 and CO. CO absorbs at two bands, and as a preliminary assessment revealed that their absorption profiles are almost identical, the higher wavenumber was selected as a representative.

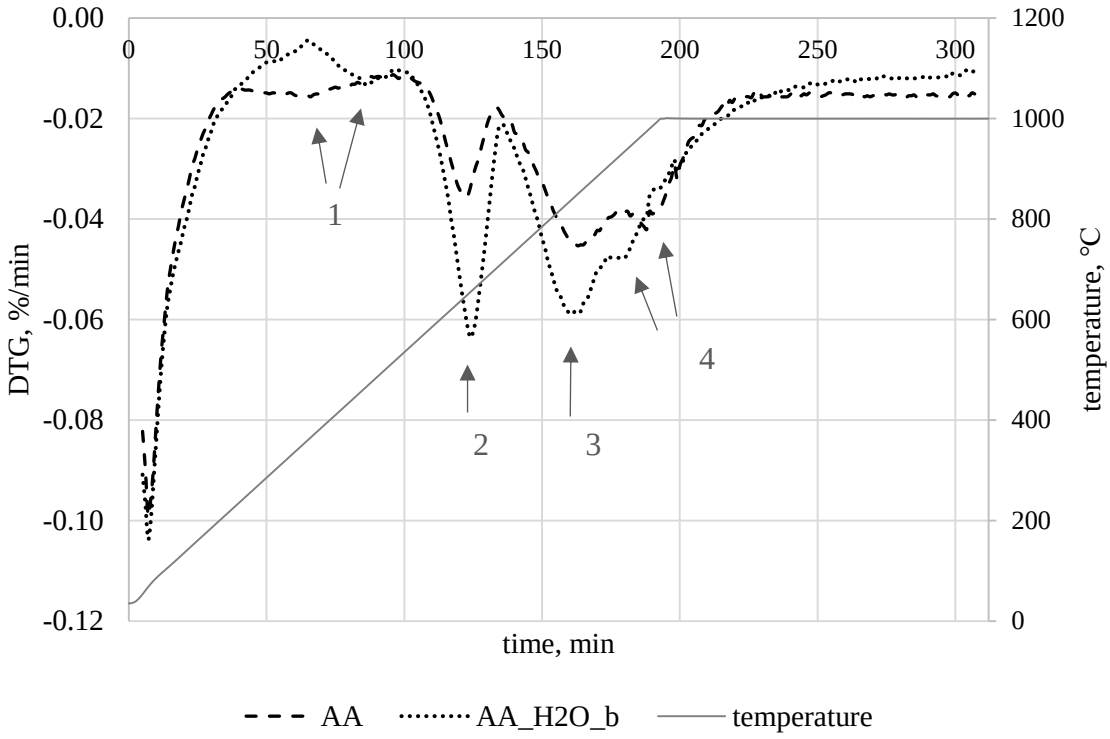

Figure 10. First derivative (DTG) of mass loss registered during the TPD-FTIR analysis of alder char activated for 80 (AA) and 140 (AA_H2O_b) min with 4 characteristic mass loss regions indicated

Although usually preformed with chemisorption instrument coupled with mass spectrometer, the TGA-FTIR analysis of pyrolysis at slow heating rate could be considered a Temperature Programmed Desorption experiment as well. It was performed *e.g.* by Gao et al. [69] for a pine saw dust examination. Since the yield of volatiles released from the raw wood is relatively high, a 10 mg sample could be used for their experiments. To obtain similar IR absorbance during activated char analysis, much higher sample mass was required for the purpose of these studies. Nevertheless, the quality of obtained spectra was still relatively poor. The drift of the baseline was measured in a blank run and subtracted from the experiment results, but an overall intensity of the selected wavenumbers absorption was still increasing constantly throughout the experiment, as presented in Figure 12. It is possible that due to a large sample mass, some low-temperature species continued to evolve at higher temperatures due to mass and heat transfer restrictions, although this would rather result in more irregular deviations, instead of a linear drift that was registered. Hence, it is more plausible, that a baseline drift in a blank run was less intense than during the char experiments and the applied correction was insufficient. Similar baseline drift could be seen

in a 3D FTIR graph of pine pyrolysis performed by Gao et al. [69] despite a smaller sample mass that was used. Despite the low resolution of the obtained FTIR data, some major peaks in CO and CO_2 elution profiles could still be distinguished. As the quantification of the spectra profiles was not performed and the apparatus' response is higher for CO_2 than CO, any ratio between the yields of those species could not be directly obtained. However, since the absorption at the certain wavenumber is linearly proportional to a corresponding gas concentration, a magnitude of an amount of a compound that was released with respect to time could be assessed. Moreover, a comparison of the characteristic temperatures for CO and CO_2 release with corresponding mass losses registered with TGA enabled some insight into the relations between the amounts of released CO and CO_2.

The main regions of mass loss during Temperature Programmed Desorption of chars could be represented by the peaks of the first derivative plot (DTG) obtained from the thermogravimetric analysis. Besides the initial mass loss related to water evaporation [23], four main DTG peaks have been distinguished, as indicated in Figure 10 and further summarised in Table 8.

The main qualitative difference between examined samples was visible at lower temperatures. 1st DTG peak could be observed at 365 ℃ (66 min) for AA measurements, while for AA_H2O_b a narrower, more pronounced peak at 475 ℃ (90 min) was detected. The CO_2 evolution profile showed a slightly increased yield at 60 min for AA test. The wide and flat shape correlated with a wide DTG profile curve at this point. The 90 min CO_2 shoulder peak for AA_H2O_b is clearly visible. Interestingly, during desorption run for this char, a depression in CO_2 yield and mass loss rate was experienced at 60 min, *i.e.* at the point where a release of some species from AA char was maximised. At lower temperatures no CO yield was detected.

A large, sharp DTG peak (no 2) occurred at 120 min of the experiment, *i.e.* at the temperature of 635 ℃. It correlated well with main CO_2 yield peak. It was slightly smaller in AA experiment and a shoulder peak at 130 min could be distinguished. The AA_H2O_b sample released more CO_2 at this region, which was confirmed by a more intense mass loss of this sample. Most likely due to an overlap, only one, large CO_2 evolution peak can be observed in this case. At this stage of the temperature program, evolution profiles did not indicate any significant release of CO. A small shoulder peak in AA_H2O_b profile could be noticed. In case of AA no CO was detected.

At higher temperatures, two overlapping peaks (no 3 and 4) occurred in both experiments. 3rd DTG peaks at 163 and 165 min for AA and AA_H2O_b, respectively, can be attributed

to the CO evolution that was most pronounced at this point of the experiment, while no significant CO_2 yield was registered. This observation suggested the decomposition of the functional groups that break up solely to CO. On the other hand, both gases release contributed to the following 4th DTG peak at 180 and 190 min for AA_H2O_b and AA, respectively. Both, CO and CO_2 evolution profiles for both chars revealed corresponding peaks, and the elution time shift between AA_H2O_b and AA matched the one registered in the DTG plots.

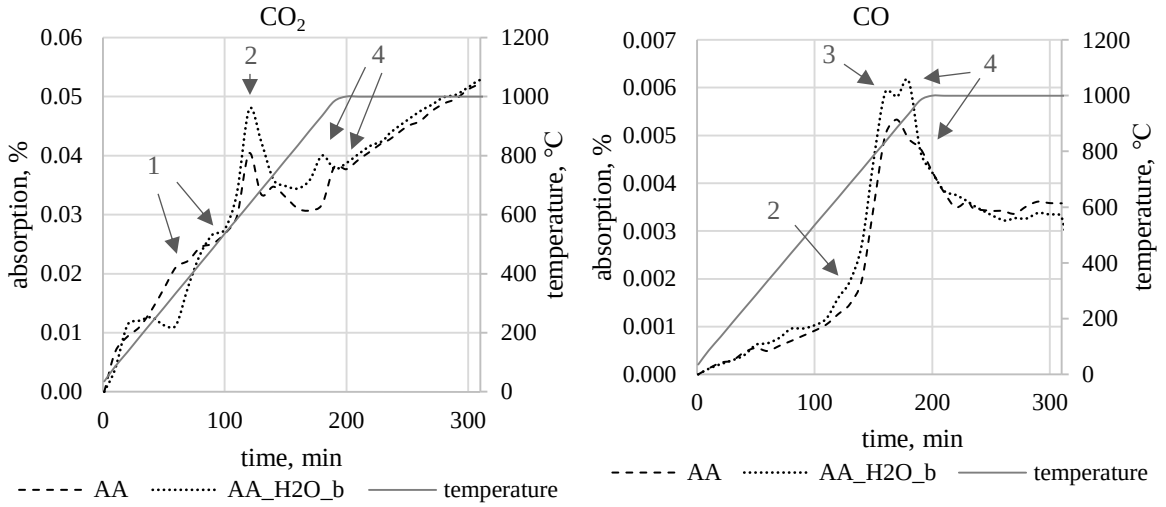

Figure 11. Evolution profiles of CO_2 and CO released from fresh activated alder char (AA) expressed as an absorption registered during an on-line FTIR analysis. Correlating temperatures of the TPD process are indicated with the solid line, correlating DTG peaks are indicated with numbers 1-4

In general, the AA char mass loss was less intense than the AA_H2O_b one, which can be expected as the prolonged activation step was likely to enhance oxygenates creation on the char surface. There was also a qualitative difference to the registered DTG curves. The dominating step of the desorption experiment of the AA_H2O_b char was the CO_2-related mass loss at 120 min. In case of AA, the 3rd and 4th steps were more intense than the 2nd one. Moreover, within those last two decomposition steps, in AA experiment the 3rd one, derived solely from CO evolution, was more intense, while in AA_H2O_b the following decomposition peak originating from both CO and CO_2 evolution was more pronounced. Based on the characteristic temperatures and released gaseous products, each desorption step could be assigned to a certain functional groups decomposition [26]. Therefore, while the quantitative difference between the examined samples could be attributed to the magnitude of the char activation/oxidation, the changes in the relative intensities between registered

mass loss steps could suggests a change in the types of O-functionalities that were created with an increase of the steam-char interaction time.

Table 8. DTG curve peaks registered for TPD of alder char activated for 80 min (AA) and 140 min (AA_H2O_b), t_i, t_f – initial and final temperature of distinguished mass loss step, t_p – temperature at the peak mass loss rate, x – indication of the species being released during the mass loss step based on the FTIR analysis

Peak	AA					AA_H2O_b				
no	t_i, ℃	t_f, ℃	t_p, ℃	CO_2	CO	t_i, ℃	t_f, ℃	t_p, ℃	CO_2	CO
1	235	535	365	x		365	535	475	x	
2	565	705	635	x		535	720	635	x	x*
3	705	935	860		x	720	910	850		x
4	935	1000	975	x	x	910	1000	935	x	x

* very weak

The characteristic temperatures for functional groups desorption varies significantly, depending on both, material parameters: surface area; pore structure; functionalities configuration; *etc.*, as well as on the TPD experiment conditions such as heating rate or reactor geometry [23]. However, some general conclusions regarding nature of the desorbed groups could be drawn based on the similar studies reported so far [14,23,26,27]. It is generally agreed upon, that the CO_2 evolution below 400 ℃ derives from carboxylic groups. Carboxylic anhydrites are reported to decompose at temperatures as low as 350 ℃ and up to 900 ℃ [23,26], yielding both CO and CO_2, with a molar ratio of 1:1. Lactones, another acidic sites type, desorb at similar temperatures, although yielding only CO_2. Phenolic groups decompose to CO between 600 – 800 ℃. At higher temperatures, above 700 ℃, some basic structures like carbonyls and quinones start to decompose, yielding CO. It was also reported [23,28,29], that at temperatures above 900 ℃ pyrone and chromene-like structures of carbon matrix can decompose into CO and possibly also to CO_2. Some cases of a high temperature CO_2 release was reported in literature, yet no particular structures could be assigned to this phenomenon [107].

Most of the reported TPD experiments were carried out for commercial carbons with a significantly diversified surface groups compositions [23,26] prepared by a liquid activation with nitric acid or hydrogen peroxide. The studies reported by Klinghoffer et al. [14] comprised TPD of gasification char from poplar wood, with the preparation method

relatively comparable to the one used in these studies, *i.e.* a gas-phase activation with H_2O/N_2 for 60 min at 750 °C. The similarities between the nature of feedstock and char preparation technique justified the comparison between the obtained results. The evolved gas analysis of poplar char tests revealed CO_2 release peaks at 350 and 700 °C. The former was attributed to carboxylic acids and surprisingly lactones, usually ascribed to higher temperatures. The latter peak was assigned to the carboxylic anhydrides, despite the lack of CO evolution at this point of experiment. The two high temperature CO peaks were however detected, and they corresponded well with the ones registered in AA and AA_H2O_b tests. In Klinghoffer et al. [14] experiment, they were attributed to the basic quinone and carbonyl sites, as expected. It is worth mentioning, that a small CO_2 peak above 900 °C was present as well, although it was not discussed in detail by the authors.

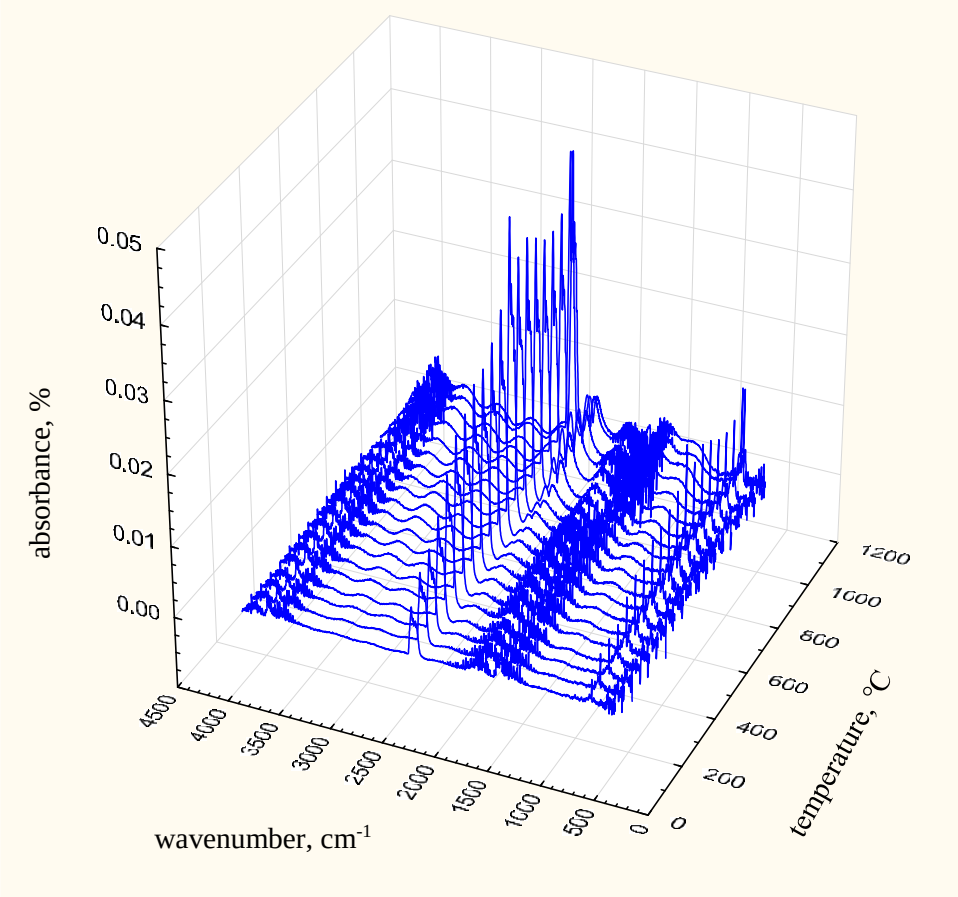

Figure 12. The online FTIR spectra of the gases evolved from activated alder (AA) char during TGA pyrolysis with respect to the linearly increasing temperature (5 K/min).

A similar TPD profiles were reported by Zhuang et al. [108] for the phenol-formaldehyde resin based carbon prepared in an oxygen gasification process. This gas-phase activation resulted in the carbon with negligibly low carboxylic acids content. The main CO_2 peak at 627 °C was attributed to carboxylic anhydrites and lactones, while the high temperature peak of CO was assigned to carbonyl groups of a basic nature.

Following the common TPD peak interpretations, the 1st registered DTG peak (Figure 10) would result from the carboxylic acids decomposition, while the 2nd arose due to carboxylic anhydrides. A weaker FTIR instrument response to CO and a generally poor resolution of the obtained spectra, could explain the lack of the expected CO yield peak from the anhydrides during AA char analysis, as the actual scale of CO evolution at this region might be obscured by a signal noise. A small amount of CO registered during the experiment with a more activated sample (AA_H2O_b) supports this hypothesis. Due to the discrepancies in the lactones desorption temperatures reported in the literature [14,23], this group might comprised either a part of the 1st or the 2nd registered DTG peak. No pronounced CO evolution at lower temperatures suggested that no significant phenolic sites were present at the char surface.

The TPD-FTIR analysis, therefore, supported the FTIR analysis results, suggesting that there are no significant amounts of hydroxyl groups on the fresh char surface and that phenols and possibly free carboxylic acids were created only during the pre-treatment for Boehm titration experiment due to hydrolysis and protonation of original active sites that were rather comprised of anhydrides and esters.

This assumption might be further justified by the nature of acidic sites. They are easily destroyed at relatively low temperatures, therefore most of them desorb during the pyrolytic step of char preparation (as can be seen in the non-activated char spectrum presented further in section 4.5). The release of acidic sites creates the active places rich in unpaired electrons and during a following activation step, introduced oxidising agent recreates acidic sites [14,27]. However, the gas-phase oxidation is expected to favour high-temperature sites creation [27]. It is therefore expected, that the recreated functionalities were comprised mostly of the more resistant, condensed structures like esters and anhydrides, rather than free carboxylic acids or phenols. Although the distinction between the particular structures that comprised these two groups (DTG peaks no 1 and 2) might be debatable, they are all unambiguously attributed to the active sites of an acidic nature.

The main CO release corresponding with DTG's 3rd peak was most likely a result of basic sites decomposition, namely carbonyls and quinones. A higher temperature 4th peak was

mainly due to some further, more resistant basic structures decomposition, *e.g.* pyrones and chromenes. It is possible, that the CO_2 released at those high temperatures was indeed correlated with some pyrone structures decomposition.

Despite the overlapping of some species release temperature zones and a week intensity of the FTIR spectra, some general observations could be drawn:

a) The CO_2 release could be assigned mainly to acidic sites decomposition that occurred at lower temperatures, represented by 1st and 2nd DTG peaks. The 3rd and 4th DTG peaks were derived from basic sites decomposition, yielding mainly CO. Comparing the areas of the registered peaks, it should be expected that a significant part of oxygen containing surface functionalities were of a basic nature. Hence, the Boehm titration, by providing acidic sites distribution, does not show the overall amount of catalytically active oxygenated structures present on the char surfaces.

b) The narrower, more intense 2nd DTG peak, compared to a wide mass loss comprised within the 3rd and 4th one, suggested a higher uniformity of acidic functionalities. The oxygen-containing, basic structures, some of them potentially embedded directly in the aromatic rings as heteroatoms, were most likely more diversified and desorbed through a wider range of temperatures.

c) Comparison between AA_H2O_b and AA char suggested, that upon the prolonged activation, as the overall amount of functionalities increased, the ratio of acidic to basic sites increased (area of the 2nd peak compared to the sum of 3rd and 4th ones). This suggested that gas-phase oxidation creates mainly acidic sites, while the basic sites occurrence might be related rather to the structural features of the material, *e.g.* surface area and carbon matrix arrangement.

Examination of the chemical properties of the samples revealed general similarities between the wood-derived biochars. They are all comprised of a carbonaceous lattice with some built-in aromatic structures. Each char also contained some AAEM species and oxygen functionalities that are considered as catalytically active sites. Although no hydroxyl groups were unambiguously determined on the surface, the presence of lactones, carboxylic anhydrites and esters were the likely acidic structures. The hydration and protonation of the surface revealed the gradation in the acidic sites strength, and the carboxylic groups were the most abundant ones, after the samples treatment. The Temperature Programmed Desorption of alder char suggested the occurrence of the oxygen structures of a basic nature. Their abundance and temperature resistance suggested that they might be highly important during the heterogeneous catalytic reactions. As the acidic sites creation was strongly

correlated to the extension of the activation process, basic sites might be related more to the overall structural properties of the chars.

The char derived from the pine possessed a slightly lower amount of AAEM species and acidic sites compared to the deciduous-trees chars. The difference might have originated either from the raw wood properties, like inorganics content and polymeric constituents structure, or it could be related to the physical properties, *e.g.* the available surface area, of the char carbonaceous matrix that acts as a support for those active sites.

4.3.2. Physical properties of the fresh, activated chars

Although the catalytic conversion over a carbonaceous material is expected to undergo selectively on the active sites, and therefore does not depend directly on the physical properties of the materials, the char morphology determines accessibility and dispersion of those sites [27]. While AAEM species presence is related rather to the inorganics content in the original feedstock and the char preparation method [7], the functional groups are highly influenced by the carbon lattice structure [27]. The matrix created during the pyrolysis of original wood is comprised of graphene-type layers [30]. Their size and arrangement determines the number of so-called "unsaturated" carbons, *i.e.* atoms located at the edges of the lattice or at the sites of structural defects [16]. Those atoms possess unpaired electrons and therefore comprise highly reactive sites within the carbonaceous matrix. A high temperature activation in a gaseous phase introduces oxygen which can reacts with unsaturated carbons creating O-containing functional groups of either acidic or basic nature. Therefore, the carbon lattice could be considered a support for the active sites [27]. Although functional groups creation itself is caused by oxidising agent, char surface area development determine the potential for those groups creation. Moreover, the unsaturated carbons themselves are considered the sites for hydrocarbons conversion. They are often reported as the most important ones, due to their high abundance and temperature resistance [14]. Additionally, the carbon planes with high π-electron density are expected to act as basic sites for conversion reactions [5]. Therefore, the morphology of the carbon catalysts is of a particular importance. It not only governs the mass transport of the gaseous compounds towards and from the catalytic active sites, as some inorganic catalytic supports, but it also acts as a catalyst itself [16,27]. Therefore, some main structural features of biochars were examined.

As was mentioned above, the surface area of the carbonaceous material indirectly influences the amount of specific active sites, but it itself possesses catalytic properties of a basic nature

in form of unsaturated carbons and π-electron rich plane. Since the exact amount and strength of those structures would be extremely difficult to quantify, the surface area itself is often considered as a quantifying parameter regarding those basic catalytic sites [16,34]. One of the most popular techniques for surface area analysis is the measurement of an isotherm of a N_2 gas adsorption and estimation of the area using BET model [34,41]. The external surface area of the sample can be calculated from t-Plot model. The difference between those to values is considered an area of the micropores within the sample. A simple approximation of the adsorption average pore width was also considered in the char comparison. It was calculated from BET analysis as 4V/A, where V is a pore volume and A is a surface area of the sample. The outsourced analyses of BET and micropores areas as well as the average pore widths of the fresh, activated chars were presented in Figure 13.

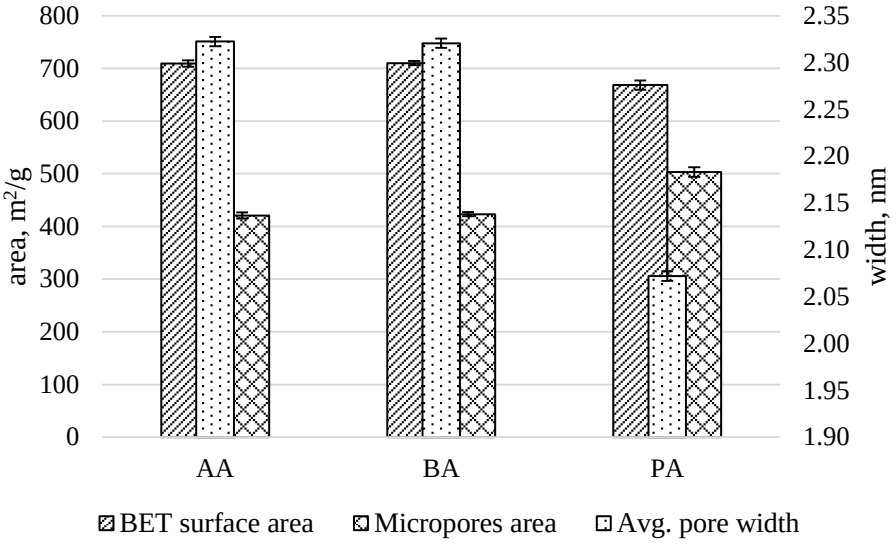

Figure 13. BET surface area and the area of the micropores, as well as the adsorption average pore width for fresh, activated chars from alder (AA), beech (BA) and pine (PA) wood

The structures of the two deciduous-trees chars (AA and BA) were almost identical, with a high surface area of approximately 700 m^2/g and a substantial microporosity, *i.e.* around 57 % of the total surface area was comprised of the micropores. The pine char (PA) had a slightly lower BET surface are of 668 cm^3/g but a significantly higher microporosity, as the micropore area comprised 75 % of the total surface. As can be expected, higher microporosity involved a lower average pore size. PA char had, on average, pores smaller by *ca.* 10 % than BA and AA chars. A lower BET surface area plausibly entailed fewer

active sites in the form of unsaturated carbons, while smaller pores hindered the accessibility to other active sites types. Higher microporosity also made PA char more prone to sintering by coke created during hydrocarbon conversion.

The most important differences between the chars, in terms of their catalytic performance, are the ones occurring at the nanoscale, *i.e.* pores structure, and atomic scale, *i.e.* AAEM and functional groups distribution. The SEM micrographs of chars taken with magnification between x100 and x3000 allowed for a general char structure observation in a macroscale. Some captured features were presented in Figure 14.

The micrographs taken at lower magnification (Figure 14 *a* and *b*), where whole particles were captured, revealed a more ruffled surface of deciduous-trees chars compared to a pine-derived one. Although this macroscale diversification between the samples was less likely to contribute to their catalytic efficacy, it suggested, that the devolatilisation and/or activation of pine was less rapid, yielding char with a smoother surface.

Although obtained SEM micrographs did not reveal the microstructure of the samples, they provided a general overview of the activated chars morphology. Some basic structural features of the original feedstock remained after pyrolysis and activation. Char particles shape and the fibrous arrangement, typical for woody materials, was preserved, as can be seen in Figure 14 *a* - *c*. Thermal treatment is known to evoke melting of some of the polymeric constituents in wood. During the devolatilisation step, lighter compounds are released from the sample. Their escape from the plasticised matrix can create gas bubbles, which are eventually perforated, leaving round craters on the forming char surface [109]. Those craters can be seen in some of the micrographs, as shown in Figure 14 *d*. A variety of original wood tissue relicts can be still present in char samples (Figure 14 *e* and *f*). Rapid devolatilisation and following steam radicals attack created an abundance of cracking, uneven structures on the otherwise rather smooth particles surface.

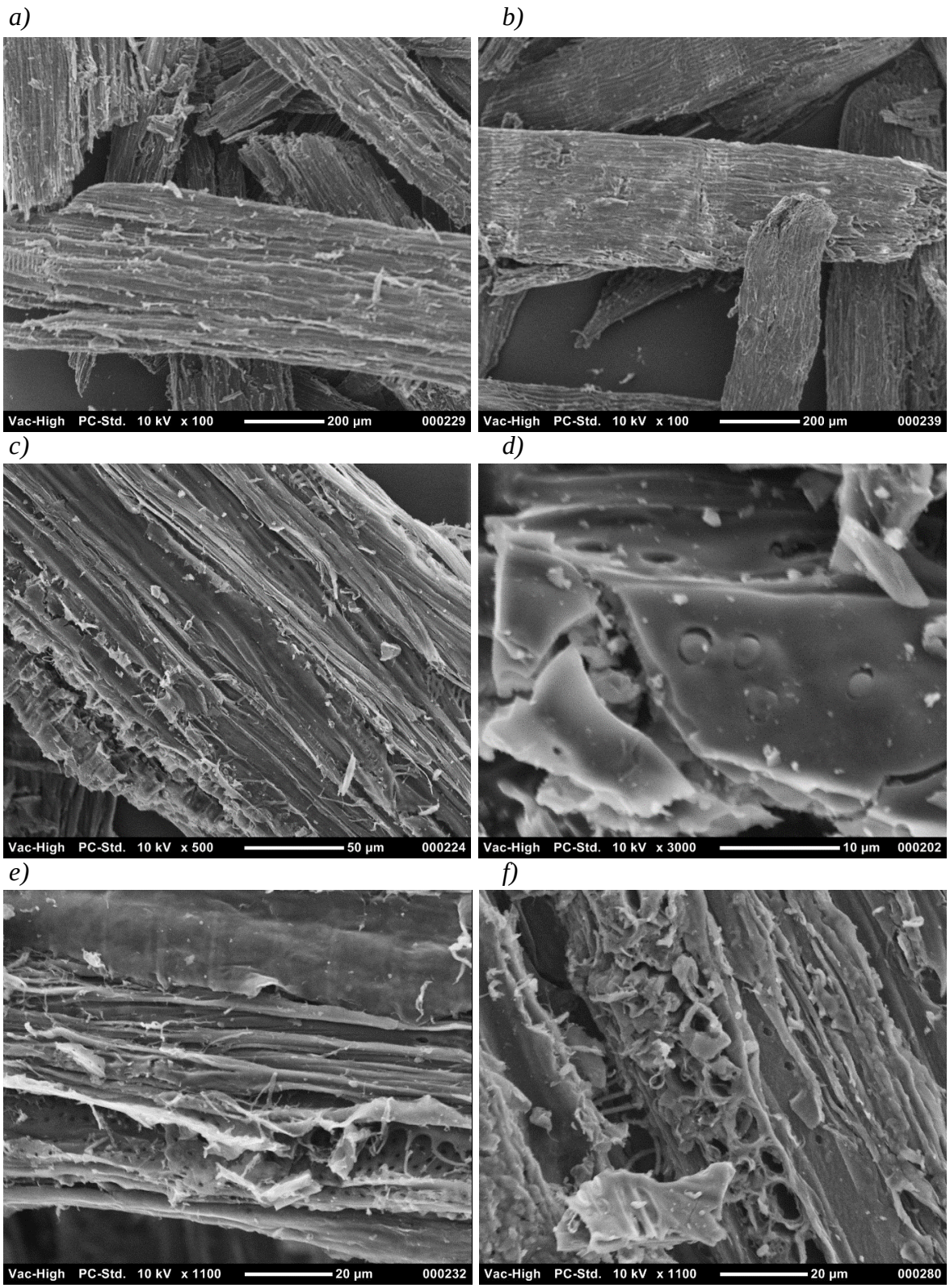

Figure 14. SEM micrographs of activated alder (a) and activated pine (b) char particles, a still fibrous structure of the alder char (c), craters left by volatiles escaping plasticised beech polymeric constituents (d) and the variety of wood structure relicts still visible in alder (e) and beech (f) chars

4.3.3. Kinetics of char oxidation

Physicochemical properties of the material are considered to have a strong influence on its catalytic activity towards hydrocarbon conversion. Carbon-based materials, contrary to inorganic catalysts, are also reactive towards oxidising agents present in the synthesis gas from the gasification. Hence, in the heterogenic tar removal over char bed, two types of reactions occur simultaneously. Hydrocarbons decompose on the char surface, while the oxidising gases gasify the char itself. This latter phenomenon was expected to occur during the steam reforming SR mode experiments in this research. Therefore, besides physicochemical examination of the catalysts, the experiment aimed to access chars reactivity towards oxidation was conducted.

To this end, small samples of finely milled chars were oxidised in TGA runs, with O_2 as an oxidising agent. The char gasification during the SR mode was overlapping with the hydrocarbon conversion over the char surface, which involved active sites occupation by the decomposing compound as well as coke deposition as a by-product of this reaction. Moreover, the gasification reaction during the SR mode was involving both, original char as well as the deposited coke layer. Therefore, only the initial step of char oxidation was considered in the TGA experiments, to establish a char nascent potential towards oxidation. The rest of the oxidation was not considered relevant for the SR mode experiments evaluation due to the discrepancies in the reaction conditions. The kinetics of the mass loss within the range of 3 – 10 % were examined, and obtained activation energies (E_a) and pre-exponential coefficients (A) for the fresh, activated chars were presented in Figure 15. The initial and final temperatures of the considered mass loss region were also provided.

The activation energy of the deciduous-trees chars were significantly lower than the E_a of pine char. This suggests that the AA and BA char were much more reactive towards oxidising agents. This observation was expected, since all performed material tests favoured those chars in terms of their potential reactivity as catalysts, as well as reactants in oxidation reactions. The lower reactivity of PA char entailed higher temperatures at which the initial mass loss occurred. The AA char activation energy was only slightly higher than BA char, yet the difference in the temperature range of the reaction was substantial. The FTIR analysis and Boehm titration revealed almost identical parameters of those chars. The surface area and porosity were also very similar. Therefore, it is plausible, that a slightly higher K content in beech char was responsible for slightly lowering its E_a and quite significantly lowering the oxidation temperatures. The lower reactivity of pine char, where both, temperature zone as well as E_a discrepancies were substantial, might have been caused mainly by its

substantially lower AAEM species content, and possibly to some extent by its higher microporosity.

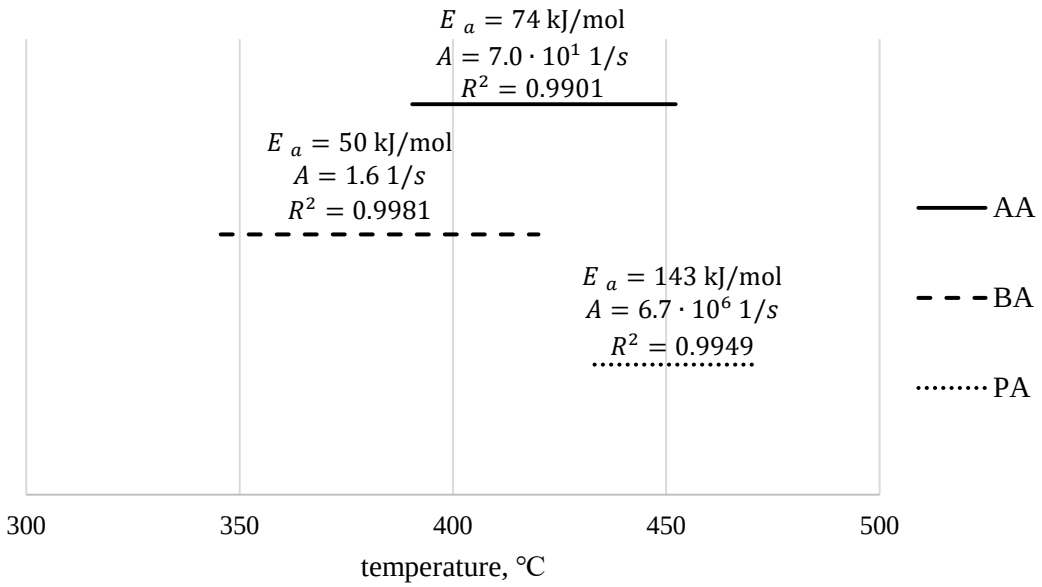

Figure 15. Activation energy E_a and pre-exponential coefficient A of initial oxidation of fresh, activated alder (AA), beech (BA) and pine (PA) char with temperature range of the considered mass loss region

4.3.4. Summary of the findings

Activated biochars with an abundance of potential active sites and well-developed surface area were prepared from three different wood species. All three biocatalysts have structure typical for the biomass-gasification derived chars. They had BET surface area of around 700 m^2/g, *i.e.* larger than inorganic catalysts (~1 – 200 m^2/g [49,110]) and smaller than the commercial, chemically activated carbons (≥1000 m^2/g [34]). They also have a significantly microporous structure, typical for biochars, compared to the commercial carbons with a higher mesopores volume [34]. As opposed to the liquid-phase, chemically activated materials [14,23], prepared biochars had a substantial amount of temperature resistant basic groups, and higher temperature acidic sites, important in high temperature processes, like tar removal. AAEM species content in biochars varies significantly due to feedstock properties and preparation technique. The concentrations detected in these studies fell into a general rage reported for similar materials [14,20].

Since all chars were wood-derived and prepared under the same conditions, their properties were generally similar. The most distinguishable differences were found between pine and deciduous-trees chars. This observation was in accordance with the distinctiveness of the

coniferous pinewood among the examined feedstocks. Pine (PA) char had approximately 30 m^2/g lower surface area, although over 18 % more micropores, 1.3 – 4.6 times lower AAEM species contents and almost 15 % less acidic active sites on its surface. The oxidation reactivity of PA char was significantly lower than other chars, as indicated by its 1.9 – 2.9 times higher activation energy, compared to deciduous trees chars. Examined differences suggest a better potential of alder and beech chars towards catalysing high temperature tar conversion processes. These findings implicate that deciduous trees might be a more suitable feedstock for a production of biochar with good catalytic properties.

4.4. Toluene conversion over biochars

The main part of this research was focused on the hydrocarbon conversion over a biochar bed. As explained in detail in Chapter 3, the basic experiment comprised toluene decomposition over a char bed in an externally heated, vertical, quartz reactor at an 800 °C isotherm. Real tar was substituted with a pure compound to ensure more uniform reaction conditions and to enable analysis of the reaction by-products. Toluene was selected as a representative of light aromatic compounds with a single, simple functional group. Light tar molecules are considered more refractory than the heavier, larger species [36,92]. Therefore, a study of a single-ring molecule was considered of a higher significance than using polyaromatics. Moreover, it was generally established that more substituted structures were more prone to decomposition [92]. Benzene is therefore considered the most difficult for removal. A complete lack of any side groups is however less interesting in terms of possible interactions with the char surface and a number of created by-products. Toluene, with a single methyl group and no oxygen atoms, provided a manageable amount of reaction products, while remaining a refractory compound suitable to representing light tars.

The tar conversion process was further simplified by introducing a controlled gaseous atmosphere, instead of a real syngas with a highly diversified composition. Toluene decomposition process was studied in two modes, one comprising pure N_2 as a carrier gas, *i.e.* pyrolysis (PYR) mode, and the second with the presence of 15.5 vol.% of steam in N_2 flow, further referred to as a steam reforming (SR) mode. This approach enabled differentiation between the high-temperature heterogeneous toluene interactions with active sites on the char surface and the potential direct toluene-steam reactions. Since biochars, as carbonaceous material, could themselves undergo oxidation, blank tests of steam reforming without toluene introduction were performed, to obtain background information on the char gasification during the appropriate SR runs. Moreover, some spent char samples were

collected for analysis to assess the changes to their properties upon their interaction with toluene. The results of all tests carried out during the main experimental work as well as the spent char analysis were summarised in this section.

4.4.1. Toluene conversion during PYR mode

Pyrolytic toluene conversion experiments were carried out according to the procedure described in Chapter 3, where the details of each test run were listed. The decomposition reaction was carried out at 800 °C, with a different feeding time for each test run. Toluene conversion as well as liquid and gaseous by-products yields were analysed post-run. All three steam-activated biochars, *i.e.* alder (AA), beech (BA) and pine (PA) chars were studied at this stage of the research.

Toluene conversion was determined as a ratio of the converted to the amount fed of the compound. It was calculated for each experimental run, *i.e.* each reaction time, according to the equation:

$$\eta_T = \left(m_{Tf} - m_{Tr}\right)/m_{Tf} \tag{8}$$

where, m_{Tf} is the total mass of toluene fed during a test run (in mg) and m_{Tr} is the mass of unreacted toluene recovered from the impinger bottle after the run (in mg).

Liquid by-products of toluene conversion were collected in the impingers and analysed post-run with GC-FID. Their yield was expressed as molar ratio of a created by-product to a converted toluene amount, calculated for each run as:

$$x_i = m_i/\left(m_{Tf} - m_{Tr}\right) \cdot M_T/M_i \tag{9}$$

where m_i is a mass of *i*-th by-product recovered from the impingers (in mg) and M_T and M_i are molar masses of toluene and *i*-th by-product, respectively (in mg/mmol).

Toluene conversion was presented in Figure 16. The initial conversion for short feeding times was high for all tested chars. Prolonging the time of char exposition to toluene flow resulted in a continuous decrease of η_T due to a progressing deactivation of catalyst. This phenomenon was commonly experienced in similar studies and was usually ascribed to the solid conversion by-product, *i.e.* coke, depositing on the catalyst surface [15,36]. Coke layer covers active sites as well as fills pores and sinters pores' mouths, decreasing surface area of a catalyst [34]. Carbonaceous coke appears on inorganic catalysts as well as on carbon-based ones. The nature of coke is expected to be similar to that of carbon matrix of the

catalyst itself, although it most likely lacks oxygenated groups and AAEM species and has lower porosity. It therefore deteriorates the inherent catalytic properties of the char, like the presence of inorganic, and it annihilates the effects of activation, like developed porosity and created functional groups.

Among tested biochars, pine (PA) char provided lower toluene conversions throughout the whole studied reaction time. This could be attributed to the overall worse catalytic properties of this char – lower amount of functional groups, AAEM species and surface area. The slope of the conversion plot was also steeper for PA, which indicated a more rapid deactivation of this char. It was suggested by Moliner et al. [41], that highly microporous structures are more prone to deactivation, since micropores get sintered more easily. More mesoporous structures are considered more stable catalysts for hydrocarbon conversion [34]. As micropores constituted 75 % of the total surface area of PA, while it represented roughly 59 % of AA and BA chars, slower deactivation of the latter could be justified.

Besides a highly likely coke deposition from toluene conversion, some liquid by-products of the decomposition were detected. The main recovered by-product was benzene (Figure 17), suggesting that some of the toluene underwent demethylation. For all studied chars, x_B increased for the initial 30 min of the conversion experiment and stabilised at a constant level afterwards. At the beginning of the process, coke deposition is expected, as suggested by the deactivation of chars. As at this stage of the experiment, benzene yield was low and it increased with progressing char deactivation, leading to a conclusion that the toluene conversions to coke and to benzene were two competing conversion pathways. Initially, toluene favoured conversion into a solid deposit, but as the char was being saturated with coke, more toluene begun undergoing demethylation to benzene. After char surface deactivation with a carbonaceous layer, benzene yield reached its stable, maximum yield. This phenomenon was also detected in the preliminary studies with a commercial activated carbon, described in detail further, in section 4.6, where the coke yield was also accessed via a gravimetric method [111]. The correlation between a coke yield decrease and benzene yield increase, followed by reaching stable levels of both, at the similar time of experiment, supported this hypothesis. Both of those reactions required an access to a char surface, since with test runs on empty reactor no significant toluene conversion was experienced, as mentioned in Chapter 3. The two conversion pathways were therefore expected to compete for the char surface access, with the coke formation being a favoured one. The deactivation of active sites on the catalyst's surface had an inhibiting effect on a further coke creation,

and most likely a less pronounced effect on demethylation, therefore the latter became more significant with time.

Toluene by-product yields in this study were reported on the basis of reacted toluene. Hence, they provided information on what share of converted toluene ended up as a certain by-product, rather than gave information on the absolute amounts of created species. As can be seen in Figure 17, there were no significant differences in benzene yields between studied samples. Since the overall toluene conversion over PA char was lower, the absolute amount of yielded benzene was adequately lower than in AA and BA tests. The matching of the plots after conversion to the presented, relative values, gave an evidence that the significance of toluene demethylation reaction in the course of the experiment was the same for all the chars, despite the difference in their catalytic affinity towards overall toluene conversion.

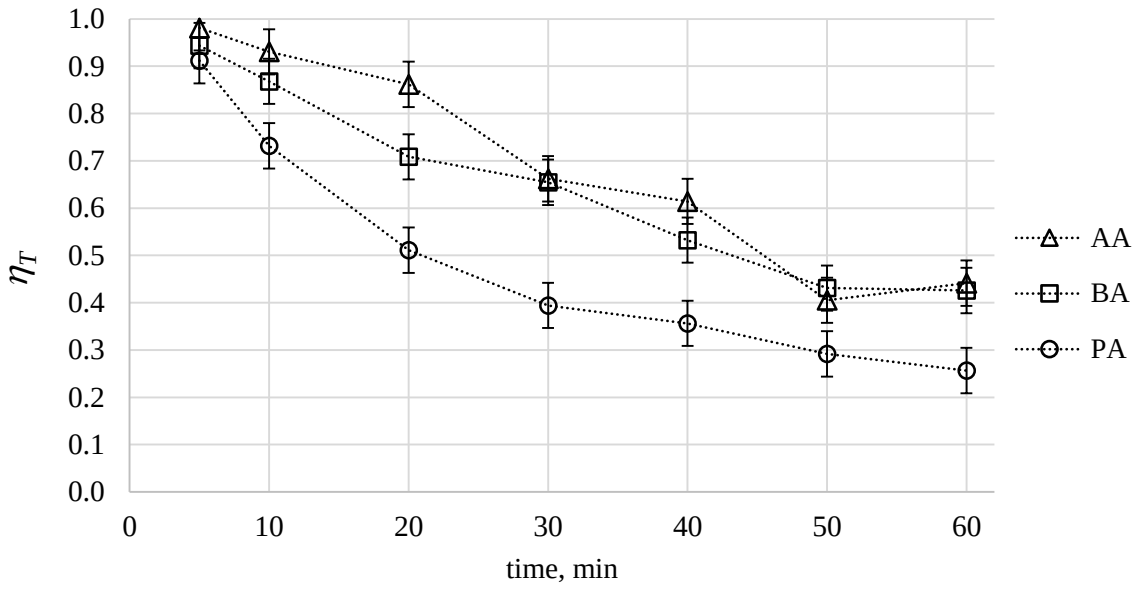

Figure 16. Toluene conversion in time during pyrolysis over alder (AA), beech (BA) and pine (PA) chars

Another group of liquid by-products was comprised of substituted benzenes that most likely resulted from recombination of benzyl and methyl radicals created during toluene pyrolytic conversion [72,79]. The relative yields of those species (based on reacted toluene) are presented in Figure 18 in ppm units, as they were two orders of magnitude lower than benzene's. Three peaks corresponding to toluene substitution products were detected with GC-FID. They were corresponding to the following species: ethylbenzene; *p*-xylene and/or *m*-xylene; *o*-xylene and/or styrene. Unfortunately, due to overlapping retention times, the differentiation between two species assign to each, the second and the third peak was

impossible. The assumption of the *o*-xylene presence in the last detected peak was justified by the findings of other xylene isomers. The presence of styrene proved to be very plausible as well, as will be explained further in section 4.7.4 where *p*-xylene decomposition by-products are detailed, including *p*-methylstyrene. Therefore, an average of *o*-xylene and styrene molar masses was used in Eq. 9 for the third peak's yield calculation.

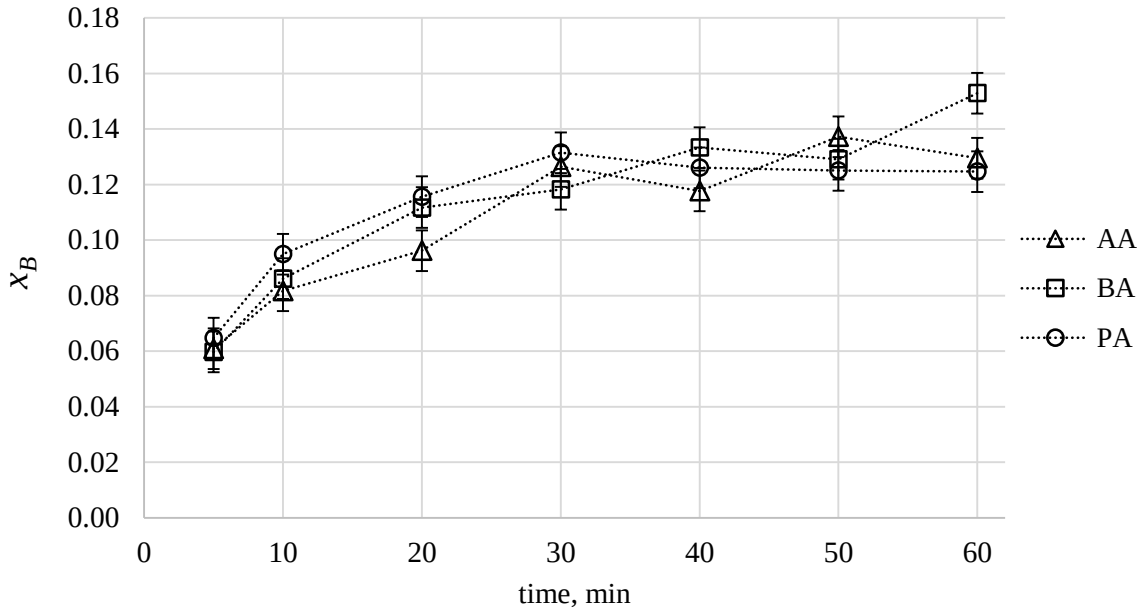

Figure 17. Benzene molecular yield (converted toluene based) for pyrolytic experiments with alder (AA), beech (BA) and pine (PA) chars

The species recovered from the impingers suggested two types of radical recombination mechanism taking place during toluene conversion. Both pathways would involve substitution on either an aromatic ring in a toluene molecule, resulting in xylene formation, or the methyl group in a toluene molecule (or already created benzyl radical), forming ethylbenzene. Due to pyrolytic conditions of the process, the ethyl- group would further undergo dehydrogenation, yielding styrene. Since the ethylbenzene yield (Figure 18 a) was substantially higher than yield of xylenes (Figure 18 b), the reaction with toluene methyl group is most likely the favoured one. This observation is in alignment with a lower energy of the C-H bond in methyl group than in the aromatic ring [71]. Methyl group in toluene molecule is an ortho, para directing one. Therefore, it could be expected, that similar yields of *o*-xylene and *p*-xylene were created, while significantly lower amounts of *m*-xylene were formed. Under this assumption, and because of a very similar FID response to both compounds, roughly 80 % of the third peak (Figure 18 c) could be ascribed to styrene,

making it the main product of toluene substitution reactions. This conclusion is in alignment with the further findings for *p*-xylene conversion tests (section 4.7.4). Since no other compounds were detected, it is likely that the recombination reactions were involving only phenyl and benzyl radicals and that the restricted gas residence time in the reaction zone prevented any following reactions, like *e.g.* methyl addition to ethylbenzene to create a propyl group. The only further rearrangement would therefore be an ethylbenzene dehydrogenation to styrene.

For all examined chars, the yields of all substituted benzenes were increased with the experiment time. This behaviour was similar to that of benzene, suggesting that the recombination reactions were competitive to coke deposition. The demethylation to benzene was also likely linked to the following toluene substitution, as it provided methyl radicals for the recombination process. Substituted benzenes formation was increasing even after benzene yield reached a plateau. This might suggest that their creation was even more dependent on the availability of demethylation products than on the char surface activity. Nevertheless, toluene recombination reactions, along with benzene formation, could be jointly considered a pathway competing to the favoured and more effective one of toluene decomposition via coking.

While comparing examined chars, the higher yields of substituted benzenes were registered in PA char tests, especially the ethylbenzene one. This observation, again, might suggest that the recombination reactions were relying more on the demethylation products than on the char surface itself, while benzene creation, initially hindered by competition with coking, required access to a char surface. Therefore, both coking and demethylation were related to char surface activity, and while their contribution to the toluene conversion was similar for all chars, the absolute amounts of created coke and benzene were lower for PA char. If, as suspected, the recombination did not rely on the catalyst surface as strongly as coke and benzene creation, it would be less influenced by the lower activity of PA. Therefore, its contribution to the overall toluene conversion was higher for PA than for AA and BA chars.

As explained in Chapter 3, gases released during the experiment were collected into a series of Tedlar bags and analysed post-run. During the PYR mode experiments, some H_2 and CH_4 were created, as presented in Figure 19. Their relative molecular yields were expressed on the reacted toluene basis. Since the sampling interval was 1.5 min and the experimental run times were equal to $t = \{5, 10, 20, 30, 40, 50, 60\}$ min, the relative molecular yield of an *i*-th gas species for the *t* time run was calculated according to the equation:

$$x_{i,t} = \frac{\sum_{n=1}^{n=n_t}\left([i]_n/[N_2]_n \cdot \dot{n}_{N_2} \cdot \tau_{int}\right)}{n_{T,t}} \quad (10)$$

where $[i]_n$ is the concentration of the *i*-th gaseous species detected in *n*-th tedlar bag (in vol.%), the $[N_2]_n$ is the concentration of the N_2 detected in *n*-th tedlar bag (in vol.%), $\dot{n}_{N_2}$ is the molar flow of N_2 fed into the reactor during the experiment (in mol/min), τ_{int} is the time of sampling interval (in min), and $n_{T,t}$ is the amount of toluene (in mol), converted during an experimental run with a feeding time *t*.

Contrary to the SR mode, described in detail in the following section 4.4.2 no CO and CO_2 was detected. This was expected due to a lack of gasification reactions in an inert atmosphere. The amounts of CO and CO_2 that might have appeared due to acidic sites thermal desorption (as registered with TPD-FTIR presented in section 4.3.1) would be below the detection limits of the applied GC-TCD analysis.

H_2 formation could be assigned mainly to dehydrogenation that accompanied coke deposition. It was commonly experienced in similar studies that as a molecule adsorb on the catalyst surface, it releases H_2 while transforming into a dense and non-reactive carbon-rich layer [15]. Some H_2 is also created during above mentioned ethylbenzene to styrene dehydrogenation, although due to minute amounts of those species, it is not expected to bring any visible contribution to the registered yields. CH_4 is expected to be created manly during toluene demethylation to benzene. CH_4 formation was increasing during the initial 20 min of the experiments similarly to benzene. The CH_4 yields oscillating within a range of 0.15 – 0.25 were of the similar magnitude as the benzene ones (0.12 – 0.14), suggesting that the creation of both compounds could be ascribed to the same conversion mechanism. Assuming that some of the created benzene was *in situ* decomposing on the char surface, the nascent benzene yield would be even higher to the one detected downward the reactor. Further studies, detailed in section 4.7.3, revealed that during a 30 min benzene pyrolysis, approximately 40 % of it was converted. Taking this assumption into account, the nascent benzene yield before its partial, *in situ* decomposition would therefore amount to 0.20 – 0.23, which would bring it even closer to the detected CH_4 yields.

Despite high measurement uncertainties for performed gas analysis, a conclusion supporting the quicker deactivation of PA char could be drawn from obtained results (Figure 19), as both, CH_4 and H_2 yields from this char reached their maxima at shorter experiment times (20 min) than the yields from AA and BA tests (50 min).

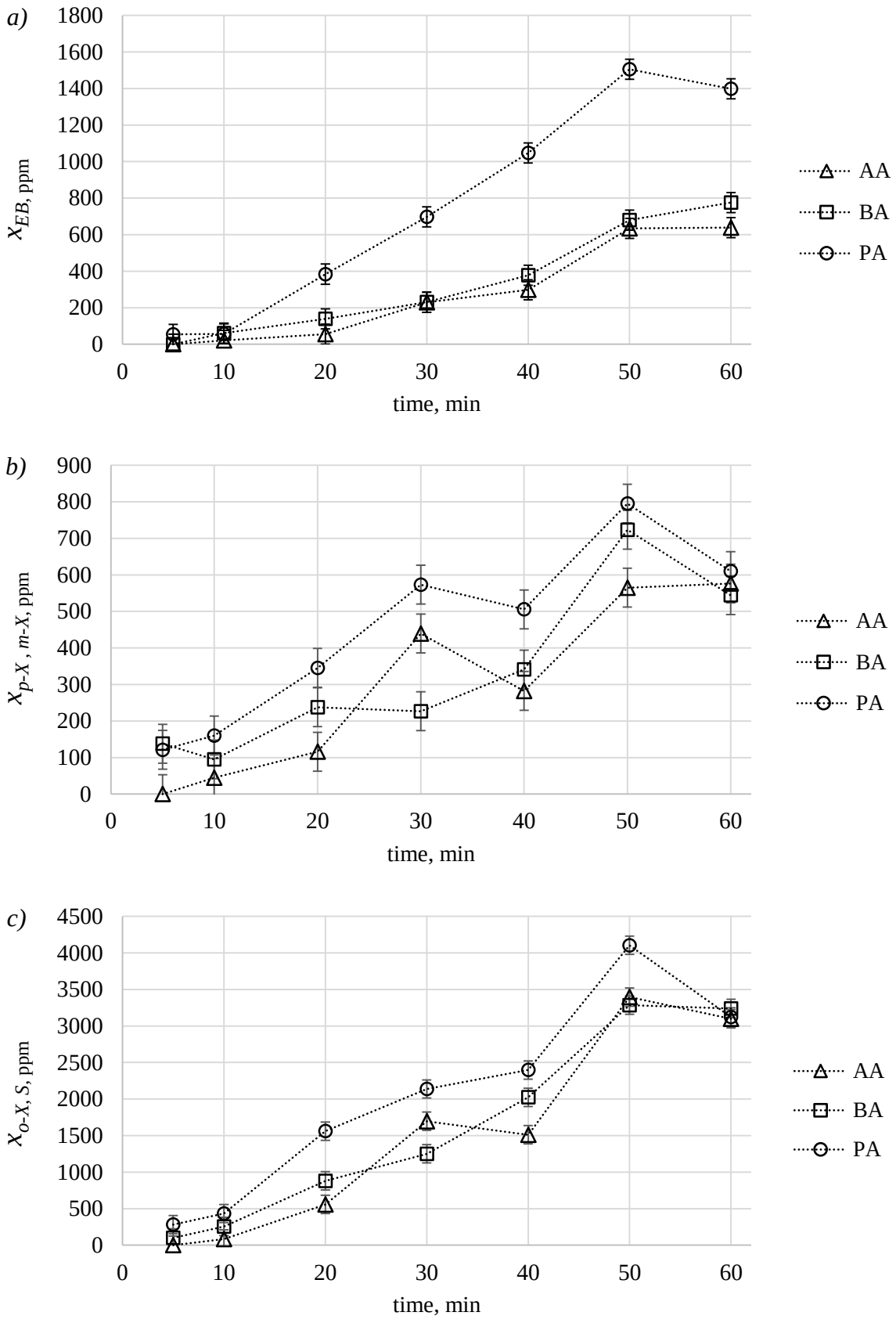

Figure 18. Molecular yields of substituted benzenes (based on reacted toluene) a) ethylbenzene, b) p-xylene and/or m-xylene, c) o-xylene and/or styrene for pyrolytic experiments with alder (AA), beech (BA) and pine (PA) chars

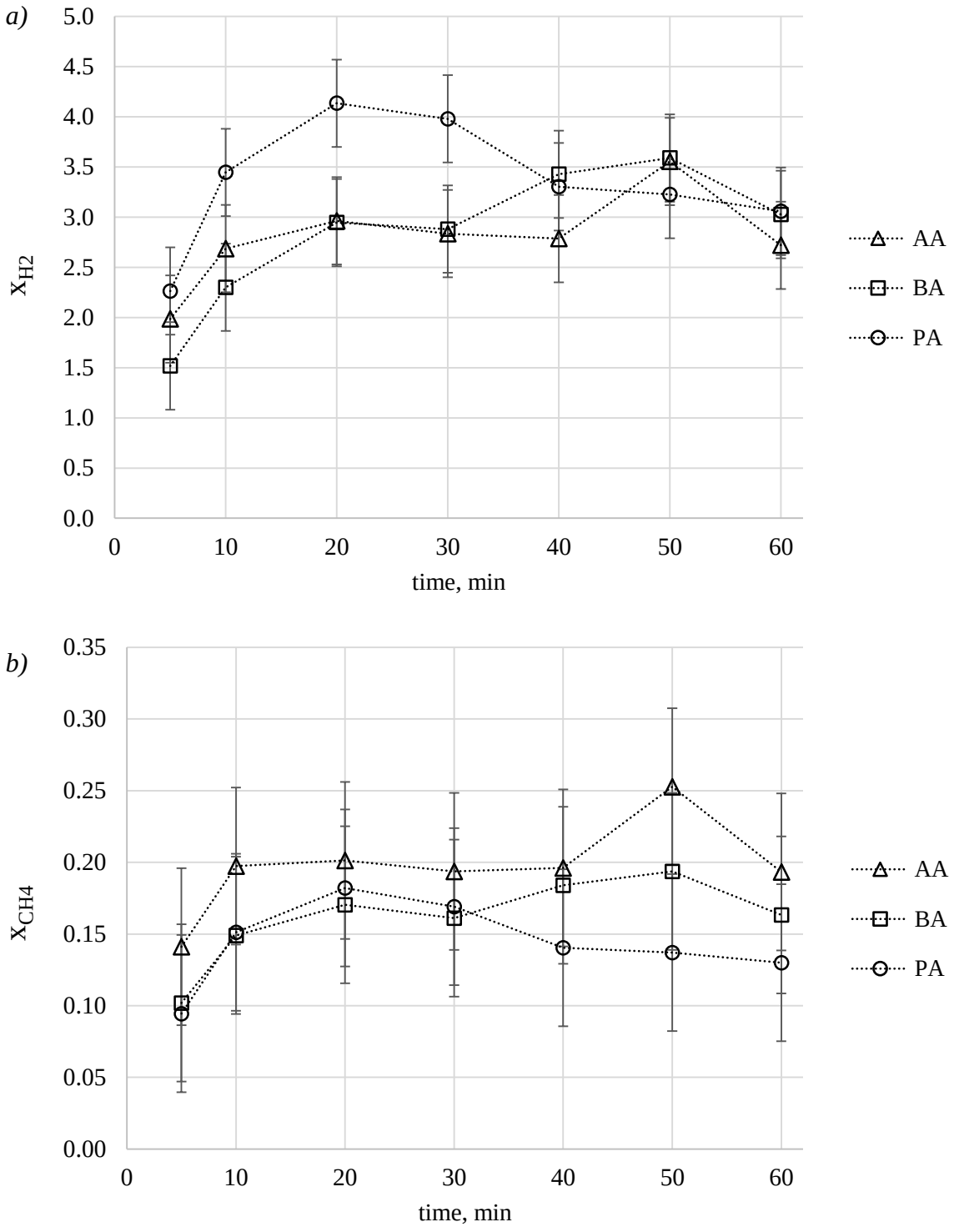

Figure 19. Relative molecular yield (based on reacted toluene) of H_2 and CH_4 released during pyrolytic experiments with alder (AA), beech (BA) and pine (PA) chars

As opposed to the SR mode or a real gasifier, studies on the pyrolysis (PYR) mode allowed isolating toluene conversion reactions from any char/coke oxidation or gas-phase interactions. Therefore, a mass balance of the toluene conversion could be easily performed.

The sum of H and C mass comprised in all detected gaseous and liquid by-products was subtracted from the mass of toluene converted during an experimental run. Therefore, an estimation on the amount of coke deposited on a char surface was obtained as presented in Figure 20 a. Due to a lower conversion of toluene over PA char, coke yield on this catalyst was significantly lower. As the 0.5 g char bed was used in each experiment, the estimated coke yield after 60 min pyrolysis comprised *ca.* 0.14 wt.% of PA and 22-23 wt.% of AA and BA chars initial bed mass.

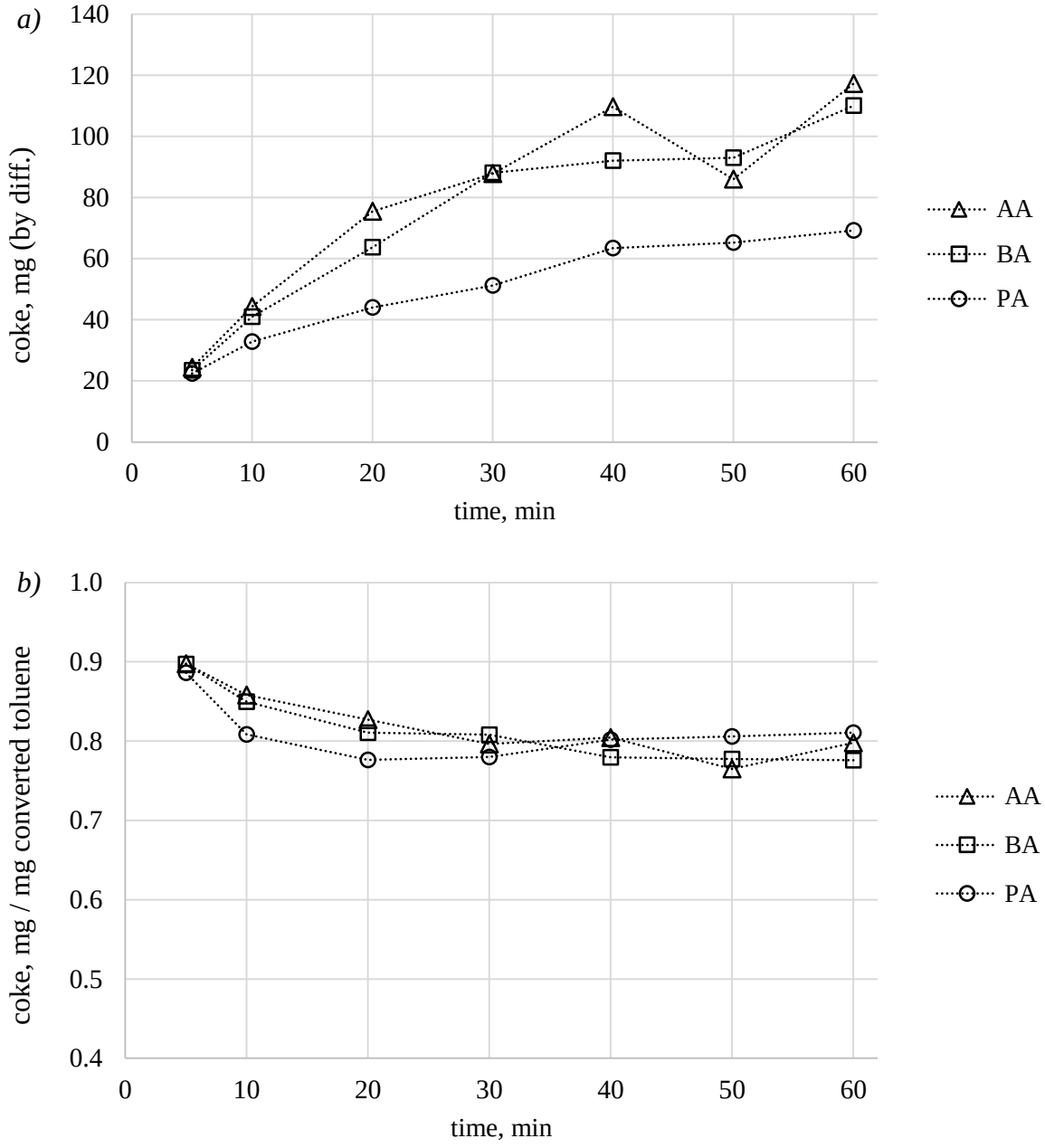

Figure 20. Deposited coke amount determined form the mass balance for toluene pyrolytic decomposition as well as coke's relative mass yield (based on reacted toluene) on alder (AA), beech (BA) and pine (PA) char

When the calculated coke yield was expressed as the mass percentage of the converted toluene (Figure 20 b), the share of toluene that decompose into coke revealed to be similar for all studied chars, and initially it was as high as 90 wt.%. This supports the generally acknowledged theory, that tar decomposition via coke formation is a dominating, primary mechanism [5,15]. However, although highly effective and favoured, it inevitably leads to catalyst deactivation, due to poor catalytic properties of the created coke layer as well as catalyst's porosity deterioration. Therefore, as the char becomes saturated with coke, the share of this reaction pathway in the overall conversion decreases, at the expanse of gaseous and liquid products yield, as well as the overall conversion itself becomes inhibited. As can be seen in Figure 20 b, a decrease in the coke formation predominance took place during the initial 20 (PA), 30 (AA, BA) minutes of the experiment. The steeper slope for PA char can be observed, which again suggests a more rapid deactivation of PA, despite a lower overall amount of coke that was deposited on its surface. Although the total BET surface are of PA char was only slightly lower than that of AA and BA chars, higher microporosity lowered the PA char's capacity for coke accumulation significantly (from 22 to 14 wt.%).

4.4.2. Toluene conversion during SR mode

Steam reforming (SR) experiments were carried out analogously to the PYR mode tests, with the only difference in the composition of gas introduced into the reactor. During the time of toluene feeding, the atmosphere was switched from inert, to an oxidising one, comprising 15.5 vol.% of steam in N_2 flow. Toluene conversion as well as liquid and gaseous reaction products were analysed, and data obtained are discussed in this section.

Toluene conversions, calculated according to Eq. 8, were presented in Figure 21. The initial conversions, for 5 min runs, were high and similar for all studied chars. Although the initial conversion values during the PYR mode, where for all the chars $\eta_T > 0.9$, were slightly higher than during the SR mode, a one-way ANOVA analysis did not indicate a significant difference between the two modes, for 5 min test runs ($p = 0.14$). Despite a similar initial efficiency, a deterioration in toluene conversion with the increasing reaction time was however slower during the SR mode. For 60 min runs in SR mode, conversion for all studied chars remained higher than 0.6, while during pyrolytic experiments, it decreased as low as to approximately 0.4 for AA and BA and below 0.3 for PA char. A milder inhibition of the conversion reaction during SR mode could be attributed to a slower char deactivation [15,36]. The presence of steam resulted in a gasification of char and depositing coke, simultaneously to toluene decomposition and coke formation. It is generally regarded, that

if a coke gasification rate is higher than a coke formation rate, a catalyst maintains its reactivity during a tar removal process [5]. However, if a catalyst is comprised of organic carbon, the oxidation of the catalyst itself would occur, diminishing the mass of the catalyst's bed [13]. In these studies, although the deactivation was not prevented completely, it was significantly slowed down by the presence of steam. The PA char performance was still slightly worse than the other two chars, but the differences were less pronounced than during the PYR mode. This observation supports the assumption that the lower toluene conversions over PA chars were caused by more extensive deactivation. Inhibition of the deactivation process diminished the negative effects of high microporosity of this char. The lower reactivity of PA char towards oxidation, determined by TGA experiments, was that the activation energy of PA char was roughly two times higher than that of AA and BA. This suggested, that the re-activation of catalysts surface with steam was less pronounced for PA char, thus lower toluene conversions were still detectable.

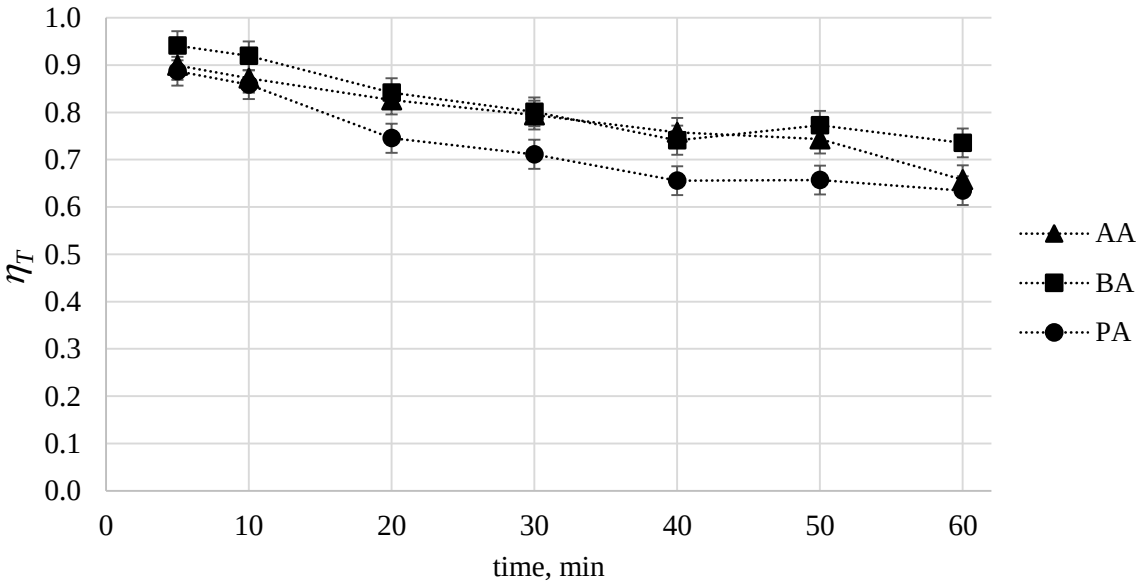

Figure 21. Toluene conversion in time during steam reforming over alder (AA), beech (BA) and pine (PA) chars

Benzene molar yields, calculated according to Eq. (9), were presented in Figure 22. A general trend in benzene formation with reaction time was similar to the one during PYR mode experiments, *i.e.* its yield was increasing within the initial 30 min before reaching a steady level. Maximum benzene yields reached during SR mode were relatively similar to the ones from PYR experiments. ANOVA analysis of the collective results for all chars in

either PYR or SR mode, suggested that the differences in x_B between the modes for experiment times of 50 and 60 min were not statistically significant, with *p*-values of 0.54 and 0.18, respectively. This would suggest that the proportion between the toluene conversion via coking and through demethylation was not affected by the introduction of steam. It is likely, that toluene decomposition in SR mode underwent in the same, heterogeneous way as during PYR mode, and steam, independently from toluene reactions, acted only as an oxidising agent for char/coke gasification. This would suggest that no steam-derived radicals attack on toluene in the gaseous phase occurred. The lack of toluene decomposition experienced during the preliminary steam reforming test in an empty reactor supports this hypothesis.

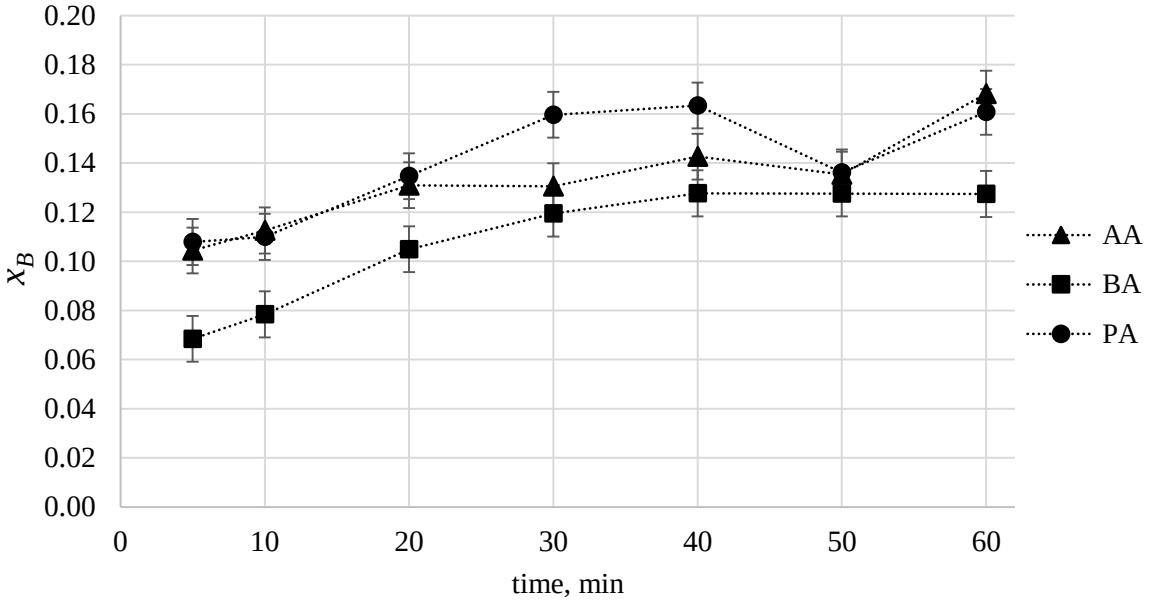

Figure 22. Benzene molecular yield (converted toluene based) for steam reforming experiments with alder (AA), beech (BA) and pine (PA) chars

Substituted benzenes were also created during the SR mode experiments with their yields increasing in time (Figure 23), although to a significantly lower extend than under a PYR mode. A maximum reached by substituted benzenes during 60 min SR experiments, correlated with the yields obtained in PYR mode at the 10-20 min of the experiment. It is therefore plausible, that a prolonged activity of the char surface, due to steam re-activation, delayed the recombination reactions of toluene. Despite a high scatter of the obtained data, slightly higher yields for the experiments with PA char could be noticed. This correlated well with less enhanced re-activation of this char, due to its lower oxidation reactivity.

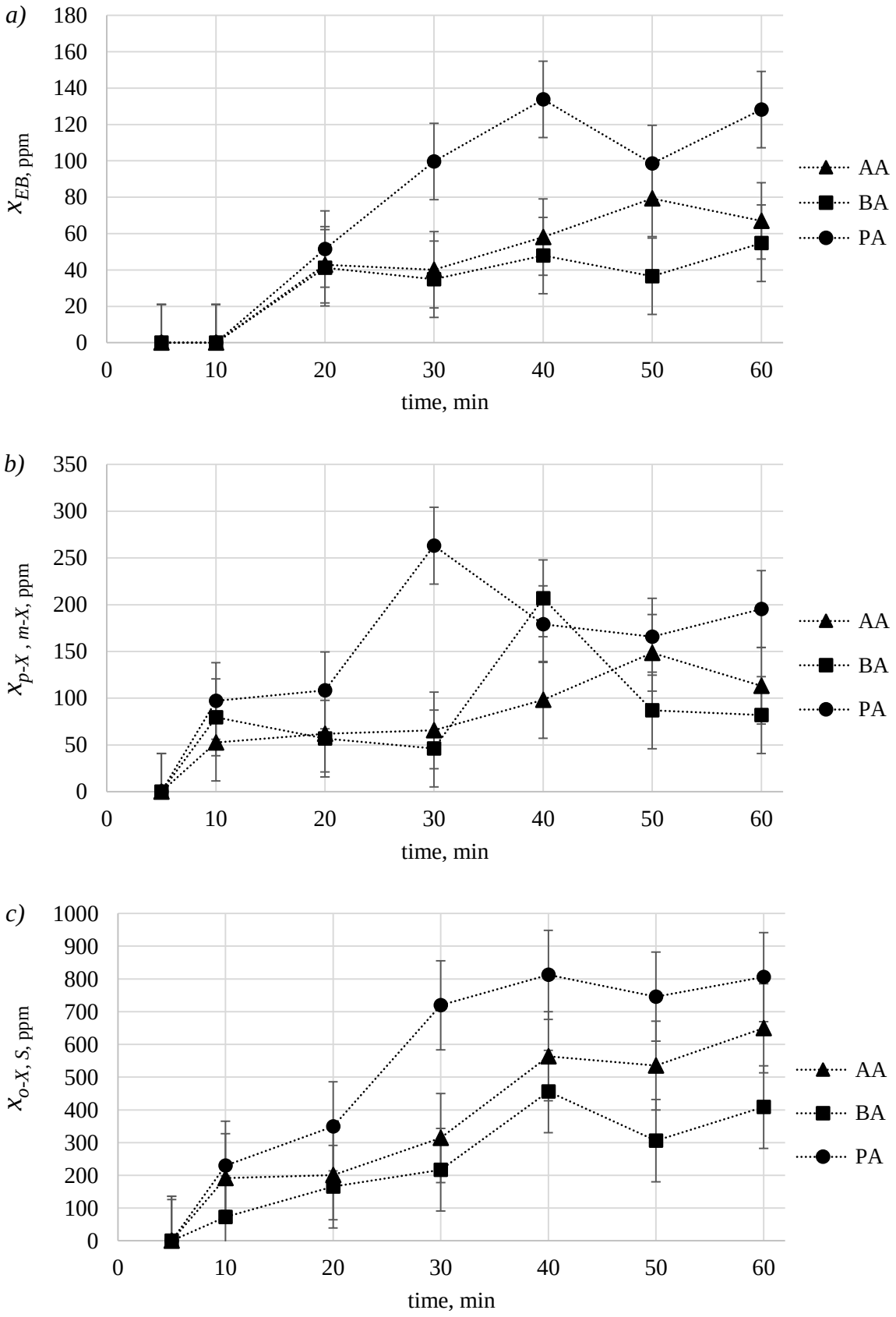

Figure 23. Molecular yields of substituted benzenes (based on reacted toluene) a) ethylbenzene, b) p-xylene and/or m-xylene, c) o-xylene and/or styrene for steam reforming experiments with alder (AA), beech (BA) and pine (PA) chars

As explained previously, since the methyl group is known to be para, ortho directing, an assumption could be made that *p*-xylene and *o*-xylene yields were similar and the *m*-xylene yield was negligibly low. A rough estimation of the styrene yield could be therefore made by subtraction of the *p*-xylene/*m*-xylene yields (Figure 23 b) from the o-xylene/styrene (Figure 23 c). This analysis would suggest that styrene was again, the most abundant type among created substituted benzenes, similarly to the PYR mode. Moreover, the ratio of estimated styrene yield to detected ethylbenzene yield for each experimental series was calculated. To capture the well-developed recombination process, ratios obtained for the 40, 50 and 60 min test runs were averaged and presented in Table 9. The ratios for SR were higher than during PYR mode for all examined samples. This suggested that dehydrogenation reaction converting ethylbenzene to styrene would be more enhanced during SR mode. Although counterintuitive, a more pronounced dehydrogenation reaction under oxidising conditions could be attributed to a catalytic effect of biochars. A use of carbonaceous materials as catalysts in an oxidative dehydrogenation of ethylbenzene to styrene was studied for the chemical synthesis purposes [27]. It was established, that ethylbenzene adsorbs on two neighbouring carbonyl groups. The following desorption involves dehydrogenation to styrene and functional groups transformation into hydroxyl ones. Finally, the oxidising agent used in the process, usually O_2, air or CO_2, regenerates carbonyl groups, yielding H_2O. It is therefore plausible that the steam introduced into the reactor also initiated this type of mechanism, thus enhancing styrene creation, especially, since the oxidative dehydrogenation is considered more effective than the classical one carried out in the inert atmosphere [27]. The enhanced dehydrogenation upon steam introduction is especially pronounced for PA char, where the ratio increased from 1.9 to 5.1, and as FTIR analysis suggested, this char might possess more basic functional groups, *i.e.* carbonyls and quinones, than the other two chars. Although the initial recombination reactions, leading to toluene methylation, were expected to rely mainly on the reactivity of the gaseous phase in the reaction, especially availability of methane, there is however, a possibility that the char surface was involved in observed effective and rapid dehydrogenation of the created ethylbenzene. The possible char involvement in dehydrogenation (both oxidising and the one during PYR mode) could explain why the overall substituted benzenes yields in PA char tests were increased due to their independence on the char activity, while the styrene/ethylbenzene ratio for PA in PYR mode was lower than for AA/BA char tests, as this particular rearrangement still relied on a catalyst activity.

Table 9. A ratio of an estimated styrene yield to a measured ethylbenzene yield averaged for 40, 50 and 60 min test runs of steam reforming (SR) and pyrolysis (PYR) modes for alder (AA), beech (BA) and (PA) char experiments

SR			PYR		
AA	BA	PA	AA	BA	PA
7.0	5.7	5.1	4.2	3.9	1.9
±1.8	±0.5	±0.7	±0.3	±0.5	±0.2

Gases released during the SR experiments with toluene were presented in Figure 24, expressed, according to Eq. 10, as a relative molecular yields based on the reacted toluene. Although most of the released gases were derived from char and coke gasification, rather than the toluene conversion itself, the relative amounts were calculated to maintain consistency with the data reported in previous sections. As expected, more of the gaseous products were yielded during SR mode. Besides H_2 and CH_4 detected during PYR experiments, significant amounts of CO and CO_2 were created in this experiment due to gasification reactions accompanying toluene decomposition. Only small increase in CH_4 yield, from about 0.2 to 0.3, was registered. This compound formation could be related mainly to toluene demethylation, and since benzene creation was not significantly affected by steam introduction, it could be assumed that the importance of this conversion pathway did not change. Increase in H_2 yield could be related to both, steam gasification of solid carbon and further secondary homogeneous reactions, as well as to enhanced toluene conversion, and thus enhanced coking, resulting in increased H_2 formation from dehydrogenation that accompany coke creation.

Comparison of the three chars revealed higher CO_2 and CO yields for AA and BA chars, which is in alignment with lower activation energies of those chars, and hence their more intensified gasification during SR mode. All gaseous species originated from char/coke gasification had relatively steady yields through the whole experiment. On the other hand, CH_4 yield increased during the initial 30 min, analogously to benzene, as the demethylation reaction was intensifying.

Because of the overlap between toluene decomposition and char/coke gasification, released gas analysis does not provide any particular insight into toluene conversion mechanisms. Therefore, in attempt to separate these two reactions, a 60 min blank test run was performed for each char, as described in detail in Chapter 3. Blank runs were carried out in exactly the same manner as the normal SR tests, with only difference being that no toluene, or any other compound, was fed to the reactor chamber. Therefore, the only undergoing reaction during

blank runs was char gasification. This reaction does not reflect exactly on the gasification reactions undergoing during a classical SR runs, because no coke gasification was occurring. It however, provided an insight into gases evolving solely from char conversion. It is also notable that since the SR reforming conditions were the same as the one for steam activation of char in the activated char synthesis procedure, the spent chars after 60 min blank runs provided a material that could be considered a fresh, activated char with a prolonged activation time (from 80 to 140 min). This opportunity was used, *e.g.* during TPD-FTIR analysis of activated alder char, described in section 4.3.1.

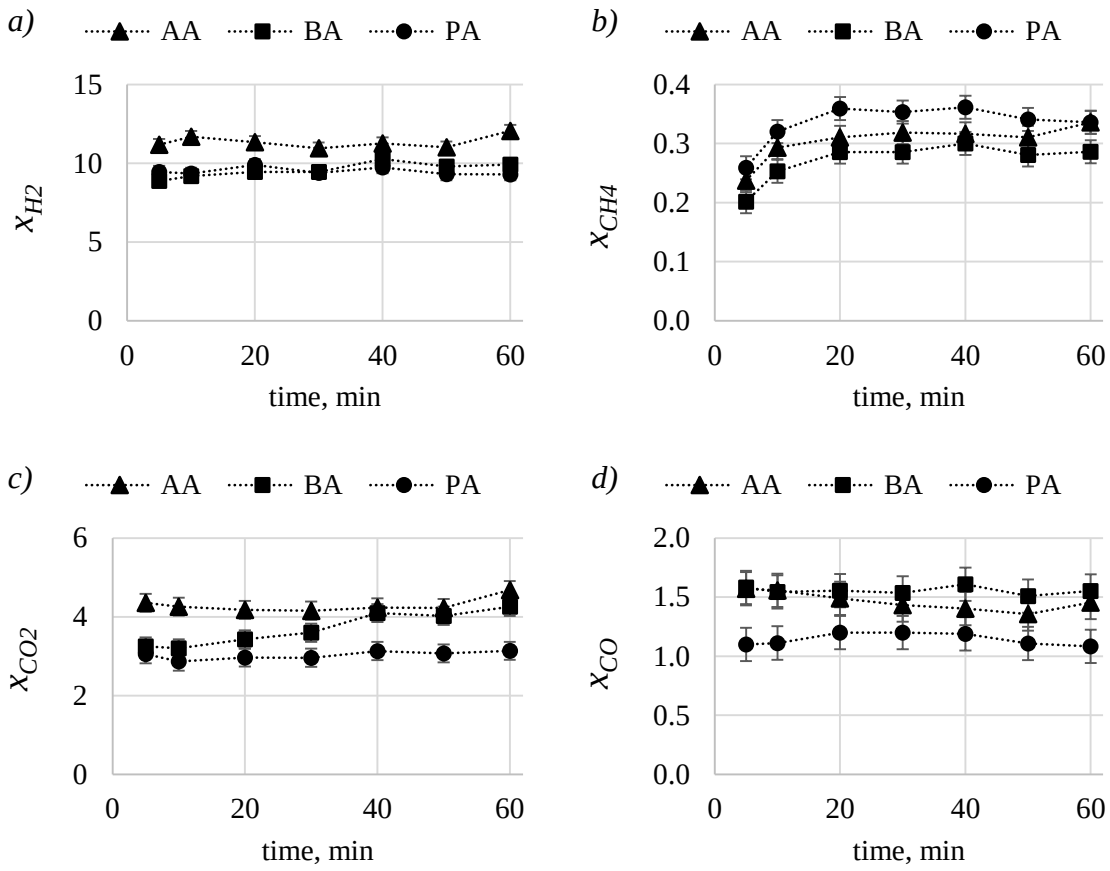

Figure 24. Relative molecular yield (based on reacted toluene) of H_2 and CH_4 as well as CO_2 and CO released during steam reforming experiments with alder (AA), beech (BA) and pine (PA) chars

Since during blank runs, no toluene was fed into the reactor, and the only occurring reaction was char gasification, the gaseous species were the only products formed during this experiment. To allow the comparison between blank runs and SR experiments, the ratios of

the gas yields from SR run to the yields from blank runs were calculated, according to the equation:

$$r_i = n_i / n_{i,b} \tag{11}$$

where n_i is the number of moles of the *i*-th gas species released during a 60 min SR run with toluene and $n_{i,b}$ is the number of moles of the *i*-th gas species released during a 60 min blank run. The results of the obtained ratios were presented in Figure 25.

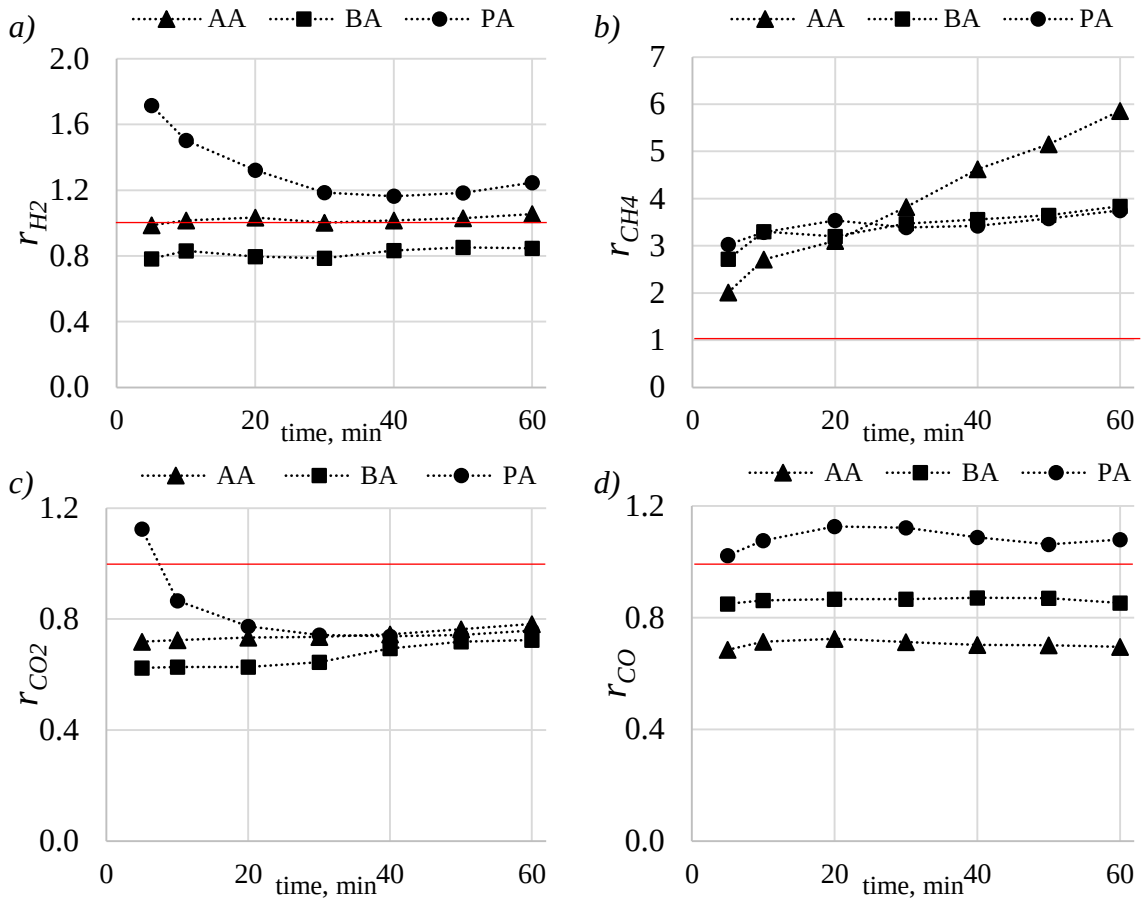

Figure 25. Ratio of the amount of a gas species released during a toluene steam reforming to the amount released during a blank run for alder (AA), beech (BA) and pine (PA) char

The ratio for H_2 release (r_{H2}) did not provide any unambiguous information on which of the compared runs favoured its formation. It might be related to a significant involvement of this species in both, steam gasification and toluene conversion process, as well as it might originate in a relatively poor detection of H_2 with TCD. In case of CH_4, however, there was a clear trend, 3-4 times higher yields of this species during toluene steam reforming, compared to a blank run. This aligns well with an assumption that most CH_4 produced during

SR mode was derived from toluene demethylation and only small contribution was due to gasification process, either due to hydrogasification of solid carbon or secondary reactions between released gases. The most important information, which was provided by comparison of SR and blank runs, was the ratios of CO_2 and CO release. Since the formation of those two was strictly related to gasification reactions of either char and coke, or char only (in blank test), ratios of those species' yields reveal the relative intensity of the gasification process. For all examined chars, $r_{CO2} \ll 1$ and in case of more reactive chars (AA and BA) $r_{CO} \ll 1$. This finding suggests a more intensified gasification of char while no toluene was fed to the reactor. Introduction of toluene conversion, simultaneously to char gasification, inhibited the letter. This phenomenon could be explained in a two-fold manner. Toluene steam reforming involves coke deposition and its following gasification. Therefore, during the SR mode experiments, gasification involved both a mixture of char and coke, and the second one is most likely less reactive towards oxidation reactions, since it was already found out to be less reactive towards catalysing hydrocarbons conversion. Another possible explanation of the gasification inhibition effect is that the toluene, during its conversion, required access to the active sites on the char structure, and those structures, acidic sites and unsaturated carbons, also played a role of active sites in steam gasification. Therefore, those undergoing reactions were competing for the same structures on the char surface, thus toluene inhibited steam access to the char surface.

The potentially worse reactivity of coke towards oxidation was examined by performing TGA oxidation kinetics analysis described in Chapter 3, for the spent chars retrieved from the reactor after toluene conversion in pyrolysis PYR mode, assuming that they were significantly coke-covered. The results comparing activation energies E_a of fresh and spent, coke-covered chars were presented in Figure 26. As can be seen, a general trend of increasing E_a values, *i.e.* deteriorating oxidation reactivity, occurred. This proves, that hydrocarbon-derived coke, not only possess less catalytic effects towards hydrocarbons conversion, but it is also less prone to undergo oxidation reactions itself. It may be a result of less active sites as well as less developed porosity of a coke layer. The second hypothesis, on toluene and steam competition for char active sites, was not examined, but it was still likely that this phenomenon contributed to the lower CO and CO_2 yields upon toluene conversion reactions introduction. The detailed studies into this subject will constitute an interesting scope for further research.

During steam reforming of toluene, simultaneous coke formation and coke and char gasification occurred. The determination of coke yield could be therefore achieved only in

conjunction with char mass balance. During SR mode, H was introduced into the reactor not only with a tar compound, but also with steam, therefore a char/coke yield was estimated based on C balance, instead of the total toluene mass. The obtained results, presented in Figure 27, can be still compared to the coke yields from PYR mode, since the H contribution to the overall toluene mass balance in that mode was below 1 wt.% for all experimental runs. Some of the obtained char/coke yields, BA at 40 min and AA at 60 min in particular, did not fit well within the general trend of the data point series. It was most likely caused by adding up of the uncertainties of numerous experimentally derived values included in the C balance calculations. However, an increase of char/coke yields with toluene feeding time could be observed for all examined materials. In SR mode, despite continuing gasification, the catalyst beds were still gaining mass, although slower than during PYR mode. This observation correlated well with a still visible, yet less significant toluene conversion η_T decrease with experiment time. Therefore, it can be concluded, that under applied conditions, the gasification rate of char/coke was lower than the rate of coke formation, for all examined chars. Steam concertation, applied during this SR runs, was reported by Hosokai et al. [15] as sufficient for maintaining char activity. For a similar gas composition, Fuentes-Cano et al. [36] established, that at temperatures lower than 950 °C, deactivation of chars still progressed. These discrepancies suggest, that the effect of steam on prolonging catalyst activity is related not only to the experiment conditions, but also to the properties of the char, like its gasification reactivity or physical structure, *e.g.* its microporosity.

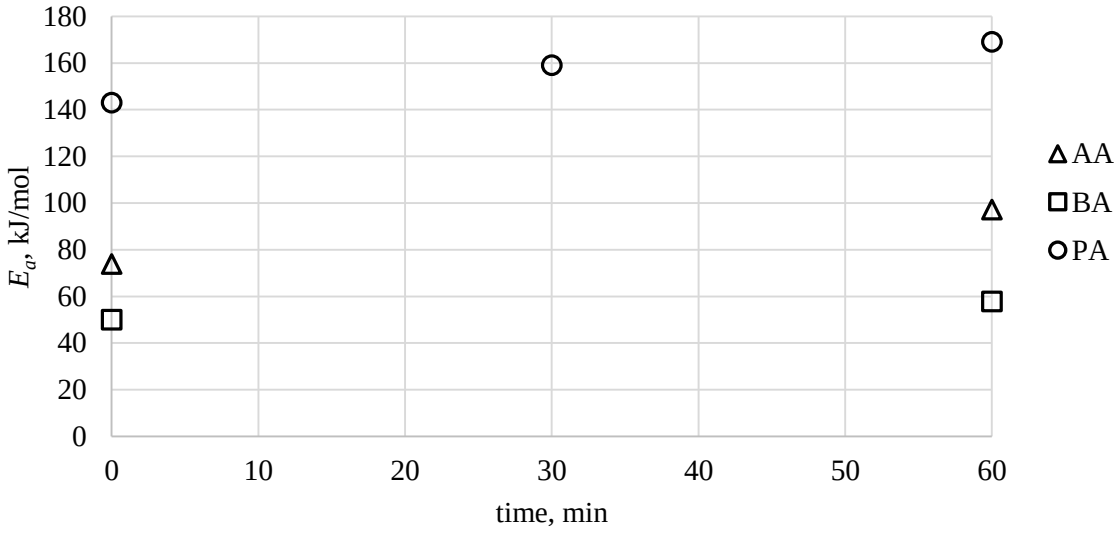

Figure 26. Activation energy E_a (fitted with R^2>0.99) of fresh (time=0) and spent in a pyrolytic toluene conversion runs chars from alder (AA), beech (BA) and pine (PA)

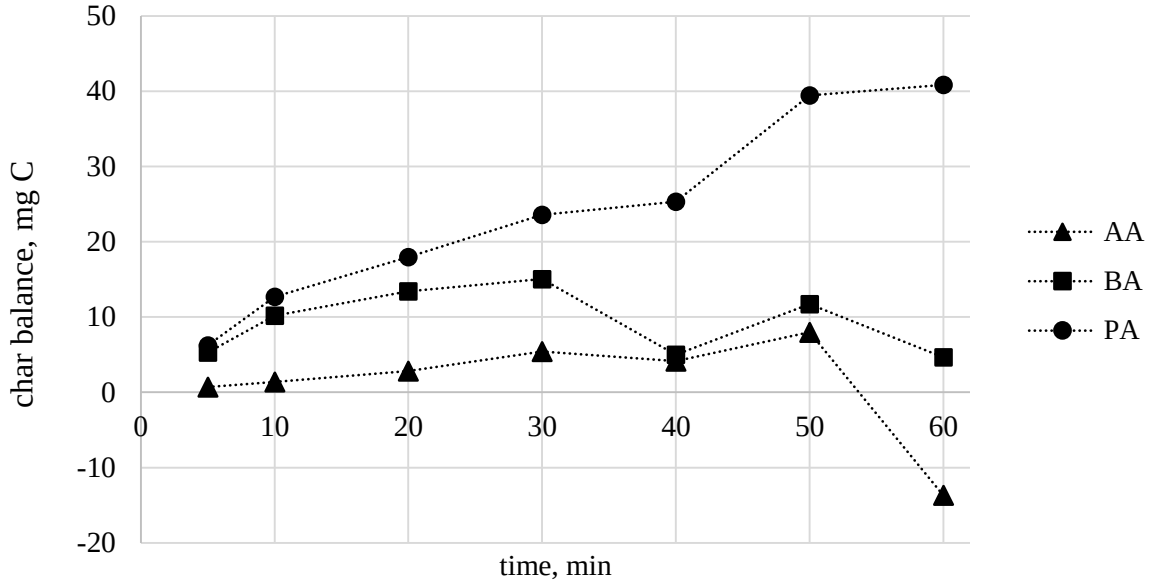

Figure 27. Char/coke yield based on C balance for steam reforming runs with alder (AA), beech (BA) and pine (PA) chars

During toluene pyrolysis, after approximately 30 min of the run, chars reached saturation point after gaining approximately 100-120 mg and 60-70 mg of coke, for AA/BA and PA, respectively. In SR mode, combined coke formation and char/coke gasification yielded roughly 10 mg and 40 mg mass gain of AA/BA and PA chars, respectively. While the coke capacity of PA char was lower than that of AA/BA char, leading to quicker deactivation and lower η_T values, the SR experiments suggest a higher char/coke yield of PA char. Most likely, this could be attributed to a more enhanced AA/BA char gasification, resulting in a lower bed mass gain, despite a higher η_T and thus plausibly higher coke formation rate.

4.4.3. Spent chars analysis

The observed char deactivation and gasification as well as expected coke layer deposition suggested some physicochemical changes to their structure. In order to gain some insight into the influence of toluene conversion and steam gasification on the catalyst bed, a basic analysis of selected spent chars, recovered from the reactor after the experimental runs, were carried out and the results were presented below.

The influence of coke covering and steam activation/regeneration of chars was examined via ATR-FTIR analysis, described in detail in Chapter 3. Fresh chars spectra, discussed in section 4.3.1, were compared with the ones of spent chars recovered from the reactor after

60 min run of pyrolytic (PYR) mode, steam reforming (SR) mode and blank runs for steam reforming (without toluene feeding) in Figure 28. Pyrolytic toluene conversion was expected to yield a significant amount of coke, approaching char saturation point. Therefore, spectra of spent chars from PYR experiments would represent what is expected to be a coke surface. The main absorption regions where oxygen functional groups were revealed in fresh chars spectra, were greatly diminished. Especially absorption within the 1300 – 900 cm^{-1} region was reduced, as it was comprised mainly of C-O and structural C-C bonds vibrations. The 1640 – 1420 cm^{-1} band remained visible, as it could be ascribed to both C=O vibrations as well as aromatic rings absorption. A dense, toluene derived coke layer is expected to comprise a significant amount of aromatic structures [47], which could explain remaining absorption. The shoulders on the main absorption regions in fresh char samples were reduced to small, sharper bands at 1374 and 1231 cm^{-1}. These bands were also present in a fresh pine char removed from the reactor during preparation process after pyrolysis but prior to the activation step, presented further in section 4.5.1.

As the pyrolytic conversion deactivated all chars, leading to a similarly flat spectra for all samples, the steam reforming of toluene influenced alder (AA) and beech (BA) chars differently than a pine (PA) char. Spectra of AA and BA chars retrieved from reactor after a 60 min SR experiment run resembled the fresh char ones. The only noticeable difference might be the lower absorption within the 1300 – 1160 cm^{-1} shoulder of the main absorption region, which would suggest that some particular C-O comprising structures were gone from the char surface. For PA_SR char, on the other hand, the high absorption region around 1000 cm^{-1} diminished significantly and its intensity become lower than the C=O, C=C region around 1500 cm^{-1}. This would suggest a more pronounced reduction of O-functionalities on PA char and/or its higher resistance to re-activation with steam. Lower PA char reactivity towards oxidation and its quicker deactivation due to coke could both serve as an explanation for PA_SR spectrum shape. As explained before, spent chars from blank runs performed at SR mode conditions, could be considered fresh chars with prolonged activation time. It can be seen in Figure 28, that AA_H2O_b and BA_H2O_b chars had more developed spectra then fresh chars, suggesting that more oxygen functionalities were created on their surface upon the extended time of steam treatment. The sharp bands at 1091 and 1049 cm^{-1} that were standing out of the main absorption region, become even more pronounced upon further activation, supporting the hypothesis, that those chars possessed some specific O-containing structures which creation was favoured during steam activation. The PA_H2O_b char, on the other hand, did not revealed any improvement in functionalities yield upon further

activation. This might be attributed to the PA char's higher activation energy, and therefore lower reactivity towards oxidation. It could also explain the highly visible decline in intensity of spectra of spent PA chars, even the one from SR mode.

The important information provided by FTIR analysis is that although during the SR mode, the deactivation of all chars was experienced, the AA and BA chars spectra remained relatively unchanged, suggesting that the amount of functional groups was not deteriorating. Therefore, it could be expected, that some other char parameters were mainly responsible for char deactivation and toluene conversion decrease during SR mode. The other conclusion that could be drawn from this analysis is that the AA and BA chars were much more susceptible to steam activation than PA char, due to their higher oxidation reactivity and therefore, indirectly, due to their higher AAEM species content.

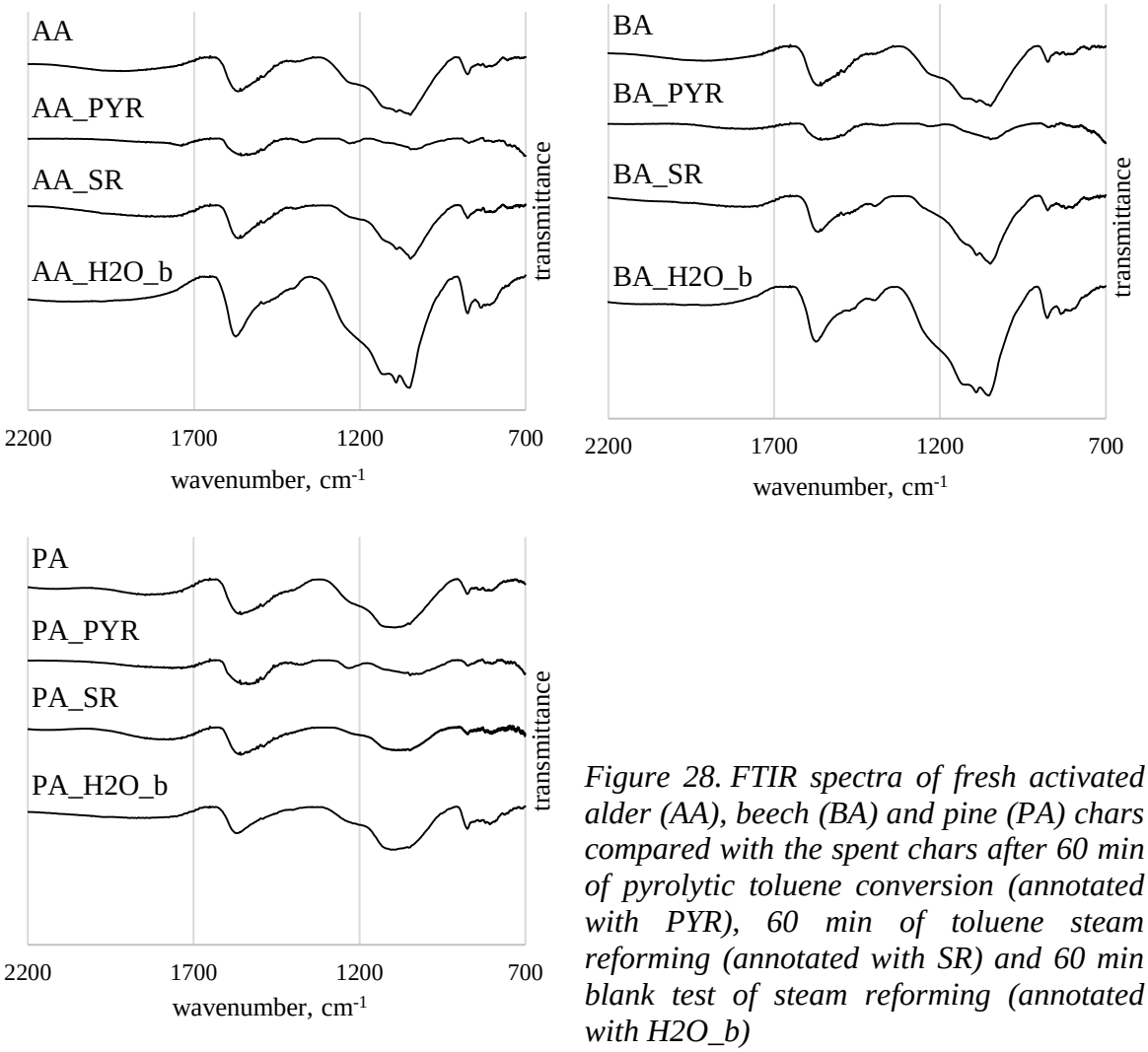

Figure 28. FTIR spectra of fresh activated alder (AA), beech (BA) and pine (PA) chars compared with the spent chars after 60 min of pyrolytic toluene conversion (annotated with PYR), 60 min of toluene steam reforming (annotated with SR) and 60 min blank test of steam reforming (annotated with H2O_b)

The re-creation of oxygen functionalities during steam reforming mode was observed for AA and BA char, while it was negligible in case of PA. However, for all examined chars, the beneficial role of steam in prolonging char activity was experienced. It was therefore expected, that the main advantages of steam-char interactions were related to the changes in char physical structure rather than the acidic sites distribution. Surface area and microporosity of selected fresh and spent chars were therefore compared to provide some insight on the char morphology changes.

In Table 10, total surface areas and microporosities of all discussed samples were summarised and their nitrogen adsorption-desorption isotherms at 77 K were presented in Figure 29 and Figure 30. All registered isotherms shapes were a composite of a type I and II with H4 hysteresis, typical for micro-mesoporous carbons [37,112]. The type I isotherm is characterised by an almost vertical increase at low relative pressures, followed by a horizontal, flatline. It is typical for a microporous materials with low external surface [112]. Type II isotherm is comprised of a steep, yet not as much as in type I, increase of adsorbed gas quantity up to a characteristic point B. It is followed by a slower yet continuous increase in adsorbed quantity at higher relative pressures. The point B is usually attributed to the end of monolayer creation and beginning of multilayer adsorption [113]. This isotherm is ascribed to non-porous and macroporous materials. The combination of those two isotherm types, *i.e.* an isotherm with an almost vertical initial part followed with some further absorption at higher pressures is commonly registered for micro-mespoporous materials. If the hysteresis occurs at the higher pressures region of I and II composite, it is usually H4 type, which suggests the occurrence of slit-shape pores. This shape of isotherm is commonly experienced in micro-mesoporous carbons [112].

Table 10. Total (BET) and micropore surface area as well as micropores contribution to the overall porosity of fresh activated alder (AA) and pine (PA) char, as well as spent AA chars after 60 min blank run (H2O_b) with steam, 30 and 60 min of toluene steam reforming (SR_30 and SR_60, respectively) and 30 min of toluene pyrolysis (PYR_30)

	BET area m^2/g	**Micropore area m^2/g**	**Micropores share**
AA	709 ±6	421 ±8	59 %
AA_H2O_b	1336 ±8	502 ±11	38 %
AA_SR_60	581 ±2	176 ±3	30 %
AA_SR_30	617 ±2	239 ±3	39 %
AA_PYR_30	272 ±1	134 ±1	49 %
PA	668 ±5	503 ±7	75 %

As can be noticed in Figure 29, fresh alder and pine chars had a relatively similar initial increase at the micropores region. It was however followed by a steeper increase in case of AA char, suggesting more developed external surface of this char, while PA isotherm shape remained slightly closer to the ideal type I. Both samples had a visible hysteresis, suggesting presence of the slit-shaped pores. The more developed external surface, and thus mesoporosity, of AA char was most likely responsible for slower deactivation of this char in toluene decomposition experiments.

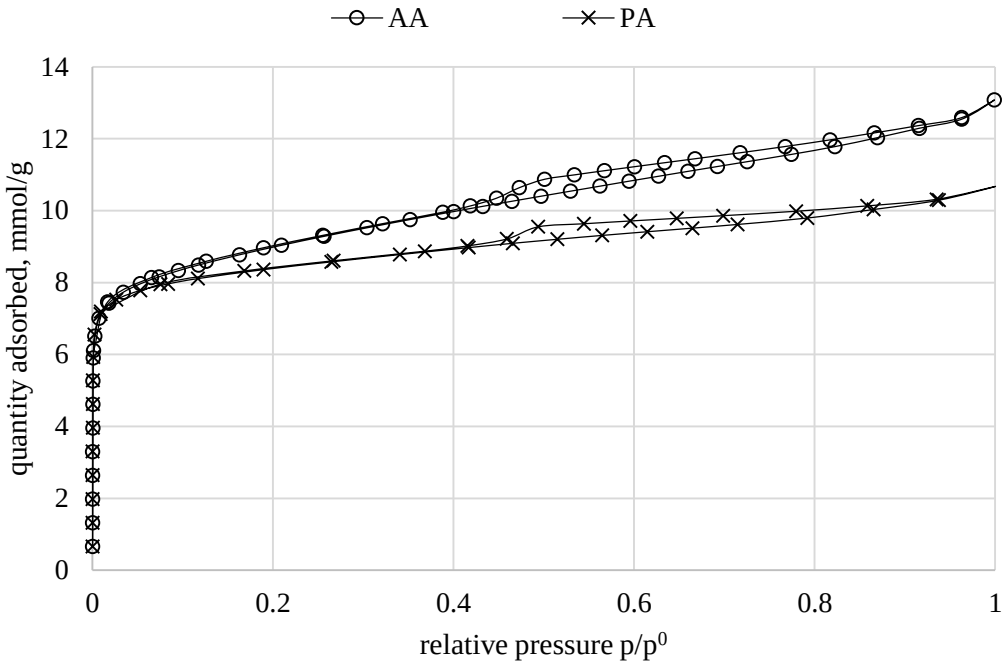

Figure 29. Nitrogen adsorption-desorption isotherm at 77 K on fresh activated alder (AA) and pine (PA) char

The changes in char morphology were further investigated for spent AA char after various treatments. The char recovered from the reactor after steam reforming blank runs (AA_H2O_b), where no compound was fed, could be considered a fresh AA char that was steam activated for an extra 60 min, compared to the original AA one. The surface area calculations revealed that while the total surface area of this char increased almost twice, the micropores creation was not significantly enhanced and the share of micropores dropped from initial 59 % to only 38 %. As could be seen in Figure 30, AA_H2O_b isotherm had a higher initial increase, although it was not as steep as in the AA char. The main difference between the isotherms was however registered in the second part of the isotherm, there the adsorption increase in the mesopores region was significantly higher and the hysteresis loop

was increased when the prolonged activation occurred. Among the activating agents, steam is generally considered as a mesopores-creating one [32,33]. It was also the case in this research, where enhanced exposition to steam created a more mesoporous structure with a higher total surface area. AA char used in analogous SR mode but with toluene conversion (AA_SR_60), where the steam activation of char was continuously competing with coke deposition and following coke gasification, the overall, total area was slightly diminished. This suggested that the steam re-activation effect was not fully counteracting coking. The coke tendency to fill micropores as well as mesopores-creating abilities of steam resulted in a char that, while possessing relatively similar total area, was much more mesoporous than the initial AA char. The micropores share was as low as 30 %. This could be also noticed in Figure 30 where the total absorbed quantity for AA and AA_SR_60 isotherms were similar, yet the latter started transition into type II at lower amount of absorbed N_2 and it was followed by a more intensified increase of adsorption at higher pressure region. The hysteresis loop was also increased, upon H_2O interactions.

The effect of coke deposition could be seen in Figure 30 b, where the spent AA chars after 30 min of toluene conversion in N_2 (PYR) and steam (SR) were compared. Coke creation non-interfered with steam gasification obviously resulted in char with a very low total surface area, since carbon deposition was occurring while nothing was removing it from the char's surface. The AA_PYR_30 char microporosity, however, was not as strongly deteriorated as in the steam reforming mode. The hysteresis loop on its isotherm was also less pronounced.

It is also worth mentioning, that while sole steam activation and sole toluene coking, *i.e.* the most extreme cases, strongly influenced total area of the char, the toluene conversion combined with steam re-activation maintained a relatively steady char BET surface area. It decreased for about 100 m^2/g within the initial 30 min of the toluene SR experiment, followed by another 40 m^2/g within the next 30 min. However, since both, steam activation and toluene conversion, had a microporosity-reducing effect, the share of micropores noted the strongest decrease during SR runs.

It can be concluded, that the main effect of toluene decomposition was the decrease of both total and micropore area, which resulted in a lower increase of the initial part of absorption isotherm. The steam activation, on the other hand, increased the total surface area but had a diminishing effect on the char microporosity that was even more pronounced than during coke deposition. This was due to an enhanced mesopores creation, that resulted in an overall higher N_2 adsorption, a stronger resemblance to the type II isotherm and a more pronounced

hysteresis loop, suggesting that the steam activation favoured mesoporous slit-shaped pores formation.

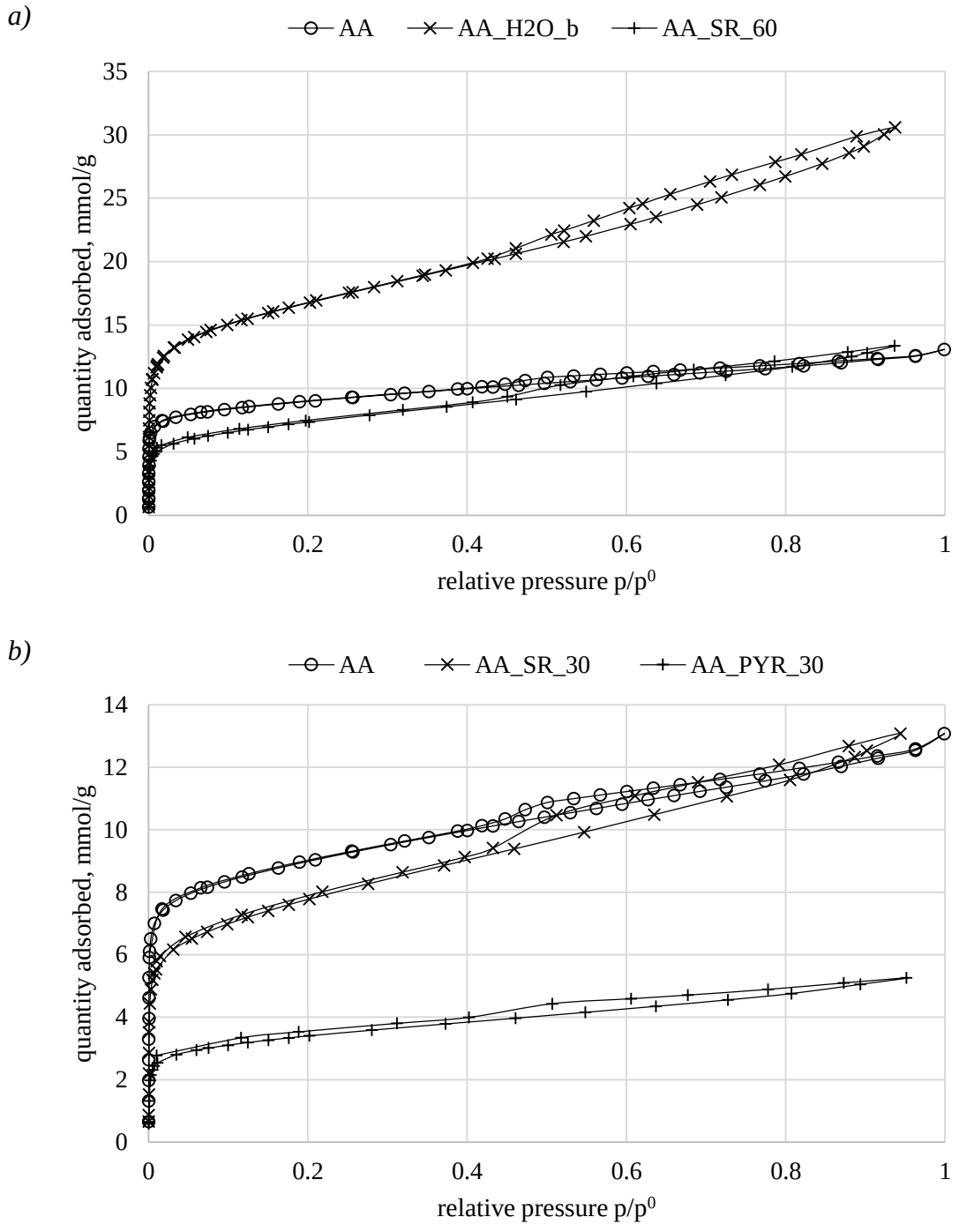

Figure 30. Nitrogen adsorption-desorption isotherm at 77 K on fresh activated alder (AA) and spent AA char after 60 min blank run (H2O_b) with steam, 30 and 60 min of toluene steam reforming (SR_30 and SR_60, respectively) and 30 min of toluene pyrolysis (PYR_30)

Coking and steam activation both had a deteriorating effect on microspores, caused by filling them up or widening them, respectively. The aligning roles of toluene and steam in microporosity deterioration, combined with an opposite effect on total surface area developments, create a wide range of potential scenarios of the char morphology changes upon the reforming process. As other gasifying agents are known to have different contributions towards pore size distribution [32,33], the overlapping and counteracting effects of oxidising gases and converting hydrocarbons in real gasifiers would be therefore even more difficult to predict. The preformed analysis suggested, that the relation between a process gas composition is one of a crucial issue in preserving char activity and therefore optimising tar reforming process.

As the initial char parameters defined an inherent potential towards catalysis of toluene decomposition, they become overshadowed by the strong effect of tar and oxidisers in a long-term reforming process, as was experienced by a more even performance of all chars during SR modes.

4.4.4. The effect of char properties on toluene conversion

Toluene pyrolytic (PYR) and steam reforming (SR) conversion over steam-activated biochars prepared from three differentiated wood species was examined as a main scope of this research. Selected woods represented coniferous and deciduous trees species with a varied hardness and chemical composition. The main differences in raw wood occurred between coniferous pine and the deciduous alder and beech due to a different amount of extractives as well as varied amount and structure of lignin polymer. Synthesised biochars proved to be relatively similar carbonaceous structures with well-developed porosity and some particular surface formations regarded as catalytically active during hydrocarbons conversion. While alder (AA) and beech (BA) activated chars properties were almost identical, the pine (PA) char revealed to be an ode one out, with a slightly lower total surface area, significantly increased microporosity, lower AAEM species and acidic sites content and possibly more basic and aromatic structure. PA char was also proved to possess significantly lower reactivity towards oxidation. It was therefore expected, that any potential differences in prepared chars' catalytic affinity towards toluene conversion would occur between the coniferous and deciduous trees chars.

Indeed, all detected discrepancies were pointing out towards slightly lower catalytic properties of the pine char. It was already proven that it had lower oxidation reactivity, and most properties determining this feature are also important in hydrocarbon conversion

catalysis [5,15,34]. Toluene pyrolytic conversion was lower when the PA char was used in experiments. Initial toluene conversion was only slightly lower than for AA and BA chars. This could be attributed to the slightly less intensive physicochemical properties that are considered important for hydrocarbons conversion, like AAEM species content, surface area and acidic active sites. However, the role of AAEM species in hydrocarbons conversion could be debatable [14,16] (as discussed further in section 4.7.5), the acidic active sites are known to decompose at higher temperatures [14,34], so their role would be important only at the beginning of the process and the slightly lower surface area was combined with an increased microporosity, therefore an overall effect of PA char structure on the initial, inherit catalytic properties was unambiguous. Therefore, the PA char handicap for the toluene conversion at the initiation of toluene conversion (5 min run) was not very pronounced. The discrepancies between PA and AA/BA chars performance become most visible with prolonging experiment time. As toluene feeding progressed, the conversion over PA char decreased much more rapidly than over the other chars. This phenomenon was attributed to a quicker PA char deactivation, which in turn was considered to be related to a more developed microporosity of this char. The difference in the shares of micropore area in overall surface of the chars was indeed very pronounced. Because of a higher microporosity, the PA char was more prone to sintering, which resulted in a more rapid deactivation and lower capacity for coke accumulation, leading to lower toluene conversions during the process duration.

It could be therefore concluded, that upon the similar feedstock, yielding similarly structured biochars, the pore size distribution played the most important role in their catalytic effectiveness, and the difference in chars performance was revealed with progressing conversion reaction time.

Steam reforming of toluene involved overlapping reactions of toluene decomposition over biochar and char/coke gasification. Oxidation of the catalytic material, along with a covering it layer of coke, prolonged the activity of char. This could be explained by two phenomena that were likely to occur. Firstly, coke removal was expected to re-open sintered pore mouths, increasing again the access to the char surface. Secondly, it was also exposing again an underlying char surface and/or re-creating oxygenated functionalities on its surface, providing active sites for toluene decomposition. However, ATR-FTIR analysis revealed regeneration of O-containing species on AA and BA chars, but not on PA chars and as all char performances decreased in the time of SR experiments, it is plausible, that surface oxygen was not a crucial parameter for maintaining char activity. Therefore, it is likely that

deactivation was related mainly to pore sintering and re-opening. The char activity during SR mode would therefore be again, as during PYR mode, related mainly to char structure. This time however, not only initial pore size distribution but also its changes upon steam activation would be of importance.

Therefore, during steam reforming runs performance of biochars depended not only on their initial catalytic properties and inherit affinity towards deactivation, but it was also dependent on their reactivity towards oxidation. As revealed in TGA studies, activation energy of PA char oxidation was roughly twice the one for AA and BA chars. The differences were attributed, most likely, to a significantly lower AAEM species content in PA chars, as they are known to have a very strong impact on the oxidation reactivity [17,18]. For all chars studied at SR mode, a decrease of the initial, high toluene conversion decreased more slowly than during PYR mode, due to activating effect of steam. Although smaller than during pyrolysis, the effect of worse PA char performance due to more rapid deactivation was still visible during SR runs. This time, it could be however attributed to both, easier PA char deactivation (due to higher microporosity) and its higher resistance to steam activation (due to its lower oxidation reactivity, indirectly related to its lower AAEM species content).

The registered differences in toluene conversion over examined chars were mainly of a quantitative nature. The distribution of the main products of toluene decomposition was the same for all chars. The competitive reactions of coke deposition and demethylation both required an access to the active char surface. As the PA char provided less of this surface, both those reactions were inhibited, yet to a similar extent, yielding similar relative amounts of products than AA and BA chars in both, PYR and SR mode. The only qualitative difference that could be observed was an enhanced yield of substituted benzenes from PA char experiments. As those were created during secondary, recombination reactions that involved primary products of toluene decomposition (*e.g.* methyl radicals), their formation was likely less dependent on the char surface accessibility (besides a possible catalytic role of char in ethyl group dehydrogenation). Therefore, recombination reactions became relatively more significant when the worse catalyst, *i.e.* PA char, was used.

4.4.5. Main principles of toluene conversion

The toluene conversion over biochar with increasing reaction duration was measured along with the yields of gaseous and liquid products, in search of information on decomposition mechanisms. The reaction was studied in an inert atmosphere (PYR mode) as well as with a presence of an oxidising agent (SR mode).

Perusal of the obtained data enabled formulation of several assumptions on the toluene conversion mechanism. Those assumptions were often supported by more than one independent analysis result and they were mostly in accordance with a current state of knowledge on hydrocarbons heterogeneous conversion [5,6,13,15,34,36]. After summarising all collected results and conclusions based on them, a coherent hypothesis on the toluene conversion pathways could be created. The basic concept of the undergoing reactions was presented in Figure 31. It was divided into four steps, occurring simultaneously, throughout a conversion process.

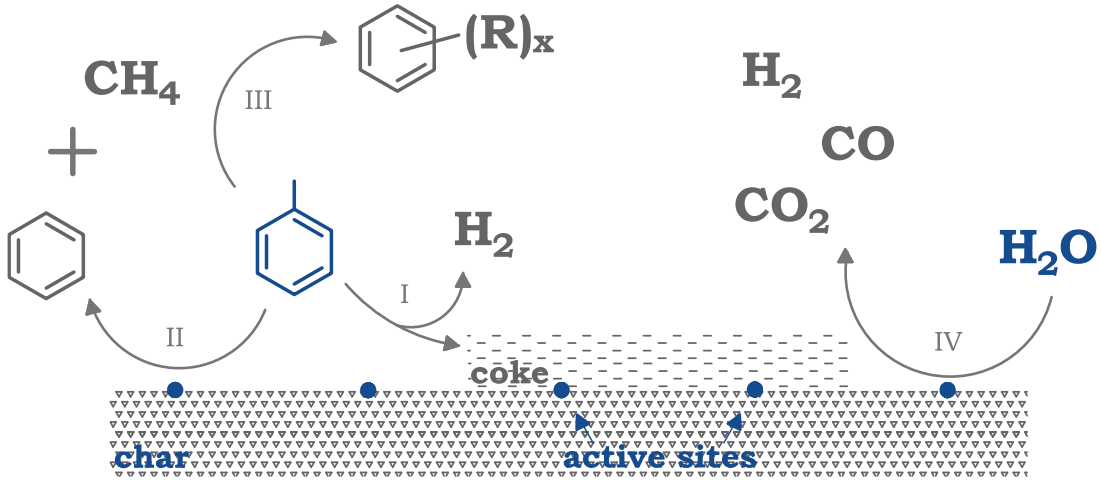

Figure 31. Schematic of the proposed toluene conversion mechanism over char surface divided into stages I – IV (compounds introduced to the reaction zone are depictured in blue, while the conversion products are grey)

During toluene pyrolysis (PYR) with no steam presence, only steps I – III occurred. With no significant toluene conversion detected in an empty reactor tests, it is expected, that all toluene conversion underwent heterogeneously, on the char surface. Another, although less expected, possibility would be that the char also released some radicals that interacted with toluene in a gaseous phase. This alternative was addressed in further, additional experiments (section 4.7.1) in a scope of "intermittent feeding" test. The basic assumption from the main experiments was, however, that the conversion involved exclusively direct toluene-char interactions. Product distribution suggested two main decomposition pathways. First one (I) involved toluene adsorption on the char surface, followed by the dehydrogenation and condensation into a dense, highly carbonaceous coke, and it was coupled with a H_2 release. Coking reaction was widely discussed by other researchers and is generally considered the main and most important of tar catalytic conversion pathways [5,15]. The toluene adsorption

occurred at various, specific char surface structures, commonly addressed as active sites. Hence, created coke remained attached to those sites, covering them, and preventing their participation in any further interactions with newly supplied toluene molecules. This phenomenon is commonly described in the literature as a catalyst deactivation. In this research, the appearance of active sites on wood-derived steam-activated char surface was proved by means of ATR-FTIR and TPD-FTIR analysis, Boehm titrations, AAEM species content evaluation, as well as surface and porosity analysis by N_2 adsorption. The coke accumulation on the char bed was confirmed by the mass balance calculations and detection of H_2 in gaseous products. Char deactivation due to coking was experienced during PYR mode of these studies as well, as a decreasing toluene conversion with char time-on-stream, as well as a deterioration in spent chars FTIR spectra intensity and in an increase of char activation energies.

Another, less pronounced, toluene conversion pathway (II) was its demethylation to benzene. While coke creation has been generally experienced in all tar conversion experiments [15,36], demethylation would be related to a particular structure of the tar representing compound selected for this research, *i.e.* toluene's methyl group. Since this reaction was less intense, and moreover, correlated with a specific functional group, it is not that commonly addressed in the literature. Some research, where this pathway was isolated as a separate conversion reaction are however available [37,83], including a preliminary experiments for this project [111]. The confirmation for the demethylation was obtained by detecting both benzene and CH_4 in toluene conversion products. Comparison of the coke and benzene yield allowed for conclusion about the dominance of the pathway I over II. The inverse proportions between benzene creation, enhancing in time, and coke formation, decreasing in time, suggested that the favoured, coke-creating reaction was slowing down due to char saturation with the deposit, increasing the significance of benzene formation. Since during this shift in product distribution, overall efficiency of toluene conversion decreased, it was concluded, that the favoured pathway (I) was also a more effective one.

The III distinguished step of toluene conversion was comprised of secondary, rearrangement reactions involving toluene substitution with methyl group and dehydrogenation. The obtained results suggested that methyl radicals created during toluene decomposition, most likely during step II, were attacking freshly introduced toluene molecules. Two substitution patterns could be distinguished. Methyl substitution was directed either towards the aromatic ring or to the toluene's methyl group, creating xylenes or ethylbenzene, respectively. The yield of xylene isomers was most likely lower than that of ethylbenzene. The lower energy

of the H-C bond in toluene's methyl group than in its aromatic ring explains this finding [71]. The ethylbenzene was further undergoing dehydrogenation to styrene, either due to an inert atmosphere of the experiment and/or catalytic effect of char. Various recombination reactions during methylated aromatics pyrolysis were previously reported [72,79], as well as their condensation into larger molecules. In this research, any more developed structures would most likely be retained by char catalyst, therefore none was detected downward the reactor. The III step of the toluene conversion was determined based on the GC-FID results of impinger bottles analysis. No other compounds, beside the described ones, were found. This suggests that in the applied conditions, the secondary reactions feature only one methyl radical substitution per new toluene molecule, as no trimethylbenzenes nor propylbenzenes were detected. This may be caused by the restricted residence time within the reaction zone. The yields of all substituted benzenes increased with experiment time. This suggested that the recombination, involving methyl radicals, underwent in gaseous phase without the direct need of the active catalyst presence, besides a plausible char contribution to ethyl group dehydrogenation. Therefore, the relative yields of substituted benzenes continued to increase with char deactivation.

A steam introduction in the steam reforming (SR) mode entailed an additional conversion step (IV). Steam-derived radicals were reacting with char and created coke in gasification reactions. This oxidation process is known to involve char active sites and most of them are considered the same as for the hydrocarbon conversion process, *i.e.* AAEM species, oxygen functionalities, unsaturated carbons [3,17]. In these studies, the gasification of the carbonaceous bed was experienced as well, as confirmed by gas analysis, where CO and CO_2 were present, unlike during sole toluene pyrolysis in PYR mode. Moreover, since the relative coke/benzene distribution was similar for PYR and SR mode, and because no significant toluene conversion was experienced in empty reactor tests with and without steam, it was concluded, that the decomposition reactions were undergoing independently to char/coke gasification and no direct toluene-steam interactions occurred. Moreover, the decrease of CO_2 and CO yield during char/coke oxidation in SR mode, compared to the pure char oxidation in blank runs, suggested, that although toluene decomposition mechanism was independent from a steam presence, the char bed gasification was inhibited, while occurring simultaneously to toluene conversion. Therefore, a conclusion of the competitiveness of toluene conversion (I and II) and steam gasification (IV) was made. This might be attributed to the lower oxidation reactivity of coke (indicated by higher E_a of spent

chars) as well as to the competition between toluene molecules and steam-derived radicals for the char active sites.

Although a basic principle of toluene decomposition mechanism seemed unaffected by the presence of steam, and char gasification with steam was inhibited by the toluene presence, the overall toluene conversion efficiency had benefited from H_2O introduction, because of a prolonged char activity and thus maintained higher toluene conversion during the experiment. It was revealed, that in some cases, steam gasification increased the content of surface groups on the char surface, yet the main contribution to the prolonged char activity was expected to arise due to the changes in surface area and porosity of the chars during SR mode experiments, registered during N_2 adsorption analysis.

The only qualitative difference between toluene conversions in two studied modes was lower yield of substituted benzenes during steam reforming. It can be explained by the prolonged activity of char surface, enhancing the overall amount of toluene to undergo reactions I and II, therefore lowering the importance of the III step, which was considered to be less dependent on the catalyst performance. The enhanced dehydrogenation of ethylbenzene to styrene was also experienced in SR mode. This was explained by the contribution of the oxidative dehydrogenation occurrence, due to the presence of both a catalyst and an oxidising agent within the reaction zone.

4.4.6. Summary of the findings

The study on tar conversion over biochars in this work was focused on toluene conversion over wood-derived, steam-activated chars. It was found that different wood feedstock produced chars similar in their nature. They all possessed physicochemical properties that attributed to their catalytic performance, *i.e.* surface area above 600 m^2/g, at least one of metals content exceeding 0.3 wt.% and acidic active sites above 250 μeq/g. In coniferous tree char, those features were less pronounced and thus its effectiveness as a catalyst was impaired, up to 40% for the most extreme conditions, *i.e.* a 60 min pyrolytic run. Despite quantitative differences between chars performance, the overall toluene decomposition mechanism was considered the same for all chars.

Main toluene conversion pathway experienced in this study was through coke creation on char surface, entailing char surface deactivation. This observation was in alignment the findings reported in literature [5,15,36]. Besides the main decomposition route, toluene conversion to benzene was experienced with a selectivity up to 15 mol%. This pathway was less intense, and it was most likely competing with coke creation, as both reactions required

access to the char surface. As char capacity for coke was continuously decreasing, the overall toluene conversion was decreasing, while the importance of benzene formation increased. After char saturation with coke at approximately 30 min, the proportions between both reactions reached a steady level. The deterioration in char catalytic performance with time, enhance secondary reactions leading to formation of small amounts of substituted benzenes (up to 0.6 mol% in total), since this reaction was less dependent on char surface access, compared to the two main conversion pathways.

The introduction of steam increased longevity of char as a catalyst in toluene conversion, by continuous gasification of forming coke and re-activation of the char surface. Thus, after 60 min of reforming, toluene conversion was maintained above 0.60 while during pyrolytic runs in decreased to 0.25 – 0.45, depending on the type of char. It seemed, however, that it did not change the toluene decomposition principles, *i.e.* heterogeneous char-tar interactions. It was expected, that the steam reforming and toluene decomposition occurred as concurrent, yet independent reactions. The simultaneousness of those reactions inhibited steam gasification rate, while postponing the decrease of toluene conversion rate.

Results of toluene conversion experiments allowed for conclusion that wood-derived biochars can be successfully used as catalysts in hydrocarbons reforming. However, due to their high microporosity, their continuous re-activation, *e.g.* with steam, is required to preserve their effectiveness during a long-term performance.

4.5. The effect of pine extractives on toluene conversion

The main differences in the efficiency of toluene conversion were experienced between activated char prepared from pine (PA) and the chars prepared from deciduous trees, alder (AA) and beech (BA). The PA char had a slightly lower surface area, less AAEM species and acidic sites, which resulted in a lowered catalytic affinity towards toluene heterogeneous decomposition. The main disadvantage of PA char was its higher microporosity, compared to other chars that resulted in a much quicker deactivation. Another important disadvantage was its lower gasification rate, making it less susceptible to regeneration during steam reforming process. All chars were synthesised in laboratory conditions during a two-step process of pyrolysis and following steam activation, described in detail in Chapter 3. Due to a standardised preparation procedure, deviations in chars structures and their active sites, created during the preparation, were therefore most likely dependent on raw materials properties. The most distinguished features of coniferous wood, compared to the deciduous one, are a structure and amount of lignin and a presence of extractives [51]. Both, lignin and

extractives are affected by a high temperature treatment. The lignin undergoes partial decomposition, and its remains contribute to a char yield. Extractives, on the other hand, are expected to be released at the initial stages of the process, due to their volatile nature. It was however established, that their presence can interfere with other wood compounds during pyrolysis, as they tend to form a layer on the fibrous wood polymers, inhibiting the volatile release form the material and enhancing secondary reactions, leading, among others, to a more enhanced coke creation [61,90].

Therefore, an attempt to remove pine extractives prior to char preparation was made in order to establish if they influence the properties of the obtained char. Original pinewood, after sieving and drying, was extracted with acetone by a Soxhlet method, as described in detail in Chapter 3. Thus, prepared material was further used for char preparation. In this section, toluene pyrolytic conversion efficiency over original and extracted-pine activated char was compared during 5 – 60 min runs. The extracted compounds were also evaluated. The main contribution of their presence to a char formation was expected to occur at the first, pyrolytic stage of the char preparation process. Hence, extractives and wood polymers interactions were further accessed by a TGA pyrolytic experiment.

4.5.1. Extractives removal and obtained char performance

An ATR-FTIR spectrum of a thin film of extracted compounds was presented in Figure 32. The differential spectrum, obtained by a subtraction of the extracted pine wood spectrum from an original wood one, was shown as well, for comparison. The main features of both spectra were similar. Because the bands registered for extractives were sharper and they corresponded directly to the removed species structures, a more detailed analysis was devoted to this spectrum. The most pronounced absorption by extractives compounds was registered at 1697 cm^{-1}. A presence of this band was also one of the main differences between raw pine and deciduous trees spectra discussed in section 4.2. While appearing in a general region of C=O vibrations, it has been commonly attributed to resin acids [103]. A left shoulder of this band most likely comprised C=O stretching in free fatty acids (1720-1706 cm^{-1}) and fatty acid esters (1750 – 1735 cm^{-1}) [114]. Another prominent feature of the extractives spectrum was a presence of 3385, 2929 and 2868 cm^{-1} bands, corresponding to –OH, $–CH_3$ and $–CH_2–$ groups, respectively. An abundance of aliphatic chains was also confirmed by methylene scissoring and methyl asymmetrical bending at 1457 cm^{-1} and methyl symmetrical bending at 1383 cm^{-1} [114]. The 1250 cm^{-1} band could be attributed to a single C–O bond in carboxylic acids [115,116]. The 1154 cm^{-1} band most

likely resulted from C–O stretching in saturated fatty acid esters [114,115]. Detection of all the above-mentioned structures suggested a high concentration of resins as well as free fatty acids and/or fatty acid esters in examined pine extractives. They might also indicate a presence of triglycerides and phytosterols, that are common wood extractives constituents as well [51]. A presence of triglycerides was additionally indicated by the occurrence of a second peak in extractives decomposition DTG curve, detailed further in section 4.5.2. All these lipophilic species are typically found in coniferous wood [58] and they can be removed with organic solvents.

Aromatic rings are commonly represented by two doublet bands. In pine extractives spectrum their presence was a most likely cause for 1606, 1594 and 1512, 1497 cm^{-1} bands, suggesting that acetone also removed a small amount of phenolic compounds, which could be expected due to its polarity [51].

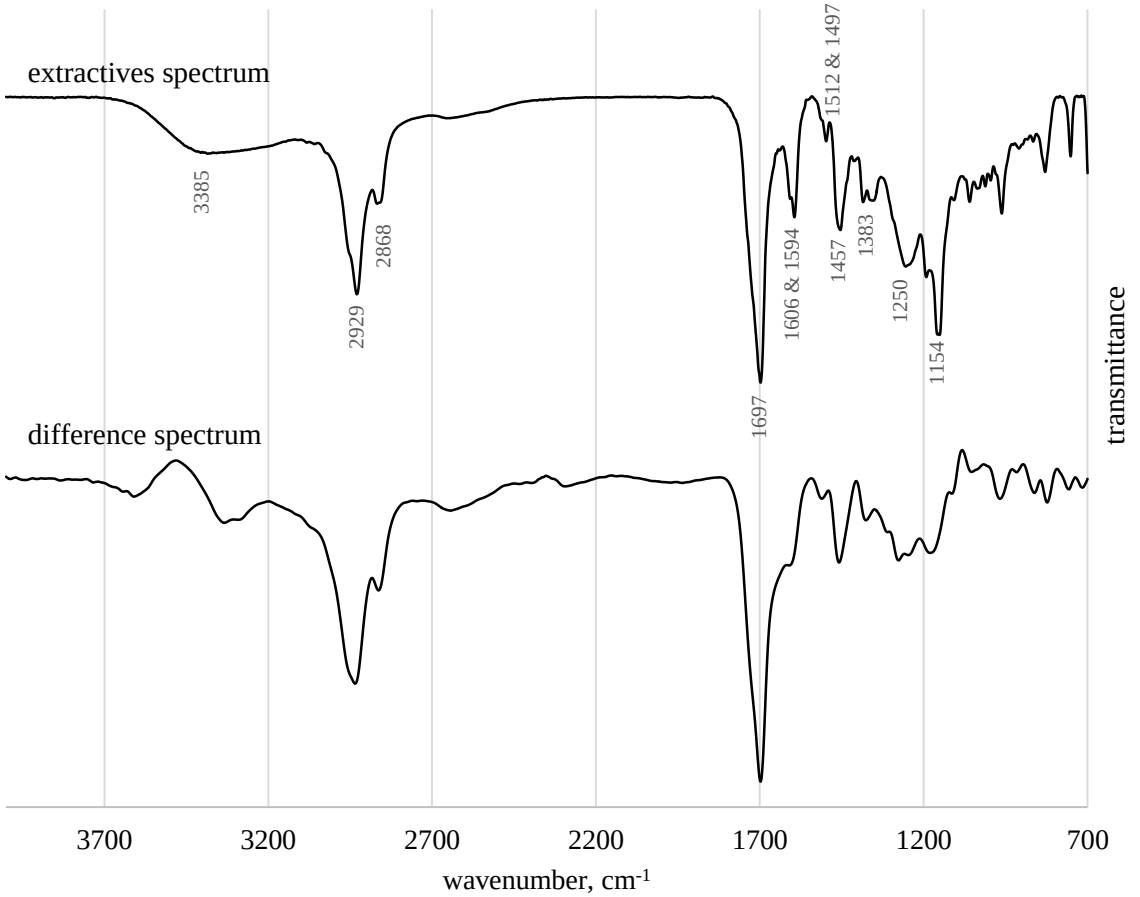

Figure 32. ATR-FTIR spectrum of a film of pine acetone extractives and a difference spectrum of extracted and non-extracted pinewood

Due to their volatile nature, extractives contribution was expected to be most significant during the first step of char preparation, *i.e.* pyrolysis. Therefore, additional chars were prepared where the steam activation stage was omitted and char preparation process was terminated after 60 min pyrolysis, followed by cooling to ambient in continuous N_2 flow. Thus obtained, non-activated pine char (P) and non-activated extracted-pine char (PE) were analysed along with the main, activated pine (PA) and activated extracted-pine (PAE) char prepared in a complete two-stage process. PAE char was used as catalysts in toluene pyrolytic conversion experiment, as detailed in Chapter 3, and compared with the results of PA char performance during the main experiment described in section 4.4.1. Toluene conversion in time was presented in Figure 33. At shorter experiment times, the efficiency of the process was increased when PAE char was used. However, by the end of the examined feeding times, toluene conversion reached similarly low values as for a char prepared from raw wood. This trend suggested that PAE char had a slightly higher capacity for coke deposition, bringing conversions closer to the ones obtained with alder and beech chars. However, PAE deactivation was relatively rapid, similarly to PA char, resulting in similarly low conversions by the end of examined toluene feeding times. Relative molecular yields of benzene, substituted benzenes, CH_4 and H_2 released during toluene pyrolysis over PAE char did not differ significantly from PA char.

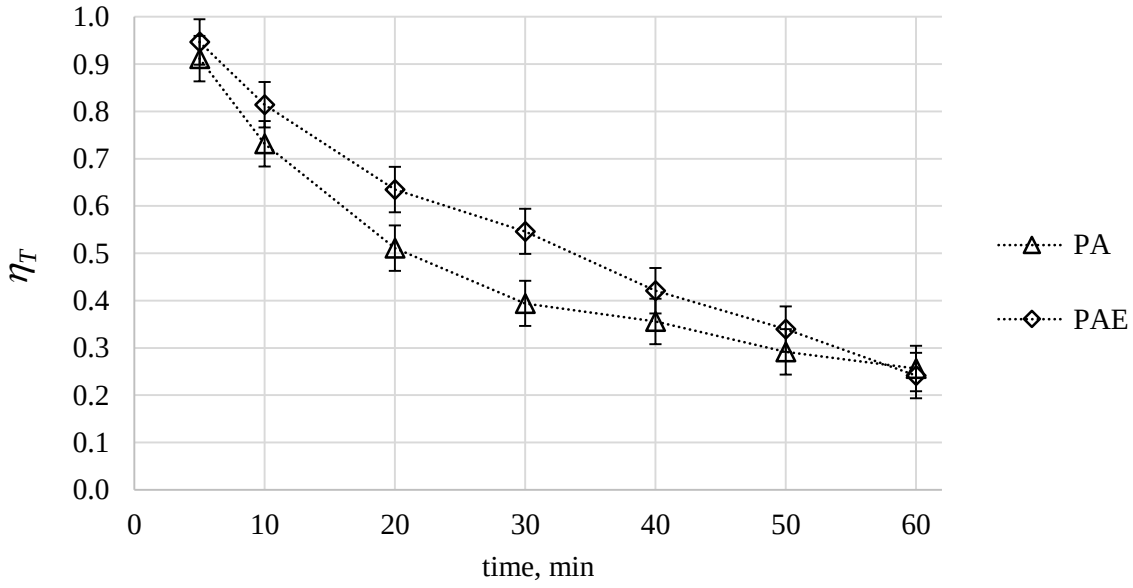

Figure 33. Toluene conversion in time during pyrolysis over activated pine (PA) and activated extracted-pine (PAE) char

In order to determine the differences in PA and PAE char that might contribute to the registered changes in toluene conversion effectiveness, PAE char properties were examined and compared with those of PA char. The AAEM species content in activated chars, as well as acidic sites distribution and activation energies for activated as well as non-activated pine chars were presented in Table 11. Functional surface groups on chars were also evaluated with ATR-FTIR spectroscopy. Fresh non-activated and activated chars, as well as spent chars after 60 min of toluene pyrolysis were presented in Figure 34. Total surface area and micropores area determined with BET and t-Plot method, respectively, of fresh non-activated and activated chars, as well as spent chars after 50 min of toluene pyrolysis were presented in Figure 35.

The chars after complete preparation process, *i.e.* pyrolysis and steam activation, had generally enhanced catalytic properties. Their surface area as well as total amount of acidic sites more than doubled upon the activation. The FTIR spectra revealed a noticeable increase of absorption within the 1630 – 1420 cm^{-1} correlated with C=O and aromatic C=C bands and a significant increase in 1300 – 900 cm^{-1} range assigned *i.a.* to C–O bands in acidic functional groups. As discussed in section 4.4.3, the steam activation also lowered microporosity of the chars. Activation energies of steam activated chars increased significantly, and the initial mass loss of char upon the oxidation was shifted towards higher temperatures. The reaction with steam during activation process partially oxidised the chars, most likely releasing more volatile components of the carbonaceous structures, making the chars more stable and resistant to the oxidation atmosphere of TGA experiments. A surface of a non-extracted pine char at consecutive stages of its preparation and utilisation was also accessed by SEM technique and the micrographs were presented in Figure 36. The pine char after pyrolysis but prior to the activation step had a relatively smooth surface with clearly visible, numerous craters. Those structures most likely resulted from a release of volatiles from melted polymeric constituents of wood during a high temperature treatment [109]. Gasification with steam that took place during an activation stage yielded char with a more uneven, cracked surface and with an abundance of small particles on its surface (Figure 36 b). In the last micrograph, a spent PA char after 40 min of toluene pyrolytic conversion was showed. The process of toluene heterogeneous decomposition and coke formation removed the small labile particles and evened the surface to some extent, although the main, widest, longitudinal cracks remained visible.

Table 11. Acidic sites distribution, AAEM species content and TGA oxidation parameters (E_a – activation energy, A – pre-exponential factor, R^2 – coefficient of determination, t_i, t_f – initial and final temperature of the analysed mass loss region) for original and extracted-pine chars (in headings: E indicates extracted and A activated)

	PA	**PAE**	**P**	**PE**
Acidic sites type, meq/g				
phenolic	0.069 ±0.006	0.065 ±0.009	0.038 ±0.035	0.043 ±0.026
lactonic	0.057 ±0.014	0.045 ±0.006	0.017 ±0.032	-0.008 ±0.035
carboxylic	0.149 ±0.014	0.188 ±0.003	0.048 ±0.024	0.113 ±0.025
AAEM species content, g/kg				
K	1.679 ±0.068	1.700 ±0.051		
Na	0.072 ±0.020	0.118 ±0.013		
Ca	3.615 ±0.181	3.909 ±0.154		
Mg	0.810 ±0.027	0.885 ±0.023		
TGA oxidation parameters				
E_a, kJ/mol	143	159	77	80
A, 1/s	$6.7 \cdot 10^6$	$1.1 \cdot 10^8$	$1.3 \cdot 10^2$	$2.5 \cdot 10^2$
R^2, -	0.998	0.997	0.998	0.998
t_i, ℃	433	440	394	392
t_f, ℃	470	472	452	447

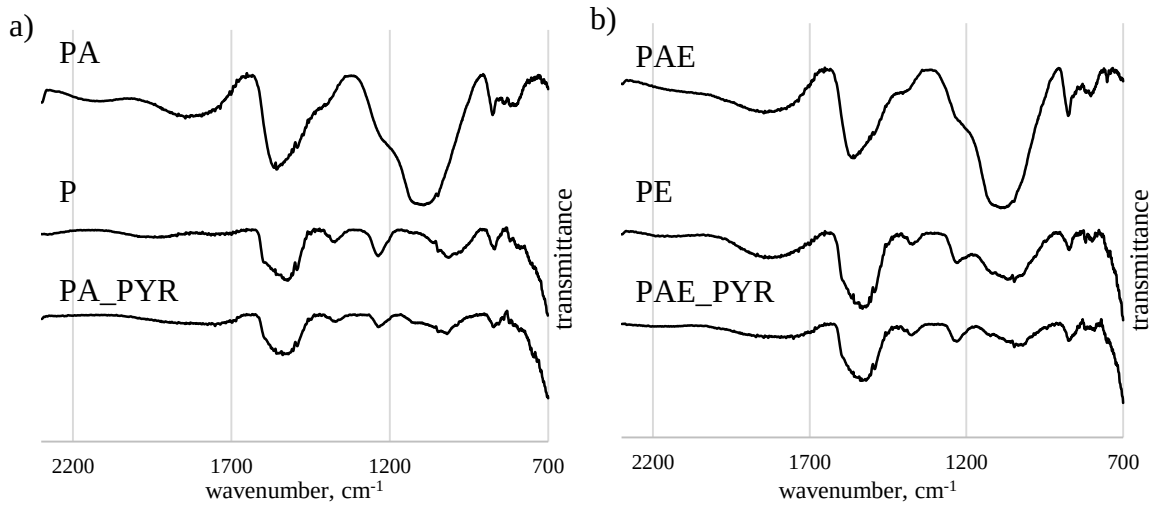

Figure 34. ATR-FTIR spectra of fresh, original and extracted-pine chars (in headings: E indicates extracted and A activated) as well as spent chars after 60 min toluene pyrolysis (PYR)

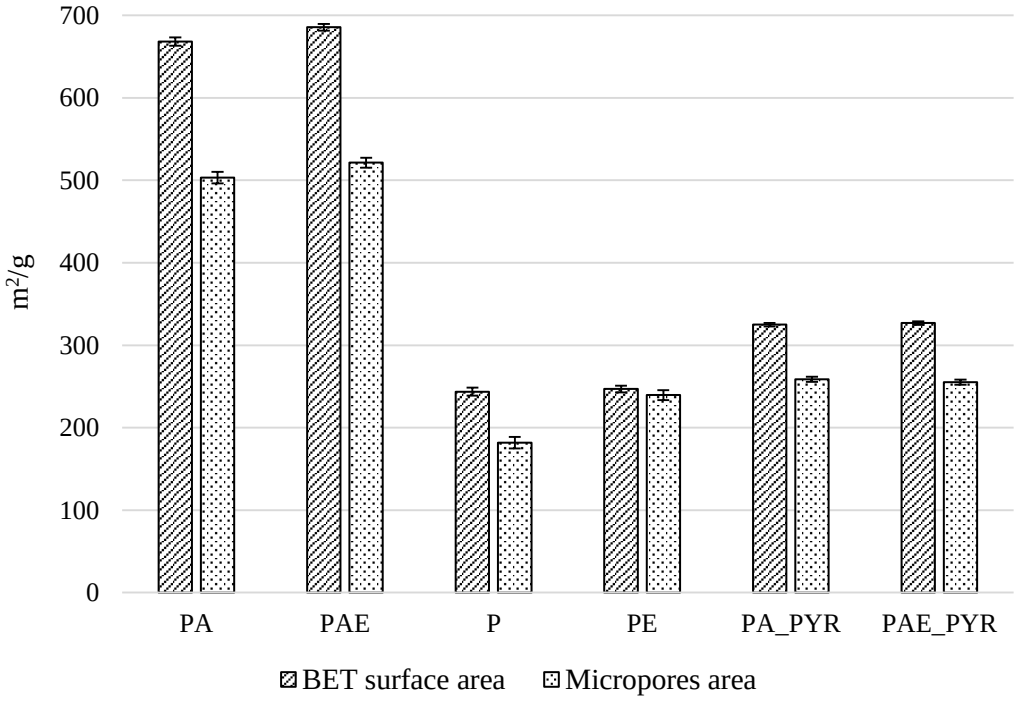

Figure 35. BET surface area and area of micropores of fresh, original and extracted-pine chars (in headings: E indicates extracted and A activated) as well as spent chars after 60 min toluene pyrolysis (PYR)

Although the most noticeable changes to chars originated from activation process, some differences between chars from extracted and non-extracted feedstock were also registered. Comparison of the non-activated chars (PE and P) revealed, that the char from extracted pine had a significantly higher amount of acidic sites (0.148 instead of 0.103 meq/g), mainly due

to an increased carboxylic groups content. Higher acidity was also suggested by a more pronounced absorption within 1150 – 1050 cm^{-1} of a C–O bonds region for PE, compared to P char. Prior to activation, both chars had similar surface area, yet the PE char had a significantly increased share of micropores, suggesting that the presence of extractives during the pyrolysis had influenced char structure. It was often reported [61,90], that the extractives layer can increase volatiles residence time within the wood particles, enhancing fixed carbon creation. It is therefore possible, that this phenomenon was more pronounced within the limited space of micropores, filling them up with solid pyrolysis products, thus yielding a less microporous char (P). As steam activation greatly enhanced catalytic properties of all chars, the effect of feedstock extraction on properties of final products was less visible. The acidity of PAE char was however still increased (0.275 and 0.298 meq/g for PA and PAE, respectively) although there were no unambiguous differences in activated chars FTIR spectra. AAEM species content in activated chars were examined, and for K and Ca, the most abundant out of four examined metals, no significant differences were found, according to an ANOVA analysis. Na and Mg content was slightly higher in PAE char, yet their concentrations were generally low and as discussed in detail in section 4.7.5, no visible effect of AAEM species on toluene pyrolysis were found. Moreover, catalytic effect of metals was found to strongly influence char oxidation kinetics and E_a of PAE char was actually slightly higher than PA, suggesting no contribution of potential AAEM species content variation in examined pine chars. Although steam activation diminished the differences between the chars, PAE char maintained a slightly increased total surface area. The micropores share in PAE was only slightly higher than in PA, yet the increased BET surface area might be, along with an increased acidity, responsible for the enhanced toluene conversion at the beginning of the process. Another possible structural change resulted from pyrolysis of extracted wood might be the amount of "unsaturated carbons" as they are also considered as catalytically active and they are correlated with the defects of the carbonaceous matrix [27,31], thus might be influenced by interferences during pyrolysis. There is however, no established method of quantifying them [16], thus no assumptions of extractives influence on their creation could be made. Upon the duration of the experiment and progressing char deactivation, toluene reached similar conversions for both deactivated chars. As can be seen from the analysis of spent chars, their surface areas were diminished and FTIR spectra were deteriorated, resembling chars prior to the activation. There were however no noticeable differences between spent PA and spent PAE chars, justifying their equally poor performance at the final stages of toluene conversion experiment.

a)

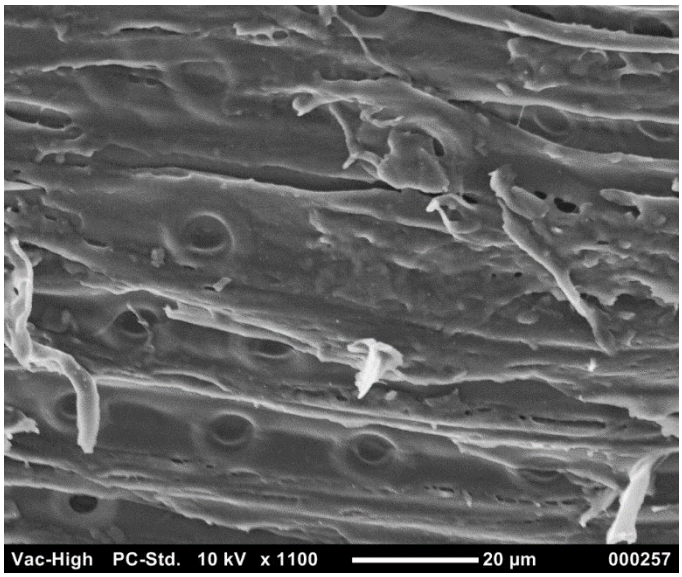

b)

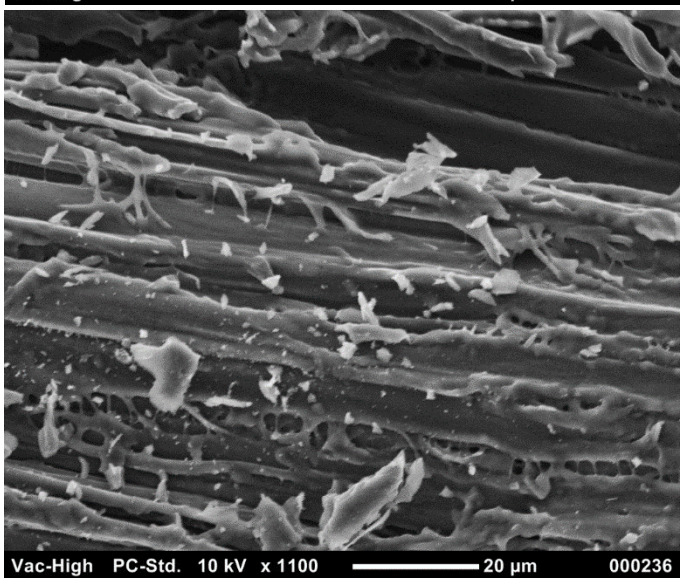

c)

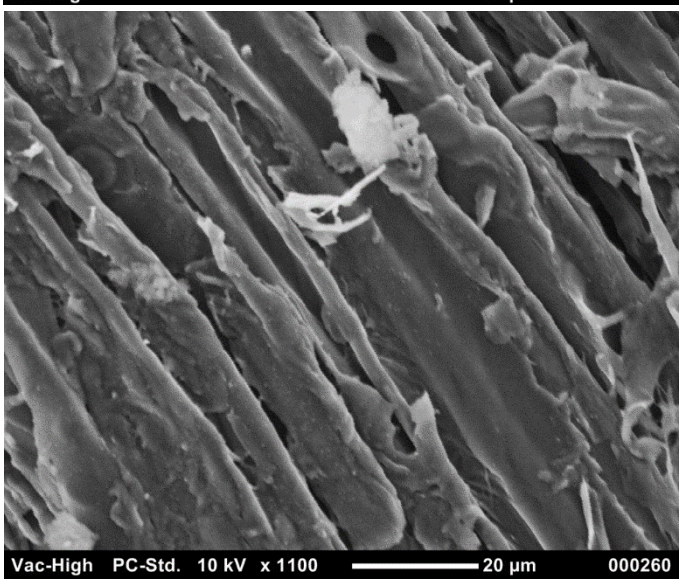

Figure 36. Scanning electron micrographs of non-extracted pine char a) before the activation (P), b) after steam activation (PA), c) after 40 min time-on-stream in toluene conversion experiments (PA_PYR)

4.5.2. Thermogravimetric analysis of pine wood pyrolysis

Wood extractives are relatively volatile compounds and they are expected to be released at the early stages of a thermal treatment. Therefore, their potential impact on the synthesised char would occur during the beginning of pyrolysis process. A thermogravimetric analysis of sample mass loss upon heating in N_2 flow was performed for original and extracted pinewood, as well as for extracted compounds. A detailed procedure of the measurements was provided in Chapter 3. Experiment was carried out for two different heating rates, 10 and 50 K/min. The latter was closer to the conditions applied during the char preparation procedure. Samples mass loss curves and their first derivatives (DTG) were presented in Figure 37. During the slower heating rate experiment, mass loss of a non-extracted sample was less rapid, as suggested by a smaller DTG peak. However, a shape of derivative was relatively similar for both, extracted and original pine, with the only difference at low temperatures, below 280 ℃. The DTG curves from the 10 K/min experiment were further deconvoluted using Gaussian distribution (R^2>0.99), as presented in Figure 38. For a decomposition of extracted-free pine, three functions were fitted, representing main wood polymeric constituents: hemicellulose, cellulose and lignin, peaking at 343, 377 and 419 ℃, respectively. As the extractives DTG shape was exhibiting three peaks at 147, 305 and 450 ℃, another three functions were applied in their deconvolution. Therefore, for a non-extracted pine derivative six Gaussian functions were fitted. Hemicellulose and cellulose decomposition derivatives peaked at similar temperatures for extracted and non-extracted wood samples. Expressed on an extractive-free mass basis, the maxima for hemicellulose and cellulose functions reached -0.537 and -0.673 %/K for raw and -0.531 and -0.675 %/K for extracted pine, respectively. This suggested that holocellulose decomposition at slow pyrolysis was not affected by the removal of extractives. The lignin peak shifted towards slightly lower temperatures, compared to the original wood decomposition. As some phenolic compounds were found in the extractives, their removal might have been related to some changes in lignin structure.

The deconvoluted curve of extracted compounds resembled some previously reported DTG plots, *e.g.* ethanol extractives from Mongolian pine [90]. The 1st, low-temperature peak might be assigned to a decarboxylation of acids or to a release of some more volatile terpenes and ketones. The temperature of a main peak corresponded well with reports on decomposition of free fatty acids and fatty acid methyl esters, which decomposed in a single step at a temperature region of 160 – 370 ℃ [117,118] and of resin acids that peaked at around 300 ℃ [119]. Triglycerides on the other hand, were reported to decompose in two

steps [117,118,120]. The first one corresponded to aliphatic chain decomposition, as it was similar to the peak derived from free acids. The second step was recognised as glycerol decomposition [117,118,120]. Reported temperatures for the second peak corresponded well with the small peak at 450 °C, registered in this study. Thus it is likely that some fatty acids were present in this form in the examined wood, especially, since they are commonly occurring in coniferous trees [58].

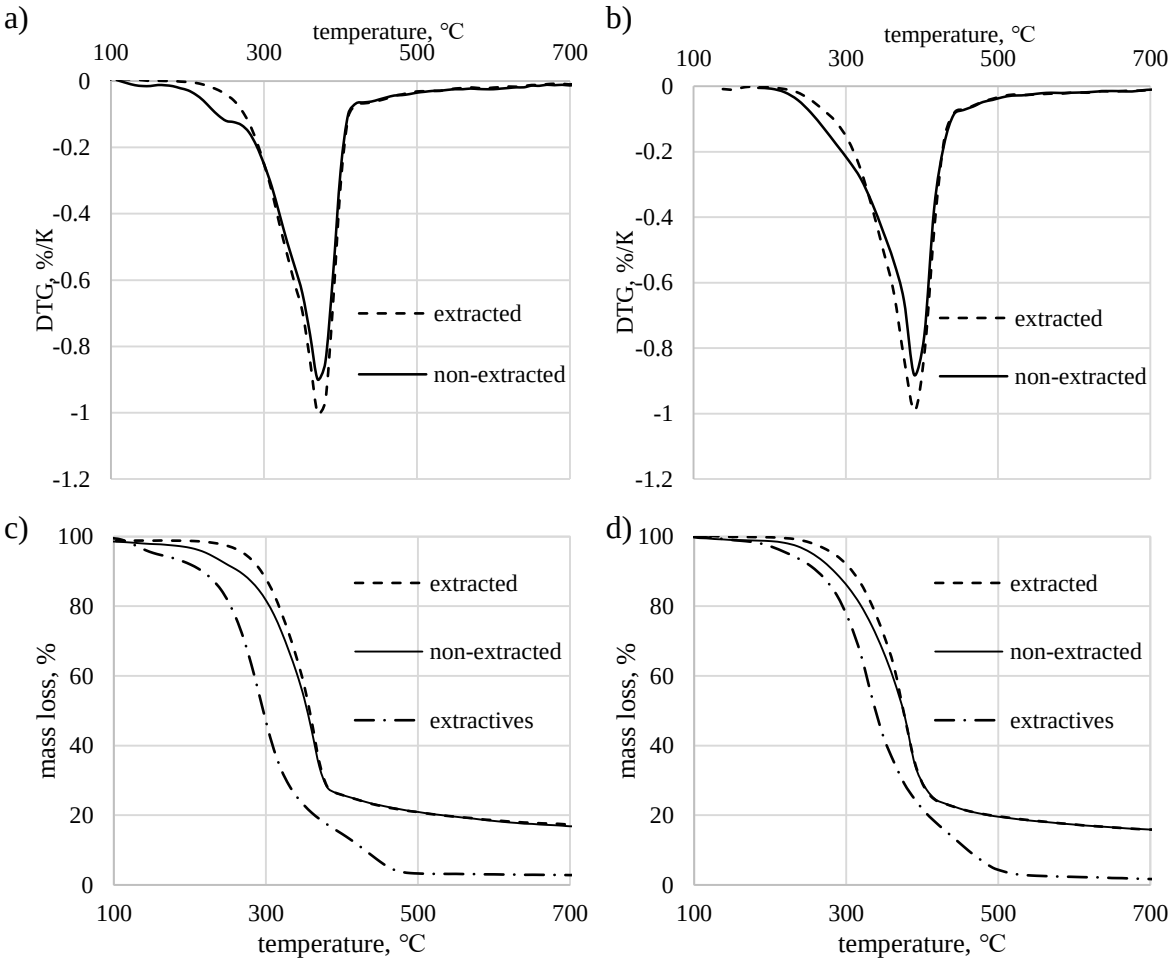

Figure 37. First derivatives DTG and mass loss curves of extracted and non-extracted pinewood obtained from TGA pyrolysis experiments at a), c) 10 °C/min and b), d) 50 °C/min heating rate

During the higher heating rate tests, that were more similar to the conditions of char synthesis, the entire shape of a left shoulder of the DTG curve changed upon a sample extraction. This suggested that a more rapid heating might have evoked some interference between the escaping extractives and decomposing wood polymers. Moreover, for a 50 K/min heating rate experiment, no clear deconvolution of the non-extracted sample could be made with the functions fitting the basic wood constituents.

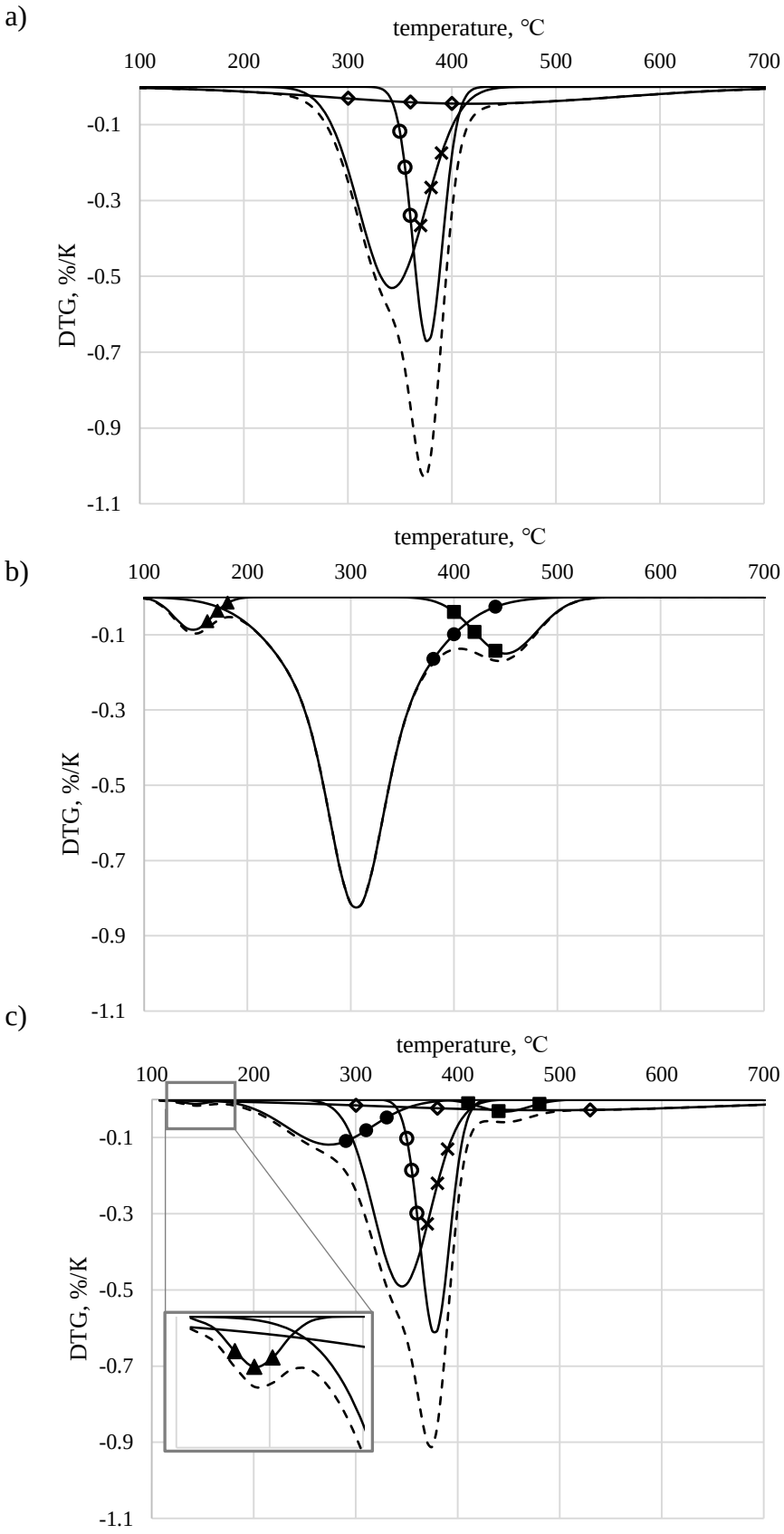

Figure 38. Deconvolution of DTG curves of a) extracted pine b) acetone extracted compounds and c) non-extracted pine pyrolytic decomposition at 10 °C/min heating rate using Gaussian functions to represent × – hemicellulose, ○ – cellulose, ◇ – lignin and ▲, ●, ■ – 1st, 2nd, 3rd extractives compounds, respectively

Some potential interactions of extractives and wood polymers were reported before. It was reported by Guo et al. [90], that presence of extractives in wood during pyrolysis favours acetic acid over levoglucosan formation as a cellulose decomposition product. A cross linking reactions between decomposing cellulose and breaking double bonds in unsaturated esters were on the other hand reported by Jandura et al. [121]. A physical interference of extractives was also reported, as their layer, covering wood fibres, inhibited volatile species evolution, resulting in their increased residence time within the particle and thus enhanced secondary tar reactions, leading to an increased char yield [61,122–124].

It is therefore plausible, that the volatile extractives compounds could escape from the sample before the main polymers decomposition during a slow heating. With an increased heating rate, on the other hand, extractives release interfered with polymers decomposition, plausibly increasing solid carbon agglomeration in restricted spaces of micropores, leading to a less microporous structure of P compared to PE char. This observation would stress out the importance of the wood pyrolysis conditions on the outcome of char structure.

4.5.3. Summary of the findings

A possible effect of extractives on char properties and its catalytic performance in toluene pyrolytic removal was examined in search for an explanation of a worse performance of extractive-rich pine, compared to deciduous-trees chars. Toluene conversion over extractives free char was enhanced by up to 30 % during the initial 30 min of the process, yet the difference ceased upon deactivation occurring with increasing time-on-stream. The improved performance at the beginning of the catalysis was attributed to an increased surface area and acidic sites in an extracted-pine char. Pine extraction brought a performance of the synthesised char closer to that of alder and beech chars at the short toluene feeding times. At 30 min of experiment, toluene conversion was 40 % lower for pine char, and only 17 % lower for extracted-pine char, than deciduous trees chars. However, at prolonged experiment times, extracted-pine char efficiency became as low as the one of the char from a raw pinewood, most likely due to a preserved high microporosity.

The main effect of extractives was experienced during the pyrolytic step of char preparation and it was diminished during steam activation of chars. The following examination of pyrolysis process suggested that higher rates increased the involvement of extractives in the formation of char structure. It is therefore expected, that optimisation of heating process in relation to wood properties might allow for obtaining a better catalyst.

The findings of this section suggest that while abundance of extractives might affect wood pyrolysis, influencing properties of the obtained char, it is not a sole factor responsible for worse performance of catalysts from coniferous, rather than deciduous, trees. Therefore, other differences between those feedstocks, *e.g.* in lignin structure, may also contribute to the observed supremacy of deciduous-wood chars.

4.6. Comparison of chars and commercial activated carbon

The preliminary studies that comprised toluene pyrolytic decomposition over commercial activated carbon (AC), described in detail in Chapter 3, were used as a reference to wood-derived char performance. Examined AC had a higher density than studied chars. Since the same catalyst mass was used for each run, an AC bed was significantly lower than that of wood-derived char. It was therefore impossible, to provide identical conditions during char and carbon tests. Moreover, as the experiment performed with AC was originally developed as a developed test rig performance test, the toluene concentration differed to the one used in the scope of the main experiment. However, since comparison of the two catalyst types provided some interesting conclusions, it was still incorporated in this project and the results were presented in this section.

4.6.1. Catalyst properties and toluene pyrolytic conversion comparison

ATR-FTIR analysis of fresh activated alder char (AA) and commercial activated carbon (AC) were presented in Figure 39. The differences between both materials are much more pronounced than the deviations between wood-derived chars used in the main experiment. The absorption intensity within the 1300 – 900 cm^{-1} of C–O vibrations region was much higher for AC sample. The maximum reached at 1063 cm^{-1} suggested an abundance of ether and ester structures. The increased absorption for wavenumbers >1720 cm^{-1}, resulting most likely from C=O vibration in esters, supported this conclusion. A more pronounced 1630 – 1420 cm^{-1} region suggested increased aromaticity and/or C=O functional groups presence. The differences in the absorption at low frequencies, <900 cm^{-1}, indicated different aromatic rings substitution patterns. A higher 875 cm^{-1} band in AA char suggested increased occurrence of a single H atoms, while the highly pronounced 778 and 797 cm^{-1} bands in AC spectrum might result from plural neighbouring H atoms on the aromatic rings matrix [65]. In case of AC sample, two small bands at 2973 and 2885 cm^{-1} appeared. As they are commonly attributed to the $–CH_3$ asymmetric and symmetric vibrations, respectively [65], they indicated that some methyl groups were present on the AC surface. These

functionalities were not detected in any of wood derived char samples, examined in this work. The most distinguishable difference between AA and AC material was the highly intensified C–O group presence. The acidic structures are profusely created during chemical activation of carbons [14], commonly used in commercial applications [23], which could give an explanation for C–O groups abundance on AC.

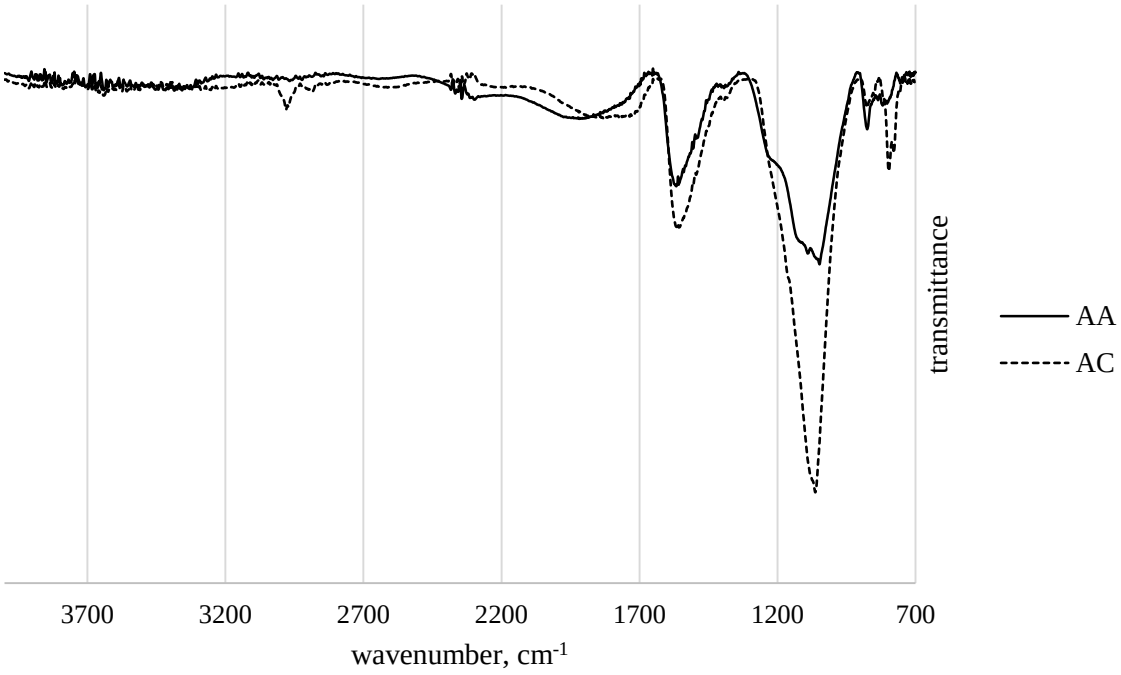

Figure 39. ATR-FTIR spectra of commercial activated carbon (AC) and activated alder char (AA) surface

Moreover, a N_2 adsorption measurement at 77 K was applied to examine AC surface area and its porosity. The total surface area estimated from BET model was 929 m^2/g and a *t*-Plot derived microporosity was 514 m^2/g. A micropores share in the total area of the AC (55 %) was therefore relatively similar to that of AA char (59 %) and lower than PA char (75 %). Total surface area of a commercial carbon was however approximately 30 – 40 % higher than wood-derived chars.

Pore structure of carbon and chars was also slightly different as can be seen in Figure 40, where adsorption-desorption isotherms of both materials were compared. A higher overall amount adsorbed for AC resulted from a higher surface area. There were also distinguishable differences in isotherms shapes, despite a similar contribution of micropores, suggested by *t*-Plot analysis. The AA char isotherm, after initial intense increase of adsorbed quantity, had a sharp bend, similar to a type I isotherm, followed by a still increasing adsorption,

characteristic for a type II isotherm. In the AC isotherm, on the other hand, the band was more mellow, suggesting an earlier transition from isotherm I to II. The hysteresis loop was also more pronounced on the AA char. The main difference between the AA and AC materials was a higher surface area of the latter. It could be also expected, that despite similar micropores area, some of the pores in AC had slightly larger diameters. The pronounced hysteresis on AA, most likely a result of steam activation, may suggest a presence of slit-shape pores on AA surface.

Toluene pyrolytic conversion over commercial activated char (AC) and wood derived chars (AA and PA) were compared in Figure 41. The AC performance was more similar to the alder than pine char. However, an initial, high conversion was maintained for a longer time, and a visible deactivation of the AC became pronounced after approximately 20 min of the test. A following decline had a relatively linear trend, similarly to AA char, while the conversion plot for PA char was more concave. A lower concentration of toluene in AC studies might contribute to a delayed start of catalyst deactivation, however it was not expected to bring out such an intense effect. A prolonged initial activity of AC is most likely partially attributed to its higher porosity and perhaps to its higher acidity. As pores become saturated with coke and acidic sites were used up or thermally destroyed, the conversion over AC started deteriorating. Similar deactivation rate of AA and AC char might be related to the similar share of micropores, while a more microporous PA deactivated more quickly, due to an enhanced sintering. Since the kinetic diameter of toluene (5.85 Å [94]) is significantly lower than average micropores size in all studied materials, it was expected that molecules were able to enter miropores. Therefore, micropores would take an active part in toluene heterogeneous conversion. However, created coke was expected to seal the mouths of smaller pores more easily, foreclosing access of the fresh toluene molecules and thus not using a full potential of the catalyst surface area. In more microporous PA char this phenomenon's contribution was more significant, causing a much quicker deactivation. The comparison suggested that the overall porosity contributed to a prolonged time of maintaining initial, high conversion, by expanding catalyst capacity for char. The microporosity of the sample, on the other hand, seemed to contribute to the rate of catalyst deactivation.

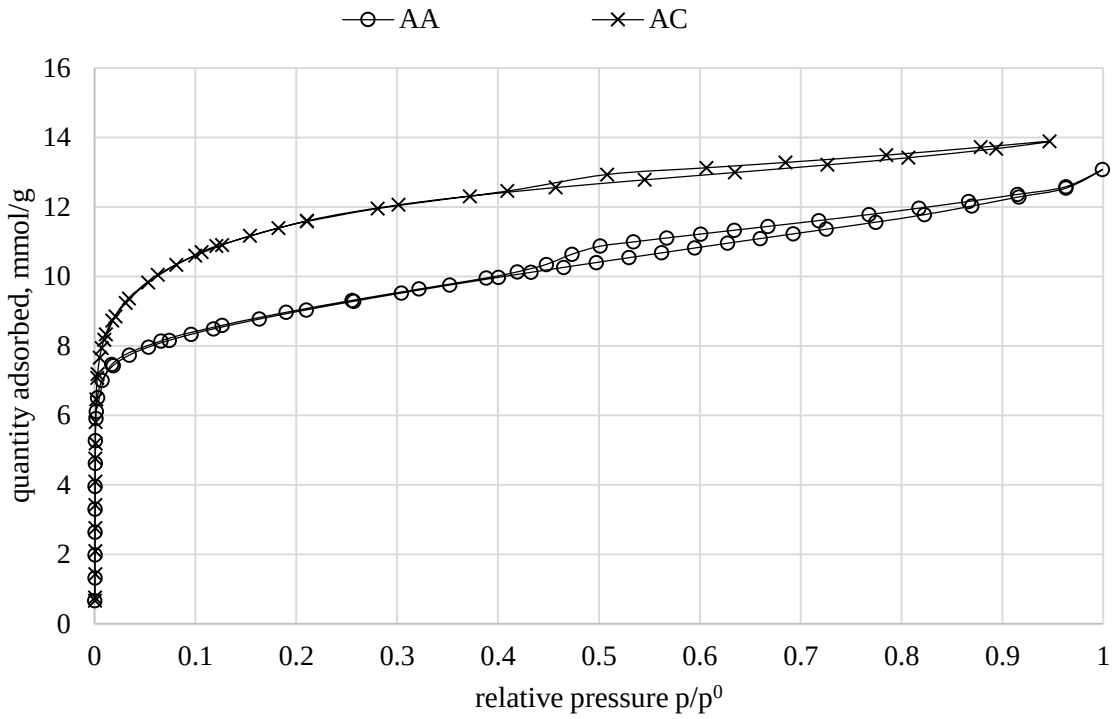

Figure 40. Activated alder char (AA) and commercial activated carbon (AC) N_2 adsorption-desorption isotherm at 77 K

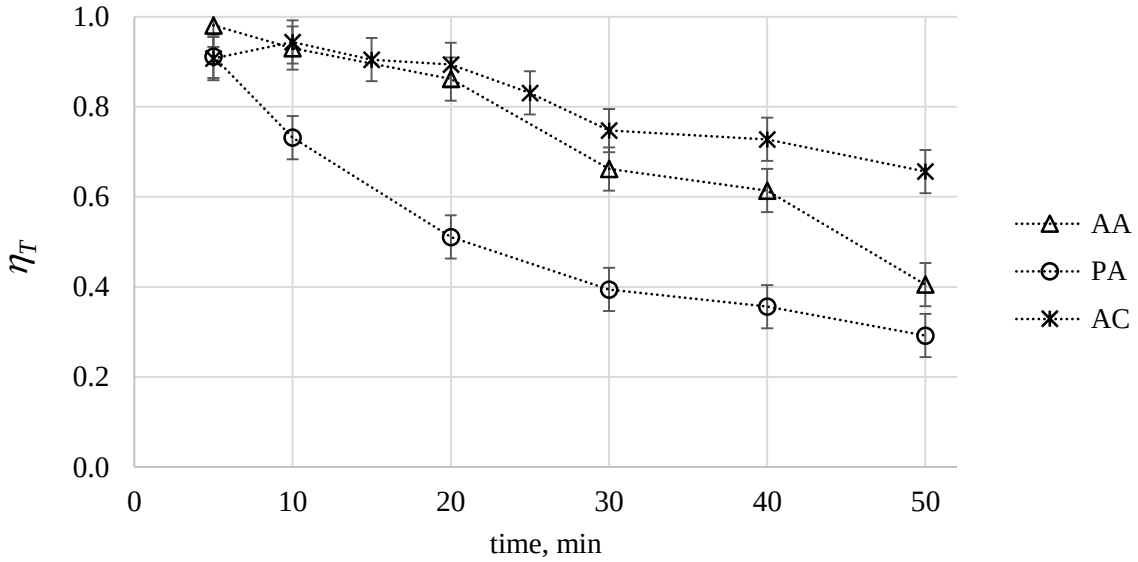

Figure 41. Toluene pyrolytic conversion over activated alder (AA) and pine (PA) char as well as over commercial activated carbon (AC)

In Figure 42 a, the relative molecular benzene yields were compared. In time, a share of toluene that underwent demethylation reached similar level for all materials.

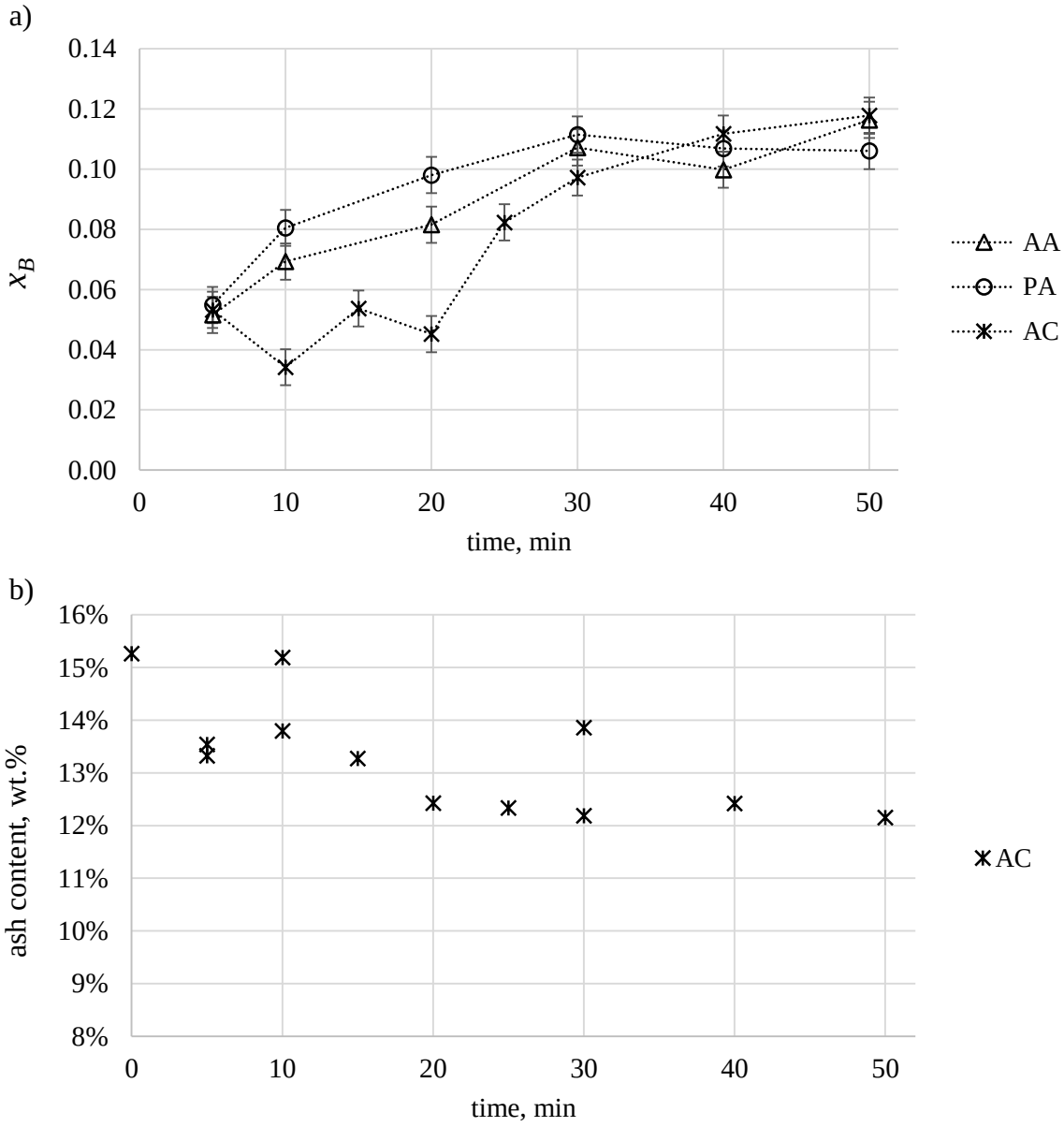

Figure 42. Relative molecular benzene yield (based on reacted toluene) for toluene conversion over activated alder (AA) and pine (PA) char as well as commercial activated carbon (AC) (a) as well as ash content in spent AC (b)

The initial benzene yield was inhibited, while the most intense coking occurred. A prolonged initial AC activity with steady toluene conversion via coking was confirmed by a delayed time of an intensification of benzene formation. Due to a relatively high ash content in AC sample, a gravimetrical assessment of deposited coke could be performed. To this end, ash content in fresh and spent AC samples was analysed and results were presented in Figure 42 b. A presence of coke deposit was expected to increase a carbon content in AC material, thus lowering an ash content. Therefore, the ash content plot would be inversely proportional to

the amount of deposited coke. A decrease in ash content in time was registered for initial 20 min of the toluene conversion process, suggesting a progressing coke deposition during this step of the process. This correlated well with the time of inhibited benzene yield and maintained initial high conversion of toluene. This observation supported a previously introduced assumption of toluene heterogeneous conversion via two competitive pathways of either coke or benzene formation. It also confirmed that coke creation was favoured and correlated with higher toluene conversions.

4.6.2. Toluene conversion kinetics and catalyst activity

Further comparison of toluene conversion over AC and AA bed was performed by calculation of kinetic parameters of the toluene initial decomposition. To this end, additional runs of toluene conversion at lower temperatures were made for pyrolytic conversion over AA and AC as well as for steam reforming over AA char. Tests were performed for the short experimental times to ensure that the conversion rate was not inhibited by catalyst deactivation. To this end, additional 5 min tests for AA and 10 min test for AC were performed at 700 and 750 ℃. Since initial conversions during the main, 800 ℃ tests were already approaching 100 %, only lower temperatures were selected for additional tests for kinetic parameters calculations. Initial toluene conversion rates for three temperatures selected for conversion kinetics calculations were presented in Figure 43. As expected, there was a pronounced effect of temperature on toluene conversion. A consequently lower conversion over AA in SR mode, compared to PYR mode, might suggest the inhibiting effect of steam at the beginning of the process. Since for the initial conversions, high activity of the char was maintained, no benefits from char gasification were expected at this early point of conversion process. The competition for char active sites between toluene and steam were however plausible, as well as an effect of an endothermic nature of the char steam gasification, both of which could contribute to the deterioration of initial conversion efficiency in SR mode. The slightly lower initial conversion in SR, compared to PYR, mode was also registered during the main experiments at 800 ℃ for other two chars. Although a *p*-value of ANOVA analysis of the registered difference was 0.12, suggesting no statistical significance between the two modes at a required, 95% confidence level, it was still possible that this occurrence was not random, especially since lower conversion at other temperatures were experienced as well.

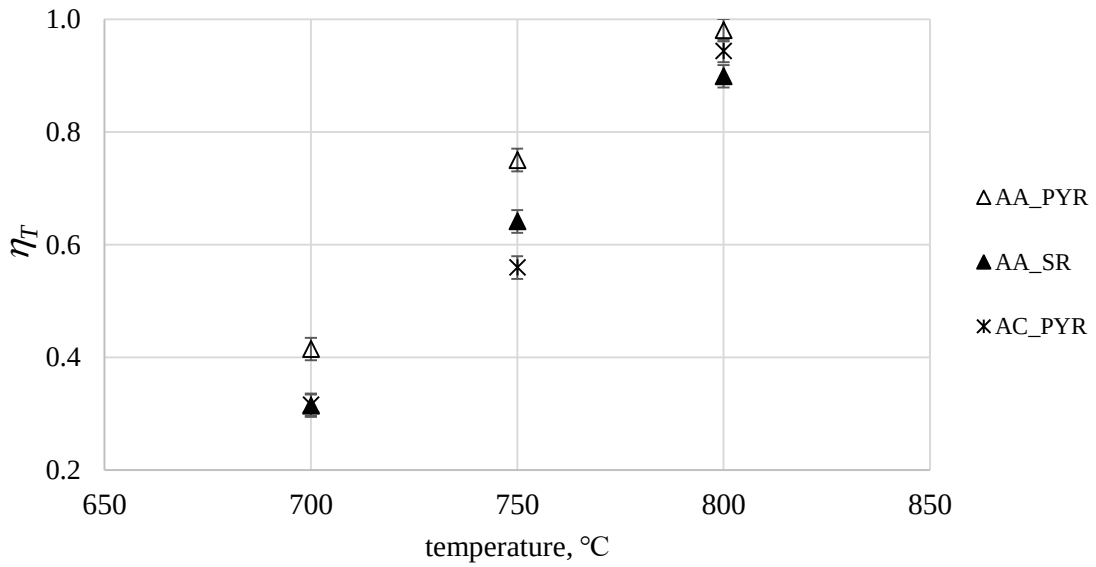

Figure 43. Initial toluene conversion over activated alder char (AA) and commercial activated carbon (AC) in either pyrolytic (PYR) or steam reforming (SR) mode for three temperatures selected for kinetic parameters calculation

Fuentes-Cano et al. [36] studied toluene conversion over coal, coconut and dried sewage sludge chars in 15 vol.% of steam at 750, 850 and 950 °C. The measurements were further used by the authors for toluene conversion kinetics calculation. To account for an observed char deactivation with time, Fuentes-Cano et al. [36] introduced an activity factor that as a function of time, visualised changes in catalyst performance. Their approach was applied in this research as well, for experimental data of toluene pyrolytic and steam reforming over wood-derived chars and AC, to enable assessment of the catalysts.

Following the work of Fuentes-Cano et al. [36], a first order kinetics were assumed and the rate coefficients were calculated for each temperature, according to the equation:

$$k = \frac{-\ln(1-\eta_T)}{\tau} \tag{12}$$

where η_T was toluene conversion over catalyst bed and τ was toluene residence time in bed. The activation energies E_a and pre-exponential factors A were calculated based on the Arrhenius plots presented in Figure 44 and they were summarised in Table 12.

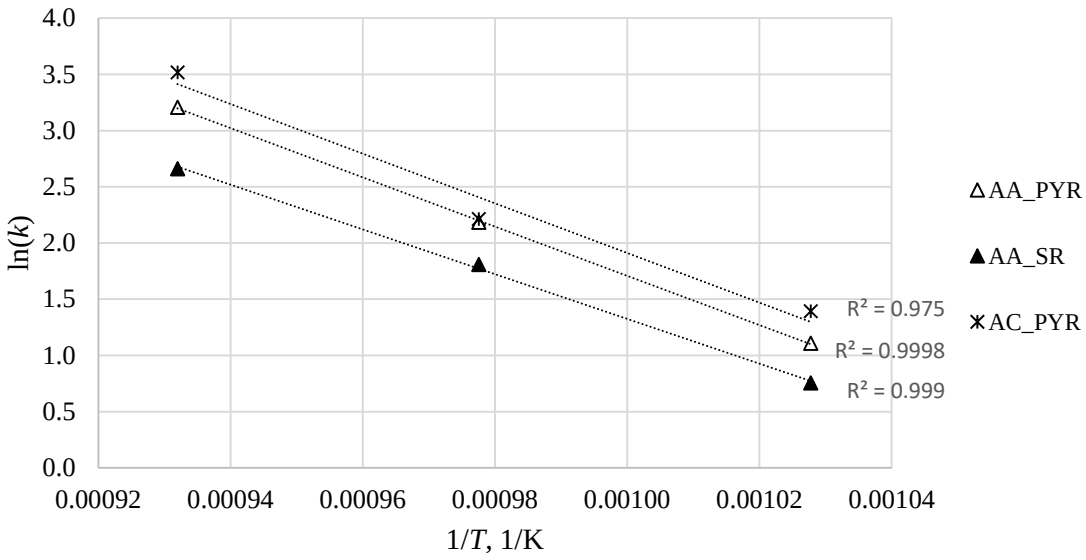

Figure 44. Arrhenius plots for toluene pyrolytic (PYR) or steam reformign (SR) conversion over activated alder char (AA) or commercial activated carbon (AC)

Activation energies for initial toluene conversion in the pyrolytic mode were similar for both AA and AC samples. The E_a of toluene steam reforming over AA char was slightly lower. This suggested that the conversion rate in SR mode was less influenced by the reaction temperature. As presented in detail in section 4.4.2, toluene conversion pathway was expected to be independent on the presence of steam. However, a concurrent gasification of char, despite constant recreation of its catalytic properties, might compete with toluene for char's active sites, inhibiting the initial conversion, as suggested by the results presented in Figure 43. The effect of reaction temperature would therefore influence toluene conversion both, directly as in PYR mode, an indirectly by affecting a char gasification rate. It is therefore possible, that the beneficial effect of increased reaction temperature was less pronounced during SR more, resulting in a lower slope of Arrhenius plot and thus a lower activation energy. All calculated activation energies were significantly lower than that reported by Fuentes-Cano et al. [36], most likely due to a higher temperature regime used in their studies (750 – 950 °C).

All tested catalyst underwent deactivation in time due to coke deposition on their surface. To account for this phenomenon, Fuentes-Cano et al. [36], in their studies on hydrocarbons conversion over biomass chars, introduced an activity factor, a, to the kinetic equation for tar decomposition:

$$-r_{tar} = kC_{tar}a \tag{13}$$

where r_{tar} is the tar conversion rate, k is the rate coefficient and C_{tar} is tar concentration. The activity factor was presented as a ratio of the rate at certain time t, to the initial rate at the beginning of the process, when catalyst was fresh and fully active ($a = 1$).

Catalyst activity expressed in this way, become a function of time. An empirical equation was proposed by Fuentes-Cano et al. to fit the activity function to experimental data:

$$a = \frac{1}{1 + k_d t_{ex}^{p}} \tag{14}$$

where

$$p = p_1 + p_2(T/1023) \tag{15}$$

In the developed equation, t_{ex} was the time of the experiment, *T* was the temperature of the catalyst's bed and p_1, p_2 and k_d were empirical parameters optimised to fit the experimental data.

Above approach was applied to the toluene conversions derived in this research as well. To this end, a rate coefficient, *k*, derived from the kinetic calculations for AA and AC tests were used. Moreover, in an attempt to fit the activity functions to PA and BA char performance as well, rate coefficients for a single measured temperature (800 ℃) were also determined and used in the activity assessment.

Table 12. Activation energy E_a, pre-exponential factor A derived from the Arrhenius plots of toluene pyrolytic (PYR) and steam reforming (SR) conversion over activated alder char (AA) and commercial activated carbon (AC) as well as coefficient of determination R^2 for linear function fitted to the experimental results

	E_a	A	R^2
	kJ/mol	1/s	
AA_PYR	182	1.79E+10	0.9998
AA_SR	165	1.65E+09	0.9990
AC_PYR	184	2.63E+10	0.9750

If an assumption of the first order kinetics was made, concentration of toluene after char bed at the time t_{ex} of the experiment was equal to:

$$C_{tar}(t_{ex}) = C_{tar,i} \cdot exp^{(-k\tau a)} \quad (16)$$

where $C_{tar,i}$ was toluene concentration before the bed, *k* was reaction rate coefficient, τ was toluene residence time in bed and *a* was the activity of the bed.

Calculated toluene conversion at time t_{ex} could be expressed as:

$$\eta_{T,calc}(t_{ex}) = \left(C_{tar,i} - C_{tar}(t_{ex})\right)/C_{tar,i} \quad (17)$$

A fitting of empirical parameters p_1, p_2 and k_d, incorporated in activity function a, could be therefore performed to match calculated conversions with the values obtained from experiments. The assumption was made that for initial conversion experiment, used to determine *k* values, $a = 1$. The following experimental conversions were used to fit the activity function. Obtained empirical parameters were presented in Table 13. Their values were relatively similar to the ones obtained by Fuentes-Cano et al. [36], where for steam reforming of toluene over coal char, coconut char and dried sewage sludge char they obtained k_d in a range of 1.6 x 10^{-3} to 3.8 x 10^{-3}, p_1 in a range of 1.15 to 2.13 and p_2 in a range of -1.32 to -0.35. As pointed out by the authors of the activity equation, those parameters were purely empirical and did not possessed any physical representation. However, relative similarities between the results obtained by the original experiment of Fuentes-Cano et al. [36] and the ones derived from this study, suggested a similar, universal trend of catalyst deactivation upon toluene conversion.

Table 13. Empirical parameters of activity function proposed by Fuentes-Cano et al. [36], *and a coefficient of determination R^2 for experimental and calculated activity fitting for activated alder (AA), beech (BA) pine (PA) and extracted pine (PAE) chars and activated carbon (AC) during pyrolytic (PYR) and steam reforming (SR) mode*

	AA_PYR	**AA_SR**	**PA_PYR**	**PA_SR**	**BA_PYR**	**BA_SR**	**PAE_PYR**	**AC_PYR**
k_d, s^{-p}	2.4 x 10^{-5}	1.9 x 10^{-4}	6.8 x 10^{-4}	1.3 x 10^{-3}	1.8 x 10^{-4}	2.0 x 10^{-3}	1.3 x 10^{-5}	3.3 x 10^{-7}
$p_1, -$	2.21	1.56	1.56	0.75	1.24	1.81	1.28	2.83
$p_2, -$	-0.63	-0.47	-0.39	0.09	0.00	-0.97	0.11	-0.71
$R^2, -$	0.95	0.95	0.99	0.91	0.98	0.87	0.98	0.93

Calculated catalysts' activities in respect to toluene conversion times were presented in Figure 45. A slower deactivation of chars during steam reforming was clearly pronounced. Activities of chars in SR mode were relatively similar and after 60 min of experiment reached values (~0.4) close to the results reported by Fuentes-Cano et al. [36] for sewage sludge char at 750 ℃ and fell between the 750 and 850 ℃ activities of coal char for 60 min toluene reforming experiments.

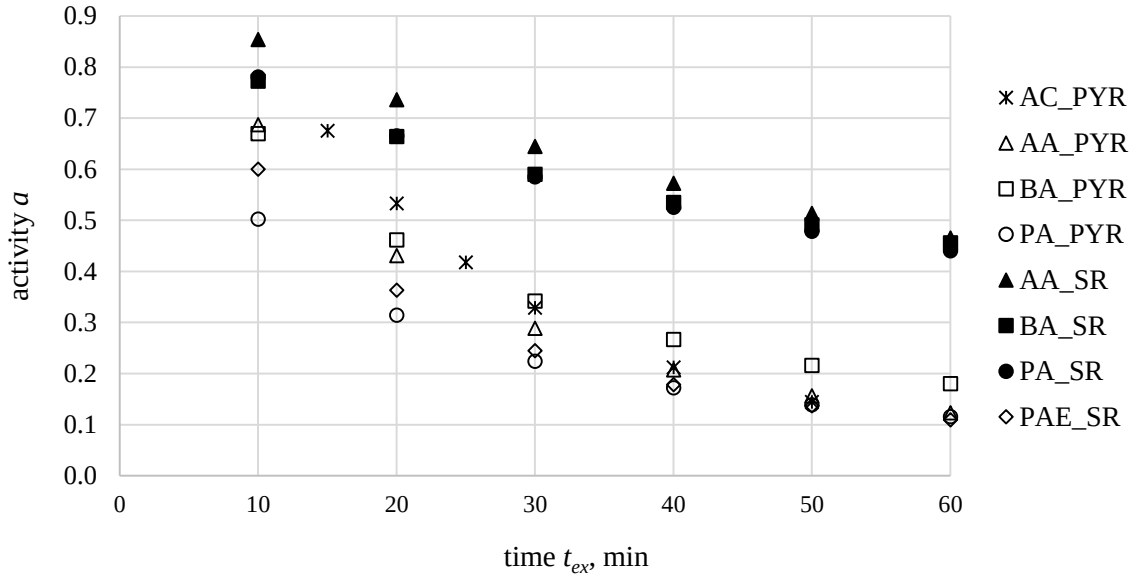

Figure 45. Calculated activities of activated alder (AA), beech (BA) pine (PA) and extracted pine (PAE) chars and activated carbon (AC) during pyrolytic (PYR) and steam reforming (SR) mode

In case of pyrolytic runs, at shorter toluene feeding times, differences in activities were pronounced. With the experiment duration, the activities became similar and very low. During an hour-long pyrolytic process, all chars performed with roughly 10 % of their initial catalytic abilities. Within the diversified activities at the earlier stages of toluene pyrolysis, an activity of PA char was significantly lower, compared to the other catalysts. The extraction of pinewood increased initial activities of pine char (PAE), bringing it closer to the deciduous trees chars (AA and BA). The AC had a higher initial activity, but it became inactive as well during a prolonged conversion. Toluene conversions derived from experiment and calculations are presented in Figure 46. As can be seen from the plot, there was a relatively good fitness of the calculated and measured values, with most points having less than 10 % deviation from the ideal fit.

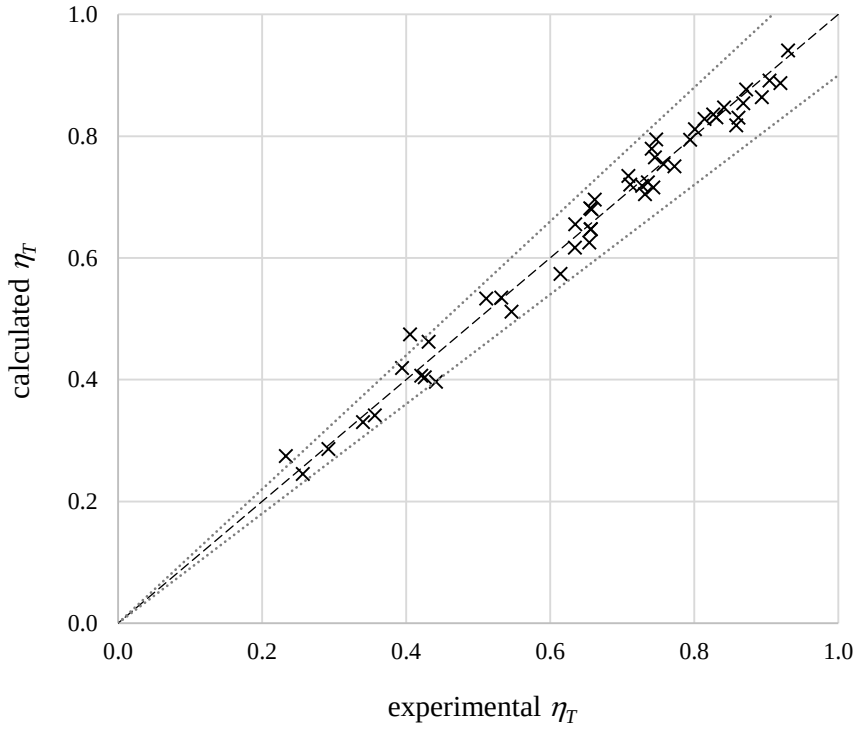

Figure 46. Accuracy of the activity fitting presented as a comparison of toluene conversion derived from calculations and measurements. Dotted lines represent a ±10 % deviation between data

4.6.3. Summary of the findings

In this section, wood-derived chars' catalytic performance was compared with that of a commercial, activated carbon (AC). Despite differences in densities of the materials, and thus a lower toluene concentration used in activated carbon runs, some conclusions could be drawn from the comparison. The initial, high conversion of toluene was preserved for longer when AC was used. A 30 % higher surface area and possibly a higher amount of surface functionalities were expected to contribute to this phenomenon. The following deactivation of AC had a similar trend to AA char, which had the same share (55-59 %) of micropores, as opposed to a more concave conversion decline of a more microporous PA char (70 %). Activation energies of toluene conversion over both AA and AC beds were similar (182 and 184 kJ/mol, respectively), suggesting analogous contribution of both materials. The AC tests were also helpful in confirmation of coke deposition occurrence and its inverted correlation with benzene creation.

Comparison of all catalysts activities, calculated according to the equation introduced by Fuentes-Cano et al. [36], revealed similarities between the chars and AC carbon in these studies and the chars presented in the source paper, *i.e.* coal, coconut and sewage sludge

chars. Calculated activities also pronounced the differences between chars properties during pyrolytic and steam reforming modes, with activity function values decreasing to ~0.10 and ~0.45, respectively, with the reaction time. Variations in the coniferous and deciduous chars activities, with the improving effect of pine extractives removal, was also observed during initial 30 min of the process.

These results suggest that wood-derived biochar and commercial activated carbon have similar abilities to catalyse hydrocarbons conversion. The effectiveness of toluene removal was found to be influenced more by coke deposition/gasification rates than the type of the applied catalyst.

4.7. Additional experiment with activated alder char

In section 4.4, a conclusion on toluene conversion principle was presented. It was based on data obtained from the main experiment and supported by some well-established findings reported in the literature [5,6,15,36,37]. However, to further clarify some aspects of tar conversion mechanism over biomass char, a series of additional experiments targeted to explain certain ambiguities of the process were performed. Since all studied chars, revealed similar qualitative contribution to the conversion process, only one was used in this part of the research. To this purpose, an activated alder char was selected, as a representative of a more efficient chars (deciduous tree derived ones) prepared from the wood of the medium hardness, among the three studied species.

The results of the main experiment of toluene decomposition suggested, that all its conversion underwent heterogeneously on a char surface and the only influence of the atmosphere in the reactor was on the catalyst bed transformations. There was however another possibility, that at high temperatures, some radicals were released from the char surface and they were further interacting with toluene in gas phase reactions. To evaluate the possibility of such a phenomenon, the intermittent feeding test was introduced to the scope of the research. It was aimed to interrupt the toluene to elute any volatiles from the char bed, to examine if after resumed toluene feeding its conversion was affected. Moreover, to further investigate the lack of toluene homogeneous conversion in the reactor, a stronger oxidising agent was used, instead of steam, in the hope of triggering some gas phase reaction, so that their intertwining with catalytic conversion could be examined. To this end, the experiment where steam was substituted with oxygen was performed.

Another unresolved issue of the toluene conversion pathways was the contribution of its methyl group to its product distribution and conversion efficiency. Therefore, two

experiments were either less or more substituted aromatic ring was used as a tar representing, were performed with benzene and *p*-xylene, respectively.

Finally, as there were some inconsistencies on the role of AAEM species in hydrocarbons, mainly methane, reforming [14,16], the experiment to evaluate the importance of inorganics on the toluene conversion was made.

4.7.1. Toluene intermittent feeding test

Preliminary tests of toluene pyrolytic conversion in an empty reactor, *i.e.* reactor tube filled with quartz wool only, without any char present, revealed no toluene decomposition. It was therefore concluded, that at the conditions of the experiments in this study, no homogeneous, gas phase reactions occurred. When an activated char bed was introduced in the scope of the main experiment, almost complete initial toluene removal (>90 %) was experienced, and it was deteriorating with char time-on-stream. The conversion process was therefore attributed to the heterogeneous toluene-char interactions, yielding mainly coke, with small amounts of benzene and trace amounts of substituted benzenes. Gases related to toluene decomposition, *i.e.* H_2 and CH_4 were also detected. Besides heterogeneous toluene-char reactions and eliminated by preliminary test results char-independent gas phase reactions, there was also a third conversion possibility. If the activated char with surface functional groups was heated up in the reactor, it might release some radicals that would further interact with toluene in indirect char-dependent homogeneous reactions. To investigate this possibility, an experiment with intermittent toluene feeding during pyrolytic conversion over activated alder (AA) char was performed. The principle of the test was to begin toluene feeding accordingly to the main experiment run, and then stop the feeding for 15 min. During this time, while maintaining desired reaction temperature of 800 °C, a char bed was purged with pure N_2 flow to elute any possible volatile species and to cease any possible chain reactions. After this time, a set of new impinger bottles were connected to the reactor's outlet and the toluene feeding was resumed. Liquid products yields could therefore be accessed separately for both feeding stages, but they could be also calculated globally, for the total run time. The comparison of total toluene conversion and its by-products yields during continuous and intermittent feeding allowed for conclusions on the char's possible role as an initiator of homogeneous toluene decomposition chain reactions. To this end, a partially deactivated, yet still catalytically active char was desired during the restarting of toluene feeding. Hence, time of the initial step was selected around the one-half of the time were pronounced, progressing deactivation of char was registered. According to a shape of toluene conversion

plot (Figure 16), this timeframe comprised initial 30 min of the toluene pyrolysis. Two intermittent feeding tests with different setups were tested. In the first mode, denoted as 10+20 min, the time of the initial step was set to 10 min, followed by the second, 20 min step. Analogously, the second setup, 15+15 min, comprised two steps, each lasting for 15 min. Therefore, a total time of each mode amounted to 30 min and they were compared with the results for the 30 min run from the main experiment in PYR mode for activated alder char, where continuous toluene feeding was carried out.

Moreover, for the 10+20 min test, toluene conversion within the initial 10 min was compared to the 10 min run of the main experiment. The conversion during the second 20 min step was compared with the main, continuous feeding experiment as well. To this end, the results for the 10 min continuous feeding run were subtracted from the results obtained in the 30 min continuous feeding run of the main experimental series of PYR mode for AA char.

The overall toluene conversion during the 30 min of continuous feeding experiment and the two intermittent feeding tests were presented in Table 14, along with the created benzene yield expressed in different forms. A pooled standard variation for toluene pyrolytic conversion was 5 % and a one-way ANOVA analysis of the obtained results suggested no statistically significant differences between the three tests. The mass of created benzene also did not statistically varied, and due to uniform toluene conversion rates, the relative benzene yields were also similar. These findings suggested, that the interactions between toluene and char undergoes on the char surface, without any homogeneous interactions in the gas phase.

The comparison of the small amounts of created substituted benzenes, however, revealed some differences in yields, depending on the applied feeding type, as was shown in Figure 47. It was found out, that beside ethylbenzene, the yields of other substituted benzenes, *i.e.* xylenes and styrene were slightly enhanced during the continuous feeding experiments. These small discrepancies might suggest an elution of volatiles created during toluene conversion, *e.g.* CH_4, ethylbenzene *etc.*, form the reactor during intermission with N_2 purging. After resuming the feeding for the second step, the recombination reactions leading to substituted benzenes formation would be initially inhibited by the lack of gaseous compounds necessary for their creation.

The additional evaluation of toluene conversion and benzene yields within the initial 10 and the following 20 min of the 30 min continuous and intermittent runs, presented in Table 15, further supported the conclusion, that two main toluene conversion pathways leading to coke and benzene, were unaffected by the intermission.

Table 14. Toluene conversion (η_T) and benzene mass (m_B) and molecular yield (x_B) for continuous and intermittent feeding during 30 min pyrolytic conversion runs

	30 min	**15+15 min**	**10+20 min**
η_T	0.66	0.64	0.69
m_B, mg	11.82	9.82	10.28
x_B (on fed toluene)	0.08	0.07	0.07
x_B (on reacted toluene)	0.13	0.11	0.11

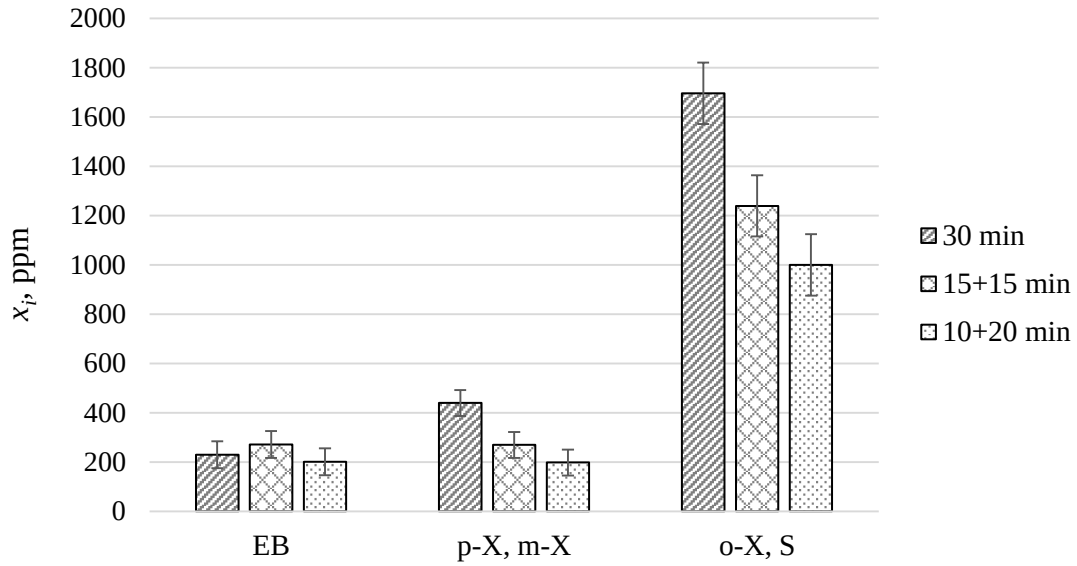

Figure 47. Substituted benzenes relative molecular yields x_i (based on reacted toluene) for continuous and intermittent feeding during 30 min pyrolytic conversion runs, where index i represents: EB – ethylbenzene, p-X, m-X and o-X – p-, m-, o-Xylene, respectively and S – styrene

The results of this experiment confirmed, that the main mechanism of toluene pyrolytic decomposition over activated char underwent strictly on the char interface as a heterogeneous, catalytic conversion, and no species potentially released from the char surface took part in the reactions. The results also confirmed, that the conversion efficiency and main products, coke and benzene, distribution was unaffected by the volatile species presence, and relayed only on char activity and its surface availability. Moreover, it could be concluded, that the activity of the char did not decreased upon the applied intermission. This suggests, at the time of the intermission, the char surface was thermally stable. It also suggests that any changes to char structure and active sites at this stage of the process were

solely the repercussions of toluene decomposition. The decrease in substituted benzenes yields upon the intermission of toluene feeding supported the hypothesis, that secondary, recombination reactions leading towards their creation were dependent more on the availability of methyl radicals than the char surface access. Therefore, their yields were relatively higher when worse catalyst (PA) was used in the main experiments (section 4.4.1) and were impaired when volatiles were temporarily removed from reactor during intermittent feeding tests. Considering a very small yields of those products, a contribution of this conversion pathway to the overall toluene decomposition efficiency is however negligible. It can therefore be concluded, that pyrolytic conversion of toluene depends on catalyst and applied reaction conditions, yet it is relatively insensitive to the continuity of the compound supply.

Table 15. Toluene conversion (η_T) and benzene mass (m_B) and molecular yield (x_B) for continuous and intermittent feeding during 30 min pyrolytic conversion runs, split into the initial 10 and following 20 min

	continuous 30 min:		**intermittent 10+20 min:**	
	first 10 min	**second 20 min**	**first 10 min**	**second 20 min**
η_T	0.93	0.53	0.93	0.57
m_B, mg	3.58	8.24	3.24	7.04
x_B (on fed toluene)	0.03	0.06	0.02	0.05
x_B (on reacted toluene)	0.03	0.11	0.02	0.09

4.7.2. Toluene conversion in a presence of O_2

No homogeneous toluene conversion was experienced during pyrolysis, either in an empty reactor, where no reactions occurred, not in char catalysed experiments, where conversion was found out to undergo only on the char surface, as indicated by intermittent feeding tests. However, a possibility of homogeneous toluene conversion during steam reforming remained unambiguous. Lack of any significant toluene decomposition during the empty reactor steam reforming tests suggested that in examined conditions, any possibly created steam-derived radicals were not sufficient to react with toluene without the catalyst presence. Char bed introduction, in the course of the main experiment in SR mode (detailed in section 0), resulted in high toluene conversions. The efficiency of toluene decomposition was correlated with char activity, which in turn was dependent on a char's reactivity towards gasification with steam. All of the above suggested, that during the steam reforming mode,

toluene was still decomposing heterogeneously on a char surface, independently to any steam-involving reactions, and the only role of steam-derived radicals was char/coke oxidation, which proved to prolong char activity.

In an attempt to gain some insight into the relations between toluene's confirmed heterogeneous and assumed homogeneous reactions in gasifying atmosphere, an experiment with another oxidising agent, yielding more reactive radicals, was performed. To this end, O_2/N_2 mixture was selected to replace H_2O/N_2. Three 40 min tests with oxygen as an oxidising agent were performed either in an absence or in presence of catalyst. The results were further compared with the ones for a 40 min SR mode run of toluene conversion over activated alder char obtained in the scope of the main experiment (detailed in section 4.4.2), as presented in Table 16. A relatively long run time was selected for these experiments to capture any effects of char deactivation/reactivation with oxidising agents in tests with catalyst bed as well as to assure steady conversion conditions in empty reactor tests.

Table 16. Oxygen tests conditions summary, toluene conversion (η_T) and some of its by-products molecular yields (x_i), where i represents: B – benzene, EB – ethylbenzene, p-X, m-X and o-X – p-, m-, o-xylene, respectively, S – styrene and BA – benzaldehyde

Test	Oxidising agent	Bed	η_T	By-products yields (base on reacted toluene)				
				x_B	x_{EB}	$x_{p-X/\mathrm{m}-X}$	$x_{o-X/S}$	x_{BA}
					ppm	ppm	ppm	ppm
1st	O_2, 3.55 vol.%	none	0.93	0.14	5613	48	10094	6558
2nd	O_2, 0.67 vol.%	none	0.16	0.27	51790	735	23728	44012
3rd	O_2, 0.67 vol.%	AA	0.78	0.08	116	118	1187	ND
4th	H_2O, 15.5 vol.%	AA	0.76	0.14	58	98	564	ND

Initially, a test with toluene conversion with oxygen was performed in an empty reactor, to determine if any homogeneous reactions with O radicals would occur at otherwise the same conditions as during H_2O/N_2 test, where there was no gas-phase toluene decomposition. The 15.5 vol.% steam concentration in N_2 flow, applied during SR mode, provided a high excess of O atoms required for complete oxidation of fed toluene. Therefore, for the first test run of oxygen experiments, a high concentration of O_2 was applied, providing a 1.3 stoichiometric O_2 excess ratio. As expected, with an abundance of strong oxidising agent, high toluene conversion was achieved in this test and it was comparable with the initial effectiveness of char catalysed decomposition, prior to char deactivation. Despite high O_2 concentration and

high toluene conversion, there were however some by-products yielded as well. Previously experienced compounds, *i.e.* benzene and substituted benzenes were detected in significant amounts. Moreover, the 1st test revealed several other compounds that were detected with GC-FID, one of which was identified as benzaldehyde. This suggested that toluene decomposition with O_2 yielded some products of incomplete combustion and, as opposed to PYR and SR modes, some of them were O-containing species as well. Toluene decomposition in an O_2-rich environment proved to be highly effective, as opposed to the tests with steam, where no conversion in homogeneous conditions in empty reactor occurred. This comparison proved a much higher toluene reactivity towards O radicals than steam-derived ones. Therefore, in the 2nd test, still in an empty reactor, the O_2 concentration was lowered, so that it provided only 0.25 of the O molecules required for a complete, stoichiometric toluene oxidation. This lowered toluene conversion significantly, down to 16 %. In the third test, the lower O_2 concentration was maintained, but the AA char was inserted to the reactor as during the main experimental series. Toluene conversions as well liquid by-products for three oxygen tests and SR reference were compared in Table 16. Moreover, gaseous products relative molecular yields for tests 2nd – 4th were presented in Figure 48. Due to char deactivation in time and a steady nature of continuous process in an empty reactor test, the gaseous yields were compared at 20th min, *i.e.* at the middle of the process, where it was expected that the catalytic conversion was not yet strongly affected by a char deteriorating performance.

A perusal of the presented results revealed significant differences in toluene conversion pathways depending on the applied conditions. In oxygen-rich environment of 1st test, toluene decomposition at 800 °C was highly efficient without any catalyst. It proved that homogeneous oxidation took place when O radicals were present in the reactor. Those gas phase reactions yielded some heavier by-products as well, suggesting not only toluene oxidation but also secondary, recombination reactions taking place in the reactor, some of them involving O-containing species formation. These findings are in an agreement with similar oxidation studies, where *e.g.* benzaldehyde and phenol creation was experienced [80]. Reduction of O_2 supply, during 2nd test, resulted in an expected decrease in toluene conversion. While excess of O_2 enabled 93% toluene conversion, providing 25% of stoichiometrically required O atoms, resulted in a conversion of only 16%. Due to this O_2 deficiency, much more secondary reaction products were created. It has to be however pointed out, that those products, despite an O-depleted atmosphere, still comprised O-containing compounds, as revealed by high yield of benzaldehyde. The 2nd test proved,

that even at gasifying, instead of fully oxidising, atmosphere, toluene homogeneous conversion occurred, when O radicals were supplied, while it was not observed with steam-derived radicals. Homogeneous toluene decomposition in O_2 atmosphere yielded CO and CO_2 (Figure 48), indicating that the conversion was carried out as a ring-opening mechanism in an oxidation reaction, rather than condensation into coke observed in catalytic experiments. Presence of toluene demethylation product, *i.e.* benzene, suggested some CH_4 formation. CH_4 was not detected during GC-TDC analysis, which would suggest either an *in situ* consumption in secondary reactions or that CH_4 yield fell below the detection limits. The latter might be expected since, absolute values of the released gases in 2nd experiment, and thus their concentrations, were particularly low, due to a low toluene conversion.

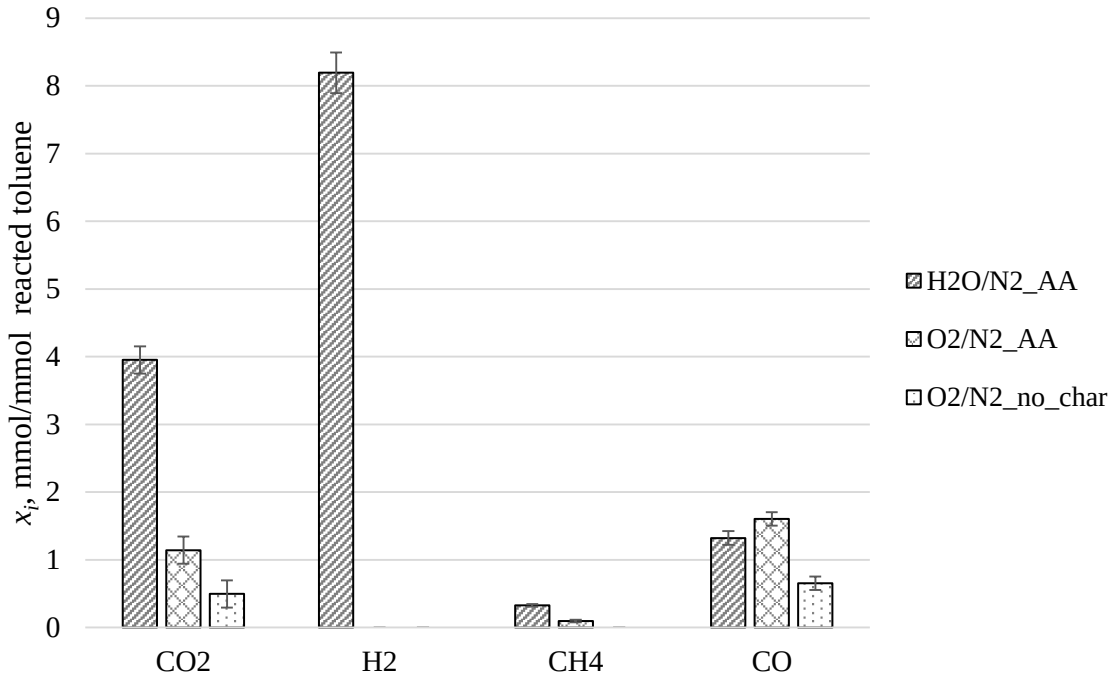

Figure 48. Molar gas yields (based on reacted toluene) for the initial 20 min of a 40-minute toluene catalytic conversion experiment over alder (AA) char in 15.5 vol.% H_2O and 0.67 vol.% O_2 as well as in an empty reactor in 0.67 vol.% O_2

Introduction of an activated alder (AA) char bed to lower O_2 concentration experiment, *i.e.* 3rd test, improved toluene conversion significantly, up to 0.78. This indicates a strong catalytic influence of the char, visible even in a presence of highly reactive O radicals. A presence of AA char significantly decreased the amount of liquid by-products. Moreover, in this test, the only detected products were the ones found in main the pyrolytic and steam reforming experiments with chars (section 4.4). There could be two reasons for the lack of

heavier compounds, including O-containing ones, further along the reaction zone. One explanation would be that all the heavier and/or oxygenated compounds created in homogeneous toluene conversion with O radicals were immediately adsorbed by the char and only the lighter by-products were eluted from the reactor. Another possibility was that in the presence of char, homogeneous toluene conversion ceased and all toluene decomposition underwent via heterogeneous reactions on the char surface. In an attempt to test the second hypothesis, additional repetition of the 3rd test was conducted where toluene was spiked with benzaldehyde, to artificially introduce this compound into the reaction chamber, at a concentration similar to the one yielded in the 2nd test. The presence of added benzaldehyde in the impinger bottles would prove that this compound formation was ceased upon char introduction to the reactor. However, no benzaldehyde was detected in these modified conditions. This observation did not provide any conclusion on the second hypothesis, of changed conversion mechanisms. It proved, however, that the first hypothesis is plausible, *i.e.* that during toluene conversion with char and oxygen some secondary products of homogeneous conversion could still be created, but they were captured within the char bed and never left the reactor. The CO and CO_2 were yielded in the 3rd experiment, as well as during the 2nd. This time, however, either it could be related to the homogeneous, ring-opening reactions of O radicals with toluene or it could be a result of char oxidation. A CO/CO_2 ratio higher than 1 in both the 2nd and 3rd test was observed, while in all the steam reforming experiments, where char was gasified, CO_2 release dominated. This observation, however, is most likely related to the nature of the oxidising agent and its reactions with carbon based materials, and it is not related to the type of the material itself. Therefore, a CO/CO_2 ratio >1 in the 3rd run does not necessarily mean that those gases were derived from gas-phase toluene ring openings. It was rather caused by the lack of steam in the reaction zone, thus no water-gas shift reaction could occur. This assumption was reinforced by the lack of H_2 detected during 3rd test, as this species would be created along with CO_2 in the water-gas shift reaction. Heterogeneous toluene conversion via coking should also release some H_2, as observed in PYR mode experiments. The lack of H_2 suggests that either dehydrogenation usually entailed by coking did not occurred in a presence of O radicals, or that it was *in situ* consumed in secondary reactions. Some CH_4 was however detected during 3rd test and this could be attributed, as in the rest of experiments, to toluene demethylation to benzene.

The comparison between tests with alder char in either O_2 or steam, 3rd and 4th test in Table 16, respectively, revealed that similar toluene conversions were achieved in both

cases. Qualitatively similar liquid by-products of toluene conversion were detected in both cases. Additional compounds created with O_2 homogeneous reactions in 2nd run were either detained by the char bed or not formed at all, as discussed above. Among the species eluted from the reactor, 3rd run with O_2 yielded significantly less benzene and more substituted benzenes than the steam reforming, *i.e.* the 4th test.

Gas composition yielded during discussed experiments varied significantly. The shift in proportions of CO/CO_2 ratio between 3rd and 4th test could be attributed to differences between H_2O and O_2 reactions with C. In an abundance of steam, a water-gas shift reaction:

$$H_2O + CO \rightleftarrows H_2 + CO_2 \tag{18}$$

would occur, leading to an increased CO_2 yield as well as an intensified H_2 formation. In oxygen tests, no H_2 was detected, although some amounts should be created during coke creation coupled with toluene dehydrogenation. It is however possible, that with the presence of O radicals, any released H_2 was instantaneously consumed in secondary, gas-phase reactions. A lower CH_4 yield during 3rd test correlated well with a lower benzene yield.

A summary amount of CO and CO_2 generated during the experiment was much higher during a steam reforming mode. As previously described in section 4.4.2, those gases in SR mode were related exclusively to char/coke gasification. In oxygen experiment, where toluene homogeneous reactions were not disproved, registered CO and CO_2 might be caused by solid carbon oxidation as well as by toluene gas-phase oxidation. However, even if all released CO and CO_2 would originate from char/coke oxidation, lower summary yield of those gases suggested lower oxidation rate of the catalyst bed, compared to steam reforming (SR) mode. It can be concluded, that although a more reactive agent was used in the 3rd test, its lower concentration resulted in slower char gasification, compared to a less reactive but more abundant steam. This suggested, that char/coke oxidation rate was more sensitive to the amount rather than quality of the provided oxidising agent. Toluene oxidation, on the other hand, was strongly dependent on the reactivity of the atmosphere and in an empty reactor, it reacted even with small amounts of O_2, while no conversion was detected even in an abundance of steam.

An inhibited gasification of char bed in experiment with oxygen should lead to an increased coke agglomeration and catalyst deactivation, compared to SR mode. To validate this assumption, ATR-FTIR spectra of spent chars were compared in Figure 49. A flatter spectrum of a surface of the spent char from 3rd test with oxygen, compared to the fresh char, indeed suggested a loss of functional groups, caused most likely by coke deposition. The

char recovered after SR mode has maintained its oxygenated structure, suggesting that during this case, a re-activation of the catalyst by steam gasification was pronounced.

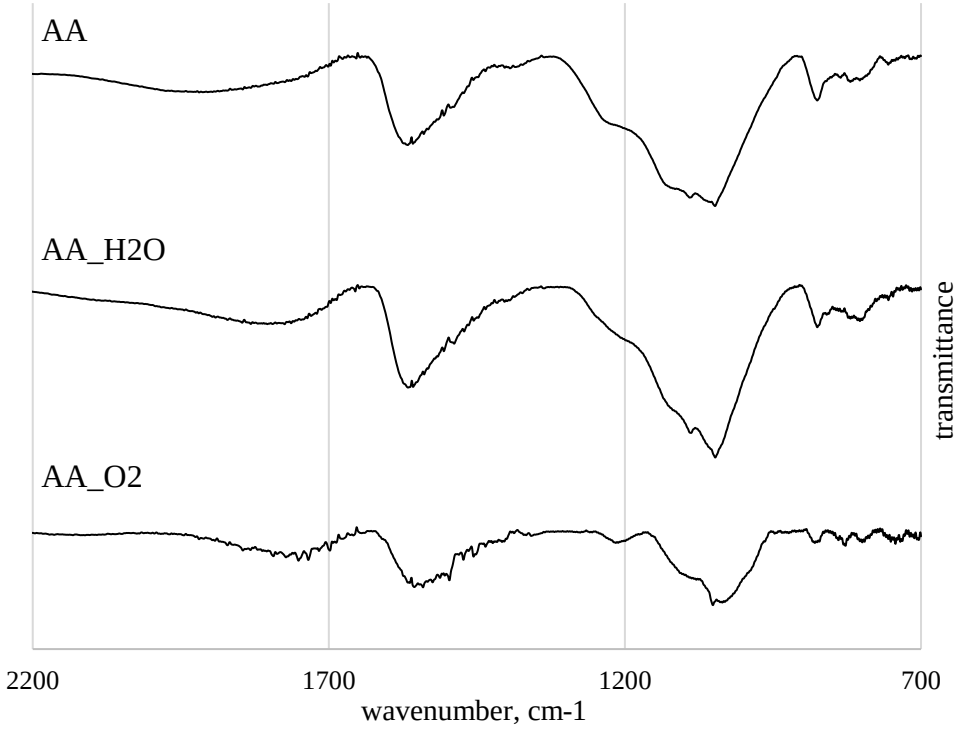

Figure 49. ATR-FTIR spectrum of fresh alder char (AA) surface, compared the spent char after 40 min toluene reforming in 3rd (AA_O2) and 4th test (AA_H2O)

Changes to the char surface upon toluene conversion with steam and oxygen were also evaluated by N_2 adsorption-desorption analysis at 77 K. The isotherms of the spent chars from the 3rd and 4th tests were presented in Figure 50. Both isotherms are a composite of a type I and II with H4 hysteresis, typical for micro-mesoporous carbons [37,112]. A steep increase at lower relative pressures, typical for type I isotherm results from adsorption in micropores. The next part in the type II shape corresponds with mesopores. The H4 hysteresis occurring at this part of the adsorption-desorption plot suggested slit-shaped pores. A higher absorbed quantity at low relative pressures for char recovered after 4th test with steam indicated more micropores, compared to the 3rd test char, while the higher total N_2 uptake suggested higher surface area. Isotherm for AA char from 4th test also had a more pronounced hysteresis. Fresh and spent AA chars' surface area determined by BET model, and micropores areas estimated with a t-Plot method were presented in Table 17. A total surface area of char decreased during both tests, however, the effect was much more pronounced in the 3rd test, proving that more coke was deposited in this case. During the 4th

test, the depositing coke and the char itself were constantly gasified with steam. It resulted in a better-preserved surface area. However, the relative amount of micropores decreased significantly from 59 to 34 %. This could be attributed to the pore widening effect of steam activation of char [33]. The test with oxygen resulted in a more deactivated char, yet the proportions between micro and mesopores remained closer to the initial ones in a fresh char.

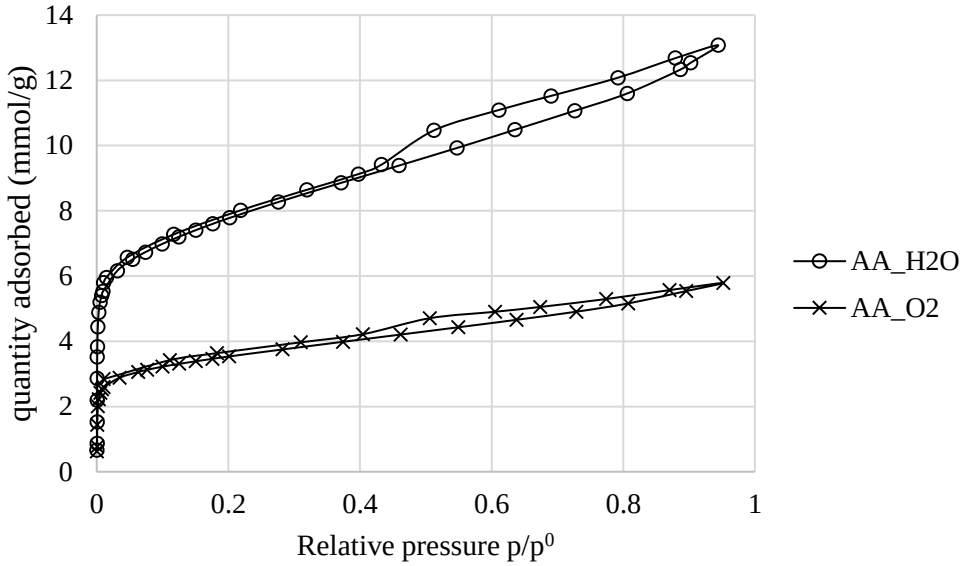

Figure 50. Nitrogen adsorption-desorption isotherm at 77 K on activated alder char recovered after 3rd (AA_O2) and 4th (AA_H2O) tests

Similar toluene conversion in 3rd and 4th tests, despite the deactivation of char during the former, could be explained by an additional toluene conversion mechanism contributing to the overall efficiently of the process. This might suggest that some homogeneous toluene reaction with O radicals, experienced in an absence of char, was still occurring even after catalyst bed was inserted. If the assumption was made, that the toluene conversion experienced in an empty bed run in 2nd test was not affected at all by char introduction, than the overall toluene conversion in 3rd test would involve 0.16 of fed toluene decomposed homogeneously and 0.62 (by diff.) decomposed on the char surface. This estimated heterogeneous part of the overall toluene conversion in 3rd test corresponds well with the pyrolytic toluene conversion over AA char in 40 min run (0.61), obtained during the main experiment (reported in section 4.4.1). Therefore, an assumption could be made, that during toluene conversion with AA char in the presence of O_2, the toluene-oxygen homogeneous interactions registered in the absence of char were maintained at a similar level. Therefore, O_2 was consumed primarily by gas phase conversion, and the char bed was not undergoing

gasification/re-activation. Concurrently to homogeneous conversion, large part of the fed toluene decomposed on the char surface, yet this decomposition effectiveness was close to the one of a pyrolytic (PYR) conversion rather than the steam reforming (SR) one, since char/coke was not oxidised. Under this assumption of O_2 consumption primarily in gas phase reactions, the former speculation about char's reactivity being more sensitive to the amount rather than strength of the oxidising agent would be no longer valid. However, the conclusion about toluene's high reactivity in the presence of even low amounts of oxygen, and lack of reactivity in the presence of excess of steam would be confirmed. Moreover, it would mean that O radicals favoured homogeneous reaction with toluene over char oxidation. This conclusion is very plausible, since the oxidation of a substituted, single-ring compound would be expected to require lower energy than a reaction with a highly dense carbon matrix of char. Moreover, homogeneous reactions are generally more rapid than the surface ones. Registered increase in substituted benzenes formation in 3rd compared to 4th test, as they were expected to form during the secondary, gaseous reactions, supported the assumption of the increased activity of gas phase interactions, including toluene homogeneous conversion. The lower benzene yield in 3rd test could be explained by the decreased char activity due to its deactivation with coke. Substantial amounts of benzene were created in homogenous reactions with oxygen, yet the contribution of gas phase conversion to the overall efficiency of the decomposition would be small. Most of the created benzene would be therefore originating from heterogeneous conversion, which in 3rd test was lower, compared to 4th, since no char/coke re-activation was experienced.

Table 17. Total (BET) and micropore surface area as well as micropores contribution to the overall porosity of fresh activated alder char (AA) as well as spent chars after 3rd (AA_O2) and 4th (AA_H2O) tests

	BET area m^2/g	**Micropore area m^2/g**	**Micropores share**
AA	709 ±6	421 ±8	59 %
AA_H2O	557 ±2	208 ±2	37 %
AA_O2	282 ±1	132 ±1	47 %

Performed tests of toluene conversion with O_2 did not provide an unambiguous answer, if the homogeneous toluene reactions are occurring during catalytic conversions in gasifying atmosphere. However, obtained results suggested, that at applied conditions, steam was not

sufficient to initiate any toluene homogeneous reactions, and in the presence of char, all conversion was undergoing heterogeneously on catalyst's surface, while the only role of steam was continuous gasification of char and depositing coke. O radicals, on the other hand, were reactive enough to decompose toluene in the gas phase, and this mechanism remained unaffected upon char introduction. The application of catalyst, in this case, initiated concurrent, independent decomposition mechanism, and toluene was decomposing simultaneously via homogeneous and heterogeneous reactions. It could be concluded as well, that, during catalytic reforming, the larger and/or oxygenated compounds were not eluted from the reactor, as opposed to homogeneous conversion. Therefore, a catalytic conversion would not only improve toluene conversion, but it also avoided releasing other unwanted volatile contaminations and conversion by-products.

It can be therefore concluded, based on the additional tests of toluene conversion in O_2, that the most efficient conversion mechanism, besides a direct combustion in an excess of O_2, is a heterogeneous catalysis involving coke creation. As the catalyst activity is very time limited, an introduction of a mild oxidised like steam could prolong the conversion by a constant re-activation of the catalyst surface. The presence of a solid carbon bed in the reforming reactor is also expected to prevent any possible heavier conversion by-products release, therefore limiting the secondary contamination of gas. The introduction of small amount of a strong oxidising agent proved to enhance the conversion, and since it most likely favours volatiles oxidation, rather than solid carbon gasification, it should not result in excessive consumption of the carbon-based catalyst during the reforming process. This experiment pointed out different roles of different oxidising agents. It can be therefore stated, that an optimisation of the reforming gases mixture composition constitutes one of the most important issues for a highly efficient and time-steady tar removal.

4.7.3. Benzene conversion over activated alder char

Toluene, as a simple single-ring aromatic with one functional group, was selected for the main part of this research, as it was considered relatively refractive, yet providing some conversion by-products, which allowed for a secondary reactions assessment. To estimate the importance of toluene's methyl group on its conversion efficiency, an additional experiment with pyrolytic and steam reforming of benzene was performed.

To this end, a 30 min benzene conversion tests over activated alder char in pyrolytic (PYR) and steam reforming (SR) modes were performed in the conditions otherwise identical to the main toluene conversion experiment. The same mass concentrations of feed benzene and

toluene were maintained, *i.e.* 12.3 g/Nm^3. The details of the main and additional tests were described in Chapter 3. The benzene conversion tests were compared with the 30 min AA test obtained in the scope of the main experiment described in section 4.4.

Toluene and benzene conversions during 30 min pyrolytic (PYR) and steam reforming (SR) experiments were compared in Figure 51. As expected, a more refractory benzene was less likely to decompose and in an inert atmosphere, its conversion was below 39 %. The introduction of steam in SR mode, although increased conversion of toluene, did not provide any significant improvement of benzene conversion. As was discussed in previous sections 0 and 0, the main role of steam was to prolong char activity by continuous gasification of catalyst bed and depositing coke. Lower benzene conversion, compared to toluene, registered in PYR mode would suggest lower yields of coke created from this compound, although the same char with the same capacity for coke was used. Therefore, if the less efficient decomposition of benzene was attributed to the more stable, thus more refractory, structure of its molecule rather than to a char deactivation, the re-activating properties of steam would not translate into enhanced conversion. Less reactive nature of benzene was also confirmed by the analysis of its liquid by-products, presented in Table 18. As significant amount of toluene underwent demethylation to benzene, while some of its molecules took part in recombination reactions creating various substituted benzenes, the only detected by-product of benzene conversion was a small yield of toluene.

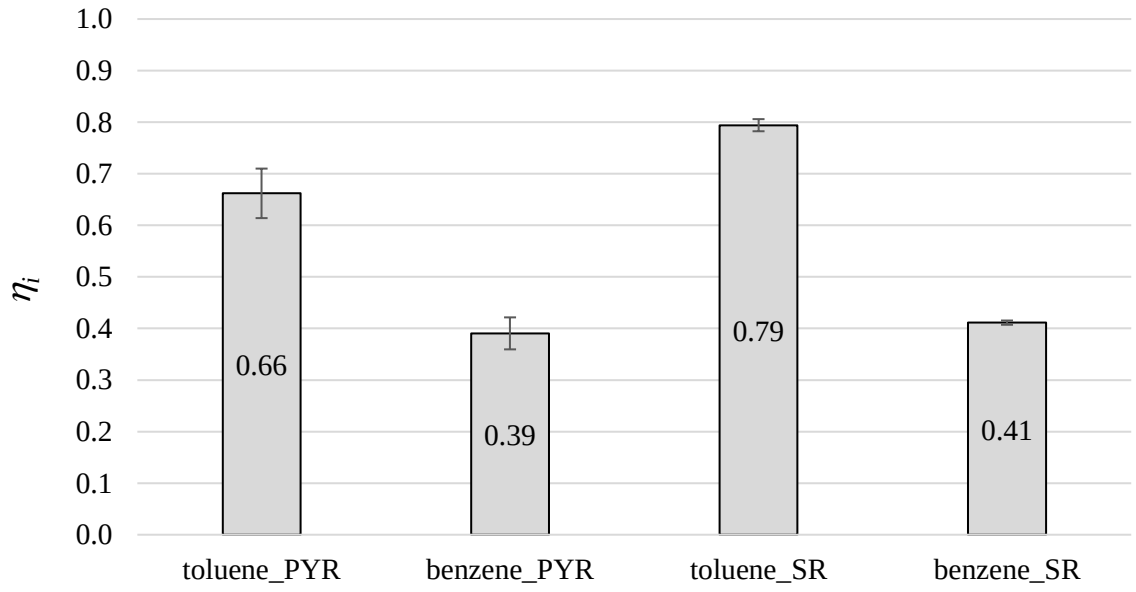

Figure 51. Toluene and benzene conversion during pyrolytic (PYR) and steam reforming (SR) 30 min experimental runs with an activated alder char bed

Table 18. Toluene and benzene pyrolytic (PYR) and steam reforming (SR) conversion liquid by-products relative molecular yields x_i (based on reacted compound), where i represents: B – benzene, T – toluene, EB – ethylbenzene, p-X, m-X, o-X – p-, m-, o-xylene, respectively and S – styrene

	x_B	x_T	x_{EB}	$x_{p-X/\mathrm{m}-X}$	$x_{o-X/S}$
	%	**ppm**	**ppm**	**ppm**	**ppm**
Toluene_PYR	12.6	-	230	439	1696
Benzene_PYR	-	339	ND	ND	ND
Toluene_SR	13.1	-	40	66	314
Benzene_SR	-	419	ND	ND	ND

Gases evolved during benzene conversion were qualitatively the same as from toluene decomposition, and their relative molecular yields, based on the reacted compound, were compared in Figure 52. In PYR mode, only H_2 and CH_4 were created. H_2, which was assigned to dehydrogenation reaction, that accompany coke creation, was formed in relatively similar amounts, provided for benzenes lower conversion. A slightly lower H_2 yield from toluene might be attributed to the fact, that some of toluene underwent demethylation to benzene instead of coking, while during benzene conversion, no significant alternative decomposition pathways were registered. The CH_4 yield was substantially higher during toluene conversion, because of before-mentioned demethylation. Interestingly, a small amount of CH_4 was released during benzene conversion as well. This might suggest that some rearrangements of benzene molecules on the char surface during coke creation released some CH_4 along with H_2. The presence of CH_4 justifies the formation of the small amount of toluene, registered in benzene conversion tests, since methyl radicals in the gas phase could initiate some substitution reactions. During steam reforming, released gases originated from both, a compound conversion as well as char/coke gasification. Therefore, some CO and CO_2 were present in the gaseous mixture as well. Steam gasification and water-gas shift reaction enhanced H_2 creation. The yields of CH_4 during SR runs became more similar for both tested compounds, since the introduction of reactive atmosphere enhanced reactions between permanent gases. It is important to stress out, that the yields presented in Figure 52, while accounting for different conversion efficiencies of toluene and benzene, distorted the contribution of gasification in the released gases composition. Hence, in Figure 52, CH_4 originated from relatively similar char gasification during less intense benzene conversion would contribute more to the absolute amount of released CH_4 then during toluene conversion, levelling x_{CH4} values for SR mode. Therefore, in Figure 53, ratios

between an absolute amount of an *i*-th gas released during the SR experiment with a compound feeding to an absolute amount released during blank test with no compound fed to the reactor were compared. The ratios were calculated according to Eq. 11 presented in section 4.4.2. As discussed previously, the CO and CO_2 ratios below 1 suggested that char gasification, which released those species, was more enhanced when no compound was fed, and it was diminished upon a compound introduction. Since benzene conversion was lower, it competition with steam for the char active sites was most likely less pronounced, therefore r_{CO} and r_{CO2} for benzene remained slightly higher. High ratios for CH_4 reflect the contribution of the compound conversion to an overall yield of this gas. Higher r_{CH4} for toluene, compared to benzene, test is related to its methyl group and a demethylation conversion pathway that was observed.

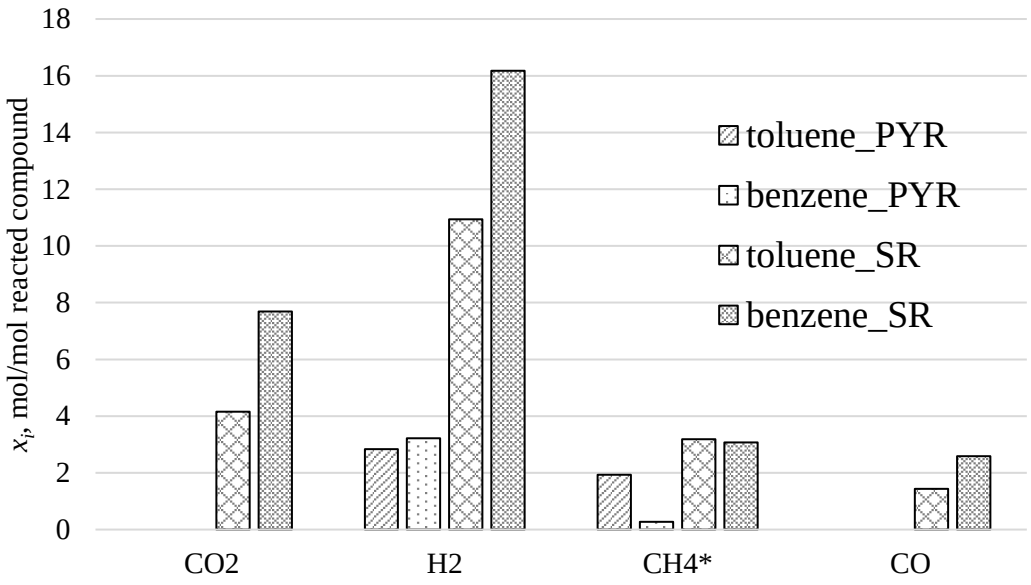

*Figure 52. Relative molecular yield (based on reacted compound) of gases released during toluene and benzene pyrolytic (PYR) and steam reforming (SR) conversion over activated alder char (*scaled – $x_{CH4} \times 10^1$ was presented due to low yields)*

A lower conversion of benzene and its insensitivity to the benefits of steam reforming was further investigated by studying properties of spent chars recovered after the tests. A total surface area and micropore area were derived from N_2 adsorption experiments at 77 K, assessed by BET and t-Plot methods, respectively. As can be seen in Table 19, in both benzene tests, the initial surface area of char was better preserved. After PYR mode tests, it was less sintered and/or coke covered and its microporosity was similar to the initial 59 %. The SR mode widened pores of the spent chars but increased the total surface area in the

case of benzene tests, suggesting a progressive activation of char despite benzene decomposition occurring concurrently. The toluene decomposition resulted in a greatly diminished surface area and microporosity of the char. The SR mode, despite undergoing gasification, did not completely prevent surface area destruction.

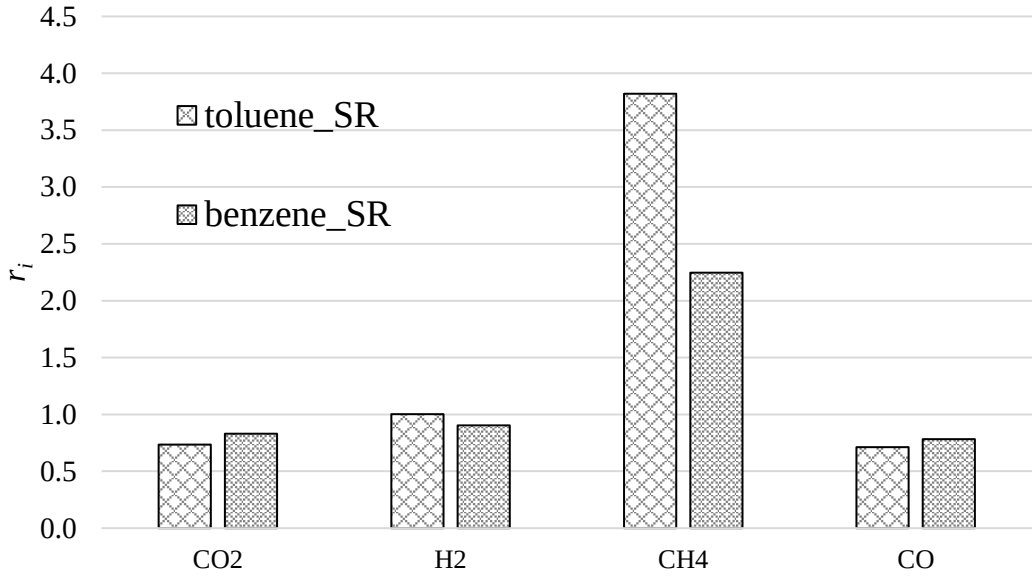

Figure 53. Ratio of the amount of a gas species released during a toluene or benzene steam reforming (SR) to the amount released during a blank run with no compound

Table 19. Total (BET) and micropore surface area as well as micropores contribution to the overall porosity of spent alder chars after 30 min pyrolytic (PYR) and steam reforming (SR) conversion of toluene and benzene

	BET area m^2/g	**Micropore area m^2/g**	**Micropores share**
toluene_PYR	272 ±1	134 ±1	49 %
benzene_PYR	401 ±2	215 ±3	54 %
toluene_SR	617 ±2	239 ±3	39 %
benzene_SR	749 ±3	343 ±4	46 %

On the other hand, the ATR-FTIR analysis of spent chars, presented in Figure 54, suggested a very similar structure of spent char after runs with benzene and toluene. The same decrease in oxygenated functionalities upon PYR mode was registered. The SR mode left both chars with the same, highly oxygenated structure. The only differences between the benzene and toluene test spent chars were visible at the low frequencies region (<900 cm^{-1}) where the

C-H vibration in aromatic rings occur, suggesting different substitutions patterns of aromatic structures in those chars.

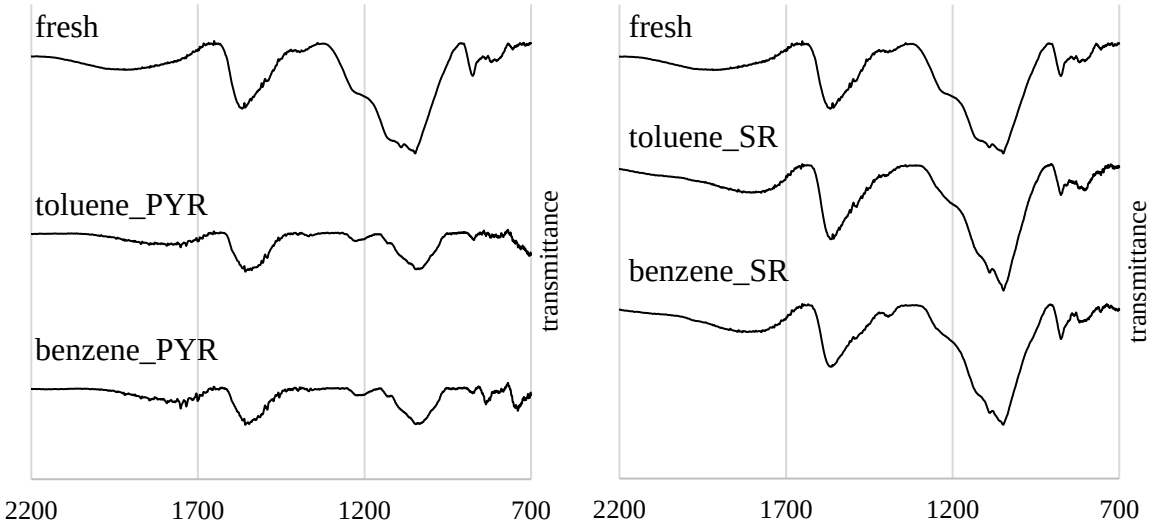

Figure 54. ATR-FTIR spectra of fresh alder char and spent chars recovered after pyrolytic (PYR) and steam reforming (SR) experiments of toluene and benzene conversion

The less deteriorated porosity and surface area in chars recovered after benzene decomposition tests corresponded well with this compound's lower conversion and thus expected smaller amount of formed coke. The similarities in char spectra might suggest that the consumption of oxygen functionalities by both compounds was similar, despite a lower amount of coke created during benzene conversion. It is possible, especially since the low frequencies of the spectra suggests differently substituted aromatic rings on spent chars surfaces, that the toluene-derived coke had a different structure to a benzene-originated one. In case of phenol adsorption, a π-π* stacking of molecules was expected, as reported by Shen [5]. It is possible, that the methyl group of toluene also allowed for some molecules piling and more developed structures formation on the char surface. It would explain the enhanced conversion and increased pore filling with toluene-derived coke, and an unaffected uptake of the surface functionalities. It could also explain benzene's higher resilience to decomposition, despite better-preserved activity of the char. Therefore, the experiment with benzene suggested, that besides the catalytic properties of char, a compounds structure could determine its conversion effectiveness and the more stable, refractive compounds would be less sensitive to the catalyst activity and its active sites availability.

4.7.4. Pyrolytic conversion of *p*-xylene over activated alder char

A difference in conversion efficiency upon the methyl group presence on the aromatic ring surface was registered during benzene with toluene comparison. The increased reactivity of the methylated ring was experienced and, for applied conversion times, it was independent to char activity and its capacity for coke. The more reactive toluene was also more prone to release some more substituted by-products as well as to undergo demethylation to benzene. Therefore, to further examine the role of methyl substituents in decomposing tar compounds, additional test of *p*-xylene pyrolytic conversion was performed, and its conversion efficiency and by-products were compared with those registered in the main experiment with toluene. Para isomer was selected as the one where methyl groups are the furthest apart, to limit any potential interactions between them. The pyrolytic (PYR) mode was studied as it yielded more substituted benzenes. The *p*-xylene was fed to the reactor with at the same concentration as benzene. The 10 – 50 min runs were performed and compared with toluene conversion ones.

Conversion of *p*-xylene was similar to that of toluene, as presented in Figure 55. It suggested that while the complete lack of methyl group, as determined in experiment with benzene, diminished conversion efficiency and significance of catalyst activity, the presence of additional methyl group did not enhance the removal process. The decrease in conversion efficiency with time was similar for both compounds, suggesting similar deactivation rate as well as similar dependency on char activity of both, toluene and *p*-xylene. The more complicated structure of the xylene molecule, however, resulted in a higher variety of liquid decomposition by-products. The yields of all species detected during GC-FID analysis of impingers content were presented in Figure 56. Structures of the discussed molecules were also shown in Figure 57, where the expected conversion pathways of *p*-xylene rearrangement were presented. The main rearrangement patterns were analogous to that of toluene rearrangement observed during the main experiment, *i.e.* demethylation and substitution followed by dehydrogenation. This time, however, due to two methyl groups, the demethylation yielded two products, toluene and benzene. It was also discovered, that the former underwent its own, secondary substitution reactions, yielding the same by-products as when it was a main component, fed to the reactor during the main experiment.

As with toluene conversion, besides the main pathway leading to coke creation, part of *p*-xylene underwent demethylation. This time, due to a presence of two methyl groups, both benzene and toluene were found as the demethylation products. Toluene yield was higher than benzene's as it was most likely a product of a first step of demethylation, and therefore

it was an intermediate in benzene formation, before the second methyl group scission. The first demethylation step of *p*-xylene yielded similar amounts of toluene to a toluene-demethylation-derived benzene yield in the main experiment, reported in section 4.4.1. A trend of increasing yield of demethylation reaction product with time, thus with char deactivation, is also similar between toluene from *p*-xylene and benzene from toluene tests. Benzene yield in *p*-xylene tests, as a product of a second step of demethylation, is relatively low and constant in time.

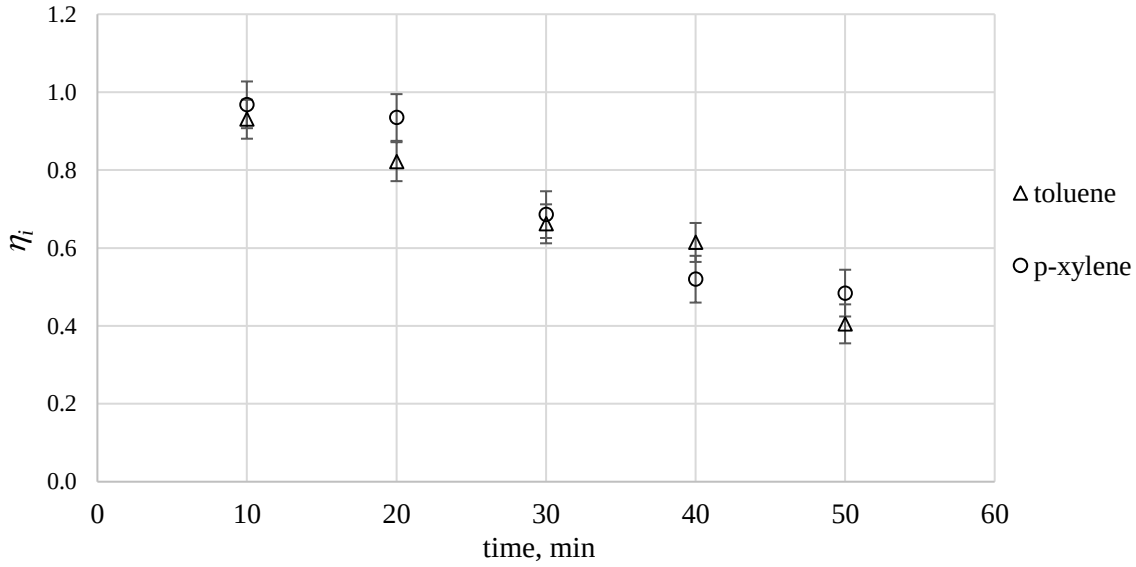

Figure 55. Toluene and p-xylene conversion in time during pyrolysis over activated alder char

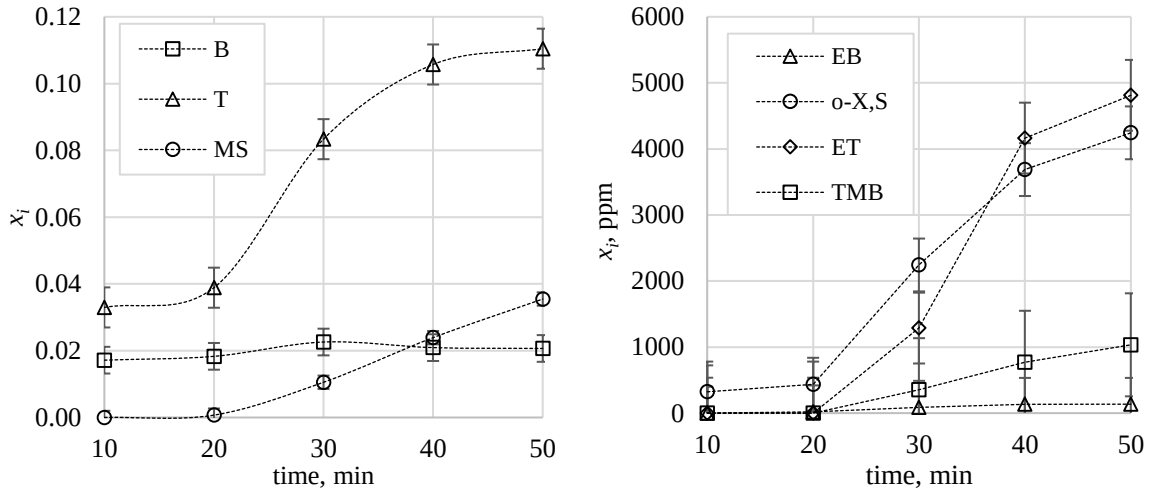

Figure 56. Relative molecular yields x_i (based on reacted p-xylene) of liquid by-products of p-xylene pyrolytic conversion over activated alder char, where i represents: B – benzene; T – toluene; MS – p-methylstyrene; EB – ethylbenzene; o-X,S – o-xylene/styrene; ET – p-ethyltoluene, TMB – 1,2,4-trimethylbenzene

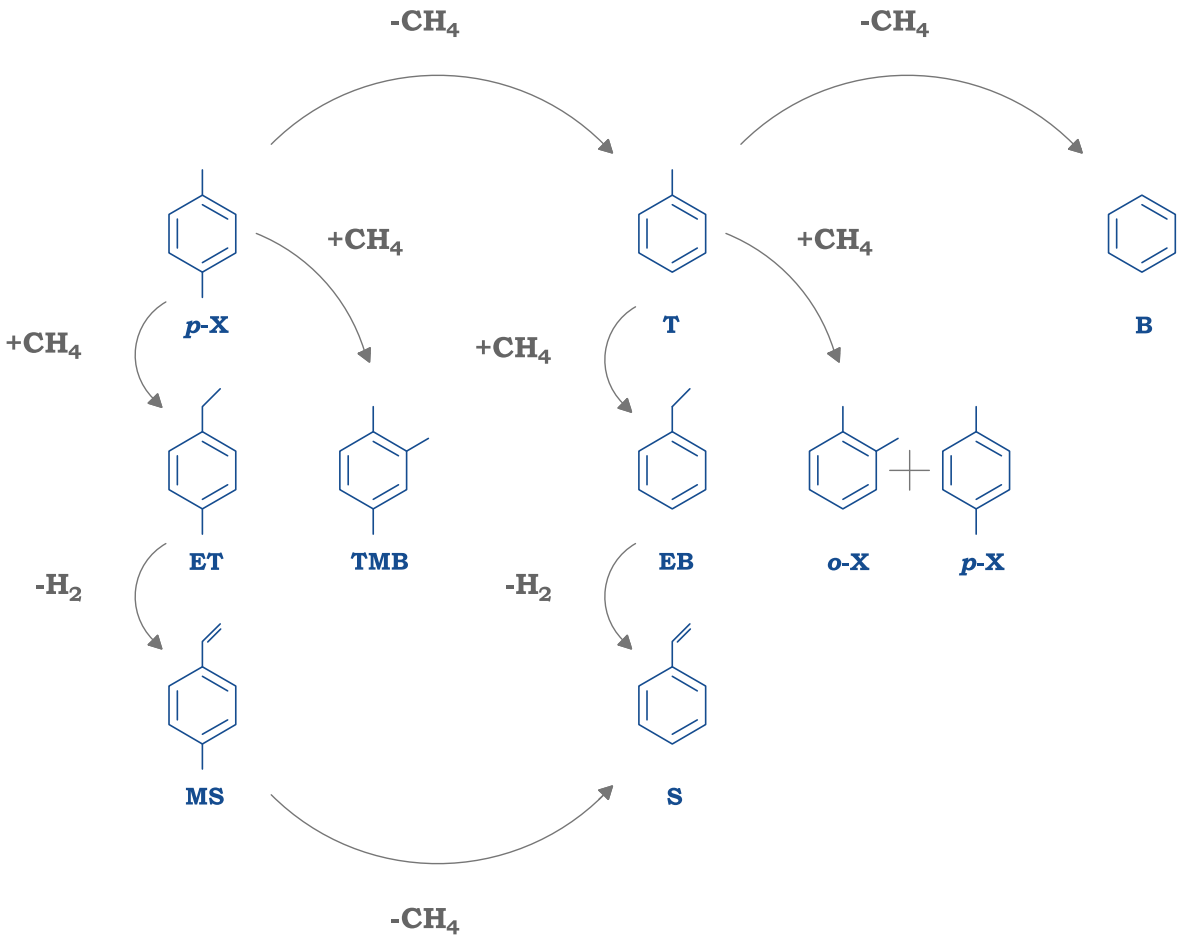

Figure 57. Proposed recombination pathways of p-xylene during pyrolytic conversion (B – benzene; T – toluene; o-X – o-xylene; p-X – p-xylene; TMB – 1,2,4-trimethylbenzene; EB – ethylbenzene; ET – p-ethyltoluene; S – styrene; MS – p-methylstyrene)

Toluene created during *p*-xylene conversion further underwent secondary rearrangements. Besides its demethylation to benzene, some ethylbenzene was also found at longer experiment times, suggesting that there was enough time for the created toluene to undergo substitution reactions. Unfortunately, for both remaining xylene isomers, FID peaks were overlapping with other compounds – *m*-xylene with unreacted share of *p*-xylene and o-xylene with styrene. It was however quite possible, that some amounts of those compounds were also created in secondary reactions of methylation. A very pronounced peak of *o*-xylene/styrene was detected and it was, similarly as in the main experiment results, attributed mainly to styrene. Moreover, p-xylene substitution reactions were experienced. Some 1,2,4-trimethylbenzene was found in the impingers, as a result of a third methyl group attaching to position 2, along the already existing groups in positions 1 and 4. No other trimethylbenzene isomers were detected. The substantial amounts of *p*-ethyltoluene were created as a result of methyl radical attack on one of *p*-xylene methyl functionalities.

It further underwent dehydrogenation to *p*-methylstyrene. This compound was detected as a separate peak on a chromatogram. Its presence, therefore, confirmed the creation of styrene in analogous dehydrogenation of ethylbenzene, during primary toluene recombination in the main experiment as well as during secondary reaction of demethylation-derived toluene in *p*-xylene tests. No other, unidentified compounds were detected during impingers content analysis. The first step of aliphatic chain formation, after methyl radical attack on the methyl group of toluene or *p*-xylene, was ceased after this step, and was most likely followed by a rapid dehydrogenation of created ethyl group. No propyl groups on the aromatic rings were created. The dehydrogenation of ethyl group to form styrenes was however strongly intensified. The amount of created styrene and *p*-methylstyrene was of an order of magnitude higher than that of their respective precursors, ethylbenzene and *p*-ethyltoluene. In *p*-xylene tests, the yield of styrene was even higher than the yield of 1,2,4-trimethylbenzene, although the former was created as a rearrangement product of toluene that was already a by-product of xylene conversion, while the latter was derived directly from *p*-xylene recombination.

The ethylbenzene yield was relatively low, as it was a product of secondary reaction of created toluene. The yield of *o*-xylene was impossible to determine due to its peak overlap with styrene. This time it was also impossible to estimate the styrene amount, since in this test *p*-xylene was not another by-product but the main compound, fed to the reactor, therefore no reference for a possible o-xylene yield was available. However, any xylene isomers creation would have to undergo through toluene intermediate and in the course of the main experiment it was established that xylenes formation from toluene was no greater than the formation of ethylbenzene. This would suggest that a negligible share of *o*-xylene/styrene peak was due to *o*-xylene and it was comprised almost exclusively of styrene. This would further indicate an extremely high styrene yield, to be solely a secondary, toluene recombination product. While styrene yield during the toluene pyrolytic conversion experiment was estimated as approximately 4 times higher than ethylbenzene (Table 9), in *p*-xylene experiment styrene yield would be 20-30 times higher than that of ethylbenzene. This suggested that large part of styrene was created in some parallel reaction, most likely in *p*-methylstyrene demethylation, since the demethylation reactions were generally intense in all performed experiments. The ration between *p*-methylstyrene and *p*-ethyltoluene was around 7, which is slightly higher, yet still comparable to the styrene/ethylbenzene ratio for main toluene PYR experiments. The yields of *p*-ethyltoluene and *p*-methylstyrene were approximately 5 and 10 times higher than respective ethylbenzene and styrene yields in the main experiment. This enhanced creation of ethyl-substituted

by-products could be attributed to an increased abundance of methyl radicals, since the fed compound possessed twice as much methyl groups as toluene used in the main experiment. 1,2,4-trimethylbenzene yield was however relatively similar to the estimated amounts of xylenes created during methyl substitution to toluene ring during the main experiment. Therefore, a more radical-rich atmosphere accompanying *p*-xylene conversion tests did not enhanced ring substitution, while it most likely improved methyl to ethyl group rearrangement.

In an attempt to summarise the rearrangement reactions of examined methylated aromatics, the graph with proposed pathways was presented in Figure 57. Besides direct compound removal via coke creation on the char surface, the recombination reactions involving methyl and hydrogen occurred. The most intense of the recombination reactions was demethylation of *p*-xylene to toluene and toluene to benzene. Moreover, the presence of methyl radicals in the reactor initiated substitution reactions, attacking a hydrogen atom in the compound's methyl group or on its aromatic ring. The former was a favoured one and it led to ethyl group creation, *i.e. p*-ethyltoluene from *p*-xylene and ethylbenzene from toluene. It was immediately followed by H_2 release to created unsaturated functional group. This dehydrogenation led to formation of *p*-methylstyrene from *p*-ethyltoluene and styrene from ethylbenzene. Moreover, it is likely, that some *p*-methylstyrene underwent demethylation to styrene. The latter of the two substitutions patterns, *i.e.* a substitution of hydrogen on an aromatic ring with a methyl group was less intense. It resulted in 1,2,4-trimethylbenzene formation from *p*-xylene as well as xylenes formation from toluene. Although it was impossible to distinguish between xylene isomers, it was expected that mainly *p*-xylene and *o*-xylene were formed from toluene, as the methyl group is known to be a *para/orto* directing one.

The main conclusions from the performed experiment with *p*-xylene feeding were that the methylated aromatic rings decomposition had some characteristic features. It involved char surface and was more dependent on its activity and surface sites than a non-substituted ring, although no difference between one and two methyl groups were observed, in terms of compound's conversion efficiency. The main conversion of methylated aromatics underwent via coking, associated with char deactivation. Second most important conversion pathway involved demethylation. Additionally, methyl group substitution reactions occurred. Substitution to the existing methyl groups, forming ethyl functionalities, was generally favoured, and enhanced by the methyl radical abundance. The aromatic ring substitution with methyl was less pronounced. Created ethyl groups were immediately and effectively

undergoing dehydrogenation, which suggested that the unsaturated C=C bond in the substituent conjugated with an aromatic ring formed an energetically favourable structure. It was also possible, that some catalytic features of char enhanced the dehydrogenation process.

Although the products of both, toluene and *p*-xylene rearrangements were released in small amounts, it is important to noticed, that they were created despite a relatively short residence times (0.16 s) and they were not removed completely by the char bed, as opposed to by-products formed in homogeneous reactions with O_2. This might suggest that the substituted benzenes were created downward the char bed. Moreover, a sensitivity of methylated by-products creation to an availability of methyl radicals indicates that in a real gasification/reforming reactor, with much more diverse gas composition, the scale of those rearrangements might become significant in terms of tar reforming and removal efficiency.

4.7.5. The influence of AAEM species on toluene conversion

The last of the additional tests was designed to determine the importance of AAEM species in the catalytic conversion of aromatic compounds. Inorganics role in solid fuels gasification and oxidation kinetics has been widely recognised [17,18]. However, the reports on their importance during methane reforming are ambiguous. *E.g.*, it was reported by Dufour et al. [16] that AAEM species do not have any significant influence on the efficiency of methane catalytic reforming over wood derived char. While the AAEM species on carbonaceous surface enhance its affinity towards reactions with oxidising agents, *e.g.* during gasification or combustion, the nature of their interactions with the oxygen-deprived toluene remain unclear. Therefore, an approach to verify the effect of AAEM species presence on toluene pyrolytic decomposition over activated alder char was made and described in this section.

To this end, fresh activated alder char (AA) was washed in HCl solution to remove inorganics including AAEM species It was further washed and dried and referred to as AA_HCl and used in a 30 min pyrolytic (PYR) toluene removal experiment, analogously to the tests performed in the scope of the main experiment. Part of the AA_HCl char was impregnated with sodium acetate to increase its Na content. It was referred to as AA_Na char and it was also used in a 30 min PYR test with toluene. The detailed procedure of char preparation for this test was described in Chapter 3.

The results of washing and impregnation of fresh alder char (AA) were examined by AAEM species content by AAS analysis (described in Chapter 3). The results, presented in Figure 58, confirmed that four examined metals content in acid washed char (AA_HCl) was

significantly reduced. AA_HCl char impregnation with sodium acetate resulted in a char (AA_Na) with a slightly increased Na content. The Na amount was higher than in the washed (AA_HCl) as well as in the original char (AA). Its concentration, however, maintained lower that the initial concentrations of the other examined metals, *i.e.* K, Ca and Mg.

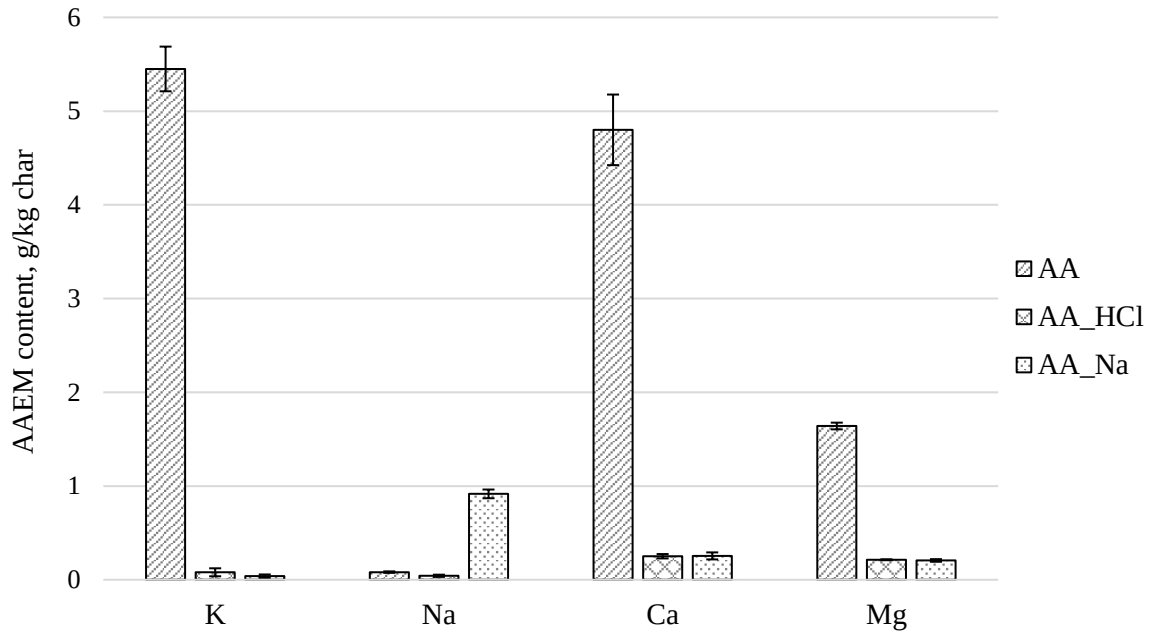

Figure 58. AAEM species content in fresh activated alder char (AA), in AA char after HCl wash (AA_HCl) as well as in AA_HCl char after impregnation with Na^+ (AA_Na)

A 30 min toluene pyrolytic decomposition test was then performed on all three chars and the obtained results were summarised in Table 20. There were no statistically significant differences between toluene conversion, as well as benzene yields, between the initial and modified chars. Substituted benzenes creation was also similar for all studied cases, with an exception of *o*-xylene/styrene yield that was slightly reduced when washed chars were used. As previously mentioned, substituted benzenes creation was expected to depend largely on the gaseous species rather than char surface properties. Registered discrepancy in styrene formation might suggest that some ethylbenzene dehydrogenation is catalysed by char inorganics and thus was inhibited by the wash.

In general, no significant differences between the performance of the original and modified chars were registered during toluene pyrolytic conversion, despite the pronounced changes in AAEM content upon the applied treatment. Further examination of original and modified chars was performed to access possible alterations to other catalytic features of the chars that

the treatment might have introduced. The ATR-FTIR spectra of all three chars were taken and compared in Figure 59 a. The acid washing of chars does not significantly influence the intensity of the char surface spectrum, it changed however the shape of a broad absorption region attributed mainly to vibrations in carbonaceous matrix structure as well as in various conformations of C–O band. The two sharp bands, characteristic for alder and beech activated chars were removed and the maximum of absorption was shifted towards higher wavenumbers. The small band around 1380 cm^{-1} was also removed as a result of the applied treatment. It is possible, that the removal of inorganics resulted in some changes to the IR absorption spectrum, *e.g.* by protonating some carboxylic salts. The most likely reason for the observed differenced is however the hydrolysis and protonation of carboxylic anhydrites and esters that were expected on the original activated char surface. This phenomenon, as described previously in section 4.3.1, was also expected to occur during char pre-treatment in Boehm titrations, resulting in high carboxylic and phenolic groups detection via this method, in contrast with the results of non-treated chars FTIR analysis. The impregnation of AA_HCl char resulted in AA_Na char with a visibly enhanced presence of both C–O and C=O bonds. Since sodium acetate was used for impregnation, the increase of the oxygen on the char surface could be explained by the acetate presence.

Table 20. AAEM tests conditions summary, toluene conversion (η_T) and some of its by-products molecular yields (x_i), where i represents: B – benzene, EB – ethylbenzene, p-X, m-X and o-X – p-, m-, o-xylene, respectively and S – styrene

Char information		η_T	**By-products yields (based on reacted toluene)**			
			x_B	x_{EB}	$x_{p-X,m-X}$	$x_{o-X,S}$
Name	**Treatment**			ppm	ppm	ppm
AA	none	0.66	0.13	230	439	1696
AA_HCl	HCl washed	0.65	0.11	230	324	991
AA_Na	HCl washed, Na^+ spiked	0.67	0.11	246	244	985

The spent chars spectra were also compared in Figure 59 b. All chars had significantly deteriorated absorption, due to deactivation. The spent chars spectra were relatively similar, although the absorption intensity decrease in the region reflecting C–O content was more pronounced when modified chars were used.

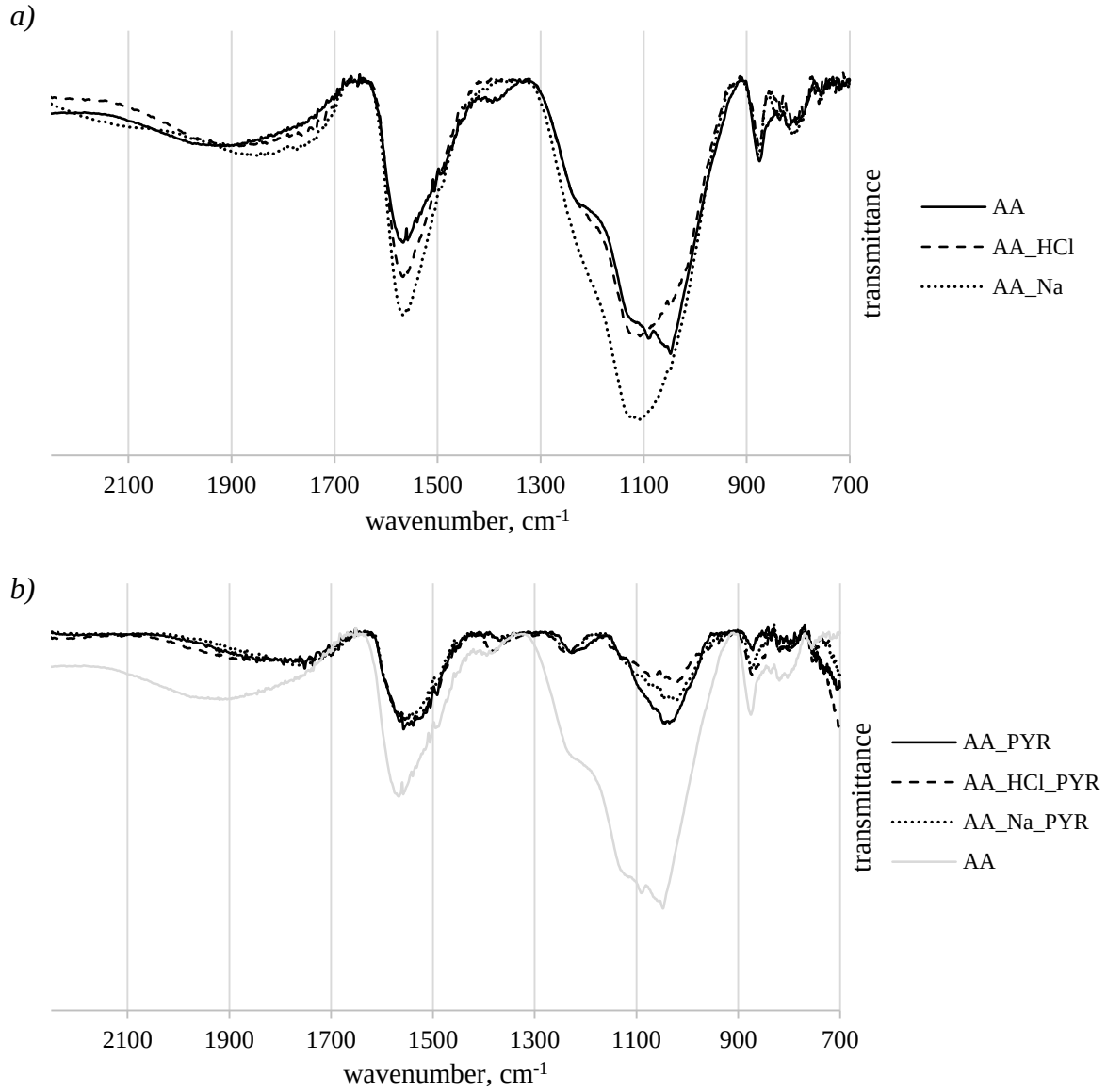

Figure 59. ATR-FTIR spectra of a) fresh, activated alder char (AA), AA char after HCl wash (AA_HCl) and AA_HCl char after Na^+ impregnation (AA_Na), as well as spectra of b) all three chars spent in a 30 min pyrolytic toluene conversion test (PYR)

To assess the changes in char physical structure, a char after final modifications, *i.e.* AA_Na char, was examined by N_2 adsorption-desorption isotherm analysis. The comparison of the modified and original sample was presented in Figure 60. A 4 % increase in total BET surface area and 8 % increase in micropore area was registered for AA_Na char, yet the shape of the isotherms and its hysteresis remained the same as for the original char (AA), suggesting that no major structural changes were evoked by the washing and following impregnation.

It could be therefore concluded, that the char treatment resulted in a significant change of AAEM species content, no significant differences in chars physical structure and a change

in the nature of their oxygen functionalities. The Na^+ impregnation, moreover, introduced additional oxygenates on the char surface. However, they were likely, derived from physisorbed acetate and thus they were expected to volatilise easily at the early stages of the process or during char heating up.

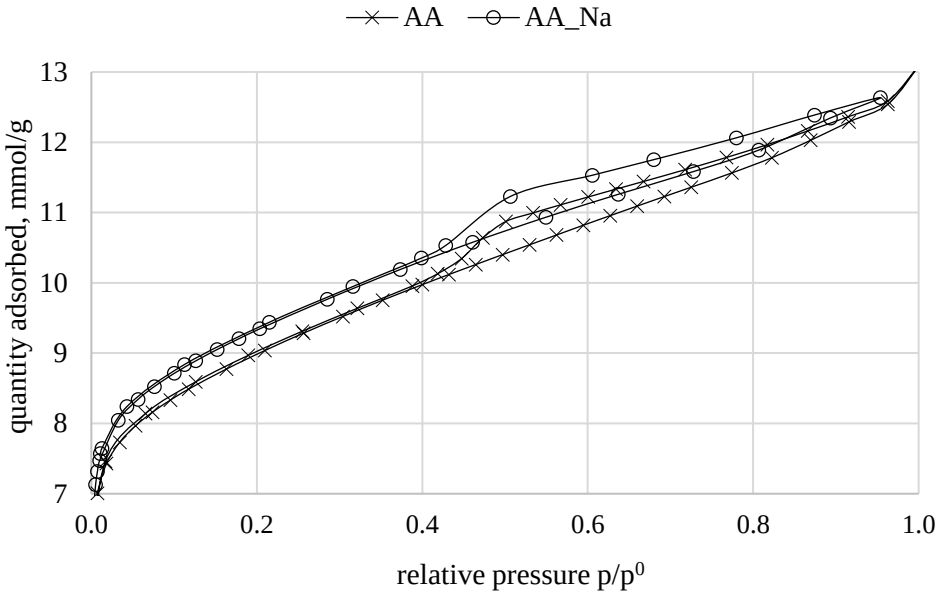

Figure 60. Nitrogen adsorption-desorption isotherm at 77 K on activated alder char (AA) and AA char after HCl washing and Na^+ impregnation. For better resolution, only the type II parts of the isotherms were presented.

The registered changes in the char samples would therefore suggest, that the washed AA_HCl char should be less catalytically active than the original char (AA), while Na^+ impregnated (AA_Na) char would be expected to have a better catalytic performance than AA_HCl char. No such tendencies were however registered in toluene pyrolytic heterogeneous conversion tests, suggesting this compound's decomposition is not particularly dependent on AAEM species.

To further investigate the observed phenomenon, a TGA analysis of char kinetics in reactions with O_2 was performed for the modified chars to compare their reactivity towards oxidation with that of an original char. The same method and initial conversion regions as during fresh char examination detailed in section 4.3.3 were considered for kinetic calculations. The obtained activation energies and the initial and final temperatures of the mass loss curves incorporated in the calculations were presented in Figure 61. Moreover, the mass loss plots and their first derivatives were compared in Figure 62. During oxidation, the expected influence of AAEM was unambiguous and very intense. The AAEM-deprived

(AA_HCl) char's activation energy more than doubled and the reaction was initiated at temperature more than 100 °C higher than the original alder char. The re-introduction of some metal cations on the char AA_Na surface somewhat reduced the activation energy and slightly lowered reaction temperatures. This indicated that char oxidation kinetic was strongly defendant on AAEM metal content. The registered mass loss curves showed clearly the differences in the char oxidation temperatures. The DTG peak on the other hand indicated different dynamics of the process. The DTG peak of AA_Na char, although occurring at higher temperatures than the original char, was shaper and higher than DTG peak of the original char, despite the higher overall AAEM content of the latter. This difference in the char oxidation intensity might be related to the different form of the original and introduced metals. The original AAEM species would be expected to occur within the whole bulk mass of the char, while the impregnation-resulted Na remained on the char surface, therefore making it more available during the reaction.

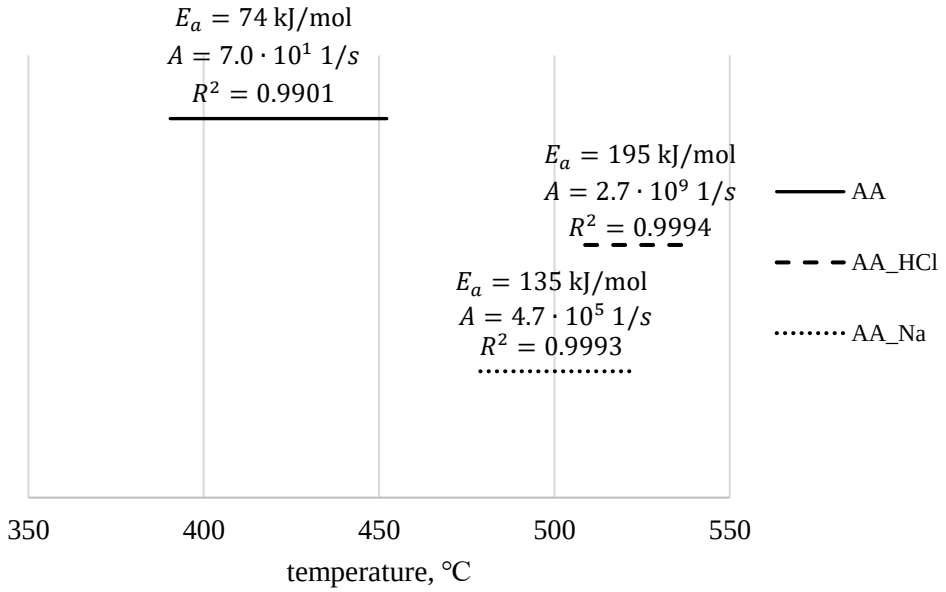

Figure 61. Activation energy (E_a) and pre-exponential factors (A) of initial oxidation of fresh, activated alder char (AA), AA char after HCl wash (AA_HCl) and AA_HCl char after Na^+ impregnation (AA_Na) with temperature range of the considered mass loss region

This experiment suggested that while AAEM species contributed significantly to char oxidation reactivity, they did not introduce any significant effects to toluene pyrolytic decomposition. It could be therefore expected, that some tar compounds heterogeneous reactions with biochar are not catalysed by AAEM species. The inorganics content and distribution in carbonaceous catalysts would however remain important in all tar reforming

processes performed in the reactive atmosphere, because of their contribution to carbon gasification and thus catalyst re-activation throughout the process. Therefore, some further research into the inorganics role in a more complicated tar reforming systems would be of interest in terms of real gasifier/reformer performance optimisation.

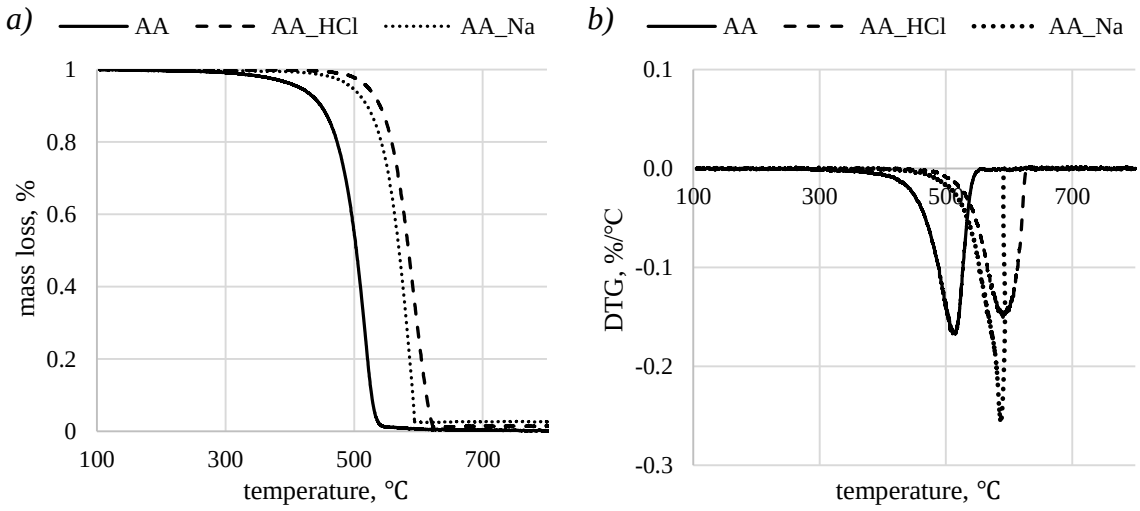

Figure 62. TGA oxidation experiment of activated alder char (AA), AA char after HCl wash (AA_HCl) and AA_HCl char after Na^+ impregnation (AA_Na): a) mass loss plots b) first derivative of a mass loss

4.7.6. Summary of the findings

In this section, series of additional experiments were performed to increase an insight into tar catalytic conversion. They were mainly aimed at verification of possible homogeneous conversion pathways during the main toluene conversion experiments, as well as at evaluation of the importance of methyl groups on compounds conversion. Moreover, an assessment of the AAEM species importance was made, since their contribution to hydrocarbons conversion remained unclear.

The course of the additional experiments reaffirmed the conclusions about toluene conversion principles derived from the main experiments described in section 4.4. Moreover, results of additional tests suggested, that:

a) No char-released volatiles contributed to toluene conversions in the conditions applied in this study.
b) Toluene conversion with N_2 and H_2O/N_2 performed during the main experiment most likely did not involve any homogeneous conversion.

c) Small amount (0.67 vol.%) of O_2 during catalytic conversion most likely initiated a homogeneous toluene conversion with O_2 along with a concurrent toluene heterogeneous conversion over char bed.
d) O_2 was favourably reacting with toluene, rather than with char in gasification reactions, while steam was involved only with solid carbon oxidation and did not react with toluene directly.
e) The lack of methyl groups on the aromatic ring resulted in a lower conversion (41 % and 49 % lower for pyrolytic and steam reforming tests, respectively), most likely due to its lower reactivity, and it was therefore less sensitive to catalyst activity. It was therefore less influenced by char regeneration with steam.
f) The introduction of second methyl group on the ring did not enhanced its conversion efficiency. It resulted in a higher yield and variety of the recombination reaction products, yet the nature of those reactions and thus their products were similar in their nature.
g) The AAEM species content greatly influenced char reactivity towards oxidation, as their removal resulted in a 2.6 times higher activation energy. However, the presence of those elements did not show any particular effect on toluene conversion efficiency. It could be therefore expected that AAEM species are irrelevant to non-oxygenated aromatic hydrocarbons pyrolytic conversion, although they might contribute to the tar reforming process by enhancing catalyst regeneration with oxidising agents.

The additional experiments revealed that the type of an oxidising agent, present during hydrocarbons conversion, might determine its role in the process, therefore, gas composition in tar reforming reactors has to be considered while designing the process. Another very important finding on AAEM species role suggests that they might not always contribute to tar reforming process. However, further studies, *e.g.* including O-containing hydrocarbons or oxidising atmosphere, are necessary to provide a full overview of metals role in tar removal processes.

CHAPTER 5

CONCLUSIONS

5.1. Introduction

The general scope of this work was focused on tar conversion over wood-derived biochars. During all experiments, tars were represented by a single, selected compound – toluene in the majority of performed tests. Conversion was carried out either under pyrolytic or steam reforming conditions. The examined biochars were prepared in a controlled, laboratory environment in a two-stage process of pyrolysis and steam activation. Three different wood species were selected for char preparation.

Two main objectives of the project were:

1) comparison of different wood species as biochar catalyst feedstock;
2) determination of toluene catalytic conversion pathways.

5.2. Summary of the experiments

This research was based on laboratory-scale experiments and analytical analyses. The initial part of the work involved designing and setting up a test rig for tar conversion investigation, as well as developing analytical procedures for required analyses. To assess a performance of the test rig, preliminary studies of toluene conversion over commercial, activated carbon were carried out. In the next stage of the work, an activated biochars preparation process was established, along with all necessary feedstock pre-treatments.

Finally, the main research was carried out and two types of laboratory work could be distinguished. The first one comprised an examination of physicochemical properties of biochars and their feedstocks by classical analytical techniques. The second type involved experiments on aromatic hydrocarbons catalytic conversion over a bed of biochar, performed in the custom-built test rig.

The conversion measurements in the test rig involved the main experiment and a set of additional tests. The main experiment was comprised of six measurement series of toluene conversion over alder, beech or pine biochar under pyrolytic or steam reforming conditions. Results of these tests enabled a comparison of biochars' performance and an investigation of toluene conversion pathways.

Additional tests involved further catalysts comparison as well as examination of selected aspects of toluene conversion. Differences between coniferous and deciduous wood, as biochar feedstock, were assessed by investigating the effect of a pinewood extractives presence on created biochar properties and catalytic performance. Toluene conversion studies were on the other hand broadened by additional tests with a modification of one of

the following: compound feeding principle, compound structure, oxidising agent type or metals content in a catalyst.

5.3. Summary of the obtained data

The experimental work performed in the test rig provided data on a model tar compound conversion for different reaction times. It also allowed for determination of liquid and gaseous by-product yields.

Analytical techniques applied for material properties investigation provided information on chemical properties of chars, including: O-containing surface functional groups, acidic sites distribution, alkali and alkaline earth metals content and oxidation reactivity. Examined physical properties involved BET surface area, micropores area and a general structure assessment via SEM micrographs.

5.4. Summary of the findings

The results obtained and a current state of knowledge on hydrocarbons catalytic conversion produced several conclusions on wood-derived biochars catalytic performance and alkylated aromatics conversion principles.

5.4.1. Wood-derived biochars catalytic performance

Wood proved to be a good feedstock for activated char synthesis. All obtained biochars had a high surface area above 668 m^2/g, well-developed porosity (with micropores areas $\geq$420 m^2/g) and an abundance of active sites, such as acidic sites exceeding 275 μeq/g. These biochars' features allowed them to catalyse hydrocarbons conversion. Observed differences in chars properties were mostly of a quantitative nature, resulting in differed efficiency of toluene conversion. Coniferous wood yielded char with less pronounced catalytic properties, *i.e.* approximately 30 m^2/g lower surface area as well as 1.3 – 4.6 times lower AAEM species contents and almost 15 % less acidic active sites, thus deteriorated toluene conversion was observed for this material. Moreover, an over 18 % higher microporosity of pine char made it more prone to deactivation due to pore sintering with coke deposit. However, the same toluene conversion pathways and their selectivity were observed for all tested biochars.

Pinewood extraction resulted in a formation of a biochar with slightly improved catalytic properties, *i.e.* 17 m^2/g higher surface area and 23 μeq/g higher amount of acidic sites. Thus, an enhanced initial toluene conversion was registered when extracted-pine char was used. However, its deactivation was still more rapid, compared to deciduous trees chars. During

the longest, 60 min tests, overall toluene conversion was as low as 25 % for both pine chars, despite the better performance of the extracted-pine one at the beginning of the process. Alder and beech chars, on the other hand, proved to be more resistant to deactivation and managed to ensure 42 % conversion under the same conditions.. This observation was in alignment with a higher share of micropores in both pine chars (75-76 %) compared to the deciduous-trees ones (59-60 %). It was therefore concluded, that higher microporosity, and therefore lower longevity of pine chars, compared to deciduous-trees chars, was related to some other distinctive feature of a pinewood, plausibly related to its lignin content and structure.

5.4.2. Alkylated aromatics catalytic conversion pathways

As a result of performed tests, an overview of a catalytic conversion pathway of methylated, single-ring aromatic compounds was proposed. Most of the compound decomposed heterogeneously on a char surface, by interacting with its active sites. The compound was attached on the surface, where it was undergoing dehydrogenation, leading to a release of H_2 combined with a formation of a dense, carbon-rich deposit, namely coke. Another, competing conversion pathway was a demethylation of an aromatic and most likely it also underwent heterogeneously, on a char surface. This reaction was less favoured, yet its significance increased with a progressing deactivation of a catalyst due to its saturation with coke. During toluene conversion, demethylation yielded benzene, with a selectivity up to ~15 %. In *p*-xylene conversion experiments, both toluene (up to 11 %) and benzene (~2 %) were formed. In both cases, corresponding amounts of methyl were released as well.

Additionally, some secondary recombination reactions between the introduced compound and its decomposition by-products were also observed. Although the role of a catalytic surface in those reactions was not clarified, the presence of gaseous radicals was found to be of an importance, as suggested by an intermittent feeding test. Therefore, those reactions, in contrast to coking and demethylation, might be of a homogeneous nature. They involved methylation of either aromatic ring or methyl group of a compound, leading to ethylbenzene and xylenes formation in toluene conversion experiments. In *p*-xylene tests, *p*-ethyltoluene and 1,2,4-trimethylbenzene were created as well. A substitution to an existing methyl group was favoured over a ring substitution, leading to higher yields of ethyl-substituted products, *e.g. p*-ethyltoluene yield was almost 5 times higher than that of 1,2,4-trimethylbenzene. An intense dehydrogenation of ethyl group was also observed, leading to styrene and *p*-methylstyrene formation. These vinyl-substituted compounds' yields were 2-8 times

greater than the yields of their precursors. During toluene conversion, recombination reactions yielded only trace amounts of substituted benzenes, adding up to 0.6 % of all products. However, *p*-xylene test revealed that its decomposition's selectivity towards *p*-methylstyrene reached almost 4 %, indicating an increasing importance of secondary reactions during a conversion of more complex compounds.

Comparison of benzene and toluene conversion indicated a significant role of the presence of methyl group, attached to an aromatic ring, in increasing compound's reactivity towards catalytic decomposition. It was established that methyl group enhanced pyrolytic conversion of a single-ring aromatic almost 1.7 times. However, *p*-xylene conversion test revealed that a further increase in methyl groups' amount did not affect compounds refractoriness, yet it intensified secondary recombination reactions, leading to a 10 times higher total yield of products of methyl addition.

Under pyrolytic conditions, alkylated aromatics underwent decomposition primarily in a heterogeneous way, via coking or demethylation on a char surface. Under the applied process parameters, steam presence did not affect toluene conversion principle. Its only role was char/coke gasification, resulting in a prolonged activity of a catalyst, allowing for a 1.5-2.5 higher toluene conversion during 60 min tests, depending on a type of char. A more reactive agent, oxygen, was able to evoke a homogeneous, ring-opening reaction of toluene. Even with a presence of char, oxygen radicals favoured a gas-phase toluene oxidation reaction over interactions with char. Therefore, a significant difference in roles of those two oxidising agents can be expected during a tar reforming processes.

Finally, an assessment of a catalytic role of alkali and alkaline earth metals in char revealed, that while they strongly enhanced reactivity of a char itself, lowering its activation energy 2.6 times, they did not affect toluene pyrolytic conversion efficiency.

5.5. Implications of the findings

The results of this work suggested, that wood-derived activated biochars are good catalysts for aromatic hydrocarbons conversion. They have relatively well-developed, active surface, regardless of wood type used for their production. High microporosity of the chars is responsible for their quick deactivation, when tar conversion is carried out in an inert atmosphere. However, this issue can be addressed by an introduction of steam that prolongs activity of the catalysts. This observation indicates an importance of maintaining oxidising conditions during catalytic tar reforming and syngas upgrading in commercial gasifiers. More microporous structure of the pine char, compared to the ones prepared from deciduous

trees, cannot be attributed to a high content of resins, as their extraction from raw pinewood did not influenced the microporosity of the prepared char. It is therefore plausible, that some other characteristic feature of conifers was responsible for a micropores development. Differences in softwood and hardwood's lignin structure might be one of the factors influencing pore distribution in chars.

Besides quantitative differences in micropores and active sites amount, all tested chars have a similar nature. They are porous, carbonaceous materials with some aromatic structures, unsaturated carbons, O-containing functional groups and AAEM metals. Those common features explain the same toluene conversion pathways that were observed for each applied catalyst. Consistency in the observed reactions as well as the types and distribution of their products indicates these determined principles of alkylated aromatics conversion are relevant for all types of woody biochar. Therefore, these mechanisms can be generally applied, *e.g.* while designing a process of a two-stage gasification of lignocellulosic feedstock.

Identified, common conversion mechanisms of alkylated aromatics comprised two heterogeneous reactions. The main was leading to coke formation. Concurrently, a competing, yet less favoured, demethylation pathway occurred. Additionally, some secondary recombination reactions of methylation and dehydrogenation took place. It was therefore established that coke formation was both, the most efficient conversion pathway and the main reason for char deactivation. Those opposing effects indicate the necessity for a catalytic material with a high capacity for coke agglomeration as well as for a constant re-activation of this material. Hence, a reactive atmosphere should be applied to achieve an effective tar reforming process.

A beneficial role of steam was observed in this work. Char re-activation due to steam gasification of coke and char prolonged high toluene conversion. Steam reforming counteracted the effect of char deactivation with coke while allowing for a further toluene-to-coke transformation. Therefore, it diminished the negative effect of this most effective conversion pathway without inhibiting the reaction itself. On the contrary, toluene conversion mechanism was not affected by the presence of steam; char/coke gasification was the only reaction involving this oxidising agent. The types of toluene conversion products as well as their distribution remained unaffected, with an exception of a lower yield of secondary, recombination products registered during steam reforming mode.

Reforming experiments with oxygen lead to different conclusions. This compound, contrary to steam, revealed a high affinity towards toluene oxidation via homogenous, ring-opening reactions. No char/coke gasification was however registered, and the catalyst deactivation

progressed equally fast as during pyrolytic toluene reforming. This surprising finding suggests crucial differences in behaviour of various oxidising agents. Obtained results revealed the need for further investigation into the nature of oxidiser-tar-char interactions. Information on the role of each oxidising agent would allow for a better understanding on secondary reactions during gasification. It can be expected that process optimisation could be carried out by an introduction of a control method for gasifying gases composition adjustment.

At pyrolytic conditions applied in this study, no solely thermal conversion of toluene occurred, as revealed by preliminary tests carried out in an absence of a char bed. Another theoretical possibility of homogeneous toluene reactions during catalytic pyrolysis, *i.e.* through radical reactions initiated by species released form a char surface, was disproved with intermittent feeding tests. An intermission in toluene supply did not affect its conversion as would be expected if any chain reactions took place. Moreover, a thermal stability of char was confirmed, as its efficiency did not diminish despite a prolonged exposition to a high temperature. These findings reaffirmed the heterogeneous nature of toluene catalytic pyrolysis, while attesting biochars suitability to serve as catalysts in high-temperature processes.

Another interesting aspect of tar conversion was the importance of methyl functional group attached to an aromatic ring. It was observed that benzene, due to a lack of any substituents, was more refractory, compared to toluene. Less reactive nature of benzene led to its lower conversion in an inert atmosphere. As the catalytic properties of char had a smaller effect on benzene, char deactivation did not hinder the efficiency of its removal as significantly as during toluene conversion. Thus, beneficial role of steam during reforming mode was not observed when benzene was used as tar-representing compound. This finding suggests that the improvement of tar removal efficiency by application of a more reactive catalyst can be achieved only for some of the tar compounds.

Further investigation into the role of methyl groups, accomplished by *p*-xylene conversion tests, suggested no additional benefits of a second substituent, as there was no difference between the efficiency of toluene and *p*-xylene pyrolytic conversion. Higher yield and diversity of secondary reaction products, *i.e.* substituted benzenes, were however observed. This could suggest that some more complex compounds could contribute to an enhanced formation of secondary tar, as their removal is similar to volatiles with a simpler structure, yet their conversion created more by-products.

The final finding of the performed research concerned the catalytic effect of AAEM species. Comparison of chars with enriched and lowered metals content revealed, that while they have a strong catalytic effect on char oxidation, they do not contribute to the efficiency of toluene pyrolytic, heterogeneous conversion. It could be therefore concluded that, at least for some of the tar compounds, AAEM species should not be considered as active sites. However, as those elements catalyse char gasification, they might still contribute to the aromatics removal, indirectly, by enhancing catalyst re-activation, when reforming atmosphere is applied.

5.5.1. Novelty of the findings

Performed research provided both, confirmation of previously reported phenomena as well as some novel and often surprising findings.

Conclusions that provided affirmation of a current state of knowledge included:

- heterogeneous nature of toluene catalytic pyrolysis;
- char deactivation resulting from toluene-derived coke deposition;
- quicker deactivation of a char with higher microporosity;
- maintained heterogeneous nature of toluene conversion during steam reforming;
- prolonged activity of char during steam reforming resulting from gasification reaction;
- lower reactivity of aromatic ring with no substituents;
- strong catalytic effect of AAEM species on char oxidation kinetics.

The studies provided following novel findings:

- differences between chars derived from coniferous and deciduous trees
- toluene conversion mainly via two, competing pathways leading to coke or benzene formation;
- increased significance of secondary reactions upon char deactivation;
- maintained toluene conversion selectivity towards benzene formation despite steam introduction;
- independence of toluene conversion and char/coke steam gasification reactions;
- no improvement in compound reactivity with a second methyl group presence;
- opposite behaviour of oxygen and steam in their affinity towards interactions with either toluene of char;
- lack of AAEM species' influence of toluene pyrolytic conversion efficiency.

All obtained results have significant implications on understanding tar conversion principles. The most surprising ones, *i.e.* different behaviour of two examined oxidising agents as well as no visible effect of AAEM species during toluene conversion, provide an interesting scope for a future investigation.

FUTURE RECOMMENDATIONS

Tar reforming over biochar catalyst is a promising and important process of upgrading a gasification producer gas. Therefore, it has been extensively studied in recent years. However, due to its high complexity, a variety of aspects still needs to be addressed.

In this work, only a few, selected issues were examined. Moreover, along with the main findings on wood-derived biochars and toluene catalytic conversion, some further, important questions arose, that would require a future investigation.

As differences between roles of steam and oxygen during toluene conversion were observed, a further investigation into this subject is advised. It would be interesting to examine the role of CO_2, as another common, yet much weaker oxidiser. Moreover, a more thorough analysis of various concentrations and complex mixtures, comprising numerous oxidising agents, might provide some valuable conclusions.

Studies of alkali and alkaline earth metals role in conversion process revealed, that while they affect carbonaceous catalysts reactivity, no effect on toluene pyrolytic conversion was found. It would be of interest, to further explore this phenomenon. It is plausible, that under reforming conditions, AAEM species would affect tar conversion process indirectly, by increasing reactivity and thus regeneration rate of a char catalyst. Extended research into AAEM role during tar conversion under different atmospheres would make an interesting objective for a future research. Moreover, determining an AAEM effect on other tar compounds conversion is very important. It is possible, that those metals may affect a conversion of *e.g.* molecules with oxygen heteroatom. Therefore, future studies comprising reactive atmosphere and other tar compounds, *e.g.* phenol or anisole, are advised.

Further extension of analytical methods applied for char properties assessment would also be beneficial for future research. A more thorough examination of char structure could be achieved by complementing N_2 adsorption test with a measurement of a CO_2 adsorption isotherm to provide high quality data on micropores distribution. Raman spectroscopy would supplement FTIR analysis with a more thorough assessment of aromatic ring structures. Basic functional groups analysis with titration and acidic sites quantification by pyridine adsorption could be of interest as well.

REFERENCES

[1] National Renewable Energy Action Plans 2020, https://ec.europa.eu/energy/en/topics/renewable-energy/national-renewable-energy-action-plans-2020.

[2] The UK Renewable Energy Strategy Cm 7686, TSO, London (2009), https://www.gov.uk/government/publications/the-uk-renewable-energy-strategy.

[3] P. Basu, Biomass gasification and pyrolysis: practical design and theory, Academic press, 2010.

[4] S. Anis, Z.A. Zainal, Tar reduction in biomass producer gas via mechanical, catalytic and thermal methods: A review, Renew. Sustain. Energy Rev. 15 (2011) 2355–2377. doi:10.1016/J.RSER.2011.02.018.

[5] Y. Shen, Chars as carbonaceous adsorbents/catalysts for tar elimination during biomass pyrolysis or gasification, Renew. Sustain. Energy Rev. 43 (2015) 281–295. doi:10.1016/J.RSER.2014.11.061.

[6] G. Ravenni, Z. Sárossy, J. Ahrenfeldt, U.B. Henriksen, Activity of chars and activated carbons for removal and decomposition of tar model compounds – A review, Renew. Sustain. Energy Rev. 94 (2018) 1044–1056. doi:10.1016/J.RSER.2018.07.001.

[7] C.Z. Li, Importance of volatile-char interactions during the pyrolysis and gasification of low-rank fuels - A review, Fuel. 112 (2013) 609–623. doi:10.1016/j.fuel.2013.01.031.

[8] K. Maniatis, A.A.C.. Beenackers, Tar Protocols. IEA Bioenergy Gasification Task, Biomass and Bioenergy. 18 (2000) 1–4. doi:10.1016/S0961-9534(99)00072-0.

[9] S. Schmidt, S. Giesa, A. Drochner, H. Vogel, Catalytic tar removal from bio syngas—Catalyst development and kinetic studies, Catal. Today. 175 (2011) 442–449. doi:10.1016/J.CATTOD.2011.04.052.

[10] D. Wang, W. Yuan, W. Ji, Char and char-supported nickel catalysts for secondary syngas cleanup and conditioning, Appl. Energy. 88 (2011) 1656–1663. doi:10.1016/j.apenergy.2010.11.041.

[11] D. Sutton, B. Kelleher, J.R.H. Ross, Review of literature on catalysts for biomass gasification, Fuel Process. Technol. 73 (2001) 155–173. doi:10.1016/S0378-3820(01)00208-9.

[12] G. Guan, M. Kaewpanha, X. Hao, A. Abudula, Catalytic steam reforming of biomass tar: Prospects and challenges, Renew. Sustain. Energy Rev. 58 (2016) 450–461.

doi:10.1016/j.rser.2015.12.316.

[13] Z. Abu El-Rub, E.A. Bramer, G. Brem, Experimental comparison of biomass chars with other catalysts for tar reduction, Fuel. 87 (2008) 2243–2252. doi:10.1016/J.FUEL.2008.01.004.

[14] N.B. Klinghoffer, M.J. Castaldi, A. Nzihou, Influence of char composition and inorganics on catalytic activity of char from biomass gasification, Fuel. 157 (2015) 37–47. doi:10.1016/j.fuel.2015.04.036.

[15] S. Hosokai, K. Kumabe, M. Ohshita, K. Norinaga, C.Z. Li, J. Hayashi, Mechanism of decomposition of aromatics over charcoal and necessary condition for maintaining its activity, Fuel. 87 (2008) 2914–2922. doi:10.1016/j.fuel.2008.04.019.

[16] A. Dufour, A. Celzard, V. Fierro, E. Martin, F. Broust, A. Zoulalian, Catalytic decomposition of methane over a wood char concurrently activated by a pyrolysis gas, Appl. Catal. A Gen. 346 (2008) 164–173. doi:10.1016/j.apcata.2008.05.023.

[17] Y. Huang, X. Yin, C. Wu, C. Wang, J. Xie, Z. Zhou, L. Ma, H. Li, Effects of metal catalysts on CO2 gasification reactivity of biomass char, Biotechnol. Adv. 27 (2009) 568–572. doi:10.1016/j.biotechadv.2009.04.013.

[18] Z. Zhang, S. Pang, T. Levi, Influence of AAEM species in coal and biomass on steam co-gasification of chars of blended coal and biomass, Renew. Energy. 101 (2017) 356–363. doi:10.1016/J.RENENE.2016.08.070.

[19] T. Sueyasu, T. Oike, A. Mori, S. Kudo, K. Norinaga, J. Hayashi, Simultaneous Steam Reforming of Tar and Steam Gasification of Char from the Pyrolysis of Potassium-Loaded Woody Biomass, Energy & Fuels. 26 (2012) 199–208. doi:10.1021/ef201166a.

[20] D. Feng, Y. Zhao, Y. Zhang, S. Sun, S. Meng, Y. Guo, Y. Huang, Effects of K and Ca on reforming of model tar compounds with pyrolysis biochars under H2O or CO2, Chem. Eng. J. 306 (2016) 422–432. doi:10.1016/J.CEJ.2016.07.065.

[21] M.H. Kim, E.K. Lee, J.H. Jun, S.J. Kong, G.Y. Han, B.K. Lee, T.-J. Lee, K.J. Yoon, Hydrogen production by catalytic decomposition of methane over activated carbons: kinetic study, Int. J. Hydrogen Energy. 29 (2004) 187–193. doi:10.1016/S0360-3199(03)00111-3.

[22] Z. Bai, H. Chen, W. Li, B. Li, Hydrogen production by methane decomposition over coal char, Int. J. Hydrogen Energy. 31 (2006) 899–905. doi:10.1016/J.IJHYDENE.2005.08.001.

[23] G.S. Szymański, Z. Karpiński, S. Biniak, A. Świątkowski, The effect of the gradual

thermal decomposition of surface oxygen species on the chemical and catalytic properties of oxidized activated carbon, Carbon N. Y. 40 (2002) 2627–2639. doi:10.1016/S0008-6223(02)00188-4.

[24] H.P. Boehm, Some aspects of the surface chemistry of carbon blacks and other carbons, Carbon N. Y. 32 (1994) 759–769. doi:10.1016/0008-6223(94)90031-0.

[25] W.J. Liu, F.X. Zeng, H. Jiang, X.S. Zhang, Preparation of high adsorption capacity bio-chars from waste biomass, Bioresour. Technol. 102 (2011) 8247–8252. doi:10.1016/j.biortech.2011.06.014.

[26] J.. Figueiredo, M.F.. Pereira, M.M.. Freitas, J.J.. Órfão, Modification of the surface chemistry of activated carbons, Carbon N. Y. 37 (1999) 1379–1389. doi:10.1016/S0008-6223(98)00333-9.

[27] P. Serp, J.L. Figueiredo, Carbon materials for catalysis, John Wiley & Sons, 2009.

[28] U. Zielke, K.J. Hüttinger, W.P. Hoffman, Surface-oxidized carbon fibers: I. Surface structure and chemistry, Carbon N. Y. 34 (1996) 983–998. doi:10.1016/0008-6223(96)00032-2.

[29] J.P. Boudou, Surface chemistry of a viscose-based activated carbon cloth modified by treatment with ammonia and steam, Carbon N. Y. 41 (2003) 1955–1963. doi:10.1016/S0008-6223(03)00182-9.

[30] H. Boehm, E. Diehl, W. Heck, R. Sappok, Surface oxides of carbon, Angew. Chemie Int. Ed. English. 3 (1964) 669–677.

[31] S.Y. Lee, J.H. Kwak, G.Y. Han, T.J. Lee, K.J. Yoon, Characterization of active sites for methane decomposition on carbon black through acetylene chemisorption, Carbon N. Y. 46 (2008) 342–348. doi:10.1016/j.carbon.2007.11.049.

[32] A.R. Mohamed, M. Mohammadi, G.N. Darzi, Preparation of carbon molecular sieve from lignocellulosic biomass: A review, Renew. Sustain. Energy Rev. 14 (2010) 1591–1599. doi:10.1016/j.rser.2010.01.024.

[33] M. Molina-Sabio, M.T. Gonzalez, F. Rodriguez-Reinoso, A. Sepúlveda-Escribano, Effect of steam and carbon dioxide activation in the micropore size distribution of activated carbon, Carbon N. Y. 34 (1996) 505–509. doi:10.1016/0008-6223(96)00006-1.

[34] F. Nestler, L. Burhenne, M.J. Amtenbrink, T. Aicher, Catalytic decomposition of biomass tars: The impact of wood char surface characteristics on the catalytic performance for naphthalene removal, Fuel Process. Technol. 145 (2016) 31–41. doi:10.1016/j.fuproc.2016.01.020.

[35] L. Burhenne, T. Aicher, Benzene removal over a fixed bed of wood char: The effect of pyrolysis temperature and activation with CO2 on the char reactivity, Fuel Process. Technol. 127 (2014) 140–148. doi:10.1016/j.fuproc.2014.05.034.

[36] D. Fuentes-Cano, A. Gómez-Barea, S. Nilsson, P. Ollero, Decomposition kinetics of model tar compounds over chars with different internal structure to model hot tar removal in biomass gasification, Chem. Eng. J. 228 (2013) 1223–1233. doi:10.1016/j.cej.2013.03.130.

[37] G. Ravenni, O.H. Elhami, J. Ahrenfeldt, U.B. Henriksen, Y. Neubauer, Adsorption and decomposition of tar model compounds over the surface of gasification char and active carbon within the temperature range 250–800 °C, Appl. Energy. 241 (2019) 139–151. doi:10.1016/J.APENERGY.2019.03.032.

[38] M.F. Tennant, D.W. Mazyck, Steam-pyrolysis activation of wood char for superior odorant removal, Carbon N. Y. 41 (2003) 2195–2202. doi:10.1016/S0008-6223(03)00211-2.

[39] N. Tancredi, T. Cordero, J. Rodríguez-Mirasol, J.J. Rodríguez, Activated carbons from Uruguayan eucalyptus wood, Fuel. 75 (1996) 1701–1706. doi:10.1016/S0016-2361(96)00168-8.

[40] M.A. Lillo-Ródenas, D. Cazorla-Amorós, A. Linares-Solano, Behaviour of activated carbons with different pore size distributions and surface oxygen groups for benzene and toluene adsorption at low concentrations, Carbon N. Y. 43 (2005) 1758–1767. doi:10.1016/J.CARBON.2005.02.023.

[41] R. Moliner, I. Suelves, M.J. Lázaro, O. Moreno, Thermocatalytic decomposition of methane over activated carbons: influence of textural properties and surface chemistry, Int. J. Hydrogen Energy. 30 (2005) 293–300. doi:10.1016/j.ijhydene.2004.03.035.

[42] J. Pastor-Villegas, V. Gómez-Serrano, C.. Durán-Valle, F.. Higes-Rolando, Chemical study of extracted rockrose and of chars and activated carbons prepared at different temperatures, J. Anal. Appl. Pyrolysis. 50 (1999) 1–16. doi:10.1016/S0165-2370(99)00022-4.

[43] L. Burhenne, M. Damiani, T. Aicher, Effect of feedstock water content and pyrolysis temperature on the structure and reactivity of spruce wood char produced in fixed bed pyrolysis, Fuel. 107 (2013) 836–847. doi:10.1016/j.fuel.2013.01.033.

[44] M. Asadullah, S. Zhang, C.Z. Li, Evaluation of structural features of chars from pyrolysis of biomass of different particle sizes, in: Fuel Process. Technol., Elsevier,

2010: pp. 877–881. doi:10.1016/j.fuproc.2009.08.008.

[45] F. Rodríguez-Reinoso, M. Molina-Sabio, M.T. González, The use of steam and CO2 as activating agents in the preparation of activated carbons, Carbon N. Y. 33 (1995) 15–23. doi:10.1016/0008-6223(94)00100-E.

[46] M. Fan, W. Marshall, D. Daugaard, R.. Brown, Steam activation of chars produced from oat hulls and corn stover, 2004. doi:10.1016/j.biortech.2003.08.016.

[47] D.M. Keown, J.-I. Hayashi, C.-Z. Li, Drastic changes in biomass char structure and reactivity upon contact with steam, Fuel. 87 (2008) 1127–1132. doi:10.1016/j.fuel.2007.05.057.

[48] F. Cherubini, The biorefinery concept: Using biomass instead of oil for producing energy and chemicals, Energy Convers. Manag. 51 (2010) 1412–1421. doi:10.1016/j.enconman.2010.01.015.

[49] S. Hosokai, J.-I. Hayashi, T. Shimada, Y. Kobayashi, K. Kuramoto, C.-Z. Li, T. Chiba, Spontaneous Generation of Tar Decomposition Promoter in a Biomass Steam Reformer, Chem. Eng. Res. Des. 83 (2005) 1093–1102. doi:10.1205/cherd.04101.

[50] S. Hosokai, K. Norinaga, T. Kimura, M. Nakano, C.Z. Li, J.I. Hayashi, Reforming of volatiles from the biomass pyrolysis over charcoal in a sequence of coke deposition and steam gasification of coke, Energy and Fuels. 25 (2011) 5387–5393. doi:10.1021/ef2003766.

[51] E. Sjöström, R. Alén, eds., Analytical Methods in Wood Chemistry, Pulping, and Papermaking, first ed., Springer, Berlin, Heidelberg, 1999.

[52] M.J. Antal, G. Várhegyi, E. Jakab, Cellulose Pyrolysis Kinetics: Revisited, Ind. Eng. Chem. Res. 37 (1998) 1267–1275. doi:10.1021/ie970144v.

[53] K. Raveendran, A. Ganesh, K.C. Khilar, Pyrolysis characteristics of biomass and biomass components, Fuel. 75 (1996) 987–998. doi:10.1016/0016-2361(96)00030-0.

[54] G. Várhegyi, M.G. Grønli, C. Di Blasi, Effects of Sample Origin, Extraction, and Hot-Water Washing on the Devolatilization Kinetics of Chestnut Wood, Ind. Eng. Chem. Res. 43 (2004) 2356–2367. doi:10.1021/ie034168f.

[55] A. Dufour, P. Girods, E. Masson, S. Normand, Y. Rogaume, A. Zoulalian, Comparison of two methods of measuring wood pyrolysis tar, J. Chromatogr. A. 1164 (2007) 240–247. doi:10.1016/j.chroma.2007.06.049.

[56] L. Burhenne, J. Messmer, T. Aicher, M.P. Laborie, The effect of the biomass components lignin, cellulose and hemicellulose on TGA and fixed bed pyrolysis, J. Anal. Appl. Pyrolysis. 101 (2013) 177–184. doi:10.1016/j.jaap.2013.01.012.

[57] D.J. Nowakowski, J.M. Jones, R.M.D. Brydson, A.B. Ross, Potassium catalysis in the pyrolysis behaviour of short rotation willow coppice, Fuel. 86 (2007) 2389–2402. doi:10.1016/J.FUEL.2007.01.026.

[58] R.W. Hemingway, W.E. Hillis, L.S. Lau, The extractives of Pinus pinaster wood, Sven. Papperstidning. 76 (1973) 371–376.

[59] R.W. Hemingway, W.E. Hillis, Changes in fats and resins of Pinus radiata associated with heartwood formation, APPITA. 24 (1971) 439–443.

[60] D.F. Zinkel, Fats and Fatty Acids, in: J.W. Rowe (Ed.), Nat. Prod. Woody Plants Chem. Extraneous to Lignocellul. Cell Wall, first ed., Springer, Berlin, Heidelberg, 1989: pp. 299–304. doi:10.1007/978-3-642-74075-6-10.

[61] C. Di Blasi, C. Branca, A. Santoro, R.A. Perez Bermudez, Weight loss dynamics of wood chips under fast radiative heating, J. Anal. Appl. Pyrolysis. 57 (2001) 77–90. doi:10.1016/S0165-2370(00)00119-4.

[62] A. Demirbaş, Analysis of beech wood fatty acids by supercritical acetone extraction, Wood Sci. Technol. 25 (1991) 365–370. doi:10.1007/BF00226176.

[63] A. Gutiérrez, J.C. del Río, F.J. González-Vila, F. Martín, Analysis of lipophilic extractives from wood and pitch deposits by solid-phase extraction and gas chromatography, J. Chromatogr. A. 823 (1998) 449–455. doi:http://dx.doi.org/10.1016/S0021-9673(98)00356-2.

[64] F.W. Claassen, C. van de Haar, T.A. van Beek, J. Dorado, M.-J. Martínez-Iñigo, R. Sierra-Alvarez, Rapid analysis of apolar low molecular weight constituents in wood using high pressure liquid chromatography with evaporative light scattering detection, Phytochem. Anal. 11 (2000) 251–256. doi:10.1002/1099-1565(200007/08)11:4<251::AID-PCA522>3.0.CO;2-P.

[65] W. Zieliński, A. Rajca, Metody spektroskopowe i ich zastosowanie do identyfikacji związków organicznych, second ed., Wydawnictwa Naukowo-Techniczne, Warsaw, 2000.

[66] R.M. Silverstein, F.X. Webster, D.J. Kiemle, Spektroskopowe metody identyfikacji związków organicznych, second ed., Wydawnictwo Naukowe PWN, Warsaw, 2007.

[67] K.B. Cantrell, P.G. Hunt, M. Uchimiya, J.M. Novak, K.S. Ro, Impact of pyrolysis temperature and manure source on physicochemical characteristics of biochar, Bioresour. Technol. 107 (2012) 419–428. doi:10.1016/j.biortech.2011.11.084.

[68] F. Jin, Y. Li, A FTIR and TPD examination of the distributive properties of acid sites on ZSM-5 zeolite with pyridine as a probe molecule, Catal. Today. 145 (2009) 101–

107. doi:10.1016/j.cattod.2008.06.007.

[69] N. Gao, A. Li, C. Quan, L. Du, Y. Duan, TG–FTIR and Py–GC/MS analysis on pyrolysis and combustion of pine sawdust, J. Anal. Appl. Pyrolysis. 100 (2013) 26–32. doi:10.1016/J.JAAP.2012.11.009.

[70] L. Zhang, J. Cai, T. Zhang, F. Qi, Kinetic modeling study of toluene pyrolysis at low pressure, Combust. Flame. 157 (2010) 1686–1697. doi:10.1016/j.combustflame.2010.04.002.

[71] G. da Silva, J.A. Cole, J.W. Bozzelli, Thermal Decomposition of the Benzyl Radical to Fulvenallene (C7H6) + H, J. Phys. Chem. A. 113 (2009) 6111–6120. doi:10.1021/jp901933x.

[72] J.-P. Leininger, F. Lorant, C. Minot, F. Behar, Mechanisms of 1-Methylnaphthalene Pyrolysis in a Batch Reactor, Energy & Fuels. 20 (2006) 2518–2530. doi:10.1021/ef0600964.

[73] J.-P. Leininger, C. Minot, F. Lorant, F. Behar, Density Functional Theory Investigation of Competitive Free-Radical Processes during the Thermal Cracking of Methylated Polyaromatics: Estimation of Kinetic Parameters, J. Phys. Chem. A. 111 (2007) 3082–3090. doi:10.1021/jp0643956.

[74] P.E. Savage, Mechanisms and kinetics models for hydrocarbon pyrolysis, J. Anal. Appl. Pyrolysis. 54 (2000) 109–126. doi:10.1016/S0165-2370(99)00084-4.

[75] C. Cavallotti, M. Derudi, R. Rota, On the mechanism of decomposition of the benzyl radical, Proc. Combust. Inst. 32 I (2009) 115–121. doi:10.1016/j.proci.2008.06.203.

[76] M.B. Colket, D.J. Seery, Reaction mechanisms for toluene pyrolysis, Symp. Combust. 25 (1994) 883–891. doi:10.1016/S0082-0784(06)80723-X.

[77] B. Shukla, A. Susa, A. Miyoshi, M. Koshi, In Situ Direct Sampling Mass Spectrometric Study on Formation of Polycyclic Aromatic Hydrocarbons in Toluene Pyrolysis, J. Phys. Chem. A. 111 (2007) 8308–8324. doi:10.1021/jp071813d.

[78] C.C. Zimmerman, R. York, Thermal Demethylation of Toluene, Ind. Eng. Chem. Process Des. Dev. 3 (1964) 254–258. doi:10.1021/i260011a013.

[79] A.R. Lea-Langton, G.E. Andrews, K.D. Bartle, J.M. Jones, A. Williams, Combustion and pyrolysis reactions of alkylated polycyclic aromatic compounds: The decomposition of 13C methylarenes in relation to diesel engine emissions, Fuel. 158 (2015) 719–724. doi:10.1016/j.fuel.2015.05.043.

[80] W.K. Metcalfe, S. Dooley, F.L. Dryer, Comprehensive Detailed Chemical Kinetic Modeling Study of Toluene Oxidation, Energy & Fuels. 25 (2011) 4915–4936.

doi:10.1021/ef200900q.

[81] M. Frenklach, K.E. Spear, Growth mechanism of vapor-deposited diamond, J. Mater. Res. 3 (1988) 133–140. doi:DOI: 10.1557/JMR.1988.0133.

[82] B. Shukla, A. Susa, A. Miyoshi, M. Koshi, Role of Phenyl Radicals in the Growth of Polycyclic Aromatic Hydrocarbons, J. Phys. Chem. A. 112 (2008) 2362–2369. doi:10.1021/jp7098398.

[83] S. Mani, J.R. Kastner, A. Juneja, Catalytic decomposition of toluene using a biomass derived catalyst, Fuel Process. Technol. 114 (2013) 118–125. doi:10.1016/J.FUPROC.2013.03.015.

[84] E.B. Ledesma, C. Campos, D.J. Cranmer, B.L. Foytik, M.N. Ton, E.A. Dixon, C. Chirino, S. Batamo, P. Roy, Vapor-Phase Cracking of Eugenol: Distribution of Tar Products as Functions of Temperature and Residence Time, Energy & Fuels. 27 (2013) 868–878. doi:10.1021/ef3018332.

[85] E.B. Ledesma, J.N. Hoang, Q. Nguyen, V. Hernandez, M.P. Nguyen, S. Batamo, C.K. Fortune, Unimolecular Decomposition Pathway for the Vapor-Phase Cracking of Eugenol, A Biomass Tar Compound, Energy & Fuels. 27 (2013) 6839–6846. doi:10.1021/ef401760c.

[86] M. Nowakowska, O. Herbinet, A. Dufour, P.-A. Glaude, Detailed kinetic study of anisole pyrolysis and oxidation to understand tar formation during biomass combustion and gasification, Combust. Flame. 161 (2014) 1474–1488. doi:10.1016/J.COMBUSTFLAME.2013.11.024.

[87] P.N. Bhandari, A. Kumar, D.D. Bellmer, R.L. Huhnke, Synthesis and evaluation of biochar-derived catalysts for removal of toluene (model tar) from biomass-generated producer gas, Renew. Energy. 66 (2014) 346–353. doi:10.1016/J.RENENE.2013.12.017.

[88] The Wood Database, (n.d.). https://www.wood-database.com/.

[89] E. Mészáros, E. Jakab, G. Várhegyi, TG/MS, Py-GC/MS and THM-GC/MS study of the composition and thermal behavior of extractive components of Robinia pseudoacacia, J. Anal. Appl. Pyrolysis. 79 (2007) 61–70. doi:10.1016/j.jaap.2006.12.007.

[90] X. Guo, S. Wang, K. Wang, Q. Liu, Z. Luo, Influence of extractives on mechanism of biomass pyrolysis, J. Fuel Chem. Technol. 38 (2010) 42–46. doi:10.1016/S1872-5813(10)60019-9.

[91] B. Holmbom, Extractives, in: E. Sjöström, R. Alén (Eds.), Anal. Methods Wood

Chem. Pulping, Papermak., first ed., Springer, Berlin, Heidelberg, 1999: pp. 125–146. doi:10.1007/978-3-662-03898-7.

[92] D.M.L. Griffiths, J.S.R. Mainhood, Cracking of tar vapor and aromatic compounds on activated carbon, Fuel. 46 (1967) 167–176.

[93] J.P.A. Neeft, Rationale for setup of impinger train, SenterNovem CEN BT/TF. 143 (2005) 1–14.

[94] J. Jae, G.A. Tompsett, A.J. Foster, K.D. Hammond, S.M. Auerbach, R.F. Lobo, G.W. Huber, Investigation into the shape selectivity of zeolite catalysts for biomass conversion, J. Catal. 279 (2011) 257–268. doi:10.1016/j.jcat.2011.01.019.

[95] R.K. Sharma, J.B. Wooten, V.L. Baliga, P.A. Martoglio-Smith, M.R. Hajaligol, Characterization of Char from the Pyrolysis of Tobacco, J. Agric. Food Chem. 50 (2002) 771–783. doi:10.1021/jf0107398.

[96] S.L. Goertzen, K.D. Thériault, A.M. Oickle, A.C. Tarasuk, H.A. Andreas, Standardization of the Boehm titration. Part I. CO2 expulsion and endpoint determination, Carbon N. Y. 48 (2010) 1252–1261. doi:10.1016/j.carbon.2009.11.050.

[97] A.M. Oickle, S.L. Goertzen, K.R. Hopper, Y.O. Abdalla, H.A. Andreas, Standardization of the Boehm titration: Part II. Method of agitation, effect of filtering and dilute titrant, Carbon N. Y. 48 (2010) 3313–3322. doi:10.1016/j.carbon.2010.05.004.

[98] R.B. Fidel, D.A. Laird, M.L. Thompson, Evaluation of Modified Boehm Titration Methods for Use with Biochars, J. Environ. Qual. 42 (2013) 1771–1778. doi:10.2134/jeq2013.07.0285.

[99] L. Tsechansky, E.R. Graber, Methodological limitations to determining acidic groups at biochar surfaces via the Boehm titration, Carbon N. Y. 66 (2014) 730–733. doi:10.1016/j.carbon.2013.09.044.

[100] R. Weber, Extracting mathematically exact kinetic parameters from experimental data on combustion and pyrolysis of solid fuels, J. Energy Inst. 81 (2008) 226–233. doi:10.1179/014426008X370997.

[101] G.I. Senum, R.T. Yang, Rational approximations of the integral of the Arrhenius function, J. Therm. Anal. 11 (1977) 445–447. doi:10.1007/BF01903696.

[102] J. Rodrigues, O. Faix, H. Pereira, Determination of lignin content of Eucalyptus globulus wood using FTIR spectroscopy, Holzforschung-International J. Biol. Chem. Phys. Technol. Wood. 52 (1998) 46–50.

[103] M. Nuopponen, T. Vuorinen, S. Jämsä, P. Viitaniemi, The effects of a heat treatment on the behaviour of extractives in softwood studied by FTIR spectroscopic methods, Wood Sci. Technol. 37 (2003) 109–115. doi:10.1007/s00226-003-0178-4.

[104] R.K. Sharma, J.B. Wooten, V.L. Baliga, X. Lin, W.G. Chan, M.R. Hajaligol, Characterization of chars from pyrolysis of lignin, in: Fuel, 2004: pp. 1469–1482. doi:10.1016/j.fuel.2003.11.015.

[105] R. Rana, R. Langenfeld-Heyser, R. Finkeldey, A. Polle, FTIR spectroscopy, chemical and histochemical characterisation of wood and lignin of five tropical timber wood species of the family of Dipterocarpaceae, Wood Sci. Technol. 44 (2010) 225–242. doi:10.1007/s00226-009-0281-2.

[106] C.G. Boeriu, D. Bravo, R.J.A. Gosselink, J.E.G. Van Dam, Characterisation of structure-dependent functional properties of lignin with infrared spectroscopy, in: Ind. Crops Prod., 2004: pp. 205–218. doi:10.1016/j.indcrop.2004.04.022.

[107] S. Haydar, C. Moreno-Castilla, M.A. Ferro-García, F. Carrasco-Marín, J. Rivera-Utrilla, A. Perrard, J.P. Joly, Regularities in the temperature-programmed desorption spectra of CO2 and CO from activated carbons, Carbon N. Y. 38 (2000) 1297–1308. doi:10.1016/S0008-6223(99)00256-0.

[108] Q.-L. Zhuang, T. Kyotani, A. Tomita, DRIFT and TK/TPD Analyses of Surface Oxygen Complexes Formed during Carbon Gasification, Energy & Fuels. 8 (1994) 714–718. doi:10.1021/ef00045a028.

[109] E. Biagini, P. Narducci, L. Tognotti, Size and structural characterization of lignin-cellulosic fuels after the rapid devolatilization, Fuel. 87 (2008) 177–186. doi:10.1016/J.FUEL.2007.04.010.

[110] L. Devi, K.J. Ptasinski, F.J.J.G. Janssen, S.V.B. Van Paasen, P.C.A. Bergman, J.H.A. Kiel, Catalytic decomposition of biomass tars: Use of dolomite and untreated olivine, Renew. Energy. 30 (2005) 565–587. doi:10.1016/j.renene.2004.07.014.

[111] A. Korus, A. Samson, A. Szlęk, A. Katelbach-Woźniak, S. Sładek, Pyrolytic toluene conversion to benzene and coke over activated carbon in a fixed-bed reactor, Fuel. 207 (2017). doi:10.1016/j.fuel.2017.06.088.

[112] Thommes Matthias, K. Katsumi, N.A. V, O.J. P, R.-R. Francisco, R. Jean, S.K.S. W, Physisorption of gases, with special reference to the evaluation of surface area and pore size distribution (IUPAC Technical Report), Pure Appl. Chem. 87 (2015) 1051. doi:10.1515/pac-2014-1117.

[113] K.S.W. Sing, Reporting physisorption data for gas/solid systems with special

reference to the determination of surface area and porosity (Recommendations 1984), Pure Appl. Chem. 57 (1985) 603. doi:10.1351/pac198557040603.

[114] E.-M.A. Ajuong, M.C. Breese, Fourier Transform Infrared characterization of Pai wood (Afzelia africana Smith) extractives, Holz Als Roh- Und Werkst. 56 (1998) 139. doi:10.1007/s001070050285.

[115] E.-M.A. Ajuong, M. Redington, Fourier transform infrared analyses of bog and modern oak wood (Quercus petraea) extractives, Wood Sci. Technol. 38 (2004) 181–190. doi:10.1007/s00226-004-0236-6.

[116] R.C. Sun, X.F. Sun, Identification and quantitation of lipophilic extractives from wheat straw, Ind. Crops Prod. 14 (2001) 51–64. doi:10.1016/S0926-6690(00)00088-1.

[117] M. Melzer, J. Blin, A. Bensakhria, J. Valette, F. Broust, Pyrolysis of extractive rich agroindustrial residues, J. Anal. Appl. Pyrolysis. 104 (2013) 448–460. doi:10.1016/j.jaap.2013.05.027.

[118] T. Dong, J. Wang, C. Miao, Y. Zheng, S. Chen, Two-step in situ biodiesel production from microalgae with high free fatty acid content, Bioresour. Technol. 136 (2013) 8–15. doi:https://doi.org/10.1016/j.biortech.2013.02.105.

[119] W.H. Schuller, C.M. Conrad, Thermal Behavior of Certain Resin Acids., J. Chem. Eng. Data. 11 (1966) 89–91. doi:10.1021/je60028a024.

[120] A. Sarı, A. Biçer, A. Karaipekli, C. Alkan, A. Karadag, Synthesis, thermal energy storage properties and thermal reliability of some fatty acid esters with glycerol as novel solid–liquid phase change materials, Sol. Energy Mater. Sol. Cells. 94 (2010) 1711–1715. doi:https://doi.org/10.1016/j.solmat.2010.05.033.

[121] P. Jandura, B. Riedl, B. V Kokta, Thermal degradation behavior of cellulose fibers partially esterified with some long chain organic acids, Polym. Degrad. Stab. 70 (2000) 387–394. doi:https://doi.org/10.1016/S0141-3910(00)00132-4.

[122] C. Di Blasi, C. Branca, A. Santoro, E. Gonzalez Hernandez, Pyrolytic behavior and products of some wood varieties, Combust. Flame. 124 (2001) 165–177. doi:10.1016/S0010-2180(00)00191-7.

[123] A. Ahmed, H. Pakdel, C. Roy, S. Kaliaguine, Characterization of the solid residues of vacuum pyrolysis of Populus tremuloides, J. Anal. Appl. Pyrolysis. 14 (1989) 281–294. doi:https://doi.org/10.1016/0165-2370(89)80004-X.

[124] C. Roy, H. Pakdel, D. Brouillard, The role of extractives during vacuum pyrolysis of wood, J. Appl. Polym. Sci. 41 (1990) 337–348. doi:10.1002/app.1990.070410126.